UNIVERSIDAD COMPLUTENSE DE MADRID

FACULTAD DE CIENCIAS QUÍMICAS

Departamento Bioquímica y Biología Molecular I

TESIS DOCTORAL

Respuesta del pulmón frente al daño por ventilación mecánica
Papel del surfactante pulmonar

MEMORIA PARA OPTAR AL GRADO DE DOCTOR

PRESENTADA POR

Virginia Egido Martín

Directora

Cristina Casals Carro

Madrid, 2014

UNIVERSIDAD COMPLUTENSE DE MADRID

FACULTAD DE QUÍMICAS

DEPARTAMENTO DE BIOQUÍMICA Y BIOLOGÍA MOLECULAR I

RESPUESTA DEL PULMÓN FRENTE AL DAÑO POR VENTILACIÓN MECÁNICA: PAPEL DEL SURFACTANTE PULMONAR

TESIS DOCTORAL DE

VIRGINIA EGIDO MARTÍN

DIRECTORA

DRA. CRISTINA CASALS CARRO

MADRID, 2013

COMPLUTENSE UNIVERSITY OF MADRID

CHEMISTRY SCHOOL

DEPARTMENT OF BIOCHEMISTRY AND MOLECULAR BIOLOGY I

LUNG RESPONSE AGAINST VENTILATOR-INDUCED LUNG INJURY: ROLE OF PULMONARY SURFACTANT

DOCTORAL THESIS OF

VIRGINIA EGIDO MARTÍN

DIRECTOR

DR. CRISTINA CASALS CARRO

MADRID, 2013

A mi padre

A mi madre

A mis princesas

The research for this thesis has been conducted in the Department of Biochemistry and Molecular Biology I of Complutense University of Madrid, under the supervision of Professor Cristina Casals.

This project has been performed in close collaboration with the Intensive Care Unit of Getafe University Hospital supervised by Dr. Andrés Esteban.

The completion of this thesis was possible thanks to the funding of the Ministry of Science and Innovation [SAF2006-04434 (FPI Grant: BES2008-009128), SAF2009-07810, and SAF2012-32728] and the support of CIBER of Respiratory Diseases (Institute of Health Carlos III-CB06/06/0002).

ABBREVIATIONS

ABCA3:	**ATP-binding cassette, sub-family A, member 3**
ALI:	**Acute lung injury**
ALT:	**Alanine aminotransferase**
ARDS:	**Acute respiratory distress syndrome**
ARDSnet:	**ARDS network**
ASMase:	**Acid sphingomyelinase activity**
AST:	**Aspartate aminotransferase**
ATI:	**Alveolar type one cells**
ATII:	**Alveolar type two cells**
ATS:	**American respiratory society**
BAL:	**Bronchoalveolar lavage free of cells**
BM:	**Basement membranes**
CBS:	**Captive bubble surfactometer**
Ch:	**Cholesterol**
CK:	**Creatinine kinase**
CRP:	**C-reactive protein**
C_{RS}:	**Dynamic respiratory system compliance**
DNPH:	**2.4-Dinitrophenylhydrazine**
DPPC:	**Dipalmitoyl phosphatidylcholine**
DPPG:	**Dipalmitoyl phosphatidylglycerol**
ECM:	**Extracellular matrix**
EGF:	**Epithermal growth factor**
ELISA:	**Enzyme-linked immunosorbent assay**
ER:	**Endoplasmic reticulum**
FBS:	**Fetal bovine serum**
FSC:	**Forward scatter**

FiO_2:	**Fraction of inspired oxygen**
HEPES:	**4-(2-Hydroxyethyl)-1-piperazineethanesulfonic acid**
ICAM-1	**Intracellular adhesion molecule 1**
IFN-γ	**Interferon gamma**
IL-1β-4-6-8-10-12-13	**Interleukin-1β-4-6-8-10-12-13**
KC	**Keratinocyte-derived chemokine**
LA	**Large aggregates of pulmonary surfactant**
LB	**Lamellar bodies**
LBP	**Lipopolysaccharide-binding protein**
LDH	**Lactate dehydrogenase**
LPO	**Lipid hydroperoxides**
LPS	**Lipopolysaccharide**
MAP	**Mean arterial pressure**
MCP-1	**Monocyte chemotactic protein-1**
MIP-2	**Macrophage inflammatory protein 2**
MMP-2-9	**Metalloproteinase-2-9**
MSC	**Mesenchymal stem cells**
MV	**Mechanical ventilation**
MVB	**Multivesicular bodies**
NFκB	**Nuclear factor kappa B**
PaO_2	**Partial pressure of arterial oxygen**
$PaCO_2$	**Partial pressure of carbon dioxide**
P_{AW}	**Peak airway pressure**
PAWP	**Pulmonary artery wedge pressure**
PBS	**Phosphate buffered saline**
PC	**Phosphatidyl choline**
PE	**Phosphatidyl ethanolamine**
PEEP	**Positive end-expiratory pressure**
PG	**Phosphatidyl glycerol**

PI	**Phosphatidyl inositol**
Pi3K	**Phosphatidyl inositol-3-kinase**
PIP	**Peak inspiratory pressure**
PL	**Phospholipids**
POPG	**1-Palmitoyl-2-oleoyl-sn-glycero-3-phosphoglycerol**
PS	**Pulmonary surfactant**
PVDF	**Polyvinylidene difluoride**
RDS	**Neonatal respiratory distress syndrome**
RNS	**Reactive nitrogen species**
ROS	**Reactive oxygen species**
SA	**Small aggregates of pulmonary surfactant**
SD	**Sprawley-Dawley**
SDS	**Sodium dodecyl sulfate**
SM	**Sphingomyelin**
SMC	**Smooth muscle cells**
SP-A-B-C-D	**Pulmonary surfactant-associated protein –A-B-C-D**
SSC	**Side scatter**
TCA	**Trichloroacetic acid**
TGF-α-β	**Transforming growth factor-alpha-beta**
Th1	**Type 1 helper T cell**
Th2	**Type 2 helper T cell**
TLR-2-4	**Toll-like receptor -2-4**
TM	**Tubular myelin**
TNF-α	**Tumor necrosis factor-alpha**
VALI	**Ventilator-associated lung injury**
VILI	**Ventilator-induced lung injury**
V_T	**Tidal volume**
γ	**Surface tension**
π	**Pressure**

Table of contents

Resumen

Summary

INTRODUCCIÓN

Aún no se tiene un pleno conocimiento de la patogénesis del síndrome de distrés respiratorio agudo (ARDS) y su forma menos severa, el daño pulmonar agudo (ALI) (2). Sin embargo, actualmente se piensa que estos síndromes comienzan con una respuesta inflamatoria que puede ser inducida por daños extra-pulmonares (sepsis, trauma severo, pancreatitis aguda, etc.) o por alteraciones directas en el pulmón (neumonía, contusión pulmonar, aspiración de ácidos gástricos, etc.) (3). Dicha respuesta inflamatoria puede conllevar alteraciones en la permeabilidad de la barrera alveolo-capilar, provocando edema intra-alveolar (3, 4). Ante este escenario, la alteración del surfactante pulmonar complica aún más la situación (5).

El surfactante pulmonar es un complejo macromolecular esencial para mantener el alveolo abierto y por consiguiente, permitir un adecuado intercambio gaseoso. Sin surfactante, el alveolo colapsaría al no disminuir la tensión superficial de la interfase aire-líquido durante la espiración (1, 6). Por tanto, una de las principales funciones del surfactante pulmonar es establecer una monocapa en la interfase aire-líquido que excluye las moléculas de agua de la interfase y por tanto disminuye la tensión superficial a 1 mN/m en la espiración (1). Para llevar a cabo su función correctamente, el surfactante pulmonar está formado por lípidos (principalmente fosfolípidos) y apolipoproteínas específicas del surfactante, denominadas SP-A, SP-B y SP-C.

El surfactante pulmonar es secretado por los neumocitos tipo II al fluido alveolar en forma de agregados grandes (LA), que generan rápidamente una monocapa estable en la interfase aire-líquido (1). Este proceso se denomina adsorción interfacial del surfactante pulmonar. Después de la adsorción, la monocapa de surfactante está sometida periódicamente a procesos de compresión durante la exhalación y de expansión durante la inhalación. Los procesos de compresión producen cambios en la tensión superficial (γ) de ~23 mN/m a ~1 mN/m para prevenir el colapso alveolar mientras que la inspiración produce la expansión de la monocapa, produciéndose un incremento de γ hasta 20–25 mN/m para mantener la estabilidad alveolar. Como consecuencia de estos ciclos reiterados de compresión/expansión se van generando vesículas no funcionales del surfactante pulmonar, denominadas agregados pequeños (SA). Estas vesículas son capturadas continuamente por los neumocitos tipo II o los macrófagos alveolares.

La alteración o déficit del surfactante pulmonar conlleva edema intra-alveolar, alteración en la *compliance* pulmonar, desajuste de la ventilación-perfusión e hipoxemia (1, 5, 6).

La presencia de una acusada hipoxemia precisa de soporte ventilatorio, cuya utilización ha requerido estudiar los posibles efectos adversos de la ventilación mecánica *per se*, conocido como daño pulmonar agudo inducido por ventilación mecánica (VILI) (7). Actualmente se considera que VILI se genera como consecuencia de volutrauma (distensión pulmonar cuando se somete a presión alveolar alta) y/o atelectrauma (causado por la apertura y el cierre cíclicas del espacio aéreo) (7). Estas alteraciones pueden estimular la respuesta inflamatoria (denominado biotrauma), resultando en daño pulmonar progresivo e inflamación sistémica (7).

Actualmente, el soporte ventilatorio para pacientes con ALI o ARDS consiste en ventilar con bajo volumen corriente (para disminuir el volutrauma) y aplicar una presión positiva al final de la expiración (PEEP) y/o un ratio de FiO_2/PEEP adecuados (para reducir el atelectrauma) (8). El PEEP aumenta la presión del espacio aéreo al final de la espiración. Sin embargo, debido a que las presiones de apertura del espacio aéreo pueden variar notablemente entre pacientes e incluso dependiendo del estado de un mismo paciente, la aplicación de PEEP para revertir o limitar atelectasis dorsal-caudal, casi siempre sucederá a costa de un exceso de distensión de las regiones pulmonares ventrales u otras áreas que tienen presiones inferiores de apertura (9).

Dada la importancia de un correcto manejo de los parámetros ventilatorios para mantener a los pacientes con ARDS y ALI (7, 8), se ha comenzado a estudiar el efecto de la ventilación mecánica en pulmones sanos. Para ello, la utilización de modelos animales expuestos a estrategias ventilatorias convencionales o dañinas es indispensable para conocer mejor los mecanismos que inducen VILI.

En esta tesis, ratas sanas han sido expuestas a las siguientes estrategias ventilatorias (10):

- Ventilación mecánica perjudicial (HV) durante 2.5 h caracterizada por alto volumen corriente (V_T = 25 ml/kg) y ausencia de PEEP ya que nuestro objetivo era provocar alteraciones alveolares causadas por volutrauma, atelectrauma y/o biotrauma.
- Ventilación mecánica convencional (LV) durante 2.5 h caracterizada por volumen corriente moderado (V_T = 9 ml/kg) y aplicación de PEEP (PEEP = 5 cm H_2O), con

el objetivo de simular la estrategia ventilatoria utilizada habitualmente en la unidad de cuidados intensivos.

- Ventilación mecánica convencional prolongada (V_T = 9 ml/kg, y PEEP = 5 cm H_2O).
- Ventilación mecánica convencional prolongada (V_T = 9 ml/kg, y PEEP = 5 cm H_2O) después de 2.5 h de exposición a una estrategia ventilatoria dañina (V_T = 25 ml/kg, y PEEP = 0). Este modelo simula situaciones clínicas en las que los pacientes con alteraciones pulmonares son ventilados con estrategias ventilatorias convencionales.

OBJECTIVOS

El **objetivo principal** de esta tesis fue estudiar los cambios morfológicos y funcionales en pulmones ventilados con estrategias ventilatorias dañinas o convencionales, así como identificar la relación entre la ventilación mecánica agresiva, la inflamación, el edema y la disfunción del surfactante para poder entender los mecanismos implicados en el daño pulmonar agudo inducido por ventilación mecánica (VILI).

En este estudio contestaremos dos preguntas que actualmente están siendo debatidas (9): si los cambios en la composición y funcionalidad del surfactante preceden al comienzo de VILI y si VILI ocurre sólo en aquellos animales que tienen inactivado el surfactante pulmonar.

Esta tesis se compone de **tres capítulos** los cuales evalúan:

- El impacto de estrategias ventilatorias dañinas en el espacio alveolar y concretamente sus efectos sobre la composición, estructura y funcionalidad del surfactante pulmonar. Además se determinaron las causas de la inactivación del surfactante tras la ventilación mecánica lesiva. *(Chapter 1)*.
- Los factores implicados en la resistencia al daño inducido por ventilación mecánica debido a que dichos factores pueden contribuir a desarrollar terapias profilácticas o intervenciones previas a la ventilación. *(Chapter 2)*.
- Las consecuencias de una ventilación mecánica convencional prolongada, con o sin previa exposición a estrategias ventilatorias perjudiciales. Este estudio permitiría determinar si la inflamación en el pulmón esta relacionada con la

duración a la exposición de estrategias ventilatorias convencionales así como dilucidar si dicha estrategia ventilatoria convencional tiene efectos beneficiosos o perjudiciales en aquellos animales previamente expuestos a ventilación mecánica lesiva. *(Chapter 3)*.

RESULTADOS Y CONCLUSIONES

Capítulo 1

El objetivo de este capítulo fue caracterizar los cambios producidos en el espacio alveolar debido a estrategias ventilatorias dañinas. La mayoría de los animales expuestos a ventilación mecánica lesiva desarrollaron daño agudo (VILI) caracterizado por: 1) presión parcial de oxígeno arterial/porcentaje de oxígeno inspirado (PaO_2/FiO_2) < 300 mmHg; 2) evidencias de alteración tisular; 3) aumento de marcadores inflamatorios tales como TNF-α y la actividad de la esfingomielinasa ácida en BAL; 4) contaminación de proteínas plasmáticas en los alvéolos y aumento de los niveles de la proteína carbonilada en BAL, e 5) inactivación del surfactante pulmonar.

Aunque la ventilación con alto volumen corriente estimuló la secreción de surfactante por parte de los neumocitos tipo II, éste fue rápidamente inactivado. La inactivación del surfactante pulmonar puede deberse a la oxidación tanto de sus componentes lipídicos como proteicos debido al estrés oxidativo, a la degradación de los mismos por parte de fosfolipasas y proteasas y a la presencia de inhibidores de las membranas del surfactante que provengan del torrente sanguíneo o bien sean secretados por las células alveolares. En concreto, hemos observado una disminución significativa en los niveles de las proteínas específicas del surfactante SP-A, SP-B y SP-C, así como una disminución en sus niveles de expresión en el tejido pulmonar. Además, hemos encontrado un aumento significativo de lípidos peroxidados en las membranas del surfactante junto con un aumento significativo de la proteína C reactiva (CRP), un inhibidor del surfactante que se inserta en sus membranas alterando sus propiedades biofísicas (1).

Conclusiones del C.1: Este estudio indica que estrategias ventilatorias lesivas producen daño directo en el pulmón, promoviendo la inflamación, el estrés oxidativo y la liberación de diversos factores, que todos juntos están implicados en la inactivación del surfactante. Dicha inactivación conlleva atelectasis manifestada por alteraciones en el intercambio gaseoso y disminución de la complianza dinámica.

Capítulo 2

Durante la realización del anterior estudio, observamos que un pequeño número de animales expuestos a estrategias ventilatorias lesivas no mostraban evidencias de disfunción pulmonar. Por consiguiente, el objetivo de este capítulo fue identificar los factores involucrados en la resistencia al daño pulmonar agudo inducido por ventilación mecánica. Para este propósito, el grupo ventilado con alto volumen corriente y ausencia de PEEP fue dividido en dos grupos según sus valores de presión arterial media (MAP) que se registraba continuamente: 1) animales susceptibles a la ventilación mecánica lesiva (sHV), caracterizados por valores de MAP inferiores a 50 mmHg y una acusada disminución de PaO_2 tras 60 minutos de ventilación: y 2) animales resistentes a la ventilación mecánica lesiva (rHV) los cuales no tenían cambios sustanciales en MAP y PaO_2 tras 60 minutos de ventilación.

El grupo sHV se caracterizó por: 1) PaO_2/FiO_2<200 mmHg; 2) alteraciones histológicas incluyendo presencia de membranas hialinas; 3) Una disminución acusada de macrófagos alveolares; 4) Edema intraalveolar; 5) Aumento de marcadores inflamatorios en BAL (TNF-α, MIP-2, MCP-1, y actividad esfingomielinasa ácida) y en plasma (MIP-2), y 6) Marcadas alteraciones en la composición y funcionalidad del surfactante pulmonar tal y como se describen en el Capítulo 1.

Por el contrario, el grupo rHV presentó una respuesta inflamatoria atenuada en el pulmón, representada por un aumento de los niveles de IL-6 en BAL acompañada de una disminución de TNF-α, MCP-1 y MIP-2, junto con ausencia de actividad esfingomielinasa ácida. La ventilación mecánica estimuló la secreción de surfactante, aislándose surfactante sin alteraciones en su composición ni presencia de peroxidación lipídica. A diferencia del grupo sHV, el surfactante pulmonar de los animales aislados del grupo rHV era capaz de: i) adsorberse y establecer una monocapa estable en la interfase aire-líquido, ii) disminuir la tensión superficiales ~1

mN/m durante la compresión, y iii) re-extenderse durante la expansión. Aunque los animales resistentes a las estrategias ventilatorias lesivas mostraron algunas evidencias de daño tisular, disminución de células alveolares y liberación de citoquinas proinflamatorias en BAL, estos animales no presentaron edema intra-alveolar y una relación PaO_2/FiO_2 normal (450 mm Hg) tras 2.5 h de ventilación.

Conclusiones del C.2: Estos resultados indican que VILI se genera solo en aquellos animales donde el surfactante pulmonar se encuentra inactivado y que hay una clara relación entre una pronunciada respuesta pro-inflamatoria y la inactivación del surfactante pulmonar. Además, estos resultados muestran que una respuesta inflamatoria atenuada junto con un aumento de la secreción endógena de surfactante activo protegen del desarrollo de edema intra-alveolar e hipoxia, sucesos típicos de animales ventilados con estrategias ventilatorias lesivas.

Capítulo 3

El objetivo de este capítulo fue dilucidar el efecto de estrategias ventilatorias convencionales prolongadas en animales previamente expuestos o no a estrategias ventilatorias lesivas.

Se determinó que los individuos expuestos por un periodo de tiempo prolongado a una ventilación mecánica convencional mostraban un aumento de infiltración neutrofílica y de liberación de citoquinas proinflamatorias en el espacio alveolar (IL-6 yMIP-2 pero no TNF-α) y en plasma (IL-6). Sin embargo, la respuesta inflamatoria no fue lo suficientemente dañina como para producir daños histológicos, alteraciones en el surfactante y disfunción pulmonar.

Por otro lado, se observó que la ventilación convencional prolongada tras ventilar los animales con una estrategía ventilatoria lesiva tiene efectos nocivos en aquellos animales que sobreviven a dicha estrategia ventilatoria r(HV+LV). Los animales mostraron edema intra-alveolar, infiltración de neutrófilos, aumento de MIP-2 en BAL y en plasma así como ligeras alteraciones en el intercambio gaseoso mientras que el surfactante pulmonar no mostraba alteraciones. Estos datos indican que las alteraciones en el espacio alveolar pueden sucederse sin alteraciones en el surfactante pulmonar. Además, estos datos apoyan nuestra conclusión de que VILI se presenta sólo en aquellos animales cuyo surfactante se encuentra inactivado, puesto

que estos animales no desarrollan VILI. Es más, un pequeño número de animales no sobrevivió a todo el proceso ventilatorio s(HV+LV) y presentó una respuesta inflamatoria exacerbada, edema intra-alveolar, evidencias de alteraciones histológicas, alteración en la composición y funcionalidad del surfactante y por consiguiente una disminución significativa de la oxigenación arterial (PaO_2/FiO_2< 200 mmHg).

Conclusiones del C.3: Estos resultados indican que: 1) la inflamación en el pulmón está directamente relacionada con la duración de la estrategia ventilatoria convencional; 2) Que una adecuado funcionamiento del surfactante pulmonar es esencial para la supervivencia de aquellas ratas expuestas a estrategias ventilatorias lesivas y/o ventilación mecánica prolongada bajo estrategias no dañinas; y 3) Los cambios en la composición y funcionalidad del surfactante pulmonar no preceden al inicio del daño pulmonar agudo inducido por ventilación mecánica (VILI).

INTRODUCTION

The pathogenesis of acute respiratory distress syndrome (ARDS) and the less severe condition known as acute lung injury (ALI) (2) is still not fully understood. However, it is currently thought to begin with an inflammatory response induced by extrapulmonary injury (sepsis, severe trauma, acute pancreatitis, etc.) or direct pulmonary injury (pneumonia, aspiration of gastric contents, pulmonary contusion, etc.) (3). The inflammatory response increases alveolar epithelial and pulmonary vascular endothelial permeability, causing alveolar filling (3, 4). The alteration of the pulmonary surfactant system complicates the clinical picture (5).

Surfactant is necessary to keep the alveolus open, thereby allowing gas exchange. Without surfactant the alveoli collapse since the surface tension at the air–water interface exerts a collapsing pressure (1, 6). Thus, one of the main lung surfactant functions is to form a stable lipid monolayer at the air–liquid interface that excludes water molecules from the interface and effectively lowers surface tension to 1mN/m on expiration (1). To fulfill this function, the surfactant extracellular membranes are composed of lipids (mainly phospholipids) and three surfactant apolipoproteins (SP-A, SP-B, and SP-C). After surfactant secretion by epithelial type II cells, the secreted, tightly packed surfactant membranes (known as large surfactant aggregates [LA]) rapidly transfer surface-active material to the air-liquid interface, forming the surfactant monolayer (1). This process is known as interfacial adsorption of surfactant. After adsorption, the surfactant film is periodically compressed during exhalation and expanded during inhalation. Compression involves changes in surface tension (γ) from~23 mN/m to ~1 mN/m to prevent alveolar collapse, whereas film expansion increases γ to a maximum of 20–25 mN/m to maintain alveolar stability. With repetitive surface compression and expansion cycles, small surfactant vesicles with poor surface activity (known as small surfactant aggregates [SA]) are generated. They are taken up continuously by alveolar macrophages and epithelial cells. Deficit or alteration of lung surfactant leads to intraalveolar edema, impaired lung compliance, ventilation-perfusion mismatch (including shunt flow due to altered gas flow distribution), and hypoxemia (1, 5, 6).

Critical hypoxemia results in the need for mechanical ventilation, thereby providing the context in which ventilator-induced lung injury (VILI) can develop (7). It is thought that VILI is generated as a result of volutrauma (intensified tissue

tensions at the junctions of closed and open alveolar units when subjected to high alveolar pressure) and/or atelectrauma (caused by the cyclical airspace opening and closing) (7). These stresses might further stimulate the inflammatory response (termed biotrauma) resulting in progressive lung injury and systemic inflammation (7).

The current respiratory support in ALI or ARDS consists of low tidal volume (to reduce volutrauma) and appropriate positive end-expiratory pressure (PEEP) and/or FiO2/PEEP ratio (to reduce atectrauma) (8).

The application of PEEP is thought to be useful in counteracting increased surface tension (thereby reversing the resulting atelectasis). PEEP increases end-expiratory airspace pressure, but since airspace opening pressures can vary markedly between and within patients, applying PEEP to reverse or limit dorsal-caudal atelectasis will almost always come at the expense of over-distending ventral lung regions and other areas having lower opening pressures (9).

Given the importance of ventilatory management for acute respiratory syndrome (ARDS or ALI) (7, 8), investigators have started to explore the effects of ventilation in healthy lungs. Animal models exposed to conventional and injurious ventilator strategies are being used to understand the mechanisms of lung injury induced by mechanical ventilation.

In this thesis, healthy rats have been exposed to the following ventilator strategies (10):

- Injurious high-stretch ventilation (HV) during 2.5 h, with high tidal volumes (V_T = 25 ml/kg) and without PEEP application since our aim was to provoke alveolar alterations caused by volutrauma, atelectrauma, and/or biotrauma.
- Conventional low-stretch ventilation (LV) during 2.5 h, with moderated tidal volume (V_T = 9 ml/kg) and application of positive end-expiratory pressure (PEEP = 5 cm H_2O), to emulate a ventilator strategy widely used in critical care units.
- Prolonged conventional low-stretch ventilation (V_T = 9 ml/kg, and PEEP = 5 cm H_2O).
- Prolonged low-stretch ventilation (V_T = 9 ml/kg, and PEEP = 5 cm H_2O) after 2.5 h exposition to high-stretch ventilation (V_T = 25 ml/kg, and PEEP = 0). This condition simulates clinical situations in which patients with pulmonary alterations are subjected to conventional mechanical ventilation.

OBJECTIVE

The **main objective** of this thesis was to study morphological and functional changes in the lungs after exposition to injurious or conventional mechanical ventilation and to identify the relationship among high-stretch ventilation, inflammation, edema, and surfactant dysfunction in order to understand the mechanisms involved in ventilator-induced lung injury (VILI). Two important questions, currently under debate (9), will be answered in this study: whether changes in surfactant composition and in surface tension precede the onset of VILI, and whether VILI occurs only in animal models when lung surfactant is inactivated.

The thesis is composed of **three chapters,** which evaluate:

- The impact of high-stretch ventilation in the alveolar space and in particular its effects on the composition, structure, and functional activity of lung surfactant. The causes of surfactant inactivation after high-stretch ventilation were assessed *(Chapter 1)*.
- Factors involved in resistance to ventilator-induced lung injury, since identification of such factors may help to develop prophylactic therapies or early interventions prior to exposition to mechanical ventilation *(Chapter 2)*.
- Consequences of prolonged conventional low-stretch ventilation, with or without previous exposition to injurious high-stretch ventilation. This would allow determination of whether inflammation in the lung was directly related to the duration of conventional low-stretch ventilation and whether prolonged conventional low-stretch ventilation has beneficial or damaging effects in surviving rats exposed to injurious high-stretch ventilation *(Chapter 3)*.

RESULTS & CONCLUSIONS

Chapter 1

The aim of this chapter was to characterize changes produced in the alveolar compartment due to injurious high-stretch mechanical ventilation. Most of the animals exposed to injurious high-stretch ventilation developed lung injury (VILI), which was characterized by 1) arterial oxygen tension/inspiratory oxygen fraction (PaO_2/FiO_2) < 300 mmHg; 2) histological evidence of tissue injury; 3) increase of inflammatory markers such as TNF-α and acidic sphingomyelinase activity in BAL; 4) leakage of plasma proteins into the alveoli and increased levels of protein carbonyls in BAL, and 5) loss of surfactant biophysical function.

Even though high-stretch ventilation stimulated surfactant secretion by type II cells, surfactant is rapidly inactivated. Surfactant inactivation can rise from protein and lipid oxidation as a consequence of oxidative stress, degradation of surfactant lipids and proteins by phospholipases and proteases, and incorporation of inhibitors in surfactant membranes leaked from capillaries or secreted by alveolar cells. Specifically, we found a marked decrease in levels of surfactant apolipoproteins (SP-A, SP-B, and SP-C) and reduced expression of these proteins by lung tissue, increased levels of lipid peroxides in surfactant membranes, and increased levels of surfactant inhibitors such as C reactive protein (CRP) that insert into surfactant membranes and critically affect surfactant physical properties (1).

Ch.1 conclusions: This study indicates that injurious high-stretch ventilation produces direct damage tothe lung, promoting inflammation, oxidative stress, and release of factors that together inactivate lung surfactant. Surfactant impairment leads to atelectasis as manifested by impaired gas exchange and decrease in dynamic compliance.

Chapter 2

During the previous study we realized that a number of animals subjected to high-stretch ventilation did not show evidence of physiological lung dysfunction. Hence, the aim of this chapter was to identify factors involved in the resistance to ventilator-induced lung injury. To this end, the high-stretch ventilated group (HV) was subdivided in two groups according to the mean arterial pressure (MAP) value, which was continuously monitored: **1) animals susceptible to high-stretch ventilation (sHV)**, showing MAP values lower than 50 mmHg and a substantial PaO_2 reduction at 60 min of ventilation; and **2) animals resistant to high-stretch ventilation (rHV)**, with insignificant MAP and PaO_2 changes at 60 min. Lung tissue, plasma, bronchoalveolar fluid (BAL), and lung surfactant were analyzed.

The sHV group was characterized by: 1) PaO_2/FiO_2<200 mmHg; 2) histological evidence of tissue injury with hyaline membrane formation; 3) prominent decrease of alveolar macrophages; 4) intraalveolar edema; 5) increase of inflammatory markers in BAL (TNF-α, MIP-2, MCP-1, and acidic sphingomyelinase activity) and in plasma (MIP-2); and 6) pronounced changes in the composition and function of lung surfactant as reported in Chapter 1. In contrast, the rHV group was distinguished by an attenuated lung inflammatory response, evidenced by increased levels of IL-6 in BAL but reduced levels of TNF-α, MCP-1, and MIP-2 and absence of acidic sphingomyelinase activity. High-stretch ventilation stimulated surfactant secretion, and high amounts of fully active surfactant with normal protein and lipid composition and absence of lipid peroxides were isolated from the lungs. Contrary to surfactant isolated from lungs of the sHV group, surfactant from the rHV group was able to: i) adsorb onto an air/water interface, ii) lower surface tension to values near 1mN/m upon compression, and iii) re-spread during expansion. Even though animals resistant to high-stretch ventilation showed evidence of some tissue injury, decrease in alveolar macrophages, and release of proinflammatory cytokines in the alveolar fluid, these animals did not exhibit plasma protein leakage into the alveolar space and showed normal PaO_2/FiO_2 (450 mm Hg) after 2.5 h of ventilation.

Ch.2 conclusions: These results clearly indicated that VILI occurred only in animal models when surfactant was inactivated and that there is a direct link between pronounced proinflammatory response and surfactant inactivation. In addition, these

results show that an attenuated inflammatory response together with increasing endogenous, fully active, surfactant pools protect against the hypoxia and protein leakage that usually occur when ventilating animals with large V_T and no PEEP.

Chapter 3

The aim of this chapter was to elucidate the effect of prolonged conventional low-stretch ventilation, with or without previous exposition to injurious high-stretch ventilation. We found that animals subjected to prolonged conventional mechanical ventilation showed neutrophils infiltration and increase of proinflammatory cytokines in the alveolar space (IL-6 and MIP-2 but not TNF-α) and plasma (IL-6). However, the inflammatory response was not damaging enough to show histological evidence of tissue injury, pulmonary surfactant alteration, and evidence of physiological lung dysfunction.

On the other hand, we found that prolonged conventional low-stretch ventilation has damaging effects in surviving rats previously exposed to injurious high-stretch ventilation (rHV+LV). Animals showed intra-alveolar edema together with neutrophils infiltration, increase of MIP-2 in BAL and plasma, and slight alterations in gas exchange, whereas pulmonary surfactant showed no evidence of impairment. These studies indicate that alveolar damage can occur without parallel surfactant damage. These animals were resistant to VILI and confirm our previous conclusion that VILI occurred only in animal models when surfactant was inactivated.

Moreover, few animals did not survive the whole mechanical ventilation process s(HV+LV) and exhibited exacerbated inflammatory response, edema, histological evidence of tissue injury, alterations in the composition and function of pulmonary surfactant, and consequently, significant decrease of arterial oxygenation (PaO_2/FiO_2< 200 mmHg).

Ch.3 conclusions: These results indicated that: 1) inflammation in the lung was directly related to the duration of conventional low-stretch ventilation; 2) proper functioning of pulmonary surfactant is essential for survival of rats exposed to injurious and/or prolonged non-injurious mechanical ventilation, and 3) changes in surfactant composition and function do not precede the onset of acute lung injury induced by mechanical ventilation.

Introduction

1. Respiratory system

Respiration defines the process by which gas exchange occurs between and organism and its surrounding environment.

Specifically, the respiratory system supplies the body with adequate oxygen for aerobic metabolism and removes its major waste product, carbon dioxide. To accomplish these features, the respiratory system must provide two physiological functions: (I) ventilation, the process by which ambient air is delivered to the alveoli which are closely related to blood, and (II) gases exchange diffusion, defined as the movement of oxygen and carbon dioxide in opposite directions across the alveoli and capillary walls (11).

The respiratory system is divided into two sections according to these functions: Upper Respiratory Tract and the Lower Respiratory Tract.

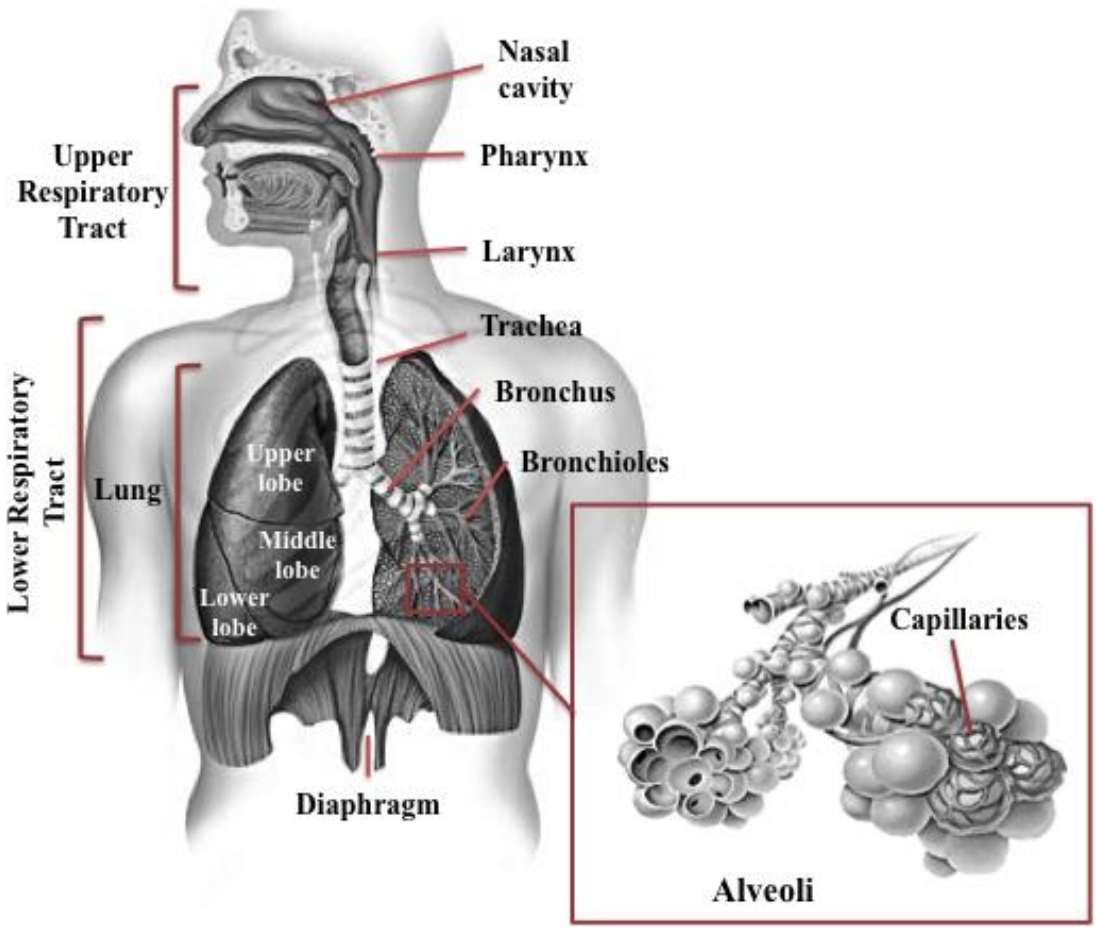

Figure 1. Respiratory System diagram.

Upper Respiratory Tract included the Nasal cavity, Pharynx, and the Larynx. Its primary function is to receive the air from the external environment and filter, warm, and humidify it before it reaches the alveoli where gas exchange will occur (12).

The Lower Respiratory Tract is conformed by the tracheo-bronchial tree and the lungs, both residing in the thoracic cavity. The airway is divided 23 times from the trachea to the alveoli sacs, conforming an airway ramification comprised by the bronchi and the smaller airways called bronchioles (13). Each bronchiole ends in an elongated space enclosed by many air sacs called alveoli, which are surrounded by blood capillaries. Therefore, the branching anatomic structure is ideal for maximizing surface area to allow optimal gas diffusion or movement of gases across the alveoli. In fact, there are 300 million of alveoli in a human (12).

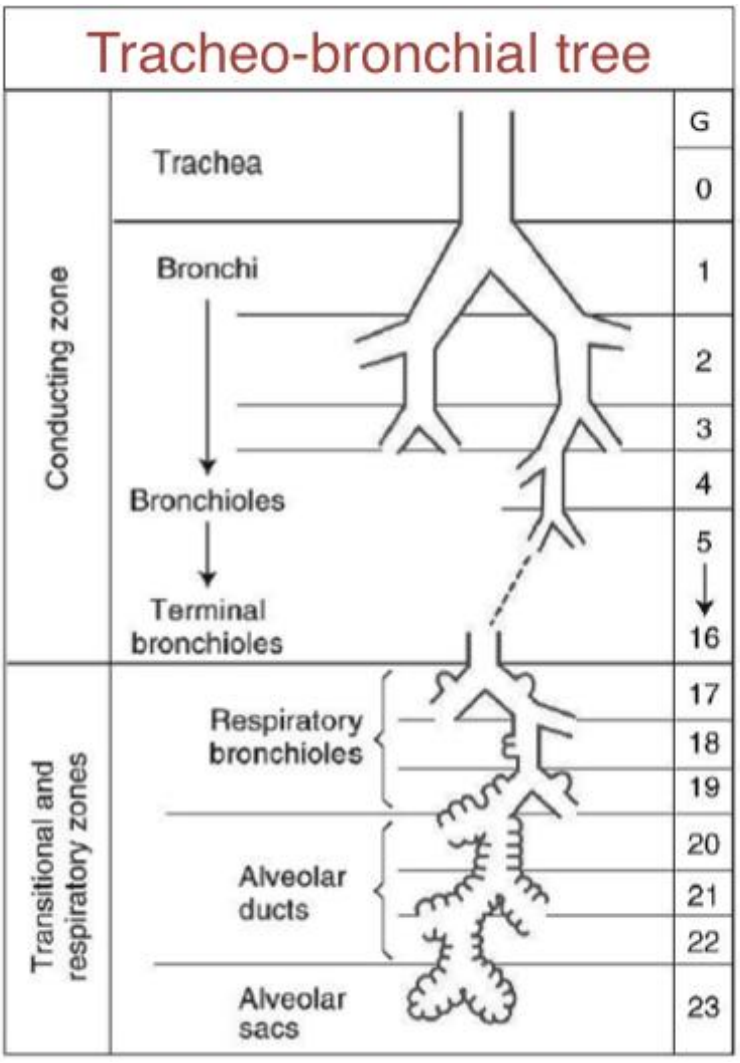

Figure 2. Tracheo-bronchial tree diagram. Schematic representation of human airways that depicts branching generations (G) beginning at the trachea (0) and ending at the alveolar sacs (23). (Modified from reference [13]).

2. Alveolar-capillary unit

The alveolar-capillary unit is highly specialized to maximize diffusion between the blood and air gases. This alveolar-capillary structure is the most extensive in the body. Specifically, the internal surface area of the adult lung is 70 to 80 m^2, of which 90% covers the pulmonary capillaries; thus the air-blood surface available for gas exchange is 60 to 70 m^2 (14).

The alveolar-capillary unit is comprised of three major constituents: pulmonary capillary endothelium, a mixture of cellular and extracellular interstitial components and the epithelial lining of the alveolus composed by epithelial lining cells and a thin layer of liquid covering the epithelial cells containing alveolar macrophages and covered by pulmonary surfactant (15).

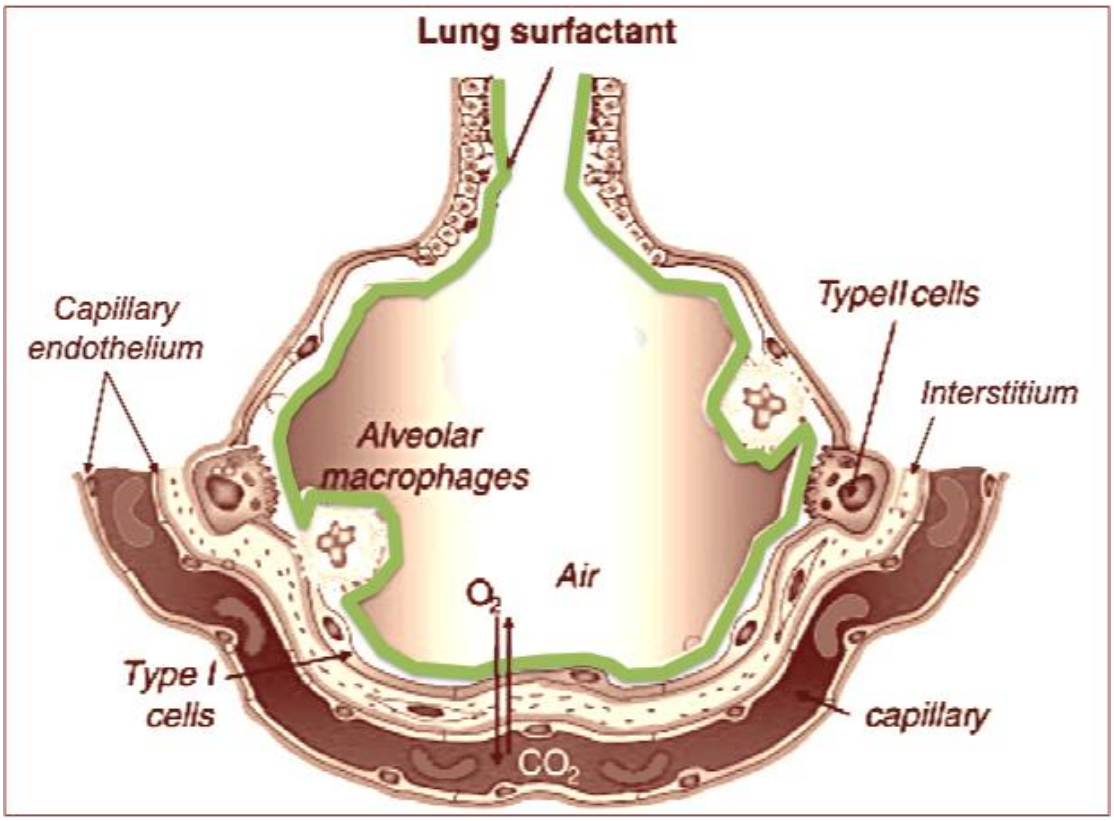

Figure 3. Schematic representation of the main parts comprising the alveolar-capillary unit. (Modified from reference (1)).

2.1. Pulmonary endothelium

The lung microvascular bed is the major collection of endothelial cells in the human body (13). Alveolar capillary endothelial cells are large attenuated cells adapted to facilitate efficient was exchange (13, 15), joined by tight junctions forming a continuous, non-fenestratred, monolayer. Their luminal surface is in contact with blood whereas their the abluminal surface rests on the endothelial basement membrane containing type IV collagen in the lamina densa providing strength to withstand rise in capillary pressure with exercise (15).

Ultrastructurally, endothelial cells had their nuclei usually oriented in the direction of blood flow, lesser presence of intracellular organelles than other cell types but a large number of plasmalemmal transport vesicles probably due to its role in the transport of macromolecules (16).

In addition to its structural role as part of the alveolar-capillary membrane, maintaining its integrity (17), pulmonary endothelium cells participate in the regulation of blood flow, coagulation and fibrinolysis (18, 19). In fact, these cells contribute to the regulation of pulmonary vascular tone by secretion of lipid mediators or maintaining nitric oxide homeostasis (20). Furthermore, endothelium cells participate in inflammatory reactions by its activation, facilitating leukocyte migration from the blood into the alveolar airspace (21). Endothelial cells activation includes changes in chemokine production and an increased of adhesion molecules expression on the luminal surface of these cells in response to stimuli such as injury or infection, leading to a dramatic increased of leukocytes migration (19).

Therefore, pulmonary endothelium possesses metabolic, structural, and immunological functions that might be deregulated during injury.

2.2. Pulmonary interstitium

The thinness and hydration state of the interstitial layer between the alveolus and the endothelial cells is critical for a proper gas exchange. The pulmonary interstitium comprises the extracellular matrix (ECM) and mesenchymal and immune cells such as fibroblasts or interstitial macrophages. ECM is conformed by the interstitial connective tissue and the basement membranes (BM) (22).

Alveolar interstitial connective tissue is mainly comprised by types I collagen, type III collagen and fibronectin (22, 23).

On the other hand, basement membranes are condensed sheet-like structures separating endothelial and epithelial cells from interstitial connective tissue.

In both rat and human lungs, the alveolar epithelial BM and alveolar capillary BM have been shown to consist of highly cross-linked type IV collagen, laminin and fibronectin (22, 23). This composition is thought to play a significant role in preserving normal alveolar structure and function. Specifically, fibronectin is believed to be involved in epithelial cell regeneration (24). Furthermore, a comparison of the level and distribution of fibronectin expression in normal and fibrotic lungs supports the hypothesis that fibronectin plays an important role in alveolar epithelial cell repair (25).

Interestingly, the rat lung had two different interstitium morphologies according to the thickness between the epithelium and the endothelium, suggesting a modulator role of alveolar epithelial cell phenotype (26, 27). Specifically, it exist a thing area where capillary endothelium and alveolar epithelium are separated by only a single fused alveolar and capillary basement membrane, and thick areas, where endothelium and epithelium are separated by their respective basement membranes and connective tissue of the interstitial space (28).

Also, interstitial macrophages are quite prominent in the lung, constituting approximately 40% of total macrophages in tissue (29). Due to their direct contact with matrix and other pulmonary connective-tissue components, it is thought that the release of mediators or enzymes by interstitial macrophages may have greater effects than those released by macrophages in the alveolar compartment (30).

2.3. Pulmonary epithelium

The alveolar epithelium is comprised of two morphologically distinct epithelial cell types, the alveolar type I (ATI) and type II cells (ATII) (31), that are continuously lined among terminal air spaces forming a barrier that is anatomically 1-cell thick (32). Consequently, ATI and ATII cells form a tight barrier, which effectively separates the alveolar air space from the vascular and interstitial spaces. However, alveolar epithelium is an order of magnitude less permeable to small solutes than the capillary endothelium (33). Thus, injury to the pulmonary epithelium increases susceptibility to alveolar flooding (34).

Interestingly, morphometric studies have demonstrated that the distribution and morphology of these cell types is remarkably analogous among mammalian species including rat and human (35).

2.3.1. Alveolar epithelial type I (ATI) cells

ATI cells comprise only ~8-9% of the parenchymal cell population within the lung, but cover ~95% of the alveolar surface (35, 36).

Morphologically, ATI cells are large squamous epithelial cells with widely spread cytoplasmic extensions, small nucleus, few small mitochondria and inconspicuous endoplasmic reticulum (ER) and Golgi apparatus (37). This morphological adaptation provides a short diffusion path for gas exchange (36). ATI cells are not metabolically active and are considered to be “inert” cells, mainly providing a barrier function. However, there is accumulating evidence that ATI cells contribute in active ion transport as well as are critical in maintaining alveolar fluid balance and resolving air space edema (38).

2.3.2. Alveolar epithelial type II (ATII) cells

ATII cells comprise ~15% of lung parenchymal cells, but cover only ~3-5% of the alveolar surface (35, 36). Typically located in the corners of alveoli, ATII cells are cuboidal in shape, with apical *microvilli* and characteristic surfactant-containing organelles known as lamellar bodies (35, 39). Known functions of ATII cells include the synthesis, secretion and recycling of pulmonary surfactant (40), regulation of alveolar fluid and electrolyte balance (41), host defense and immunomodulation (40). In addition to their synthetic and secretory capacities, ATII cells function as the stem cell of the alveolar epithelium and have a central role in alveolar epithelial repair (42).

2.4. Pulmonary surfactant

As previously described, the alveolar epithelial cell surface is lined with a thin fluid layer, denominated the alveolar lining layer, which is covered by a film of pulmonary surfactant (PS) (15).

PS is a surface-active lipoprotein complex. The main function of PS film is to stabilize the alveoli by the reduction of surface tension at the air-liquid interface, preventing the alveolar collapse during end-exhalation (43). In addition, PS possesses non-surface tension related functions such as host defense and pathogen barrier functions, which makes PS physiologically essential (6).

Deficiency or dysfunction of PS causes severe respiratory diseases (6). Specifically, the first pathology associated with PS alterations was the Neonatal Respiratory Distress Syndrome (RDS) in the late 50s (44). This syndrome is originated by an immaturity of the epithelium to synthesize and secrete a sufficient amount of PS due to prematurity (45). Conversely, accumulation of PS in the alveolar airspaces, as in pulmonary alveolar proteinosis, can be deleterious leading to gas exchange impairment (46).

In addition, qualitative alterations of PS have been also involved in other pathologies such as Acute lung injury (ALI) and its severe form, Acute Respiratory Distress Syndrome (ARDS) (6, 46). These pathologies displays symptoms similar to RDS but they can affect patients from any age, having mortality rates of ~30-40% (3, 47).

Therefore, research in PS biology in the past three decades leaded to open new lines of study focused on the development of potential surfactant replacement therapies (46). Hence, the study of PS has both physiological and clinical relevance.

2.4.1. Composition

Comparative biological studies suggest that PS exist in all air-breathing vertebrates but with slightly composition differences (6, 48). However, PS composition in mammals is outstandingly similar among species, i.e., approximately 90% lipids and 10% proteins by weight (wt.) (6, 49).

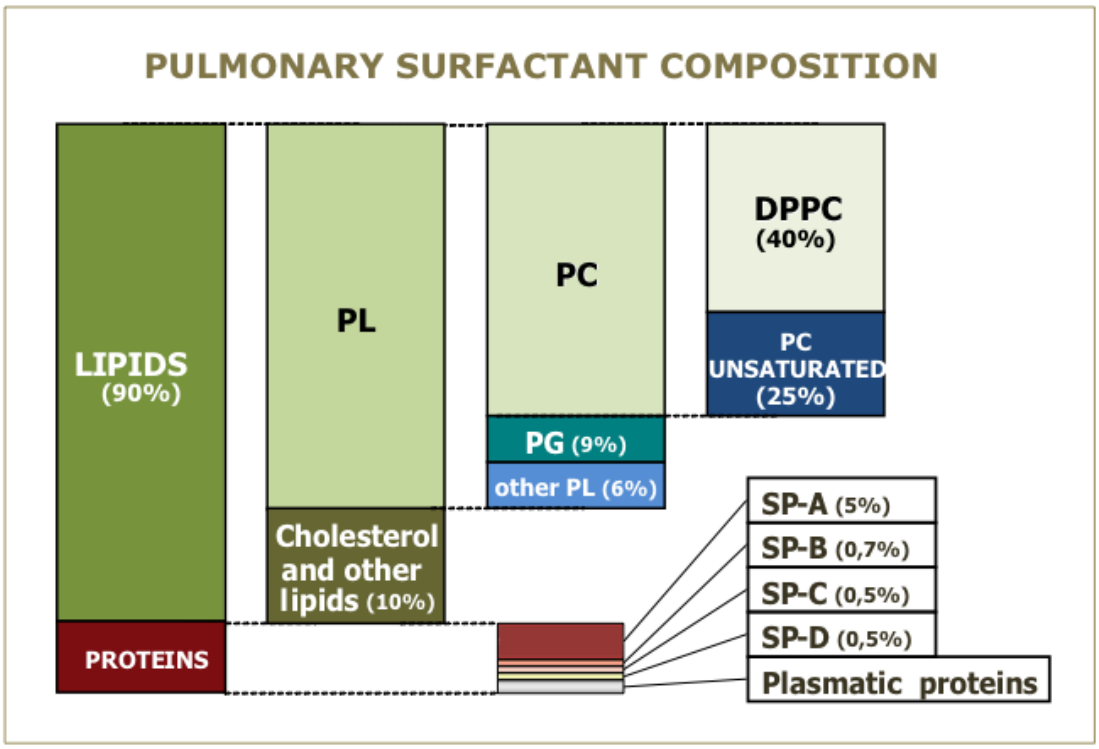

Figure 4. Pulmonary Surfactant composition diagram. PL: phospholipids; PC: phosphatidylcholine; PG: phosphatidylglycerol; DPPC: dipalmitoylphosphatidylcholine; SP-A, SP-B, SP-C and SP-D: pulmonary surfactant protein (SP) -A, -B, -C, -D.

2.4.1.1. Lipid composition

The lipids consist mainly of phospholipids (PL, ~90–95% wt.) with asmall amount of neutral lipids (~5–10% wt.), primarily cholesterol (6, 50).

Interestingly, the most prevalent class of PL in PS is phosphatidylcholine (PC), which accounts for ~80% of the total PL from most mammalian species. PC may have either saturated or unsaturated acyl chains, whose length and saturation have an impact on the fluidity of the lipid (51).

Although notable exceptions exist (52), in most cases ~40% of the PC is dipalmitoylphosphatidyl choline (DPPC) (16:0/16:0 PC) (6). DPPC is a long-chained, disaturated and zwitterionic (i.e. carry no net electrical charge) PL, mainly responsible for reducing surface tension (γ) values to near-zero values upon film compression. Despite its high capacity to reduce surface tension, DPPC does not adsorb or re-spread to the surface quickly enough *in vivo*. At 37ºC, DPPC typically exists in a gel phase, i.e., with its acyl chains in a rigid close-packed arrangement

allowing to form a condensed monolayer upon compression and resisting high surface pressures (50).

In contrast, unsaturated lipids at 37ºC exist in a liquid crystalline phase and cannot form a condensed monolayer in a highly compressed state. These lipids are more fluid-like because of the double bond. Therefore, the presence of unsaturated lipids in PS helps in fluidizing and re-spreading DPPC and other saturated lipids (51).

Other PL classes that are also present in lung surfactants but in minor proportion, include phosphatidylethanolamine (PE), phosphatidylglycerol (PG), phosphatidylinositol (PI), phosphatidylserine (PS) and sphingomyeline (SM). These lipids also help in the adsorption and re-spreading of DPPC. At physiological pH, PC PE or SM are zwitterionic, while PG, PI and PS are anionic or negatively charged (6). Anionic PL as a group accounts for ~15%of the total PL and have been shown to interact with the cationic surfactant protein B and C, being critical for the proper functioning of PS at the air/alveolar liquid interface (53).

Finally, neutral lipids constitute 10% wt. of the PS with cholesterol accounting for approximately 80-90% wt. Its main function resides in its ability to maintain the balance between fluidic and rigid lipid phases in PS (51).

2.4.1.2. Protein composition

Besides the aforementioned lipidic components, four surfactant proteins (SPs) are also present in PS. They are named pulmonary surfactant protein (SP)-A, -B, -C and -D, based on the nomenclature proposed by Possmayer (54).

Interestingly, SPs can be separated in two groups according to their role accomplished in the PS system as active inhibitors of a broad spectrum of foreign pathogens or as regulators of the interfacial surface tension (55).

Hence, the first group are large hydrophilic SPs, SP-A and -D, are members of a family of collagenous carbohydrate binding proteins, known as collectins, or calcium-dependent (C-type) lectins. Collectins consist of oligomers of trimeric subunits, which are able to recognize, inhibit and inactivate a wide range of foreign pathogens (55). Conversely, the small molecular weight hydrophobic SPs, SP-B and-C, are tightly associated with PS film at the air–liquid interface contributing to regulate the structure, integrity and composition of the surface lipid film (6, 55-57).

Among these PS-associated proteins, SP-A is the most abundant by mass (but not by molar ratio), accounting for ~5% wt. of PS, with SP-D, accounting for ~0.5% and SP-B and SP-C constituting together approximately~1-1.5% (58).

Collectins

SP-A

SP-A (630 kDa) is a large multimerichydrophilic glycoprotein consisting of 18 subunits, each weighing 28-36 kDa conformed by four structural domains (59):

(I) N-terminal segment involved in intermolecular disulfide bond formed by 7–10 amino acids.

(II) Collagen-like domain formed by 79 residues characterized by 23 Gly-X-Y repeats with an interruption near the midpoint of the domain of Pro-Cys-Pro sequence that is responsible for the formation of SP-A characteristic supra-quaternary structure (59, 60). The collagen-like domain of mammalian SP-A functions as scaffolding that amplifies the ligand binding activities of globular domains. Moreover, collagen-like domain is responsible for the binding of SP-A to some receptors on the surface of alveolar macrophages and epithelial cells (61).

(III) Neck region located between the collagen and the globular domain conformed by a 35 amino acid segment with high α-helical propensity.

(IV) C-terminal globular domain composed by 115 residues, including four conserved cysteins that form two intra-molecular disulfide loops and 18 highly conserved amino acid residues common to C-type leptines. The basic structure of the globular domain consists of a structural core conformed of α–helical and β–strands (59). This conformational shift enhances lipid binding and allows Ca^{2+}-dependent binding of oligosaccharides, protein self-association and SP-A-mediated lipid aggregation (59, 61, 62).

The human SP-A locus consists of two similar but non-identical genes, SP-A1 and SP-A2, each approximately 5 kb in length and a truncated and nonfunctional pseudogene that shares 85% similarity with the SP-A 3´ untranslated region (63); however in other mammals such as rats (64) there is a single-copy gene.

The human SP-A locus has been assigned to chromosome 10q22-q23 near the loci for SP-D and MBP, suggesting that this area of chromosome 10 is involved in the evolution of collagenous C-type lectins (63). Recently, it has been found that SP-A1 and SP-A2 are in linkage disequilibrium, indicating close physical association. In fact, it has been detected opposite transcriptional orientation suggesting that both genes might share cis-acting regulatory elements (65). Indeed, it is thought that both gene products are expressed in a 2:1 ratio (SP-A1:SP-A2) and associated through their collagenous domains to form heterotrimers (66).

SP-A is modified after translation in the ER and Golgi (cleavage of the signal peptide, proline hydroxylation, and N-linked glycosylation) and assembled into a complex oligomeric structure that resembles a flower bouquet (59, 61, 62). SP-A assembly is an intracellular process that can be conceptualized in two parts: the folding of monomeric subunits into trimers (Figure 5a) and the association of six trimers into an octadecamer (59) (Figure 5b). Interestingly, mammalian SP-A is not only assembled in supratrimeric oligomers but also forms multimers by self-association of the protein in the presence of Ca^{2+}.

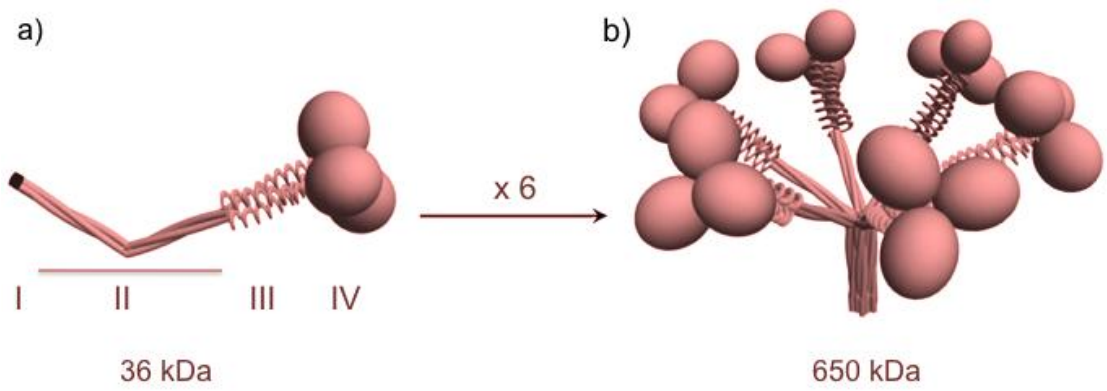

Figure 5. Models of trimeric (a) and oligomeric (b) forms of SP-A. All human SP-A structural domains are depicted: I) NH_2-terminal segment; II) collagen-like domain with a sequence irregularity, which divides the collagen-like domain in two parts; III) neck region; and IV) COOH-terminal globular domain. (Figure modified from reference [55])

Supratrimeric oligomerization and multimerization of mammalian SP-A seems to be needed for many of its functions, such as host defense and immunosuppressive SP-A high-affinity binding capabilities (to lipids, carbohydrate-bearing surfaces, and proteins) (59).

SP-A participates in alveolar innate immune defense, together with SP-D and other proteins and peptides, by direct killing of microorganisms or by indirect killing through enhancing the uptake of pathogens by phagocytes (55).

SP-A can bind to some micro-organisms such as Gram negative bacteria (67), that may lead to either bacterial killing and/or bacterial aggregation. Bacterial aggregation facilitates phagocytosis mediated by the collagen tails of SP-A, initiating a proinflammatory response (61). As well, SP-A contributes to phagocytosis of some virus like respiratory syncytial virus, influenza virus A or herpes simplex virus type 1 (68-70).

Also, SP-A binding to receptors results in an antiinflammatory response (71, 72) and prevents the persistence of inflammation, which is detrimental to the lung. For example, SP-A regulates signaling pathways in macrophages in response to microbial recognition that controls inflammation like toll-like receptor-2 (TLR-2) signaling pathway (73). As well, SP-A binds to various receptors of ATII cells including P63 (74) and SPAR (75), to activate the phosphatidylinositol 3-kinase (PI3K) pathway triggering in last term the expression of pro-inflammatory genes (75).

Finally, SP-A is mainly associated with PS and has some properties related to its ability to bind and aggregate PS membranes:

(I) Together with SP-B, contributes to the formation of tubular myelin.

(II) Improves the rate of surfactant adsorption to an air–liquid interface.

(III) Protects PS membranes against inactivation by transudated serum proteins (59, 62).

SP-D

As SP-A, SP-D (520 kDa) is also a member of the family commonly known as collectins that are involved in the first line of defense against fungal, bacterial, and viral infections (76).

SP-D as other collectins is assembled as oligomers of trimeric subunits, specifically formed a cruciform structure in which four homotrimeric subunits self-associate at their N-termini to form highly ordered SP-D dodecamers (Figure 6b).

Each subunit (43 kDa) consists of four regions (Figure 6a): (I) a short N-terminal non-collagen sequence; (II) a very long collagen domain of 59 Gly-X-Y repeats; (III)

ashort linking domain, the ‘neck’ region that connects the collagen domain to the fourth region; and (IV) C-terminal carbohydrate recognition domain (CRD) (55).

Some studies suggested that folding of the CRD, trimerization of monomers, triple helix formation, the amino-terminal association of trimeric subunits and the formation of inter-chain disulfide cross-links occur in the rough ER whereas oligosaccharide maturation occurs in the Golgi immediately prior to secretion (77).

As previously described, SP-D gene have been localized in the region of 10q22.2–23.1 close to SP-A (63, 76). Conversely, a single gene encodes human SP-D. However, protein, cDNA, and genomic sequencing together suggest the existence of a number of SP-D alleles, some of which are characterized by amino-acid substitutions in the coding region. Therefore, the SP-D gene encodes at least one, and probably two, untranslatedexons at the5´-end of the gene, similar to SP-A (76).

SP-D plays complex role in innate immunity in the alveolus by decreasing inflammation and promoting clearance of pathogens from the respiratory tract without stimulating a secondary immune response. The functions of SP-D have been investigated at different levels according to the interaction between effector cells and pathogens.

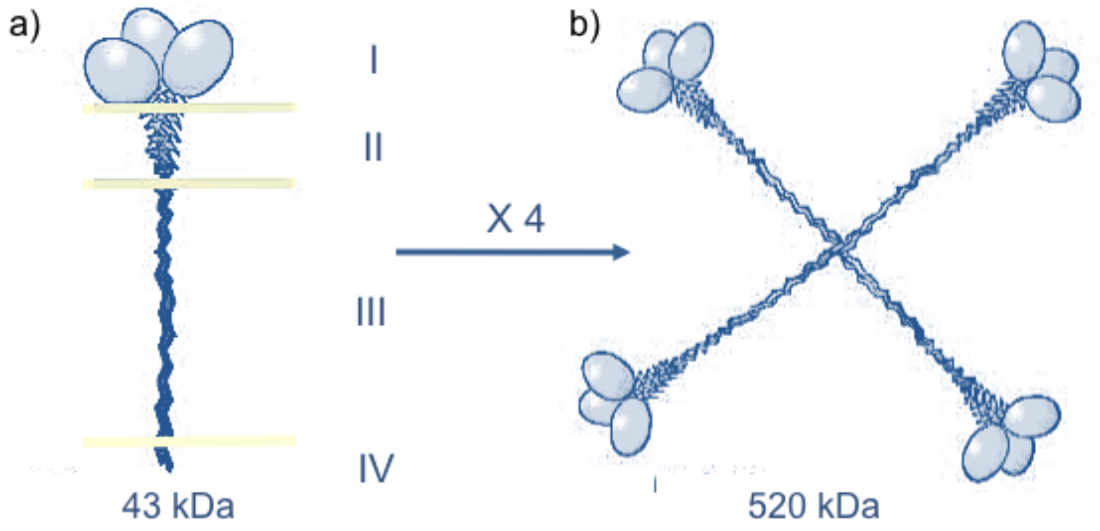

Figure 6. Models of trimeric (a) and oligomeric (b) forms of SP-D. All structural domains of SP-D are represented: I) NH_2-terminal segment; II) collagen-like domain; III) neck region; and IV) COOH-terminal globular domain.

First, SP-D binds to carbohydrate structures of several pathogens such as influenza A virus, a variety of gram-negative bacteria including *Klebsiella pneumoniae*, *Pseudomonas aeruginosa*, *Hemophilus influenzae*, and *Escherichia coli* or opportunistic fungal pathogens such as *C. neoformans*, *Aspergillus fumigatus* conidia and *Candida albicans*, leading to their inhibition (76-79).

Second, SP-D binds to leukocytes such as alveolar macrophages and dendritic cells modifying their activities by: (I) opsonization or other effects mediated by the specific interactions of the leukocyte with SP-D-coated organisms; (II) direct effects of SP-D on phagocyte function; and (III) SP-D-mediated alterations in particle presentation secondary to aggregation (77).

However, all these mechanisms may be operative, alone or in combination, in specific microbial-phagocyte interactions.

Also SP-D−/− knockout mice show that they have impaired host defense upon injury or infection instead of an exaggerated inflammatory response, heightened susceptibility to inflammatory stimuli, infections or allergic sensitization (55). Furthermore, immune cells in the lung of SP-D−/−mice display multiple abnormalities including altered morphology and constitutive release of pro-inflammatory mediators (55).

Hydrophobic peptides

SP-B

Though SP-B comprises only~10% (w/w) of SPs, its absence or dysfunction due to mutations results in respiratory failure and death shortly after birth (80).

Human SP-B mRNA is produced from a single gene located on chromosome 2 at a site syntenic with the murine SP-B gene located on chromosome 6 (81, 82). The SP-B gene is first transcribed/translated into a significantly larger monomeric pre-pro-protein of approximately 42 kDa,which is processed to a smaller, lipid-associated peptide in the distal secretory pathway within the type II cells (46, 83).

The monomeric pre-pro-protein is first N-glycosylated on regions flanking the mature SP-B sequence (83). These flanking arms are cleaved at several steps among trans-golgi, multi-vesicular bodies (MVB) and proximal lamellar bodies (LB) where proteases such as napsin A, cathepsin H and pepsinogen C are involved (46, 83).

Once finishing the protein processing, the mature form of SP-B results in a 79 amino acid homodimer of approximately 18 kDa (84), contained in the LB of the secretory pathway of ATII.

Analysis of the sequence of SP-B reveals that this protein belongs to the family of the saposin-likeproteins. Each SP-B monomer (9kDa) possess small folds of around 80 amino acids containing amphipathic alpha-helices and three intramolecular disulfide bridges that link Cys-8–77, Cys-11–71, and Cys-35–46 (85, 86). The remaining cysteine at position 48 establishes the intermolecular bond responsible for dimerization of SP-B that does not take place until the cleavage of the flanking arms is completed. This bond is a disulfide linkage that presumably constrains the protein's flexibility and contributes to the remarkable thermal stability of the secondary structure (87) and the unusual resistance to both acid and proteolytic degradation.

Although it still lacks a three-dimensional model of the structure and disposition of SP-B in surfactant membranes, it has been proposed that SP-B interacts superficially with the surface of bilayers and monolayers, through amphipathic helical motifs (88).

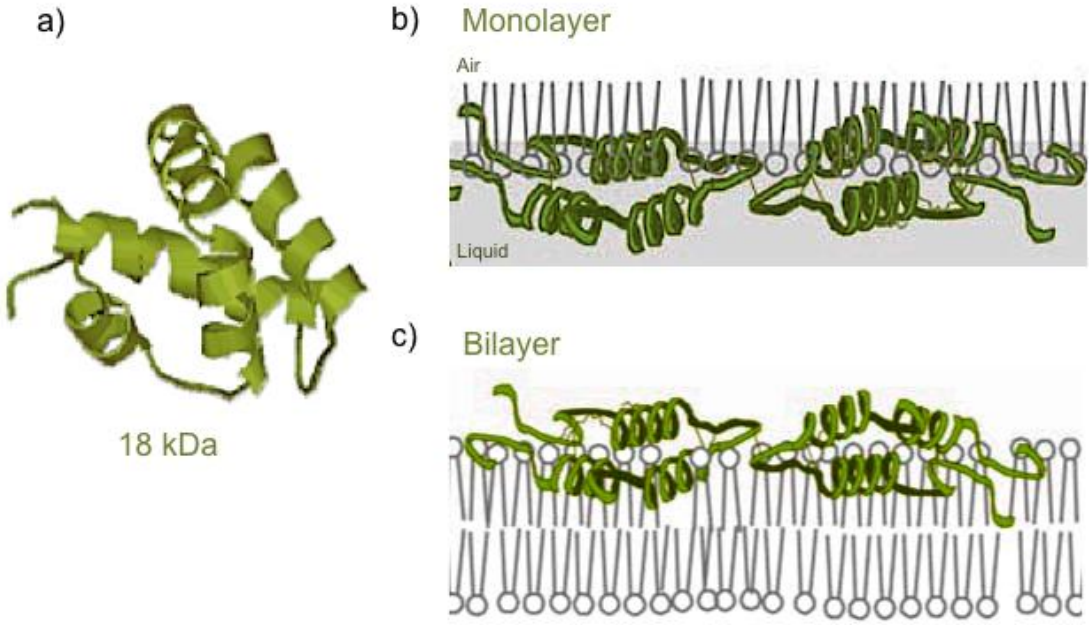

Figure 7. Models of the homodimer of SP-B (a) and its models of interaction with lipid monolayers (b) and bilayers (c).

In fact, all saposin-likeproteins have activities related to interacting with and inserting todifferent extents into PL membranes (85), but SP-B is the only member of the family that is permanently membrane-associated, partially due to its high hydrophobicity (56). Also the net positive charge of SP-B likely promotes a certain selective interaction of SP-B with the anionic PL fraction of surfactant, and particularly with PG (89) though there is a certain controversy due to whether SP-B prefers PG-enriched or PC-enriched membrane regions (90). Conversely, it has been established that SP-B is distributed specially in disordered regions of membranes and interfacial films (56).

Therefore, SP-B facilitates organization of PS membranes in the lamellar body, likely through its ability to promote membrane-membrane contacts, perturbation of lipid packing, and membrane fusion (46). Furthermore, SP-B promotes a rapid and efficient adsorption of surfactant PL into the air–liquid interface and modulates the stability and dynamic behavior of interfacial surfactant films subjected to continuous compression–expansion cycling (45).

On the other hand, SP-B deficiency, arising from mutations in the human gene (SFTPB) or disruption of the mouse locus (Sftpb), results in vesiculated LB with few or no bilayer membranes and electron dense inclusions (46). Most importantly, severe SP-B deficiency (i.e., ~75% reduction in SP-B content in the airspaces) results in fatal RDS (91). Indeed, SP-B expression is altered in several acute and chronic lung diseases contributing to their pathogenesis (80).

SP-C

SP-C (4 kDa) is a non-homologous protein considered the most specific protein in terms of biophysical activity of PS and tightly linked with lung differentiation in mammals (56). Surprisingly, animals lacking expression of a functional SP-C are able to breath and therefore survive (92), suggesting that the action of SP-C is not as critical as SP-Bs. However, deficiencies in SP-C are irretrievably associated with severe respiratory pathologies (80).

Human SP-C gene is organized into six exons and is localized in the short arm of chromosome 8 (93). Differential splicing of the primary transcript, localize primary at 5´and 3´of exon 5, leads to several SP-C RNAs, but the SP-C RNA of ~0.9 kb encodes a pro-protein of 197 amino acid in human or 194 amino acids in rat (93-95).

Like SP-B, SP-C is first synthesized as a pro-protein. During its biosynthesis, the transmembrane segment of proSP-C, which will be afterwards the main part of the mature protein, is oriented with its N-terminal end exposed to the cytosol and the C-terminal side to the lumen of the ER (95).

The cytosolic domain encodes information required for intracellular trafficking of SP-C to the MVB/LB compartments (96). Here, assembly of SP-C into PS membranes is coupled with proteolytic processing of proSP-C precursor, to liberate N-terminal and C-terminal propeptides (46). Specifically, the generation of the 35-amino acid mature peptide involves a removal of 23-25 residues of N-terminal pro-peptide and 133-139 residues from the C-terminus of the pro-protein (94). Also, SP-C is post-translationally modified by addition of palmitoyl groups via thioester bonds to Cys-5 and Cys-6 (97). Interestingly, it is suggested that the processing machinery of SP-C maturation might be shared with SP-B as cathepsin H seems to be implicated (96).

Subsequently, fusion of the MVB with a LB leads to SP-B-mediated incorporation of SP-C-containing luminal vesicles into existing PS membranes that are eventually secreted into the airspaces. Thus the highly hydrophobic mature SP-C maintains its transmembrane orientation throughout biosynthesis (46).

As a result, mature SP-C is a small hydrophobic lipopeptide of 35 amino acids, containing palmitoylated cysteines, which is co-purified with SP-B and PL in chloroformic extractions of PS (98). Its three-dimensional structure consisted in a rigid α-helix covering approximately two thirds of the sequence and an unstructured N-terminal segment containing palmitoylated cysteines (97) (Figure 8a). In membranes, the helical segment of SP-C adopts a transmembrane orientation, adapted to traverse the DPPC bilayer in a fluid state(46) (Figure 8b and c).

SP-C, with lower activity that SP-B, is also able topromote adsorption and transfer of PL into the air–liquid interface (99).

Also, it has been suggested that SP-C could contribute to the remodeling of composition and structure of the interfacial films due to its exclusion of the monolayer during compression together with its intrinsic ability to interact and disrupt PL membranes with both α-helical segment, and N-terminal regions (100-102). Furthermore, it has been detected that SP-C promotes the formation of multilamellar structures associated with interfacial films during compression of surfactant films

(103). For that purpose, the presence of palmitic acid chains esterifying the cysteines in the N-terminal segment of the SP-C molecule seems to be critical to maintain this association (104).

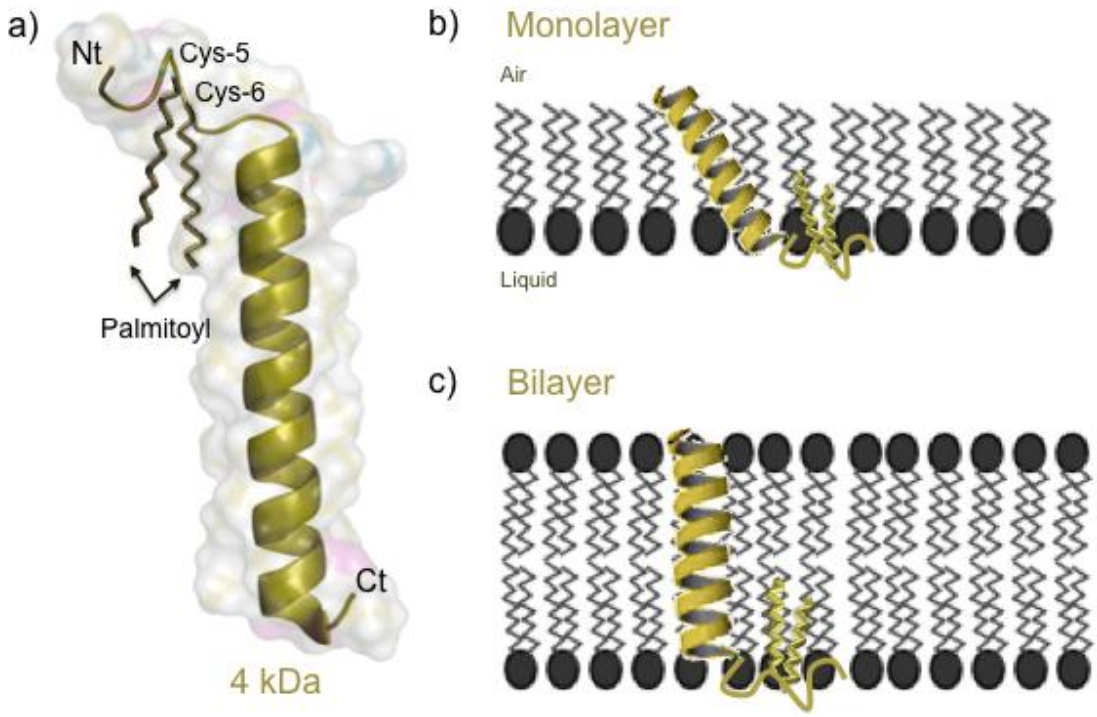

Figure 8. Model of the monomer of SP-C (a) and its models of interaction with lipid monolayers (b) and bilayers (c). Nt: Amino-terminal region; palmitoyl groups bonded to Cysteine (Cys) 5 and 6 are indicated with black arrows. Ct: Carboxyl-terminal region.

On the other hand, increasing evidence indicate that SP-C is also involved in immunomodulation that is critical for the stability and host defense of the airways (80). Interestingly, SP-C-deficient mice were found to be susceptible to bacterial and viral infections showing excessive inflammation (105, 106) and more vulnerable to develop severe outcomes in bleomycin-induced fibrosis (107).

A well, several studies observed that the amino-terminal segment of SP-C binds LPS suppressing inflammation (108-110) and SP-C-containing surfactant vesicles bind and interfere with toll-like receptors mediating the inflammatory responses in macrophages (105).

2.4.2. Metabolism

ATII cells are mainly responsible of the synthesis, storage, secretion, and even recycling of almost all components comprising PS. Here we divided the metabolism of PS in three sections: Synthesis and processing; Secretion; and Recycling and turnover.

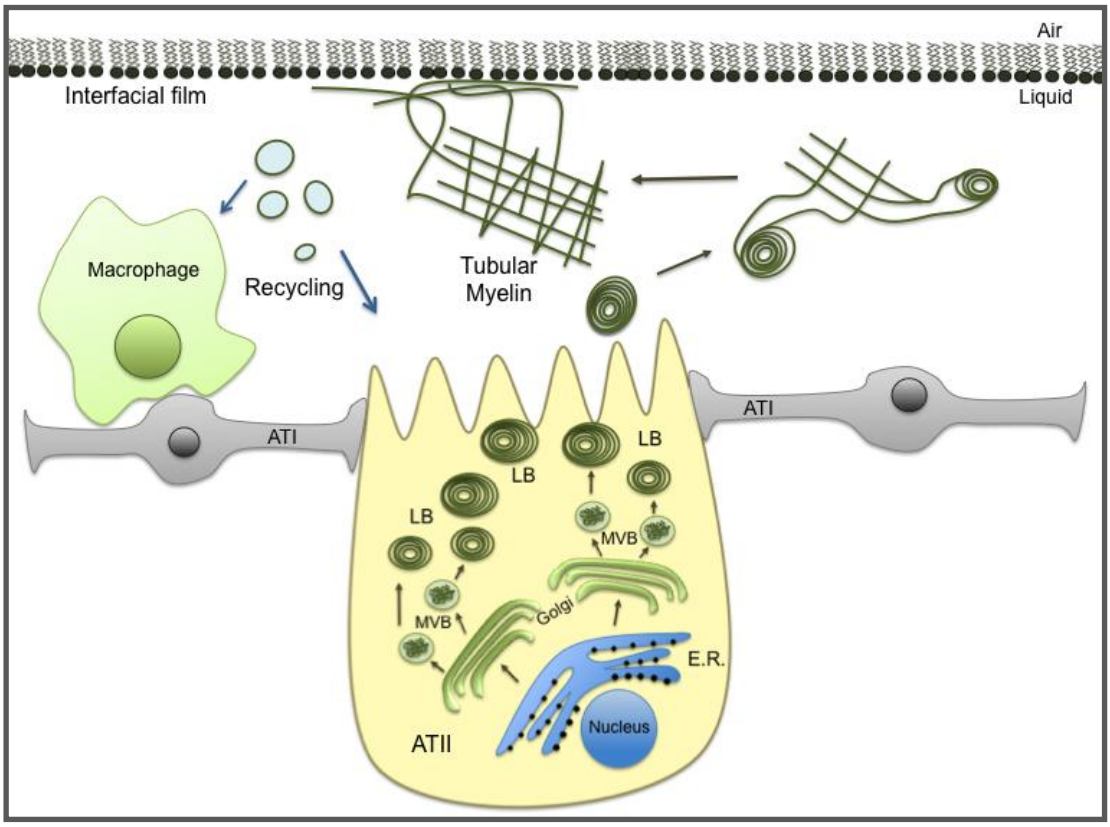

Figure 9. Diagram of the metabolism of pulmonary surfactant. ATI: alveolar type I cells; ATII: alveolar type II cells; E.R.: endoplasmic reticulum; MVB: multi-vesicular bodies; LB: lamellar bodies.

2.4.2.1. Synthesis and storage

The PL and proteins of PS are synthesized in ATII cells, assembled in lamellar bodies and extruded into the alveolar lumen by exocytosis.

Phospholipids synthesis

As SPs synthesis and processing has been mentioned in the last section, here we briefly summarize the synthesis of main important lipids of PS.

Phospholipids are composed of a glycerol backbond, two fatty acids and a polar phosphorylated moiety. This composition conferred to the PL amphipathic properties. The fatty acids required for PS lipid synthesis might be recruited from circulation as free fatty acids or triacylglycerols in lipoproteins but also might be synthesized *de novo* by ATII cells from several precursors such as glucose, lactate or acetate (111). All diacylglycerol phospholipids are synthesized in the ER through a chain of biochemical events beginning with the formation of phosphatidic acid, which is hydrolyzed to diacylglicerol. Subsequently, specific enzymes transform this product generating compounds with several polar heads, like PC, PG or PI (112). Interestingly, as previously mentioned, half of the PC in PS is DPPC, accounting for ~40% of total surfactant PL (6). Two pathways contribute to the production of DPPC, *de novo* synthesis andremodeling via lysoPC. However, the latter pathway accounts for up to 75% of DPPC in ATII cells and involves deacylation of unsaturated PC at the sn-2 position by a Ca^{2+}-dependent phospholipase A2 (14, 46).

The regulation of PL synthesis in the lung is influenced by developmental and hormonal factors affecting several rate-limiting metabolic steps. Corticosteroids and thyroid hormones enhance the activity of several enzymes within the PL synthetic pathway whereas insulin, epithermal growth factor (EGF) or transforming growth factor α (TGF-α) influence PS production (112, 113). Interestingly, some of these factors e.g. glucocorticoids, are directly involved in the control of AMPc production, which in last term regulate SP levels (114, 115).

Storage

Pulmonary surfactant complexes are assembled in ATII cells and stored in form of tightly packed membranes in the LBs (e.g. the characteristic storage granules of PS in ATII cells) (Figure 10) (116). They consist of a limiting membrane surrounding about 20-70 tightly packed PL bilayers, or lamellae, arranged in a hemisphere (117, 118). These organelles belong to the endosomal–lysosomal pathway and their maturation requires proper trafficking of proteins and lipids along the regulated exocytic pathway (119).

As previously mentioned, it has been postulated that SP-B and SP-C are synthesized in the ER and processed through the Golgi and MVBs reaching LBs (120). Conversely, though SP-A is also synthesized and processed in ER and Golgi,

now it is widely accepted that it is secreted into the extracellular media by a different pathway and probably interacts with PS membranes once in the alveolar space (121).

As well, the major surfactant PLs are synthesized in the ER. Three pathways of intracellular lipids transport has been postulated: vesicular transport, non-vesicular transport, and diffusion at membrane contact sites (122).

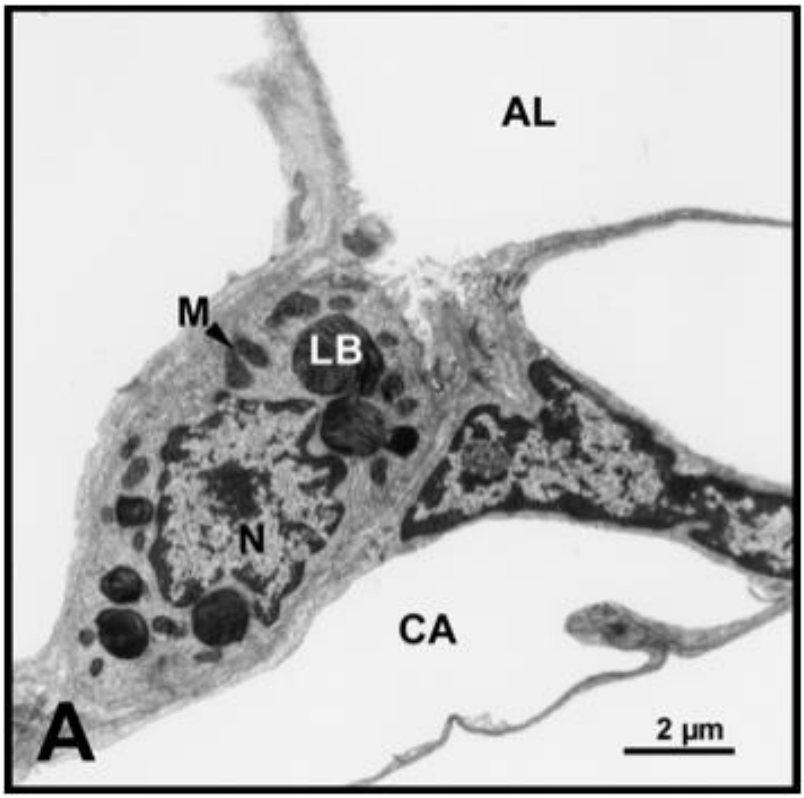

Figure 10. Ultrastructural appearance of alveolar epithelial type II cells by electron microscopy (bar=0.2µm). Lamellar bodies (LB), nuclei (N), mitochondria (M), alveolar lumen (AL), capillary (CA). (Image from Fehrenbach et al. Respiratory Research 2005.)

Vesicular transport plays an important role in trafficking newly synthesized SPs andis also important for recycling of PS proteins and lipids via the endocytic pathway. However, though there are some evidences of PS lipids vesicular transport from the ER to the LB (123) a separate study found that inhibition ofvesicular transport did not inhibitincorporation of newly synthesized lipid intothe LB (124).

The non-vesicular transport pathway can answer these results due to the localization of the ABC transporter (ABCA3) to the limiting membrane of the LB (125, 126). Indeed, as ABC transporters typically move substrateout of the cytosol,

being liable that ABCA3 would be an essential transporter of PL into the LB. In fact, disruption of the Abca3 locus results in neonatal lethal RDS associated with loss of LBs (127, 128).

Another postulated mechanism for PL transfer from ER to LBs is via diffusion or facilitated exchange at membrane contact sites that would require the participation of accessory proteins to ensure the formation of transient contact sites between the appropriate donor (ER) and acceptor (LB) organelles (122). However, these pathways remain as an important and unresolved question.

There are several classes of LBs according to their packaging statement from round–concentric-like membranes to very tightly packed piles of membranes (56). These types areusually linked with the proximity with the alveolar surface. Thus, when LB acquired the final packed state, they are found near the alveolar surface to be extruded into the alveolar lumen by exocytosis.

2.4.2.2. Secretion

PS secretion requires the transportation ofLB to the apical membrane of ATII cells. According to several stimuli such as cholinergic and β-sympathomimetic agents, Ca^{2+} ionophores, purine agonists and the most important, alveolar stretching, the limiting LB membrane is merged with the plasma membrane of ATII cell, extruding the LB into the hypophase (e.g. thin aqueous layer covering the ATII cell surface) by exocytosis (Figure 11a) (129, 130).

In the hypophase, the tightly packed surfactant membranes comprising the LBs tend to reorganize to form a loose network of interconnected membranes named tubular myeline (TM) (Figure 11b). It is not clear how the structural transformation of surfactant membranes is triggered, but potential effectors include changes in the hydration of surfactant complexes, pH, presence of surfactant apoproteins or calcium concentration (50–52).

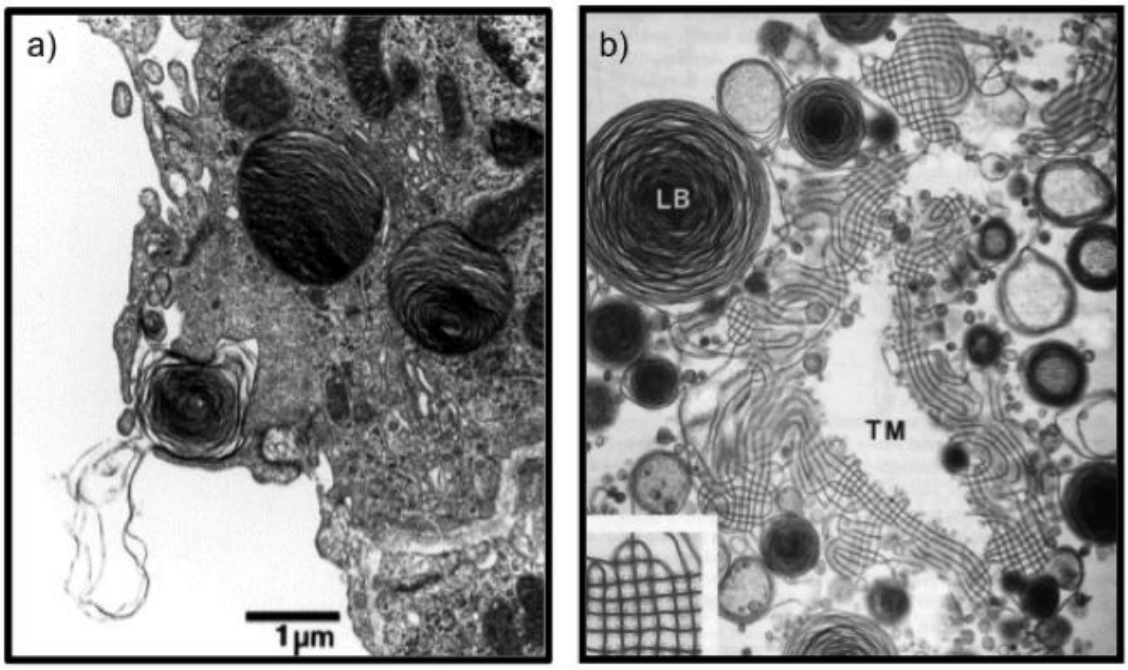

Figure 11. Electron micrographs sections (bar=0.1 µm). a) A lamellar body in the process of exocytosis from a type II cell. (Figure from reference [122]). b) Lamellar bodies (LB) are seen forming tubular myelin (TM). Inset: detail of tubular myelin showing small projections in the corners, thought to represent SP-A (Image from reference [34]).

TM is composed of large square elongated tubes, constituted primarily of PL (DPPC and PG), proteins SP-A and SP-B, and Ca^{2+} (6), ranging in size from nanometers to microns (53,54). Membranes in TM arrange in an ordered pattern, whose dimensions are related with the molecular size of SP-A macromolecule, suggesting that SP-A is the main determinant for TM organization. Though the mechanisms of TM are still under discussion, it is likely that TM formation requires: (I) close contacts between opposing DPPC-rich membranes mediated by SP-A; (II) SP-A self-association mediated by Ca^{2+}, and (III) membranes fusion mediated by SP-B (59). As SP-A is mainly implicated in innate defense (59), current thinking assumes that TM structure plays also some role in optimizing clearance of pathogens.

Subsequently, PS components of TM are transferred to form a surface-active film at the air–water interface of alveoli by rapid adsorption. In this case, SP-B and SP-C are thought to facilitate PL transfer (specifically DPPC) from TM to the surface film (56, 58).

Traditionally, the PS film has been considered to be a monolayer (131, 132). However, several studies using different techniques (133-136) conclude that at least part of the PS film is thicker than a single monolayer. Specifically, plus the surface monolayer, there are at least one lipid bilayer closely and apparently functionally associated with the interfacial monolayer (Figure 12). These multilayers structures could provide additional stability to PS monolayers, thereby allowing the attainment of very low surface tension (6).

Therefore, upon compression of the PS film during expiration, SPs induce the formation of unsaturated phospholipids-rich multilayers that remain associated with a monolayer enriched in saturated PL species. After inspiration, some of the lipids in the reservoirs are re-adsorbed into the surface film, helped by the hydrophobic peptides in order to avoid significant loss of material (57).

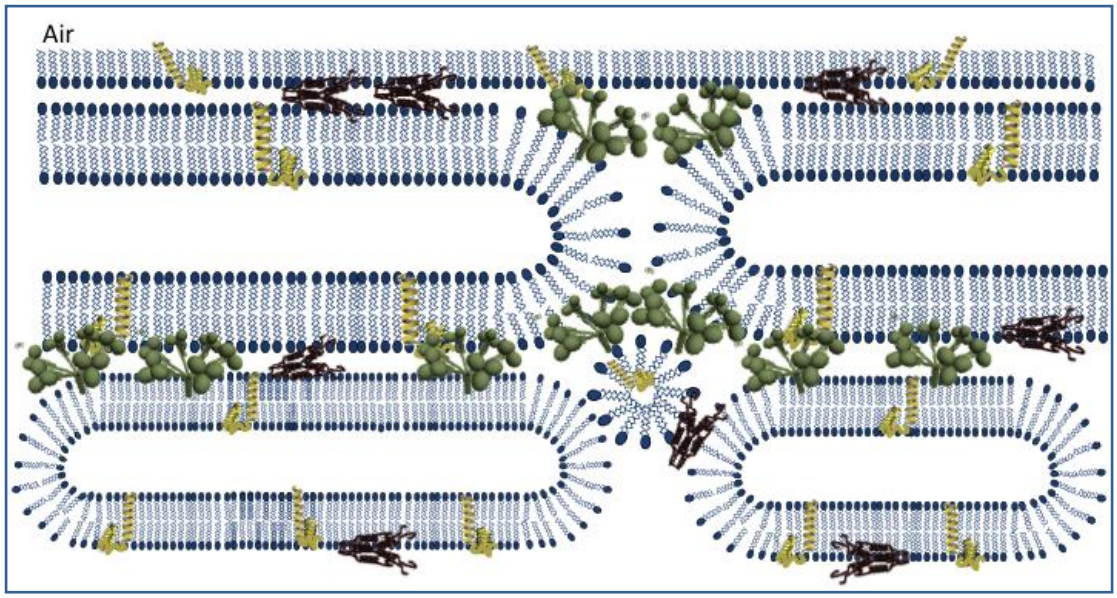

Figure 12. Diagram of a multilayer interfacial surfactant film structure.
It depicted the possible interaction between pulmonary surfactant-associated proteins with the monolayer in the air-liquid interface and the bilayers associated**.**
Yellow: SP-C; Red: SP-B; and Green: SP-A.

2.4.2.3. Recycling and turnover

Compression-expansion cycling during respiration leads to progressive conversion of the surface-active fractions of PS into lesser active lipid/protein complexes (46). The inactivation of PS may result from detachment of small PS particles from the air-liquid interface, changes in lipid/protein association, and oxidation of lipid and protein species of PS without rejecting the possibility of inactivation byincorporation of materials inhaledfrom the upper airways (6, 137). Maintenance of a fully functional surfactant film therefore requires continual film refinement through efficient removal of spent PS and incorporation of newly secreted complexes (46).

These lesser active PS complexes are small vesicular forms named small aggregates (SA) that represent used PS destined for clearance and re-uptake. These aggregates can be separated by centrifugation of lung lavage fluid from the fraction of heavy, large aggregates (LA) forms containing more surface active material i.e. tubular myelin, lamellar bodies and proteins (138). Measurement of aggregate conversion is used experimentally to estimate PS inactivation, being correlated the increment of SA with lung injury (139, 140).

SA is continuously taken up by ATII cells for recycling or, toa lesser extent (5-10 % of total), cleared by alveolar macrophages (141) (Figure 13). However, it has been demonstrated that alveolar macrophages depletion significantly affects PS metabolism (142).

The surfactant lipids that are recycled back into the ATII cells can either be catabolized for *the novo* lipogenesis in lysosomes or reutilized intact in the LB were the biosynthetic and endocytic pathways converge. The estimated turnover period of PS range from 4 to 11h (143).

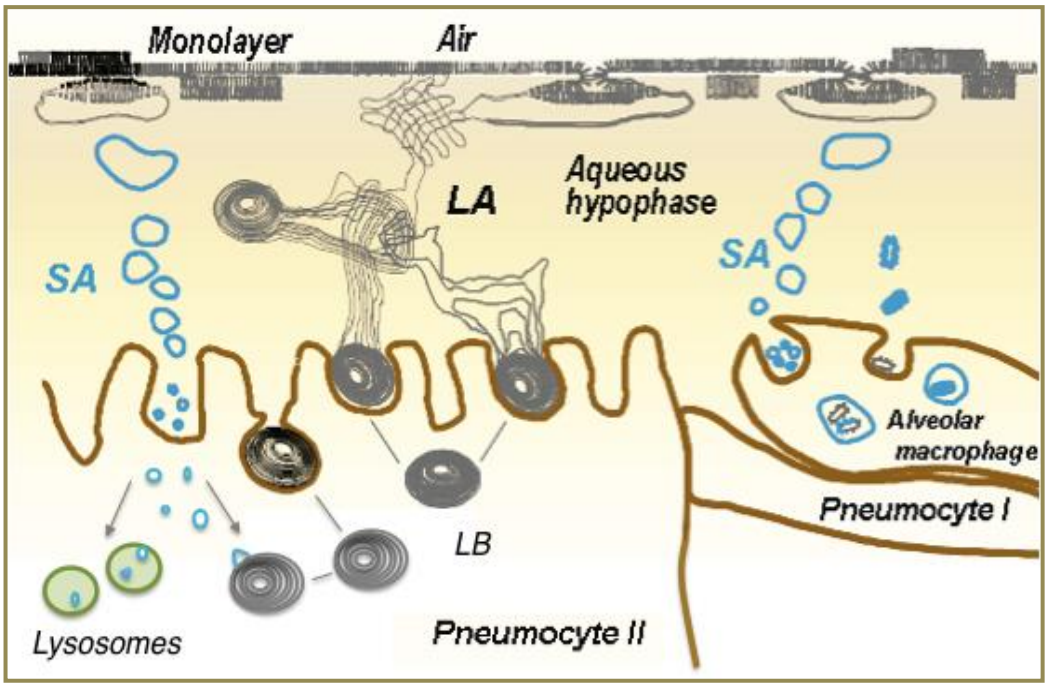

Figure 13. Diagram of recycling and turnover of pulmonary surfactant LA: large aggregates or functional fraction of pulmonary surfactant; SA: small aggregates or inactive fraction of pulmonary surfactant; LB: lamellar bodies.

2.4.3. Functions

The main functions of PS system are: (I) reduce the surface tension in the alveolar air-liquid interface; (II) Alveolar-capillary fluid homeostasis maintenance; and (III) Host defense against pathogens and inflammation. These functions can be accomplished by the whole PS system or specifically by one of its components.

2.4.3.1. Surface tension reduction in the alveolar air-liquid interface

Molecules at an interface between two phases, like the alveolar air-liquid interface, are subjected to specialized conditions that generate associated forces manifested as surface tension (144).

Specifically, because liquid molecules at the interface have strong attraction toward the bulk of the liquid (i.e. water is a strongly polar substance with a significant intramolecular attractive forces) with no equivalent forces above the surface because air molecules are dilute, this imbalance leads to minimize surface area of the alveoli, raising the surface tension (144).

PS is a surface-active lipoprotein complex which has energetic preference to the interface due to its amphipathic condition. As a result, PS film ubication at the alveolar air-liquid interface decrease the net unbalanced attractive forces between interfacial region and bulk liquid molecules, lowering surface tension (51).

The resulting PS surface film is compressed and expanded during breathing and lowers and variances surface tension in a dynamic way. As alveolar size decreases during exhalation, PS film is compressed and surface tension reaches very low values (<1 mN/m compare with 70 mN/m for pure water at 37ºC). Conversely, when alveolar size increases with inspiration, the PS films is expanded, and surface tension proportionaly increases (~23 mN/m at 37ºC). This dynamic variation of surface tension with area allows alveoli of different sizes to coexist stably at fixed pressure during respiration (51).

Therefore, idealicing the alveoli shape as spherical cavities, it can be applied the Laplace-Young law which enounces that the pressure (π) inside the alveoli is directly proportional tosurface tension (γ) and inversely proportional to alveolar radius (r).

As a result, small alveoli resist collapse at end expiration because their surface tension is low, and alveolar inflation is better distributed during inhalation because the ratio of surface tension to area is more uniform in different-sized alveoli (Figure 14) (51).

Moreover, by reducing surface tension throughout the lungs, PS decreases the pressures (work) needed fot pulmonary inflation. Interestingly, there is a direct conection between the surface activity of PS and pulmonary pressure-volume mechanics. The physologic consecuences of PS deficiency or dysfunction includes atelectasis, uneven inflation and severe ventilation/perfusion alterations present in the lungs of preterm infants with RDS (144).

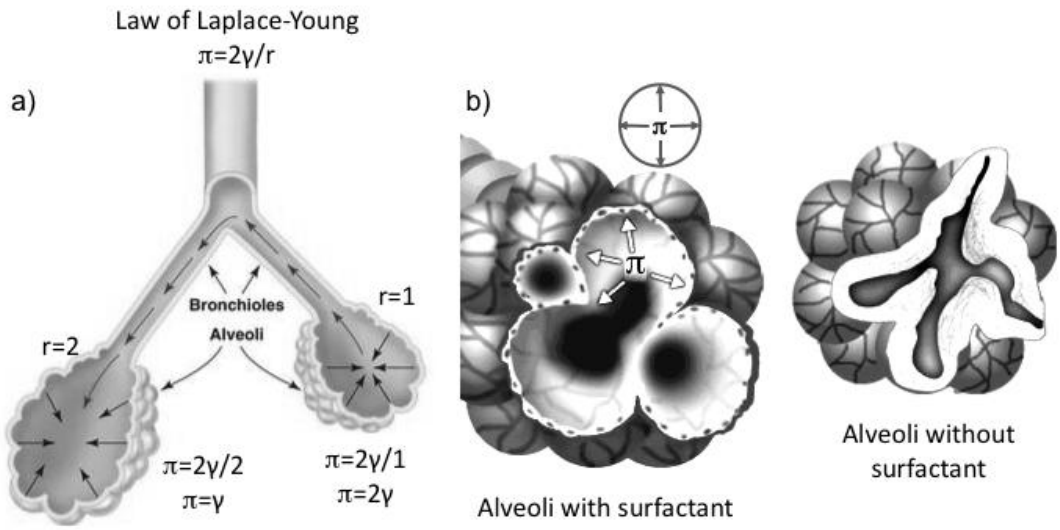

Figure 14. Surface tension in the alveolar air-liquid interface. a) Law of Laplace-Young illustrated. The small alveoli tend to empty into the large one in order to balance the pressure difference between them. b) Alveoli with presence (normal state) and absence (collapse state) of pulmonary surfactant. π: pressure; γ: surface-tension; r: ratio.

2.4.3.2. Alveolar-capillary fluid homeostasis

PS also plays a role in homeostasis maintenance of the alveolar fluid, thereby preventing edema formation. Edema is defined as an abnormal accumulation of fluid in the interstitium followed by fluid compilation in the alveolar space.

The net flow fluid (Q) across the alveolar-capillary membrane is generally expressed using the Starling equation:

$$Q=K_f\,([P_c-P_i]-R[\pi_c-\pi_i])$$

Therefore the net fluid movement between compartments is determined by six factors:

1) The filtration coefficient (K_f): is the constant of fluid permeability of the capillary wall. Therefore, a low value indicates a low capillary permeability whereas a high value indicates a highly water permeable capillary typical of several damages like ARDS.

2) The hydrostatic pressure difference across the capillary, which is determined by the difference between the capillary hydrostatic pressure (P_c) and the interstitial hydrostatic pressure (P_i, which is negative).

3) The reflection coefficient (R) is used to correct the magnitude of the oncotic pressure gradient taking into account the efficiency of the capillary wall to prevent protein leakage. It can have a value from 0 to 1, being 0 total protein leakage and 1 absence of protein flow.

4) The oncotic pressure difference across the capillary, which is assessed by the positive difference between plasma colloid oncotic pressure (π_c) and interstitial colloid oncotic pressure (π_i).

Therefore, under normal conditions, the balance of Starling forces across the alveolar-capillary membrane favors a net flow of fluid out of the microvascular space into the interstitium (145, 146).

The resulting small net filtration is balanced by lymphatic drainage of the interstitium, which also contributes to the subatmospheric pressure in the interstitial spaces, favoring fluidfiltration. However, an excess of fluid accumulation in the interstitium leads to fills progressively the alveoli (145).

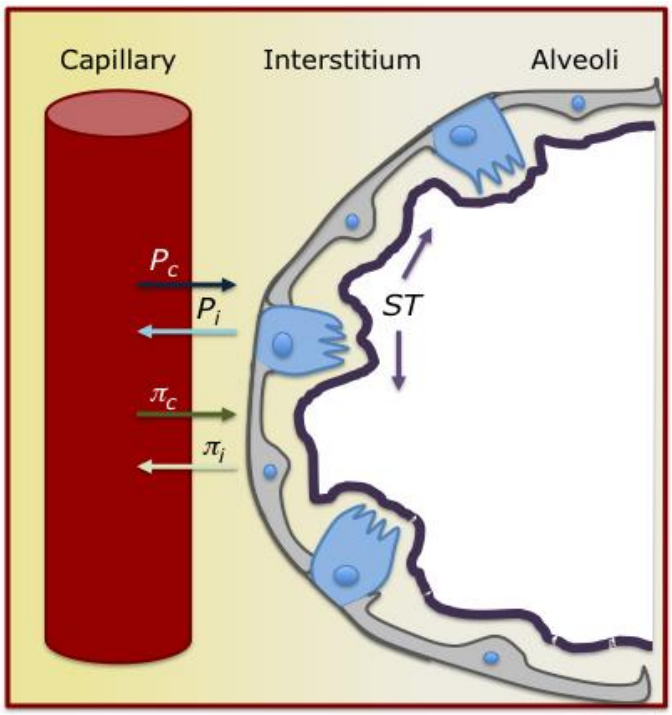

Figure 15. Diagram of the forces implicated in the net flow of fluid from the capillary to the interstitium. Pc: capillary hydrostatic pressure; Pi: interstitial hydrostatic pressure; πc: plasma colloid oncotic pressure; πi: interstitial colloid oncotic pressure.

PS contributes to maintain constant the negative levels of P_i by keeping intra-alveolar pressures due to its action of decreasing surface tension and alveoli area proportionally during expiration. Consequently, PS inactivation results in a surface tensionincrement causing a reduction in the negative value of P_i, altering the hydrostatic pressure difference and consequently increasing the net fluid movement to the interstitium and subsequently to the alveolar space (147). Interestingly, intra-alveolar edema promotes PS inactivation triggering ALI, leading to a damaging feedback.

2.4.3.3. Innate host defense

PS is involved at several levels in host defense mechanisms:

Physical barrier: The alveolar epithelium is a potential pathogens gateway as it is the greater surface contact of the organism with the environment. Consequently, the inhaled pathogens that manage to evade the defense mechanisms of the upper airwaysface PS. Thus, PS is the first defensive barrier at the alveolar space hindering the adhesion of the incoming particles to the alveolar epithelium and facilitating their removal through mucocilliary transport (148).

Inhaled particles interaction: PS-collectins SP-A and SP-D mainly accomplish this function (see section 2.4.1.2). Both collectins are able to bind a wide range of ligands including allergens, LPS and other surface molecules of bacteria, virus or fungi (148). As a result, the complex pathogen-collectin can be eliminated either directly by enhancing the membrane permeability (149) or indirectly by improving the aggregation, opsonization and clearance of these pathogens via leukocytes (55, 148).

Immunomodulatory interaction with leukocytes: Almost all components of PS are able to accomplish immunomodulatory activities.

Recent studies have illuminated a potentially important roleof surfactant PL in altering the immune response. PL, specifically anionic lipids appear to act as immunosuppressive mediators by inhibiting responses such asrelease of reactive oxygen species and proinflammatory cytokines (80, 148). Specifically, phosphatidil glycerol (POPG) attenuates or even blocks TLR-2 and TLR-4-dependent inflammatory processes and prevent infection of some virus (150, 151). Also,

dipalmitoylphosphatidyl glycerol (DPPG) inhibit viral infection by blocking attachment of the virions to host cells (152). On the other hand, DPPC, the major PS phospholipid, blocks epithelial cell expressed TLR4 activation by limiting translocation of TLR-4 to membrane lipid raft micro domains (153) and induced expression of several macrophage innate immune receptors (154).

As well, some studies suggested that the hydrophobic peptides SP-B and SP-C have an inmunomodulatory role (148) (see section 2.4.1.2). SP-B-deficiency is suggested to impair the ability of the lung to counteract LPS-induced inflammation and promotes an inflammatory status mediated by alveolar macrophages and ATII cells (155, 156). On the other hand, SP-C may be involved in host defense as it interacts with both LPS and the pattern recognition molecule CD14 found on phagocytes to reduce it response (88, 110, 157).

Additionally, collectins can also modulate the host inflammatory response independent of activities against microbial agents. Specifically, SP-A and SP-D play a major role regulating inflammation by hastening the clearance of apoptotic cells and impeding the release of cytokines and other proinflammatory products. Moreover, some experiments depicted that SPA or SP-D knockout mice, have increased the presence of proinflammatory cytokines and inflammatory response resulting due to infection (55).

2.5. Pulmonary immune system

The lung is constantly exposed to environmental pathogens, allergens and toxicants. Therefore, this system had developed robust defenses to protect itself against the deleterious effects of such challenges (158). The mechanisms of pulmonary defense can be divided into non-specific defenseandspecific defense accomplished by the innate immune system.

Non-specific defenses are mechanisms of physical removal such as cough and expectoration, lymphatic flow from the alveolus to the lymph nodes, and mucociliary clearance (158). The innate immune system includes soluble factors like proteins that bind to microbial products and leukocytes that ingest particulates and kill microorganisms (159).

The soluble constituents of airway and alveolar fluids have acritical role in the innate immune defense in the lungs. There are a wide range of soluble factors in the

alveolar and airway aqueous fluids accomplishing this role suchlysozyme, which is lytic to many bacterial membranes; lactoferrin, which excludes iron from bacterial metabolism; IgA and IgG, being IgG the most abundant immunoglobulin in alveolar fluids (160); defensins, which are antimicrobial peptides released from leukocytes and respiratory epithelial cells (161); LPS-binding protein (LBP) and soluble CD14 (sCD14), which are key molecules in the recognition of LPS by alveolar macrophages and other cells in the alveolar environment (162, 163); and complement proteins and surfactant-associated proteins (SP-A and SP-D) that serve as additional microbial opsonins (see sections 2.4.1.2 and 2.4.3.3).

Cellular innate immune mechanisms include inflammatory cells such as alveolar macrophages, neutrophils, monocytes, lymphocytes, and eosinophils. Alveolar macrophages account for approximately ~95% of airspace leukocytes, with ~1 to 4% lymphocytesand only ~1% neutrophils (160).

Alveolar macrophages represent the most important defense system both for non-specific phagocytic defense and for antigen triggered immunity via activation of T-lymphocytes and neutrophils recruitment (164-166).

Morphologic studies have shown that alveolar macrophages are large, mature cells, with an increased cytoplasm/nucleus ratio, which resembles other tissue macrophages. These cells reside within the alveolus and are often seen protruding from the alveolar epithelial walls into the lumen of the lungs (30).

Macrophages are highly heterogeneous cells that can change their function in response to local signals in their environment. They are commonly divided into subpopulations based on their functional phenotype. However, rather than being separated subpopulations, macrophages represent a spectrum of phenotypes, and they can switch from one phenotype to another in response to signals present in the environment.

The two commonly known sub-populations are named classically activated macrophages, and alternatively activated macrophages. Exposure to interferon-γ (IFN-γ) stimulates the first classic pathway of activation that yields M1 macrophages with efficient capacitiesfor phagocytosis, antigen presentation and production of Th1 cytokines, including IL-1β, IL-6, IL-12, and tumor necrosis factor-α (TNF-α), that are all important for clearance of intracellular and bacterial pathogens. Conversely, the alternatively activation take place when macrophages

gather with IL-4 and IL-13, involving Th2 responses and antiinflammatory functions (165, 166).

Interestingly, though alveolar macrophages are critical for the normal function of the innate and adaptive immune responses during host defense, they might be also implicated in the abnormal function of these same systems when they drive inflammatory diseases.

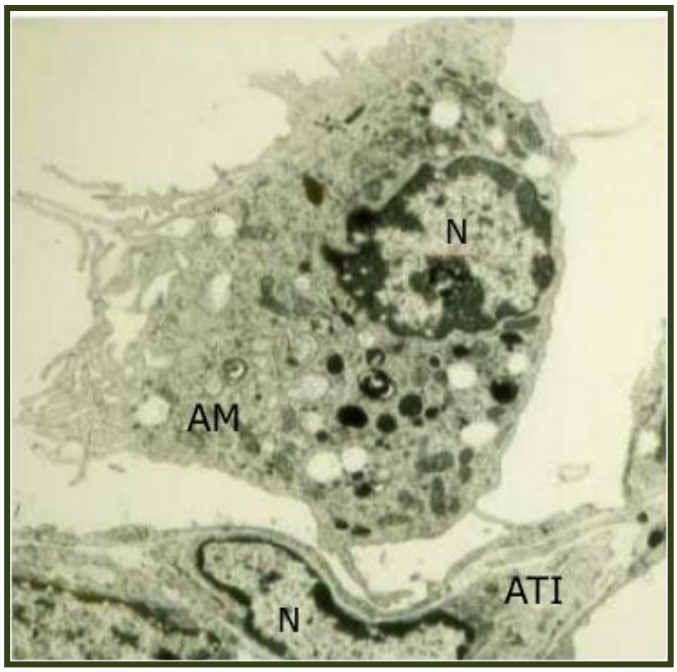

Figure 16. Ultrastructural appearance of an alveolar macrophage by electron microscopy. Alveolar macrophage (AM); alveolar type I cell (ATI); nuclei (N). (Image from © 2005, Angeline Warner, D. V. M., D. Sc.)

As alveolar macrophages are the primary sentinel cells which sensed pathogens and elaborated a cytokine response, neutrophils are key effector cells of the innate immune system recruited by macrophages (164). These cells are recruited through the pulmonary capillaries and into the air spaces, being initiated by the upregulation of adhesion molecules on pulmonary endothelial cells (167). Intravasated neutrophils phagocytose microbes, which are killed by reactive oxygen species, antimicrobial proteins, and degradative enzymes. Neutrophils also produce proinflammatory cytokines that recruit and activate other cells of the innate and adaptive immune system. Thus, alterations in neutrophil functions predispose the lung to respiratory infections and may exacerbate inflammation (164).

3. Acute lung injury

Acute lung injury (ALI) results from a dysregulated inflammatory response, and can progress to severe respiratory failure termed the acute respiratory distress syndrome (ARDS).

The first description of ARDS was published in 1967, when Ashbaugh and colleagues described patients in intensive care units with an onset of respiratory failure characterized by hypoxemia refractory to oxygen therapy, decreased lung compliance, and diffuse alveolar infiltrates on chest radiograph, preceded either by severe trauma, viral infection, or acute pancreatitis (168).

Thereafter, Murray and colleagues proposed a 4-point lung-injury scoring system based on the statement that severity of lung injury determines survival. This 4-point score was assessed by measurements of lung function, lung compliance, and degree of pulmonary edema (169). However, the clinical usefulness of this score was limited because it could not be used to predict outcome in the first 24 to 72 h after the onset of ARDS.

In 1994, the American-European Consensus Conference Committee on ARDS proposed the currently widely accepted defining clinical criteria to distinguished ALI and ARDS based on the extent of hypoxemia (defined by a ratio of the partial pressure of arterial oxygen [PaO_2] to the fraction of inspired oxygen [FiO_2]) (Table 1). In addition, acute onset, presence of bilateral infiltrates seen on lateral chest radiograph and a pulmonary artery wedge pressure (PAWP) <18 mmHg or no clinical evidence of left atrial hypertension are the other defining features of ALI/ARDS (2).

Table 1. Definition of Acute Lung Injury (ALI) & Acute Respiratory Distress Syndrome (ARDS) from the American-European Consensus Conference 1994 [163].

	ONSET	OXYGENATION	CHEST RADIOGRAPH	PAWP
ALI	Acute	PaO_2/FiO_2<300 mm Hg	Bilateral infiltrates	<18 mmHg/ no left atrial hypertension
ARDS	Acute	PaO_2/FiO_2<200 mmHg	Bilateral infiltrates	<18 mmHg/ no left atrial hypertension

PaO_2: partial pressure of arterial oxygen; FiO_2: fraction of inspired oxygen.

3.1. Epidemiology

3.1.1. Incidence

ALI/ARDS mortality rates have declined over the last 2 decades. In the 1980s, mortality rates were approximately 60–70% (170-172). However, these rates must be interpreted with caution, as accurate estimations were difficult to assess due to the lack of uniform definitions and diagnosis criteria until the 1994 consensus definitions together with the presence of etiologic variations, geographical variation and inadequate documentation (173).

In 2003, Goss and colleagues (174) used the NIH-funded ARDS network database to prospectively identify ALI patients from 1996–1999, estimating an incidence of 64.2 cases per 100,000 person-years. More recently, Rubenfeld and colleagues (175) estimated that there are 200.000 cases of ALI each year in the United States, associated with 74.500 deaths, estimating a 39% mortality that accords with mortality rates of 40-60% previously assessed in other studies (3).

3.1.2. Risk factors

The American-European Consensus Conference in 1994 defined several clinical disorders capable of triggering ALI divided according to the mechanism through which they cause lung damage (2). Thus, the first group of the disorders causes direct injury to the lung whereas the second group induces lung damage indirectly (Table 2). For example, pneumonia and aspiration of gastric contents belong to the most common causes of direct ALI whereas the most common causes of indirect ALI are sepsis and severe trauma with shock and multiple transfusions. Specifically, sepsis has a higher mortality rate than major trauma (43 vs. 11%) whereas pneumonia and aspiration have intermediate mortality rates (36 and 37%, respectively) (176).

Other factors that influence mortality appear to be age and race. Rubenfeld and colleagues (175) found that mortality was significantly lower in patients 15–19 years of age (24%) compared to patients 85 years of age or older (60%). On the other hand, racial inequalities also occur, e.g. African-Americans and Hispanics have a higher 60-day mortality rate (33%) compared to Caucasians (27%) (177). Finally, patients with multiple comorbidities, chronic alcohol abuse, or chronic lung disease, have an increased risk for ALI development (3).

Table 2. Clinical disorders associated with development of ALI & ARDS, as identified by the American-European Consensus Conference Committee 1994 (2).

DIRECT INJURY	INDIRECT INJURY
Diffuse pulmonary infection (e.g. Pneumonia)	Sepsis
Aspiration	Transfusion-related
Lung contusion	Pancreatitis
Near drowning	Sever non-thoracic trauma
Toxic inhalation	Cardiopulmonary bypass

3.1.3. Outcomes

Patients who survive ALI have been shown to have a reduced health-related quality of life (178) and persistent functional limitation largely as a result of muscle wasting and weakness. In fact, mild lung function alterations such as gas-exchange deficit with exercise and residual impairment of pulmonary mechanics persist after the resolution of the syndrome, but these abnormalities seem to be asymptomatics (179) and in most patients, pulmonary function returns to normal within 6-12 months (180).

3.2. Pathogenesis

Acute lung injury is a disorder of acute inflammation that causes disruption of the lung endothelial and epithelial barriers. Cellular characteristics of ALI include loss of alveolar–capillary membrane integrity, excessive transepithelial neutrophil migration, and release of proinflammatory, cytotoxic mediators (173).

In humans, the intrapulmonary inflammatory response begins before the onset of clinically defined ALI and is most intense in the first 3 days after the onset of ALI/ARDS (181, 182). This acute phase is characterized by the leakage of protein-rich edema fluid and inflammatory cells into the alveolar space together with the formation of characteristic hyaline membranes. This ALI stage, also named exudative phase, rises as a consequence of both endothelial and epithelial cell injury with increased permeability of the alveolar-capillary barrier (3, 183, 184) (Figure 17).

The subsequent histopathological stage of ALI (after ~1-2 weeks), known as the proliferative phase, is characterized by the proliferation of ATII cells along alveolar septa and the onset of epithelial regeneration (184). Under normal conditions, the denuded basement membrane is re-epithelialised with restoration of normal alveolar architecture and epithelial fluid transport capacity and rapid re-absorption of alveolar edema. However, in some patients alveolar edema persists, mesenchymal cells fill the alveolar spaces leading to a fibrotic stage (3).

3.2.1. Endothelial and epithelial injury

Disruption of the alveolar-capillary barrier is a well-established mechanism responsible for the influx of protein-rich edema fluid into the air spaces during the

initial phase of ALI (183). Therefore, the alteration of any of the components comprising the alveolar-capillary barrier may lead to the development of pulmonary edema that entails physiological events including hypoxemia and reduced lung compliance in ALI/ARDS patients (185).

During ALI, microvascular endothelium is injured by proinflammatory cytokines, activated immune cells and reactive species leading to an increased of capillary permeability. This alteration allows the efflux of protein-rich fluid into the interstitium, ultimately crossing the epithelial barrier into the distal airspaces of the lung (183). Several studies have documented increased release of von Willebrand factor (186-188) and upregulation of intracellular adhesion molecule-1 (ICAM-1) (189, 190) following endothelial injury. Also, endothelial damage contributes to leukocyte recruitment, coagulation disorders and vascular leakage.

On the other hand, the loss of epithelial integrity contributes importantly to edema formation for several reasons. Normally, ATI and ATII cells form tight junctions with each other, selectively regulating the epithelial barrier. Their alteration leads to disruption of normal fluid transport via down-regulated epithelial Na channels and Na^+/K^+ATPase pumps, impairing the resolution of alveolar flooding (3, 183).

As a result, increased permeability of this membrane during the acute phase of ALI leads to the influx of protein-rich edema fluid into alveolar space. Also, epithelial injury alters PS production by ATII cells (191), predisposes the lung to fibrosis during the later phases of ALI (192) and what is more, it allows the development of sepsis in those patients with pneumonia due to the entrance of bacteria into circulation (193).

3.2.2. Inflammation

Aberrant activation of the immune system (i.e., increase in neutrophils and cytokines) contributes to pulmonary edema in ALI and ARDS (194). Normally, >90% of the alveolar cells in the alveolar fluid are alveolar macrophages and >2% are neutrophils. However, in ALI this ratio is reversed and neutrophils comprised >90% of the alveolar fluid cells (195).

Macrophages contribute to ALI by regulating inflammatory and immune responses through the release of several mediators including cytokines, chemokines, metalloproteases or reactive oxygen species (ROS) (195). As well, endothelial and

ATII cells can also produce several cytokines and chemokines under numerousALI stimuli (196-199). Furthermore, some of the ALI mediators can up-regulate various surface molecules on the endothelial and epithelial surface allowing leukocytes, primary neutrophils, to adhere and migrate across the alveolar-capillary barrier (200-202).

In fact, a marked neutrophil accumulation is characteristic of the acute phase of ALI, suggesting that these cells play an important role in the pathogenesis of lung injury as they are considered primary perpetrators of inflammation (203-205).

Excessive and/or prolonged activation of neutrophils contribute to basement membrane destruction and increased permeability of the alveolar–capillary barrier (205, 206). Specifically, elastase, a widely studied neutrophil mediator, seems to degrade epithelial junctional proteins and possess pro-apoptotic and direct cytotoxic effects on the epithelium (207, 208). Furthermore, ARDS patients with increased levels of granulocyte-colony stimulating factor (a neutrophil anti-apoptotic factor) in the lung lining fluid, have poorer outcomes (209).

On the other hand, a complex balance of pro- and anti-inflammatory cytokines appears to initiate and regulate the inflammatory response in ALI (3, 182). Cytokines are low-molecular weight soluble proteins that transmit signals between cellsinvolved in the inflammatory response (210).

IL-1β and TNF-α are unrelated early response cytokines as they are found in the early stages of ALI and are able to initiate further inflammatory responses. Several human studies determined that both cytokines play a role in mediate ALI as well as maintaining the inflammatory response (211). Besides, they are able to induce additional cytokine production including IL-6 and IL-8 (212). IL-6 is a pleiotropic cytokine with multiple functions such as stimulation of acute phase proteins, T-cells activation or even inhibits IL-1β and TNF-α production (213). IL-8 belongs to the CXC chemokine family that has significant neutrophilchemotactic activity (214).

In patients with ALI/ARDS, those proinflammatory cytokines are persistently elevated in plasma and are strongly predicative of mortality (215-217). As well, IL-1β, TNF-α and IL-8 are elevated in the alveolar fluid of ARDS patients (211, 215, 218). Thus, systemic and local production of proinflammatory cytokines initiates and amplifies the inflammatory response and the subsequent injury in ALI and ARDS.

However, the presence of several specific inhibitors of proinflammatory cytokines including IL-1-receptor antagonist (IL-1ra), soluble TNF receptor (sTNF-R) and auto-antibodies against IL-8 and non-specific antiinflammatory cytokines like IL-10 and IL-11 has been described to modulate inflammatory lung injury. Nonetheless, their low presence in the alveolar fluid of ARDS patients is associated with increased mortality rates (3, 182). Therefore, a balance between pro- and antiinflammatory mediators may lead to a solving proliferative phase or a proliferative phase leading to fibrotic processes.

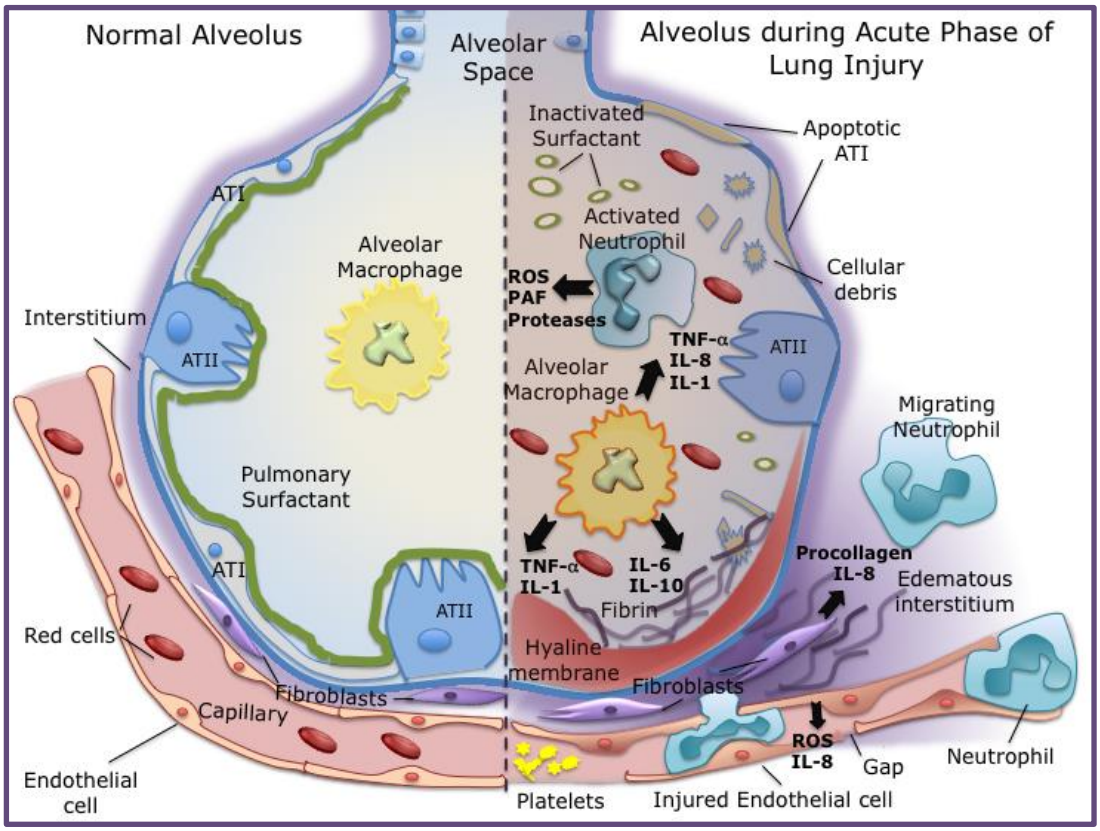

Figure 17. Pathophysiology of the acute phase of acute lung injury. Left side represents a normal alveolus; Right side represents an injured alveolus characterized by an edematous and an inflammatory state in the acute phase of lung injury. Alveolar Type I cell (ATI); Alveolar Type II cell (ATII); Interleukin (IL)-1-6-8-10; TNF-α: Tumoral necrosis factor α; ROS: Reactive Oxygen Species.

3.3. Treatment

Currently, treatment of ALI is based in both ventilatory and non-ventilatory strategies. However, for many years, treatment of ALI was limited to the supportive treatment of organ failure and treatment of the underlying cause of lung injury. Improvements in this supportive treatment, rather than the success of a particular therapeutic intervention, are thought to account for the recently observed decline in mortality from (60-70% to ~30-40% (3)).

The best evidence for the value of a lung protective strategy in patients with ALI is a study by the ARDS Network (ARDSNet) comparing conventional mechanical ventilation with a lung protective strategy of ventilation. This study reported a 22% reduction in mortality in patients ventilated using protective ventilation together with more ventilator free and non-pulmonary organ failure-free days (219). Moreover, clinical risk factors including sepsis, aspiration, pneumonia, and trauma did not affect the efficacy of the protective strategy of ventilation (176).

Despite significant advances in the understanding of the pathogenesis of ALI, specific pharmacological interventions, including surfactant therapy, inhaled nitric oxide, glucocorticoids and other antiinflammatory agents, have shown little benefit al phase III trials (173, 220).

There has been considerable preclinical data supporting the potential value of β-2 agonist therapy for the treatment of ALI as it has been suggested that they able to decrease inflammation and upregulate alveolar salt and water transport, hastening the resolution of alveolar edema (221-223). However, only a randomized trial in the UK recently demonstrated that intravenous salbutamol significantly lowered extravascular lung water (224).

Currently lines of investigation are focused on the potencial benefits of enteral feeding (225), the use of statins, which are normally used for the prevention or treatment of cardiovascular diseases and also have significant antiinflammatory, immunomodulatory, and antioxidant effects (226-228), and treatment with bone marrow-derived mesenchymal stem cells (MSCs) as they possess the ability to differentiate into many types of cells and also are able to secrete paracrine factors that reduce the severity of ALI (e.g. growth factors, factors that regulate barrier permeability and antiinflammatory cytokines) (229, 230).

3.4. Animal models

Modeling human disease in animals has contributed significantly to our understanding of lung physiology in health and in disease (231).

As human studies provide important descriptive information about the onset and evolution of the physiological and inflammatory changes leading to formulate hypothesis about the mechanisms of injury, animal models provide a bridge between patients and the laboratory bench to test these hypothesis (232).

The hypotheses formulated in human studies are difficult to test in humansbecause of the many clinical variables that are difficult to control in critically ill patients. Therefore, these hypotheses can be tested directly in animal models together with the results of *in vitro* studies in order to assess their relevance in intact living systems. Without animal models there would be no way to test clinical hypotheses generated in patients using intact biological systems, and there would be no way to validate the importance of fundamental laboratory findings without going directly to human experimentation (232).

Ideally, animal models of ALI should reproduce one or more features of human ALI, including rapid onset (hours) after an inciting stimulus, evidence of pulmonary physiological dysfunction (e.g., abnormalities of gas exchange, decreased lung compliance), histological evidence of injury to the lung parenchyma (endothelium, interstitium, epithelium), and evidence of increased permeability of the alveolar-capillary membrane. As well, the evolution of the injury and repair should also be reproduced, as the responses of the lungs to injury change with time. Ideally, the injury should evolve over time if the animals are supported for prolonged periods or even if specific studies focus on a narrow time frame (4, 232). However, no single animal model reproduces all of the characteristics of ALI/ARDS in humans, and most of the existing animal models are relevant for only limited aspects of human ALI/ARDS (4, 232).

There are many anatomical and physiological differences between animals and humans that influence the response of the lung to an acute injurious stimulus and affect the evaluation of lung injury (233):

(I) Respiratory rate: in humans an adult respiratory rate of ~12–16 bpm whereas in mice rise to ~250–300 bpm, rendering absolute respiratory rate inadequate as a parameter of ALI in mice (4, 5).

(II) Gross and microscopic anatomy: mice and rats have different lobar anatomy, fewer branches of the conducting airways proximal to the terminal bronchioles. As well, both, alveoli and thickness of the blood–gas barrier are smaller in the lungs of mice and rats compared with humans.

(III) Inflammation: rodents have fewer circulating neutrophils (~10–25%) than humans (~50–70%) and do not express defensins. The neutrophil collection of CXC chemokines differs between rodents and humans (keratinocyte-derived chemokine KC [CXCL1] and macrophage inflammatory protein [MIP-2] in rodents and IL-8 in humans) (232, 234).

(IV) ALI settings: murine lungs rarely demonstrate hyaline membranes under enhance permeability situations.

(V) ALI development: in humans, ALI is developed in patients affected by the mechanisms involved in a primary illness (e.g., sepsis) and/or therapeutic modalities used for supportive care (e.g., mechanical ventilation) whereas animal studies frequently use young mice with no comorbidities (232).

For all of these reasons, the responses of animal and human lungs to an injurious stimulus cannot be expected to be identical or perhaps even similar.

To address this problem in 2010, an Official Committee was established in American Thoracic Society (ATS) Workshop (4) to determine the main features that characterize ALI in animal models and to identify the most relevant methods to assess these features. They concluded that the main features of experimental ALI include histological evidence of tissue injury, alteration of the alveolar capillary barrier, presence of an inflammatory response, and evidence of physiological dysfunction; they recommended that, to determine if ALI has occurred, at least three of these four main features of ALI should be present. However, the Committee emphasized that the list of ALI features is intended as a guide for investigators in which they might choose according to the experimental questions addressed and the specific aspects of each experimental design chosen.

Commonly used animal models are based on clinical disorders that are associated with ALI/ARDS in humans. Investigators have tried to reproduce each of these risk factors in a variety of animals, and the frequency with which each model has been reported is shown in Table 3 (232). Each model has their own characteristics, advantages and similarities with ALI human models. However, animal models of

ventilator-induced lung injury are the more frequently studied because is the only model that has affected clinical practice and improved survival in humans (232).

Table 3. Percentage of the different animal models used to study Acute Lung Injury.

ANIMAL MODELS OF ACUTE LUNG INJURY	%
Mechanical Ventilation	30
LPS	19
Live bacteria	16
Hyperoxia	12
Bleomycin	10
Oleic acid	5
Cecal ligation and puncture	4
Acid Aspiration	3

Table modified from reference (226).

4. Ventilator-induced lung injury

Mechanical ventilation (MV) is routinely used for decades to provide respiratory support in critically ill patients. However, its safety for the treatment of ARDS patients has been a matter of concern ever since its introduction into medical practice (235). Yet already in 1974, Webb and Tierney demonstrated for the first time that MV could generate lung lesions in intact animals (236). Since then, several experimental and clinical studies have been performed to clarify the potential drawbacks of MV and its subsequent outcomes according to the strategy applied.

Currently, we should take into account two different concepts related to MV alterations, ventilator-associated lung injury (VALI) and ventilator-induced lung injury (VILI). VALI is referred to the additional injury imposed on a previously injured lung by MV in either clinical settings or in experimental studies (also termed as two-hit experimental models (237)). Conversely, the term VILI is regarded as a sole method to generate lung injury, which is the direct application of an injurious

MV strategy (238). Here, we are going to focus mainly on VILI and its pathogenesis.

4.1. Determinants of VILI

4.1.1. Mechanical determinants

Barotrauma vs. Volutrauma

The term *barotrauma* is used to describe the lung damage attributable to MV with high peak pressures (239). However, a study performed by Dreyfuss and co-workers (240) suggested that lung distension was more important to cause lung injury than airway pressure *per se*, coining the term *volutrauma*. In order to elucidate this, they ventilated rats with identical peak pressures using high or low tidal volumes (V_T). As a result, they observed that rats subjected to high V_T-high pressure ventilation developed pulmonary edema whereas those subjected to low V_T-high pressure ventilation did not. Subsequently, other groups confirmed and replicated these findings in other experimental models (235, 241, 242).

Therefore, the important fact is trans-pulmonary pressure (i.e. the pressure across the lung: airway pressure [alveolar pressure] – pleural pressure) and not the airway pressure itself (243).

Atelectrauma

It is important to highlight that ARDS patients had their lungs heterogeneously injured leading to their alveoli to pass thought one of three following conditions: (I) fluid-filled or collapsed, and thus closed and not inflated; (II) collapsed or filled with fluid at end-exhalation, but opened and air-filled at end-inspiration; or (III) expanded and aerated throughout the respiratory cycle (244).

As the collapse of an alveolus causes shear stress not only on its own walls but also on those of adjacent alveoli, heterogeneously MV lungs are susceptible to cyclic damage by shear stress resulting from repetitive alveolar collapse and overdistension (or recruitment-derecruitment), termed *atelectrauma* (239).

Thus, the application of positive end-expiratory pressure (PEEP) effectively opens the distal airways, maintaining recruitment throughout the ventilatory cycle (243).

The application of PEEP during VILI development has been associated with a preservation of the integrity of the alveolar epithelium besides few alterations including endothelial blebbing and interstitial edema (240). However, the influence of PEEP in VILI mustbe studied with caution according to the V_T used.

Protective ventilatory strategies: Low V_T and PEEP

The bases of lung protective strategies reside in: (I) prevention alveolar overdistention by limiting V_T/ airway pressures; and (II) to maintain alveolar recruitment throughout the respiratory cycle through the addition of PEEP.

Webb and Tierney (236) showed that edema was lessened by PEEP application during MV with high peak airway pressures and they attributed the beneficial effect to the preservation of PS activity.

Later studies demonstrated that V_T reduction, maintaining the same level of PEEP, significantly reduced both endothelial and epithelial injury and this was associated with lower histological lung injury severity scores (245). Furthermore, clinical trials reported significant decreases in the levels of both pulmonaryand systemic inflammatory mediators in patients ventilated using lung protective strategies (246). Moreover, the ARDSnet trial determined a reduction of 22% in the mortality rates of those patients MV with lower V_T (6 ml/kg) compared to those ventilated with traditional V_T (12 ml/kg) (219). Besides, the protective effect of PEEP was highlighted by Amato and colleagues, which demonstrated that the use of high levels of PEEP to alveolar recruitment resulted in improved 28 day-mortality (247).

4.1.2. Biotrauma

Barotrauma/Volutrauma and *atelectrauma* has been considered the principal causes of VILI until the *biotrauma* hypothesis emerged (248).

Biotrauma relies on the hypothesis that lung tissue stretching might result in lung injury through the release of inflammatory mediators and leukocyte recruitment (249, 250). This inflammatory reaction may not be exclusively of lungs, it may also involve systemic circulation, altering distal end-organs and therefore providing an explanation to the observation that most patients with ARDS die from multiple organ failure rather than hypoxemia (7, 251).

This hypothesis is supported by several clinical trials that observed that ARDS patients ventilated with a protective strategies exhibited lower bronchoalveolarlavage fluid and/or plasma concentrations of inflammatory mediators than patients ventilated with control strategies (252-254). Intriguingly, one of these studies observed an increased of most of antiinflammatory cytokines rather than proinflammatory (254), emphasizing that it remains unclear whether mechanical ventilation affects the balance of cytokines toward pro- or anti-inflammation (255).

Accordingly, experimental studies also suggested that MVcould influence the proinflammatory/antiinflammatory balance in the lungs. Specifically, Tremblay et al. (250) showed in unperfused rat lungs that high V_T ventilation with zero PEEP resulted in a dramatic increased of proinflammatory cytokines levels (TNF-α, IL-1β and macrophage inflammatory protein [MIP-2]) in lung lavage compared with controls. However, using the same model of unperfused rat lungs, others found only slightly higher IL-1β and MIP-2 bronchoalveolar lavage fluid concentration in injuriously MV rats compared with control ones, together with no changes in TNF-α lung lavage levels among groups (256, 257). The authors concluded that injurious MV strategies do not necessarily result in primary production of proinflammatory cytokines in the lungs (257).

As a result, the concepts *barotrauma/volutrauma*, *atelectrauma* and *biotrauma* are currently considered as interrelated and not exclusive in the induction of stress failure since the mechanical determinants seem to induce *biotrauma*. Thus, ventilation with high V_T or pressures can cause release of proinflammatory mediators by a number of different mechanisms, all of which appear to be clinically relevant (248):

- Injurious MV can cause stress failure of the plasma membrane and epithelial and endothelial barriersleading tonecrosisand subsequent liberation of inflammatory mediators that will stimulate other intact cells to produce such mediators.
- Stress failure of the barriers causes loss of compartmentalization with the consequent spreading of inflammatory mediators throughout the body.
- MV with increasing positive pressures raises the pressure in the pulmonary circulation and thus vascular shear stress, stimulating endothelial cells.
- Less injurious ventilation strategies that do not cause tissue destruction can elicit release of mediators by more specific mechanisms, presumably through activation of stretch-activated signaling cascades, termed as

mechanotransduction. As the sensing mechanism of these physical forces and the translation into cellular signals is largely unknown, several experimental studies *in vitro* and *in vivo* observed that mechanical stretch induce distinct patterns of gene expression including genes involved in immunity and inflammation, stress response, metabolism and transcription processes (258, 259).

4.2. Pathogenesis

4.2.1. Microscopic pathology

Animal lungs injured by MV present a pattern of atelectasis, severe congestion and enlargement due to edema, which is associated with severe endothelial and epithelial abnormalities, the structural counterpart of permeability alterations (235, 236, 240, 260, 261).

Tsuno and coworkers (262) microscopic examination revealed that baby pig lung's subjected to high-pressure MV during 22h presented severe diffuse alveolar damage,with hyaline membranes, alveolar hemorrhage, and neutrophil infiltration. Also, small animals experimental studies depicted that under high peak pressures there were wide spread alterations of endothelial and epithelial barriers observed by electron microscopy (240, 260, 261, 263) together with edema presence. Specifically, they observed ATI cells discontinuities with some areas completely destructed leaving a denuded basement membrane, hyaline membranes filling the alveolar spaces and endothelial cells alterations including their detachment from their basement membrane resulting in the formation of intracapillary blebs or even endothelial cell breaks, allowing direct contact between neutrophils and the basement membrane (240, 261).

However, there is an obvious relationship between the duration and severity of the mechanical injury and the overall appearance of the lung. Also, the animal model used entails different outcomes. Thus, edema is developed so rapidly in small animals that the lack of time prevents neutrophil infiltration. In contrast, larger animals need several hours to produce patent edema, time enough for activation, adherence, and significant migration of neutrophils into airspaces (262, 264).

4.2.2. Alveolar edema

As previously described, VILI may produce breaks in the alveolar-capillary barrier leading to alveolar hemorrhage (240, 260, 261). Thus, this disruption can be also promoted by non-uniform mechanical lung inflation altering microvascular pressure, termed shear stress (235). However, alveolar edema presence could be alsoproduced due to alterations in the alveolar-capillary barrier permeability.

Experimental studies have implicated epithelial and endothelial permeability changes in the presence of high content-protein edema in the alveolar space (243).

Increase of epithelial permeability to small hydrophilic solutes occurs as lung volume increases, being this a physiologic phenomenon. The clearance of aerosolized ^{99m}Tc-DTPA increased when the functional residual capacity was increased by applying PEEP during MV (265), or during spontaneous ventilation (266) in sheep. The same observation has been made in humans (267, 268).

However, only major increasesin lung volume alter epithelial permeability to largemolecules during static inflation (235). Hence, some studies depicted that increased static inflation of fluid filled lung lobes in sheep led to the passage of larger solutes across the epithelium, a finding observed inother models (269, 270). Moreover, the redistribution of ^{125}I-labelled albumin intothe extravascular space in MV rats demonstrated the presence of increased microvascular permeability (261). Furthermore, similar experimental studies in other species confirmed the alteration of endothelial permeability to solutes of both small and large molecular weight (271, 272).

In contrast to the clear evidence for increased permeability, relatively little is known about the contribution of hydrostatic pressures to the development of pulmonary edema in MV (243).

4.2.3. Inflammation

The role of the innate immune response and inflammation in the pathogenesis of VILI has been widely studied in recent years. Researchers have used a variety of experimental models to determine the effects of MV or mechanical strain on the expression of biological markers of inflammation or injury, including animal models,

ex vivo lung preparations and isolatedalveolar epithelial cells (238).

The role of inflammatory cells

Although many resident lung cells can produce inflammatory mediators, alveolar macrophages have a large capacity for cytokine and chemokine production, as well as nitric oxide and reactive nitrogen species elaboration (273). Specifically, several studies depicted a possible role of alveolar macrophages in the initial pathogenesis of VILI.

Mechanical deformation of human alveolar macrophages *in vitro*, has been shown to increase the expression of IL-8 and matrix-metalloproteinase-9 (MMP-9) together with an increase in nuclear translocation of the transcription factor nuclear factor kappa-B (NFκB) after 30 min of cyclic strain (274).

Frank and colleagues work also suggests that macrophage activation is an early and critical event in the initiation of VILI. They demonstrated that addition of bronchoalveolar lavage from rats exposed to injurious MV during 20 minutes induced the activation of naïve primary alveolar macrophages in culture. Furthermore, they observed that macrophage depletion decreased ventilator-induced endothelial and epithelial injury (273), supported by Eyal and co-workers (275).

In addition to macrophages, neutrophils have been un-equivocally implicated in the pathogenesis of ALI and ARDS (276) and seem to be the major effector cells in the generation of the tissue injury characteristic of VILI (277).

One of the first studies proposing that MV could lead to an inflammatory response used a model of neutrophil depletion by nitrogen mustard. Kawano et al. (264) demonstrated that the neutrophil-depleted animals had markedly improved oxygenation and decreased pathologic evidence of injury after MV versus a control group treated with the lavage and ventilatory protocol alone.

Further evidence for the central role of the neutrophil in VILI has been provided by the work of Zhang and colleagues. In this study, alveolar lavage fluid obtained from ventilated patients with ARDS was incubated with neutrophils from normal volunteers. As a result, markers of neutrophil activation were significantly higher in those ventilated conventionally compared to those ventilated with a lung protective strategy (278). Interestingly, alveolar recruitment of neutrophils by instilling a chemmoatractant does not result in lung injury (279), indicating that other mediator

possibly cytokines, are necessary to activate leukocytes.

The role of inflammatory mediators

It is widely accepted that increased production of cytokines in the lung plays a key role in VILI. To examine the mechanisms of cytokine generation during MV, *in vitro*, *ex vivo* and *in vivo* models have been conducted (256).

Upon stretch, cultured alveolar cells produce inflammatory mediators such as TNF-α IL-1β, IL-6, IL-8, IL-10 (274, 280). There are several reports of MV increased cytokines and chemokines in whole-animal models. Specifically, MV with high V_T results in increased levels of the proinflammatory cytokines in lavage fluid, including TNF-α and MIP-2 (281-283). However, other models under injurious MV detected no significant changes of TNF-α in the alveolar lavage though other proinflammatory levels were augmented (284).

Also, the use of isolated lung models allowed determining changes in the levels of many inflammatory mediators in VILI. The work of Tremblay and co-workers (250) previously mentioned, demonstrated that high V_T, zero PEEP MV induced a greater increase in airspace of TNF-α IL-1β, IL-6, IL-10, MIP-2, and interferon-γ than low V_T with or without PEEP application. Furthermore, similar to the study of Tremblay et al (250), Veldhuizen and colleagues (285) found that in isolated mouse lungs, ventilation with a tidal volume of 20 mL/kg without PEEP resulted in significant increased in BAL levels of TNF- α and IL-6.

On the other hand, clinical studies seem to support the concept that injurious MV promotes a pulmonary inflammatory response and cytokine decompartmentalisation. Ranieri and colleagues (246) reported significant decreases in bronchoalveolar fluid and plasma concentrations of many inflammatory mediators (TNF-α, IL-6 and IL-8) in patients MV with a lung protective strategy. Moreover, the ARDSnet trial depicted that patients ventilated with a lung protective strategy had a greater decrease in levels of plasma IL-6 (219).

Despite the fact that low V_T MV ameliorates the inflammatory response, some studies confirmed that subjects subjected to MV may develop a proinflammatory state (286, 287). In fact, it is not yet established the ventilatory strategy that is the most effective in limiting inflammation.

Other mediators implicated in VILI include coagulation factors, such as

plasminogen activator inhibitor-1, hormones, such as angiotensin-II and lipid derived mediators, such as cyclooxygenase and lipoxygenase (288). As well, some studies observed the implication of metalloproteases in the early stages of VILI (289) and ROS production in response to elevated mechanical stress (290-292).

4.2.4. Pulmonary surfactant alterations

PS plays a role in VILI in two related ways. Firstly, PS dysfunction or deficiency seems to amplify the injurious effects of MV and, secondly, MV itself can impair PS function thereby exacerbating the existing damage (243).

It is widely accepted that mechanical stretch of ATII cells in vitro stimulates surfactant release (293). As well some animal models observed that total PS increased (294, 295). However, injurious MV strategies of high V_T and zero PEEP lead to alterations in functional PS and a decreased LA/SA ratio (285, 294, 296-298).

PS biophysical function impairment may contribute to VILI in several ways (243): (I) Alveoli and airways tend to collapse with generation of shear stress as they are reopened; (II) The irregular expansion of lung units increases regional stress forces through interdependence; (III) The transvascular filtration pressure is increased, promoting edema formation (299).

In addition, PS system is thought to have important immunoregulatory functions (148), which may become impaired through MV.

Therefore, improving the presence of an increased pool of functioning PS might lessen lung injury by MV as some studies suggested that surfactant therapy contributes to reduce mortality in the neonatal respiratory distress syndrome and may decrease lung injury (300).

4.2.5. Consequences following VILI

Abnormal or dysregulated repair processes are associated with increased morbidity and mortality following ALI/ARDS (301). However, the factors leading either to the fibrotic phase or resolution are incompletely understood. Nevertheless, some studies suggest that some transcriptional responses in ALI genes involved in inflammation and repair are differentially expressed simultaneously very early in the

course of injury (302), and many mediators are common to both processes. This is further supported by evidence that patients with well known chronic fibrotic lung disorders have persistently elevated levels of ALI related cytokines and chemokines in alveolar lavage samples (303, 304).

Regarding to VILI, few studies have been conducted in order to characterize the potential mechanisms that occurs during resolution and repair following injurious MV (305-307). These studies observed that MV induced severe injury in the lungs characterized by histologic injury and edema, but they were able to repair spontaneously in the absence of further ventilation. Furthermore, Curley and co-workers (306) studied the evolution of several inflammatory and fibroproliferative markers throughout two-weeks, detecting that proinflammatory cytokines returned to baseline within 24h, while anti-inflammatory remained increased for48 h. Moreover, VILI generated a marked but transient fibroproliferative response, which restored normal lung architecture represented as absence of evidence of fibrosis at 7 and 14 days.

Also, González-López et al (308) studied the mechanisms of repair after VILI using a model of injurious MV followed by a protective MV strategy during 4 hours. They also observed that surviving animals were recovered from the injury characterized by increased cell proliferation, lower levelsof collagen, and higher levels of MIP-2 and MMP-2.

Therefore, these data suggest that VILI may be potentially reversible, and that the repair process depends on both an adequate inflammatory response and extracellular matrix remodeling. However, further investigation must be done in order to elucidate the precise roles of the factors involved in the resolution and repair processes following VILI.

Objectives

The lung is a delicate organ that can develop significant dysfunction in response to minor injury. The pathophysiology of acute respiratory distress syndrome (ARDS) or the less severe condition known as acute lung injury (ALI) (2) is currently thought to begin with an inflammatory response induced by extrapulmonary injury (sepsis, severe trauma, acute pancretitis, etc.) or direct pulmonary injury (pneumonia, aspiration of gastric contents, pulmonary contusion, etc.) (3). The inflammatory response increases alveolar epithelial and pulmonary vascular endothelial permeability, causing alveolar filling (3, 4). The alteration of the pulmonary surfactant system complicates the clinical picture (5).

Lung surfactant serves to stabilize the alveoli and distal airways at low lung volumes (1), and deficit or alteration of this macromolecular complex strengthens intraalveolar edema, impairs lung compliance, andresults in ventilation-perfusion mismatch (including shunt flow due to altered gas flow distribution) and hypoxemia (1, 5, 6). Critical hypoxemia results in the need for mechanical ventilation, thereby providing the context in which ventilator-induced lung injury (VILI) can develop (7). It is thought that VILI is generated as a result of volutrauma (intensified tissue tensions at the junctions of closed and open alveolar units when subjected to high alveolar pressure) and/or atelectrauma (caused from the cyclical airspaceopening and closing) (7). These stresses might further stimulate the inflammatory response (termed biotrauma) resulting in progressive lunginjury and systemic inflammation (7).

The current respiratory support in ALI or ARDS consists of low tidal volume (to reduce volutrauma) and appropriate positive end-expiratory pressure (PEEP) and/or FiO_2/PEEP ratio (to reduce atectrauma) (8). The application of PEEP is thought to be useful in counteracting increased surface tension (thereby reversing the resulting atelectasis). PEEP increases end-expiratory airspace pressure, but since airspace opening pressures can vary markedly between and within patients, applying PEEP to reverse or limit dorsal-caudal atelectasis will almost always come at the expense of over-distending ventral lung regions and other areas having lower opening pressures (9).

Given the importance of ventilatory management for acute respiratory syndrome (ARDS or ALI) (7, 8), investigators have started to explore the effects of ventilation in healthy lungs. Animal models exposed to conventional and injury ventilator strategies

have being used to understand the mechanisms of lung injury induced by mechanical ventilation.

In this thesis, healthy rats have been exposed to two different ventilator strategies (10):

- Injurious high-stretch ventilation (HV) with high tidal volumes (V_T = 25 ml/kg) and without PEEP application (ZEEP = 0 PEEP).
- Conventional low-stretch ventilation (LV) with moderated tidal volume (V_T = 9 ml/kg) and application of positive end-expiratory pressure (PEEP=5 cm H2O and FiO_2/PEEP ratio of 0.3/5).

The **main objective** of this thesis was to study morphological and functional changes in the lungs after exposition to injurious or conventional mechanical ventilation and to identify the relationship among high-stretch ventilation, inflammation, edema, and surfactant dysfunction to understand the mechanisms involved in ventilator-induced lung injury (VILI). Two important questions, currently under debate (9), will be answered in this study: whether changes in surfactant composition and in surface tension precede the onset of VILI, and whether VILI occurs only in animal models when lung surfactant is inactivated.

The **thesis is composed of three chapters** which evaluate:

1. Lung injury after high-stretch ventilation with a complete analysis of the composition, structure, and functional activity of lung surfactant as well as the causes of its inactivation after high-stretch ventilation (*Chapter 1*).
2. Factors involved in the resistance to ventilator-induced lung injury, since identification of such factors may help to develop prophylactic therapies or early interventions, prior to exposition to mechanical ventilation (*Chapter 2*).
3. Consequences of prolonged conventional low-stretch ventilation, with or without a previous short exposition to injurious high-stretch ventilation. This would allow determination of whether inflammation in the lung was directly related to the duration of conventional low-stretch ventilation (with FiO_2/PEEP ratio of 0.3/5) and whether prolonged conventional low-stretch ventilation has beneficial or damaging effects in surviving rats exposed to injurious high-stretch ventilation.

Materials and Methods

1. Animals and experimental model.

Male *Sprague-Dawley* (SD) rats (Harlan Iberica, Spain), weighing 325-375 g were acclimated to day/night cycles of 12 hours and fed with *purina* fodder (Nestlé S.A. Vevey, Switzerland). The animals were anesthetized with ketamine (90 mg/kg) and diazepan (5 mg/kg) by intaperitoneal route and the anesthesia was maintained during the intervention by a continuous perfusion of ketamine (50mg/kg/h) and midazolam (8mg/kg/h) through the femoral vein (infusion rate 10 mL/kg/h). The administration of these drugs was made under sterile conditions.

Once anesthetized, a surgical tracheotomy was performed and a 14-*gauge*cannula was secured in place and connected to a mechanical ventilator (Babylog 8000 Plus Dräger, Germany). In addition, a 20-*gauche* catheter was inserted into the left carotid artery for monitoring arterial blood pressure (Hewlett Packard, Model 66S, Geneva, Switzerland). The surgical process was performed under sterility conditions. Body temperature was maintained constant during the experimental procedure using a self-regulated heat source (Challomer Ltd. Marketing, England).

Experiments were carried out following the Principles of Laboratory Animal Care (EU 609/86 CEE, Real Decreto 1201/05 BOE 252, Spain) and the guidelines for the care and use of experimental animals of University Hospital of Getafe (UHG). UHG Institutional Review Board approved the protocol.

We established two mechanical ventilation strategies according to often settings applied in clinic and experimental studies (10):

- Low-stretch group, ventilated with conventional parameters: Tidal Volume [V_T] = 9 ml/kg, positive end-expiratory pressure [PEEP] 5 cmH_2O.
- High-stretch group, ventilated with injurious parameters: V_T = 25 mL/kg, zero PEEP**.**

In both groups, respiratory rate was 70 bpm, inspiratory time 0.35 sec., expiratory time 0.56 sec. and FiO_2 0.35.

The animals were ventilated for an equilibration period of 30 min using the low V_T ventilation parameters. Then, the assigned ventilator strategy was administered randomly starting at t=0 min. Dead-space ventilation (the volume of air inhaled that does not take part in the gas exchange) was increased in animals ventilated with high V_T

(by increasing the length of the ventilatory circuit) to attain comparable values of $PaCO_2$ (30-40 mmHg) during the ventilation period. The animals were ventilated with the parameters assigned during the time established in each experimental design (detailed in each chapter).

2. Registration of hemodynamic and ventilatory parameters.

At the beginning and end of each ventilator strategy (according to the experimental design) were registered the following parameters: mean arterial pressure (MAP) and mechanical ventilator parameters including peak inspiratory pressure (PIP), peak airway pressure (P_{AW}) and dynamic respiratory system compliance (C_{RS}).

3. Biological sampling.

At the end of the ventilatory period animals were sacrificed by exsanguination and subsequently we proceed to sampling (Figure 1).

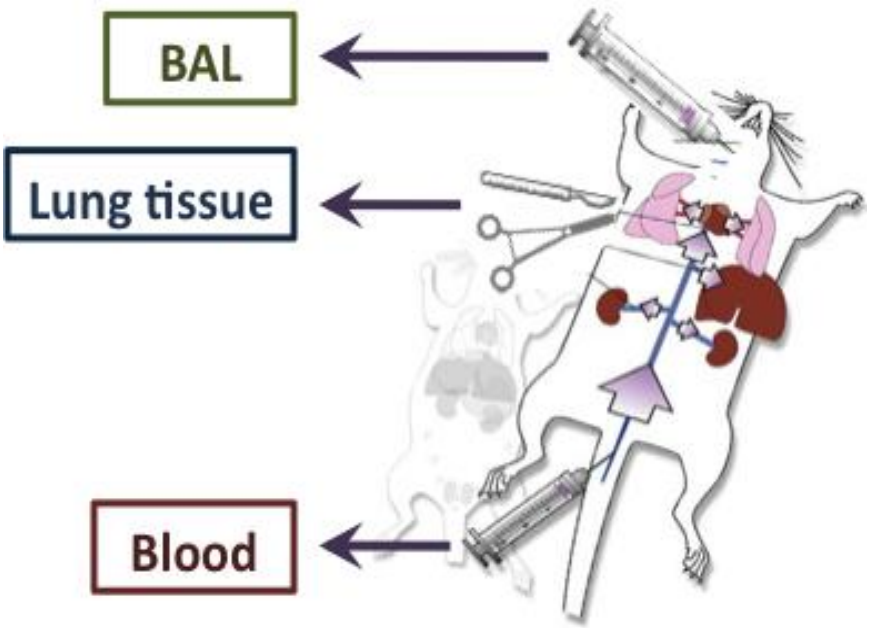

Figure 1: Sampling diagram.

Plasma: Blood samples were drawn at end times (according to the experimental protocol) to determine arterial blood gases and perform biochemical analysis.Also, 2 ml of blood were centrifuged at 3500 rpm during 10 min at 4ºC and the resulting plasma was store at -80ºC until its utilization for damage markers determination (Figure 2).

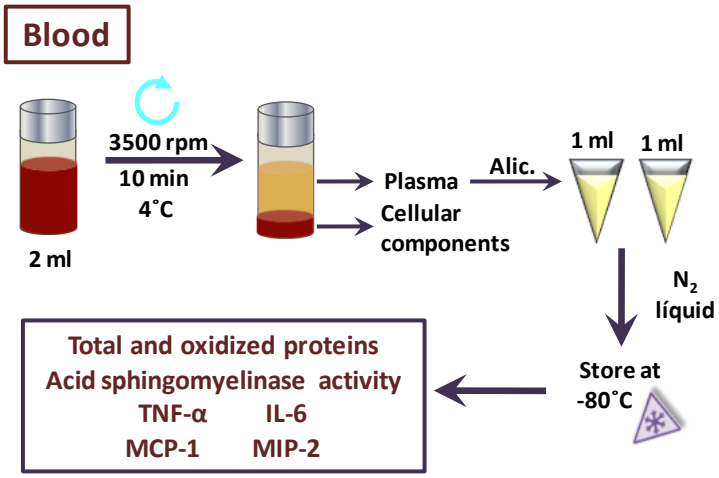

Figure 2: Plasma collection procedure.

Cell-free bronchoalveolar lavage: bronchoalveolar lavage was performed instilling 4 times 10 ml of saline (NaCl 0.9%) at 4ºC. The bronchoalveolar lavage acquired was centrifuged at 400g for 10 min at 4ºC to obtain the *pellet* of alveolar fluid cells. Total bronchoalveolar lavage cell-free (BAL) volume was recorded and stored at -80ºC in order to isolate pulmonary surfactant (PS). An aliquot was separated to perform biochemical analysis (Figure 3).

Lung tissue: cardiopulmonary block was extractedonce lungs were washed. The left lung was expanded by intratracheal instillation of 10 ml formaldehyde with 20 cm H_2O pressure for histological analysis. On the other hand, the lower lobe of the right lung was divided in 3 pieces and stored at -80ºC avoiding tissue deformation to perform gene expression analysis (Figure 4).

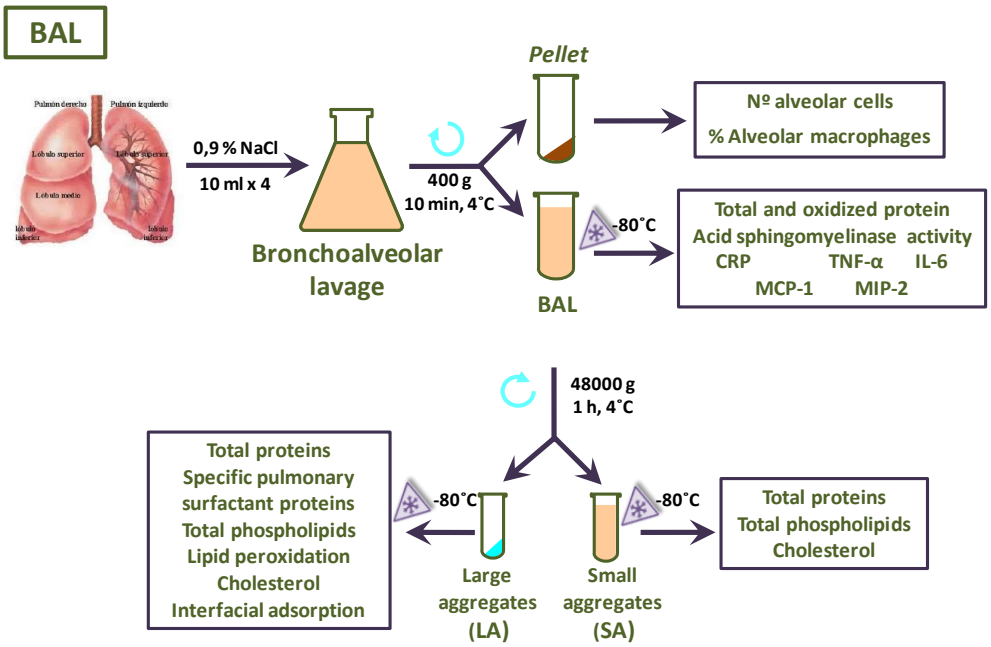

Figure 3: Bronchoalveolar lavage free of cells (BAL) processing and isolation of Pulmonary Surfactant fractions.

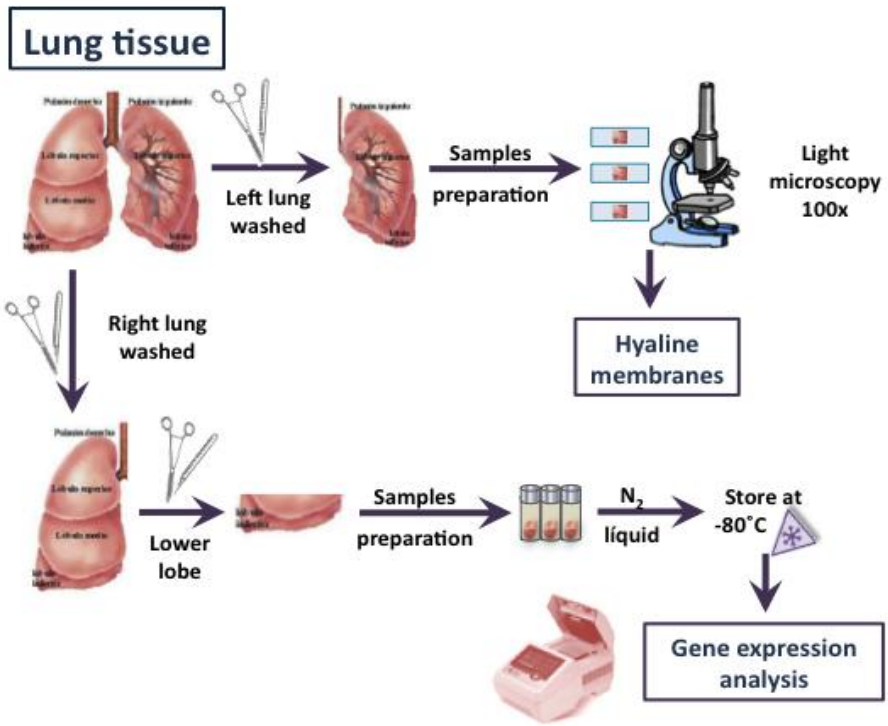

Figure 4: Lung tissue collection process: sampling to accomplish gene expression and histological analysis.

4. Arterial blood samples analysis.

Determination of arterial blood gases was accomplished using a blood gas analyzer (Gem Premier 3000, IL Instrumentation Laboratory). Levels of lactate, glucose, creatinine, lactate aminotrasferase (LDH) and creatinine kinase (CK) in arterial blood were assessed using a chemical analyzer (Integra 700, Roche Diagnostics).

5. Alveolar fluid cells analysis

Cellular *pellet* obtained from bronchoalveola rlavage centrifugation was resuspended in 1 ml of a solution 1:1, PBS: *Streck Cell Preservative* (Streck, Omaha, USA). Total number of BAL cells was determined assessing cell viability with trypan blue dye exclusion by counting in a Neubauer chamber (Marienfeld, Germany) using 15 μl of cell suspension.

Flow cytometric analysis of BAL cells

Cells were washed with PBS, centrifuged at 1500 rpm during 10 min at 4ºC and resuspended in a final volume of 2 ml of PBS. This cell suspension was used to assess alveolar macrophages and neutrophils proportion in alveolar fluid cells using a Fluorescence Flow Cytometer (FACScalibur, BD Biosciences, San Diego, USA).

This determination was accomplished performing a specific surface labeling using the following specific monoclonal antibodies: mouse anti-rat CD11c (AbDserotec, Oxford, UK), which recognizes specifically rat alveolar macrophages and mouse anti-rat RP-1 (BD Biosciences, San Diego, USA), which binds to rat peripheral blood neutrophils. Subsequently, cells were incubated under darkness conditions with a fluorescein (FITC)-conjugated goat anti mouse IgG secondary polyclonal antibody (AbDserotec, Oxford, UK).

In order to avoid unspecific unions, cells were incubated with RPMI media supplemented with 10% bovine fetal serum (FBS) during 30 min previous to the incubation with specific antibodies. Among incubations, cells were washed with PBS and centrifuged at 1200 rpm during 5 min at 4ºC. Monoclonal antibody rat IgG2A (AbDserotec, Oxford, UK) was used as negative control in both cases.

After specific incubations, cells were washed and resuspended in 500µl of PBS. 10.000 total events were counted and analyzed using BD CellQuest Pro™ Software (BD Biosciences, San Diego, USA) applying settings previously described to obtain specific forward (FSC)/ sideward (SSC) scatter plots of alveolar fluid cells from rodents (309, 310).

6. Histological analysis.

Samples preparation

Pulmonary hilium zones from the left lung were collected and fixed with formol buffered 10% during 48h. Subsequently, samples were dehydrated performing an increment alcohols procedure (70º-96º-100º), fixated with xilol and submerged in paraffinduring 1h each process. Each paraffin block was cut in 7µm sections and stained by haematoxylin-eosin technique. Briefly, samples were dewaxed with xilol and rehydrated with decreasing graded alcohols procedure (100º-96º) during 10 min each, before washed them with distilled water. Subsequently, samples were submerged in eosin-phloxine during 5 min, dehydrated again by increment alcohols procedure and fixated with xilol to assemble them. Slides were stored at room temperature, and protected from light before use.

Injury score quantification

A modify injury score was used to quantify pulmonary damage (311, 312) examining10 random fields for each section by light microscopy (40x). A score of 0, 1, 2or 3 was assigned if none, one, two or more than two membranes were found, respectively. The mean of all values of the examined fields was assigned as a measure of the degree of lung injury (305).

7. Isolation of large and small aggregates of pulmonary surfactant.

BAL was centrifuged at 100,000g for 1h at 4ºC in an ultracentrifuge XL-90 model (Beckman Coulter, Fullerton, USA) to separate the large surfactant aggregates (LA) constituted by multilamelar vesicles of phospholipids and PS specific apolipoproteins SP-A, SP-B and SP-C (313) from the small non-functional surfactant

aggregates (SA), which remain in the supernatant (314)(Figure 3). The resulting precipitate, LA fraction, was resuspended with 400 µl of saline 0.9%, reconstituted with a potter and aliquoted and stored at -80ºC. 2 ml of supernatant, SA fraction, were collected stored at -80ºC until it analysis.

8. Total amount of phospholipids quantification.

Lipid extraction was performed to determine the content of total phospholipids (PL) in LA and SA, by chloroform-methanol extraction (315) using 1 ml of SA and 50 µl of LA led to 1 ml by adding NaCl 0.9%. The organic phase of each sample was evaporated with a rotary evaporator R (Büchi, Flawil, Switzerland) and resuspended with 1 ml of chloroform/methanol (2/1, v/v). Total amount of PL from SA and LA was assessed from the organic extracts obtained by an analysis described by Rouser and col. (316) of phosphorous quantification.

Briefly, samples (200µl of LA and 300 µl of SA) and standards (KH_2PO_4 0.05 mg/ml) were dried in a sand bath before adding 450 µl of perchloric acid 70% ($HClO_4$) and incubate covered during 30 min at 260ºC to accomplish the mineralization of the phosphorous. The quantification of mineralized phosphorous was achieved through a colorimetric reaction by adding ammonium molybdate (2.5%, w/v) which conform a complex with phosphorous. This complex was reduced by adding ascorbic acid (10%, w/v), which formed a colored compound after 8 min at 100 ºC of incubation stooped with ice. Absorbance was measured at 820 nm in a spectrophotometer model DU 800 (Beckman Coulter, Fullerton, USA) and color absorbance values were directly related to phosphorous concentration by interpolation into a calibration curve built with known concentration standards.

9. Lipid peroxidation assessment.

Lipid hydroperoxides (LPO) present in the organic extracts of LA were assessed by the FOX method (317). This process is based on the ability of LPO to oxidize Fe^{2+} to Fe^{3+}. This oxidation is detected using thiocyanate ion as chromogen. To this purpose we used the Lipid Hydroperoxides Kit from Cayman (Cayman Chemical Company, Ann Arbor, USA). Samples (1.5 nmol PL/µl) and standards (13-hydroperoxy acid-

octadecadienoic acid [13-HpODE] 50μM) were incubated covered during 5 min at room temperature (RT), with 4.5 mM ferrous sulfate reagent in 0.2 M hydrochloric acid and ammonium thiocyanate 3% methanol (v/v). Absorbance at 500 nm was measured in a spectrophotometer model DU 800 (Beckman Coulter, Fullerton, USA)and color absorbance values were directly related to LPO concentration by interpolation into a calibration curve built with known concentration standards (0 to 5 nmol/mlof 13-HpODE).

10. Cholesterol quantification.

The presence of cholesterol (Ch) in LA and SA was determined by a colorimetric enzymatic assay using the CHOD-POD Enzymatic Colorimetric kit (Spinreact, SantEsteve de bas, Spain). The method is based on the *cholesterol oxidase* activity in a set of chained reactions ending in the formation of a colored compound. A first reaction is performed by *cholesterol esterase*, which breaks down Ch esters into Ch and fatty acids. Total free Ch in each sample is then oxidized by *cholesterol oxidase* into 4-cholestenone and H_2O_2. The colorimetric reaction takes place between H_2O_2, phenol and 4-aminophenazone to produce quinonimine, a substance with a rosy color. Briefly, 10 μl of Ch standard (200 mg/dl), LA and SA (1:10) samples were mixed with 1 ml of reactive mixture containing the enzymes above mentioned in a PIPES buffer pH= 6,9 and phenol. This mixture was gently blended and incubated during 10 min at RT until its absorbance lecture at 505 nm in a spectrophotometer model DU 800 (Beckman Coulter, Fullerton, USA).

11. Total protein determination.

Total content of protein was determined in BAL, LA and SA samples by a colorimetric reaction based in Lowry method (318), modified by adding sodium dodecyl sulfate (SDS). This method is based on the denaturalization and exposition of protein tyrosine phenolic groups by copper ions under alkaline conditions. Therefore, samples and standards (albumin) were mixed with a solution composed by sodium tartrate 2% (w/v), cupric sulfate 1% (w/v), sodium carbonate 2% (w/v) and one pellet of sodium hydroxide (Merck, Darmstadt, Germany) and incubated for 15 min at RT.

Subsequently, they were incubated during 30 min with Folin-Ciocalteau reactive (Merck, Darmstadt, Germany), turning the yellow color of Folin-Ciocalteau reagent into blue due to Folin-Ciocalteau reduction by tyrosinresidues. The absorbance was read at 700 nm with a spectrophotometer model DU 800 (Beckman Coulter, Fullerton, USA) and color absorbance values were directly related to protein concentration by interpolation into a calibration curve built with known concentration standards.

12. Oxidized proteins quantification.

The presence of oxidized proteins in BAL was determined evaluating their carbonyl content by a spectrophotometric assay binding 2.4-dinitrophenylhydrazine (DNPH) (319). DNPH reacts with protein carbonyls, forming a Schiff base to produce the corresponding hydrazone, which can be analyzed spectrophotometrically. Therefore, 100 µl of BAL samples per duplicate were incubated with DNPH 10mM in HCl 2.5 M during 1 h at RT in darkness and mixed every 15 min. Then, samples were precipitated with trichloroacetic acid (TCA) at 10% during 5 min in ice and subsequently they were centrifuged at 10.000g during 10 min at 4ºC and washed with ethanol/ethyl acetate (1:1, v/v). Finally, proteins were solubilized in 500 µl of guanidinium hydrochloride 6M (FlukaBiochemika, Buchs, Switzerland) and centrifuged at 10.000g for 10 min at 4°C to remove insoluble material traces. Carbonyls were measured spectrometrically at 370 nm in a spectrophotometer model DU 800 (Beckman Coulter, Fullerton, USA). The determination of carbonyls concentration was assessed by inserting the absorbance of each sample into the following equation: Protein Carbonyls (mol/ml) = $[(Abs.)/0.022\mu M^{-1}cm^{-1*}]$ * [500µl (resuspension vol.)/ 100µl (sample vol.)]* The actual extinction coefficient for DNPH at 370nm.

13. Damage markers quantificationin BAL and plasma:

TNF-α

TNF-α presence was evaluated in BAL and plasma samples in duplicated, using the same volume in both types of samples. This valuation was assessed with the BD Biosciences ELISA Colorimetric kit (San Diego, CA, USA) TNF-αrat specific. A polystyrene plate (Maxisorp ®, Nunc, Rochester, USA) was incubated overnight (o/n)

at 4ºC with a monoclonal antibody anti-TNF-α. The next day, after a washing process with PBS/Tween-20 0.05% (v/v), the plate was blocked for 1 h at RT with PBS/FBS 10% (v/v) to prevent non-specific binding. Then, the plate was incubated for 2h at RT with the samples and the calibration curve formed by the TNF-α standard between 2000 to 31.25 pg/ml. After this period, a new washing step was performed to remove unbound protein followed by an incubation with a second anti-TNF-α biotinylated during 1h. Subsequently, another wash was done to remove unbound antibody and the plate was incubated 30 min with a streptavidin-peroxidase reagent, which binds to the biotinylated antibody, until it was washed for the last time, to remove unbound reagent.Finally, the plate was developed with tetramethylbenzidine (TMB) and once the reaction was stopped with 2N sulfuric acid and phosphoric acid 1M, the absorbance was read at 450nm in the plate reader DIGISCAN ELISA plates (AsysHitech GmbH, Eugendorf, Austria).

IL-6

The amount of IL-6 was determined in BAL and plasma samples in duplicate, using the same volume of sample, being the plasma previously diluted ½. This quantification was assessed using a Quantikine ELISA kit Rat IL-6 Immunoassay (R&D Biosystems, Minneapolis, USA). First, it was mixed 50 ul of PBS/FBS 10% (v/v) with 50 ul of the samples and 50 ul of the IL-6 standard to perform a standard curve (2000 to 62.5 pg/ml IL-6 standard) in a polystyrene plate whose wells have bound a monoclonal antibody anti-rat IL-6. The plate was incubated for 2h at RT. Subsequently, after a wash with PBS/Tween-20 0.05% (v/v) to remove unbound protein, the plate was incubated another 2h at RT with a second polyclonal anti-IL-6 coupled to peroxidase, which binds to the IL-6 antibodies previously attached to the plate. After this period, a new washing process was performed to remove unbound antibody and then, the plate was incubated half hour with a reagent mixture made 15 min prior to use, containing hydrogen peroxide and TMB. Finally, the reaction was stopped with dilute hydrochloric acid and the absorbance was read at 450nm in the plate reader DIGISCAN ELISA plates (AsysHitech GmbH, Eugendorf, Austria).

MCP-1

The amount of MCP-1 was evaluated in BAL samples (dilution ½) and in plasma (¼ dilution) samples in duplicate, using the same sample volume. This quantification

was carried out using a Quantikine ELISA kit JE/MCP-1 Rat Immunoassay (R&D Biosystems, Minneapolis, USA). First, 50 ul of the samples and 50 ul of the standard curve (500 to 15.6 pg/ml MCP-1 standard) were mixed with 50 ul of PBS/FBS 10% (v/v) in a polystyrene plate whose wells having attached a monoclonal antibody to rat JE/MCP-1 and incubated for 2h at RT. Subsequently, after washing the plate with PBS/Tween-20 0.05% (v/v) to remove unbound protein, the plate was incubated for 2 h at RT with a second antibody polyclonal anti-rat JE/MCP-1 coupled to peroxidase, which joins the MCP-1 previously bound to the antibodies attached to the plate. After this period, a new washing process was performed to remove unbound antibody and then the plate was incubated during 30 min with a reagent done 15 minutes prior to use, containing hydrogen peroxide and TMB. The reaction was stopped with dilute hydrochloric acid and the absorbance was read at 450nm in the plate reader DIGISCAN ELISA plates (AsysHitech GmbH, Eugendorf, Austria).

MIP-2

MIP-2 was determined in BAL and plasma samples in duplicate, using the same sample volume. This quantification was assessed using a Quantikine ELISA kit Rat CINC-3 Immunoassay (R&D Biosystems, Minneapolis, USA). Initially, 50 ul of the samples and 50 µl of the standard curve (1000 to 31.2 pg / ml CINC-3/MIP-2 standard) were added in a polystyrene plate and mixed with 50 ul of PBS/FBS 10% (v/v). The samples were incubated for 2 h at RT in this plate, whose wells are attached to the specific monoclonal rat antibody CINC-3/MIP-2. Then, after washing with PBS/Tween-20 0.05% (v/v) to remove unbound protein, the plate was incubated for 2h at RT with a second polyclonal antibody anti-CINC-3/MIP-2 coupled to peroxidase that will stick with the MIP-2 antibodies previously attached to the plate. Subsequently, a new wash process was performed to remove unbound antibody and then, the plate was incubated 30 min with a reagent containing a mixture of hydrogen peroxide and TMB made 15 minutes before use. The reaction was quenched with dilute hydrochloric acid and the absorbance was read at 450nm in the plate reader DIGISCAN ELISA plates (AsysHitech GmbH, Eugendorf, Austria).

C-reactive protein

C-reactive protein (CRP) was measured in BAL samples in duplicate, using a specific rat ELISA kit of Chemicon (Millipore, Billerica, USA). To perform this assay the same volume was used in both types of samples being diluted at least 1:20 the BAL samples. First, samples and standards (133.3 to 4.9 mg/ml to perform a curve) were incubated for 30 min at RT in a polystyrene plate whose wells have attached a specific rat antibody anti-CRP. After a washing process with PBS/Tween-20 0.05% (v/v) to remove the unbound proteins, a second anti-CRP antibody coupled to peroxidase was incubated for 30 min at RT in order to bind the CRP previously bonded to the antibody attached to the plate. Finally, after another washing process, the plate was incubated with TMB developing reagent and the reaction was stopped with phosphoric acid for read the absorbance at 450nm in an ELISA plate reader DIGISCAN (AsysHitech GmbH, Eugendorf, Austria).

14. Acid Sphingomyelinase activity determination.

Acid sphingomyelinase (ASMase) activity was determined in BAL and plasma samples performing an enzymatic assay. This assay is based on the ASMaseactivity, which catalyze the hydrolysis of radio labeled sphingomyelin (SM) to ceramide and radio labeled phophocholine.

To this end, first it was dried by evaporation 10.15 nmoles of sphingomyelin (SM) composed by unlabeled SM (Sigma-Aldrich, St. Louis, USA) and [N-methyl-14C] SM (0.15 nmol ([N -methyl-14 C] sphingomyelin, 0.74 µCi/mol (GE Healthcare, Buckinghamshire, UK). Then, the SM was rehydrated in 90 µl of a buffer composed of 0.2M sodium acetate pH 5, 0.5% Triton X-100 and 0.1 M zinc chloride, for 1 h at 45°C under continuous shaking. The rehydrated SM was gently mixed with 10µl of BAL or plasma samples before incubate them 2 h at 37ºC to carry out the enzymatic reaction. Subsequently, the enzymatic reaction was stopped performing an organic extraction (section 8) (320) and it was collected the upper aqueous phase containing 14C-phosphocholine in a liquid scintillation vial (MP Biomedicals, Irvine, USA).Finally, the cpm of the samples were quantified in a liquid scintillation ISODATA gamma counter (Polymedco, Inc., Cortlandt Manor, USA) for 5 min/tube.

15. Determination of PS-associated proteins SP-A, SP-B and SP-C levels by Electrophoresis and Western blot analysis.

To analyze the levels of specific surfactant proteins SP-A, SP-B and SP-C, first an electrophoretic analysis of LA samples was performed by one-dimensional sodium dodecyl sulfate-polyacrylamide gel electrophoresis, using running gels of 12% for SP-A and SP-B, and 18% for SP-C. Reducing conditions (5% β-mercaptoethanol) were used for SP-A analysis and 1 μg of total protein was applied. In the case of SP-B and SP-C, the same amount of PL (5 nmol for SP-B and 3 nmol for SP-C) was applied. After electrophoresis, samples were transferred to a nitrocellulose membrane (SP-A and SP-B) or a polyvinylidenedifluoride membrane (PVDF) (SP-C) using a Bio-Rad Transblot Cell (Bio-Rad, Hercules, USA). The transfer was performed at 300mA constant during 1h, using 25 mMTris-HCl, pH 8.3, 192 mMglycine, and 20 % (v/v) methanol as transfer buffer.

PS-associated proteins immunodetection was performed using the SNAP^{TM}i.d. System (Millipore Corporation, Bedford, USA). For this purpose, blots were assembled in a hydrated holderand placed in the system chamber with the well side up. Rapidly, blots were blocked with a PBS containing 0.05% of low fat dry milk. Immediately, the vacuum was applied and, when the well was emptied, it was realized a washing step with PBS/Tween-20 0.1% (v/v) without turn off the vacuum. When the well was completely empty, the vacuum was turned off and the incubation of the primary antibody during 10 min was performed. To this, we used the following polyclonal antibodies developed in rabbit: anti-porcine-SP-A, anti-porcine-SP-B and anti-recombinant-human-SP-C. Subsequently three washing steps were performed before incubate during 10 min with the vacuum off with the second antibody anti-rabbit-IgG coupled to peroxidase (Sigma-Aldrich, St. Louis, USA). Finally, another wash step was performed and the blots were removed from the holder system and incubated with the chemiluminescent detection reagent ECL (Western Immobilon, Millipore Corporartion, Bedford, USA) for 1 min. In all cases, proteins were visualized by superimposing a film on the blot to carry out its development in the developing machine (Curix 60, Agfa, Mortsel, Belgium).

Quantification was achieved by densitometric evaluation using Quantity One software (Bio-Rad Laboratories, Hercules, USA).

16. Gene expression analysis by real time–PCR.

Total RNA was isolated from the lower lobe of the right lung using the RNeasy plus Mini Kit (Quiagen, Hilden, Germany) according to the protocol provided by the supplier. Lung tissue was weigh and freeze with N_2 liquid to immediately pulverize it using a mortar and pestle underRNase-free and freezing conditions. Grind powder was homogenate using a lysisbuffer provided by the supplier containing β-Mercaptoethanol (1:100) and a sterile needle (25-*gauche*). The homogenate was centrifuged 3 min at 16000g at RT and the supernatant was transfer to *gDNA eliminator* columns (used to eliminate DNA traces) provided by the supplier and centrifuged 30 sec at 8000g at RT. The fluid was collected, mixed with ethanol 70% and transferred to*RNeasy spin*columns, which retain RNA in the membrane. Columns were centrifuged 30 sec at 8000g at RT until all the fluid had passed and the eluate was discarded. Subsequently a wash process was performed and columns were treated with the RNase-free DNAse Set (Quiagen, Hilden, Germany) during 20 min to remove possible DNA contaminations. After several wash steps, columns were centrifuged 1min at 16000g to eliminate traces and finally the RNA was eluted with 40µl RNase-free water supplied. The amount of RNA extracted was measured at 260 nm in a spectrophotometer ND-1000 (NanoDrop Technologies, Wilmington, USA).

cDNA synthesis was performed with the Transcriptor High Fidelity cDNA Synthesis kit (Roche, Mannheim, Germany) using 1µg total RNA as input. The RNA was first incubated at 65ºC during 10 min (RNA denaturalization) in a Thermal-cycler C-1000(Bio-Rad, Hercules, USA) with the random hexamer primers supplied. Then, it was added a master mix containing: Transcriptor RT Reaction Buffer (5x), protector RNase inhibitor (40U/µl), deoxynucleotide mix (10mM) and transcriptor reverse transcriptase. All was gently mixed and tubes were incubated with the following thermo-cycling program: 25ºC during 20 min (primers annealing), 55ºC for 1 h (cDNA synthesis) and 85ºC during 5 min (enzyme inactivation). Then, the cDNA was stored at-20ºC until the PCR design.

Real-time PCR (RT-PCR) was developed using the Universal Probe Library technique (Roche, Mannheim, Germany). This method is based on the identification ofimput sequences of the target genes using the ProbeFinder online software provided by Roche (www.universalprobelibrary.com). This software designs an optimal qPCR

assay combining the best probes and primers according to their organisms specificity, absence of cross-hybridations, intron-spanning amplicon, and a small amplicon size. The primers selected by this software were analyzed and re-design in some cases using PrimerSelect application (Lasergene Core Suite Software, DNASTAR, Madison, USA) and finally ordered to be synthesized (Sigma-Aldrich, St. Louis, USA) (Table.1).

RT-PCR was performed in triplicates using the appropriate probes and primers (20 μM) for each target gene, mixed with FastStart Universal Probe Master (Rox, 2x) (Roche, Mannheim, Germany) to reach a final volume of 8μl. Allsample mixes (10μl) were gently blended and transferred to a 384-well microplate (Applied Biosystems, Life Technologies, USA) which was incubated with the following thermo-cycling program: 94ºC during 10 min (initial DNA molecule denaturalization), 94ºC for 10sec (DNA denaturalization) and 60ºC during 45 seg (primer annealing and DNA chains extension), being repeated 40 times the two last steps in The LightCycler® 480 Real-Time PCR System (Roche, Mannheim, Germany).

Results were analyzed using the ΔΔCT method (321), normalizing with the expression levels of β-actin. The final data were represented as the normalized fold change expression.

Target gene	Primer Forward	Primer reverse	Probe
SP-A	5´-CAAGGGAGAGCCTGGAGAAAG-3´	5´-CTGAGGACTCCCATTGTTTGC-3´	**50**
SP-B	5´-CTGATCAAGCGGGTCCAAGC-3´	5´-GGCAGATGCCACCCACCAC-3´	**76**
SP-C	5´-GTAGCAAAGAGGTACTGATGG-3´	5´-CACGATGAGAAGGCGTTTGAG-3´	**74**
ASM	5´-CAGCCTTATGGTCCTTTCAG-3´	5´-CAGGATTGTTGGTCTCTTTTTC-3´	**62**
MMP-2	5´-CGTAACTCCACTACGCTTTTC-3´	5´-CTTGCCGTCAAATGGGTATC-3´	**60**
TGF-β1	5´-CCTGGAAAGGGCTCAACAC-3´	5´-CGTACACAGCAGTTCTTCTC-3´	**1**
β-ACTIN	5´-GGCCAACCGTGAAAAGATGAC-3´	5´-GACCAGAGGCATACAGGGAC-3´	**64**

Table 1: Primers and probes design with the ProbeFinder software by Roche used to realize real-time-PCR assays.

17. Biophysical function of Pulmonary Surfactant.

Interfacial Adsorption:

The ability of LA to adsorb onto and spread at the air–water interface was tested at 25ºC in a Wilhelmy-like high-sensitive surface microbalance, coupled to a King-Clements Teflon dish (322, 323) (Figure 5). 450 nmol of LA phospholipids from each samplewas injected into the hypophase chamber of the Teflon dish containing 6 ml of buffer (pH 7.0) composed by 5 mM Hepes, 150 mM NaCl, and 5 mM $CaCl_2$, altogether under continuous stirring to avoid diffusion from being the limiting step of adsorption. Interfacial adsorption was measured following the variation in surface pressure (π) as a function of time, using a platinum plate coupled to the microbalance (KSV Instruments). The surface pressure (π) is related to the surface tension (γ) by the following expression: $\pi = \gamma^0 - \gamma$, where $\gamma^0$is the surface tension of the liquid in the air-liquid interface without the surfactant presence, which its value is 72 mN/m. Therefore, when PS establish a monolayer in the air-liquid interface, the surface tension decreases up to the equilibrium γ values between 22-25 mN/m and consequently, the π arise values between 47-50 mN/m.

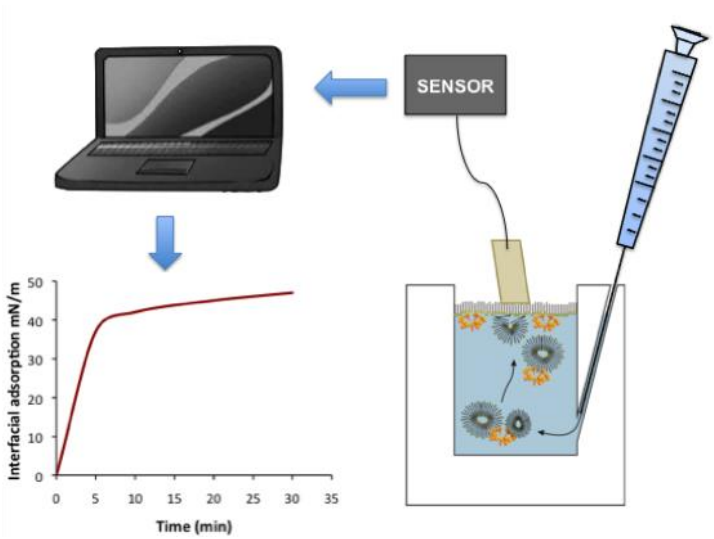

Figure 5: Schematic representation of a Wilhelmy microbalance for interfacial adsorption measurements**.**

Captive Bubble surfactometer

Captive bubble surfactometer (CBS) is an experimental set up designed to evaluate the surface activity of surfactant when it is adsorbed onto the air-liquid interface of an air bubble enclosed in a controlled environment chamber. This system, not only emulates the air-liquid interface of alveoli and its movements during respiration, but also allows controlling several parameters such as temperature, humidity or pressure, essentials for the adequate surfactant functionality.

CBS was designed, built and optimized in the late 80's by Dr. Samuel Schürch in order to study the behaviour of the native and synthetic surfactant films in physiological relevant conditions (324).

Surface area (A_b), volume (V_b) and surface tension of the bubble(γ_b)are calculated in the CBS from the diameter and height of it, by monitoring, recording with a video-camera (Model 765, Pulnix USA), and then digitizing with the computer software CBpost Ver1.5 © (325)

Dr Samuel Schürch and Michael Schoel from the University of Calgary in Canada, built the CBS setup used in the experiments done in this thesis, for the Complutense University of Madrid.

Components of the CBS system (Figure 6):

The chamber is a glass cylinder fixed to a metal base with a 2 mm hole in diameter at the bottom, through which the air bubble is created (0.0035 to 0.040 cm^3). The other side of the chamber is sealed with anagarose plug (1%, w/v) to create a hydrophilic environment that prevents the adhesion of the bubble. The agarose capis adjusted to a piston, which will start to compress and expand the space between the plug and the metal base, when initiating experimental process.

This system is filled with approximately, 1.5 mL of a monolayer buffer (Tris 5 mM, NaCl 150 mM) containing sucrose 10% in order to increase the density of the aqueous subphase, leading the surfactant against the bubble and avoiding its dilution in the subphase. Besides, the chamber is placed in a metallic jacket used as a water bath thermostated by a heat external source strictly controlled by the computer. This jacket

also has a transparent side that allows observe the bubble and locate the IR video camera in front of it. This complex is positioned and adjusted by two screws in a holder to begin the procedure.

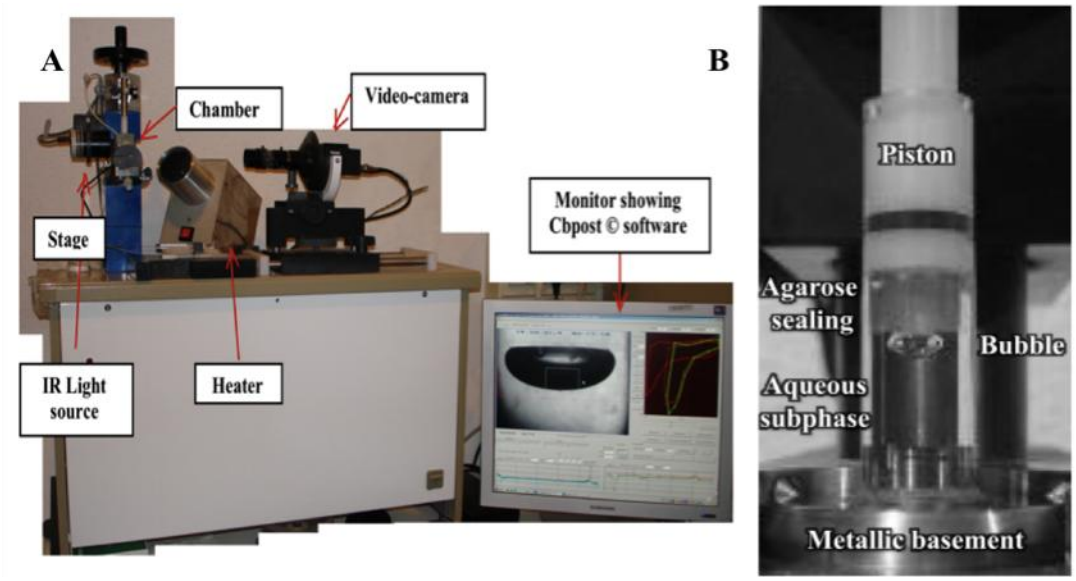

Figure 6: Schematic representation of the CBS device (A) and a detailed view of the bubble chamber (B).

Experimental protocol:

Before starting the experimental protocol, a degasification procedure was essential to ensure that any other bubble alters the results. This step involves the expansion of the bubble in the sealed chamber for 10 min, to allow small bubbles formed in the aqueous subphase join the expanded one.

To accomplish CBS experiments we used LA samples with a concentration of 20.0 ± 2.5 mg/ml of PL. This value was determined as a critical concentration to observe differences between groups.

The CBS allows determining if the surfactant measured fulfills its dynamic properties, which are:

- Very rapid interfacial adsorption (Initial adsorption)
- Low surface tension upon compression (less than 2mN/m) (Dynamic cycles)
- Efficient re-extension upon expansion. (Post-expansion adsorption**)**

As a result, the protocol used simulates each feature respectively accomplishing the following steps:

(I) Initial adsorption (IA) kinetics: registers the ability of the surfactant to reach the interface and form a film able to reduce the surface tension to the equilibrium. PS (150 nL) is applied with a syringe connected to a transparent capillary close to the bubble without contact, transferring the material onto the interface. This event can be visualized through the changes in the bubble shape during 5 min after the aplication of the material. The more flattens the bubble, the more surface tension is reduced. Therefore, the equilibrium surface tension reached with surfactant presence of 22-23 mN/m in less than 5 sec, from the inicial surface tension of the aqueous subphase of 70 mN/m (Figure 7).

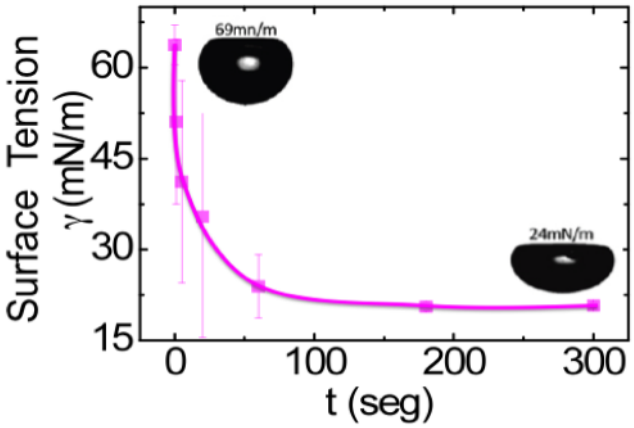

Figure 7: Initial Adsorption: changes in the surface tension detected by the alteration of the bubble shape.

(II) Post-expansion adsorption (PEA) kinetics: allows analyzing the reorganization and spreading of surfactant in an enlarged interface. To that purpose, after the initial adsorption experiment, the chamber is carefully sealed and, the bubble volume is re-determined before expanding the bubble to a maximum size of 0.15 cm^3 controlled by the software. After the bubble expansion, the changes in surface tension were registered during 5 min, visualized by the changes in the bubble shape described previously in IA (Figure 8).

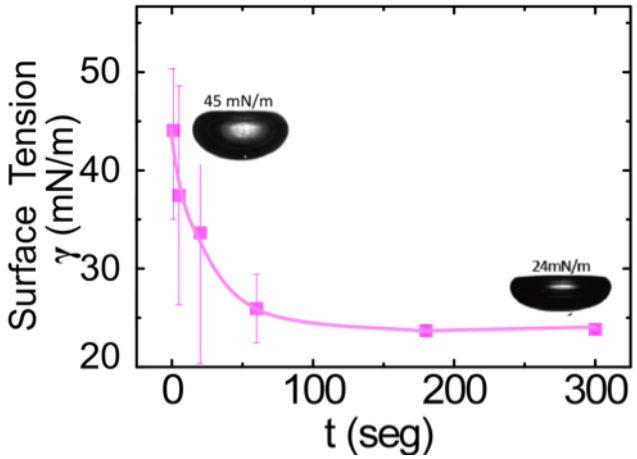

Figure 8: Post-expansion adsorption:changes in bubble shape due to decrease of thesurface tension in function of time during the subsequent adsorption to expansion.

(III) Quasi-static compression and expansion cycles: the air bubble is subjected after the adsorption of the surfactant, to four discrete step-wise compression-expansion consecutive cycles to permit the relaxation and reorganization of the material after each area change. This step, permits to analyze in detail the behaviour of surfactant, as consequence of using cycling speeds much slower than those associated with breathing, which allows the detection of structural features such as phase changes, three-dimensional restructuration and progressive purification of interfacial films.

To this purpose, first the initial bubble volume was established as the maximum bubble volume during PEA. Then, the bubble was compress up to the volume required to achieve the minimum surface tension without reaching the interfacial film collapse (Figure 9). This event can be detected because the bubble area decreases without reducing the surface tension. Therefore, the cycles were performed with 1 sec delay between de compression steps and reducing 20% its previous volume.

Usually, the first quasi-static cycle is different from the other three, because presents a higher hysteresis loops. This means that the energy provided by the compression is used to reorganize the material at the interface and purifies the material instead of reducing the surface tension. In addition, thanks to this event, subsequent cycles will show progressively lower hysteresis and less compression will be needed to reduce the surface tension to minimum.

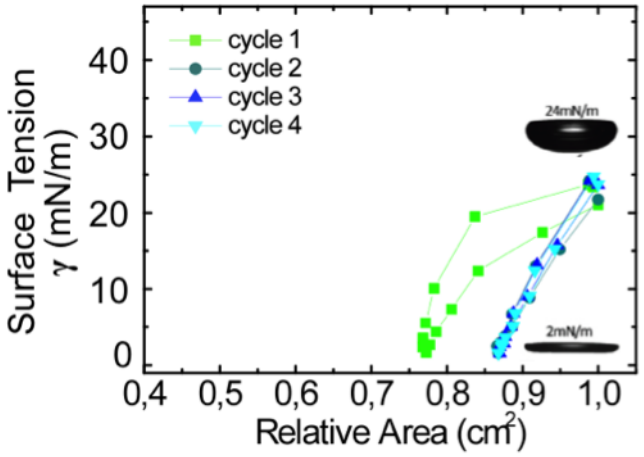

Figure 9: Quasi-static compression and expansion cycles: changes in the bubble shape related with the surface tension/ area isotherms obtained during the quasi-static cycling process.

(IV) Compression and expansion dynamic cycles: reproduces the compression-expansion of continuous cycles, simulating the physiological human respiratory rates (20 cycles/min) in order to observe the real stability and functionality of the surfactant in the interface (Figure 10). In the present study, 20 cycles/min were performed according to previous CBS studies in high-stretched rats (326) and the cycles 1, 10 and 20 were represented. This step was carried out after ending the quasi-static cycles, using the maximum and minimum volumes of the quasi-static cycles.

A functional surfactant decreases the surface tension to the maximum recurrently with the minimal compression and exhibiting reduced hysteresis, despite the speediness of the cycles that avoids the possibility of relaxation or reorganization.

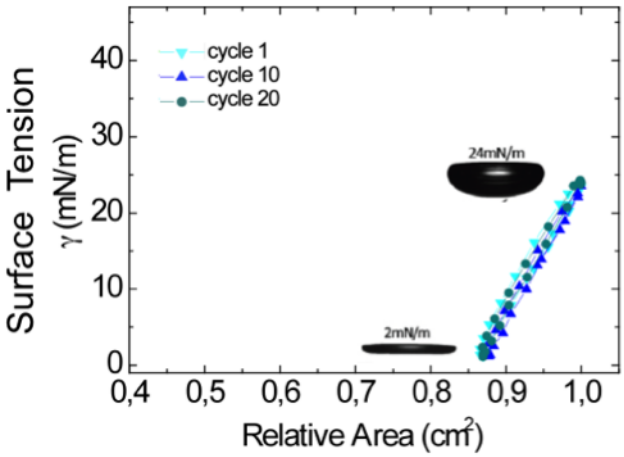

Figure 10: Dynamic compression and expansion cycles: changes in the bubble shape associated with the surface tension/ area isotherms achieved during the dynamiccycling process.

18. Statistical analysis

Data are represented as mean ± standard error of mean (SEM) of individual measurements. Means were normally distributed (Shapiro-Wilk test). Differences between means of each group were analyzed using a one-way analysis of variance (ANOVA) followed by a Bonferroni pos hoc analysis. A two-tailed unpaired Student´s T test was performed when required. A confidence level of 95% or greater ($p < 0.05$) was considered significant. The statistical analysis was performed using Sigma Plot 11.0 statistical software.

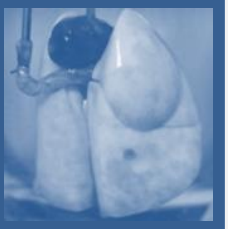

Chapter 1

Characterization of alveolar injury due to high-stretch ventilation

1. ABSTRACT

The aim of this study was to characterize changes produced in the alveolar compartment due to injurious high-stretch ventilation.

Sprague-Dawley rats were randomly assigned to control conditions [no mechanical ventilation (n=15)], low-stretch [V_T = 9 ml/kg, positive-end expiratory pressure (PEEP) = 5 cm H_2O (n=24)] or high-stretch [V_T = 25 ml/kg, PEEP = 0 cm H_2O (n=24)] ventilation strategies and monitored for 150 min. Subsequently, lung tissue, plasma, bronchoalveolar fluid (BAL), BAL cells, and isolated surfactant were analyzed.

The high-stretch ventilation group, presented several factors implicated in acute lung injury, such as leakage of proteins into the alveoli, release of inflammatory mediators, oxidative stress in the alveolar compartment, decrease of alveolar fluid cells and hyaline membranes deposition, together with factors involved in the alteration of pulmonary surfactant system such as protein contamination, surfactant oxidation and decrease of surfactant-associated proteins, as depicts alteration of surfactant metabolism and its biophysical function impairment. All this alterations in the alveolar space are coupled with impaired gas exchange and decrease in dynamic compliance, rendering the lung susceptible to atelectasis. Furthermore, we detected slightly alterations in the low-stretched group like decrease of alveolar fluid cells and increase of some damage markers in the alveolar space.

This study indicates that injurious high-stretch ventilation produces direct damage to the lung, promoting inflammation, oxidative stress, edema and release of factors that together inactivate pulmonary surfactant. Lung surfactant impairment leads to atelectasis as depicted by impaired gas exchange and decrease in dynamic compliance.

2. INTRODUCTION

The acute respiratory distress syndrome (ARDS) and acute lung injury (ALI) are common respiratory syndromes in critically care units associated with elevated mortality rates (47). However, their only effective treatment to date is mechanical ventilation (MV) (173). Thus, many studies have been undertaken in order to improve the ventilator strategies and therefore achieve a decrease in their currently mortality

rates of 43% (47, 168, 173). However, these researches also discovered that ventilate with certain strategies characterized by high tidal volumes (V_T) or lack of positive end-expiratory pressure (PEEP) administration lead to aggravate and even develop lung damage *per se*, outcome denominated ventilator-induced lung injury (VILI) and widely used as animal model of ALI characterization (7). Since then, a wide range of VILI models has been conducted in order to elucidate the main factors attributable to this alteration.

As a result, a large number of studies concluded that tissue injury, characterized by thickening of the alveolar wall or alveolar type I cells necrosis, is a main feature of VILI, which is tightly linked to alterations in alveolar-capillary barrier permeability (235). In particular, the alteration of the alveolar–capillary barrier is an important mechanism responsible of alveolar edema presence, which is characteristic of VILI (236, 327). Also, many other studies highlighted some physiological data, such as hypoxemia, as a key feature of VILI (328).

On the other hand ,the role of the innate immune response and inflammation in VILI has been broadly studied, being demonstrated that most of alveolar cells are capable to release inflammatory mediators, including IL-1β, IL-6, IL-8, IL-10 and TNF-α (238). However this field remains controversial, as some studies observed an increase of cytokines release in lungs ventilated without PEEP (250) whereas other studies reported no association between VILI and productionof proinflammatory cytokines in the same animal model (257).

As well, different studies were focused on elucidate the role and outcome of pulmonary surfactant (PS) in VILI. PS is a surface-active lipoprotein complex secreted as its active fraction, called large aggregates (LA), by alveolar type II cells (ATII), which accomplish its main function: to stabilize the alveoli by the reduction of surface tension at the air-liquid interface, preventing the alveolar collapse during end-exhalation (329). Several *in vivo* and *ex vivo* investigations concluded that PS biophysical function is impaired in VILI (295-298, 330). *Ex vivo* studies, determined together with PS dysfunction some alterations in PS metabolism and composition, such as cholesterol increase in LA or hydrophobic PS-associated proteins RNA levels decrease (295, 297, 330). Conversely, fewer studies have been conducted *in vivo*, detecting similar alterations (296, 298). Therefore, further investigation must be done in order to elucidate the mechanisms and factors that lead PS alterations in VILI.

Therefore, the aim of the present study was to characterize the impact of high-stretch ventilation in the alveolar space and in particular its effects on the composition, structure, and functional activity of lung surfactant assessing the causes of surfactant alterations.

To accomplish this objective, we characterize physiological, histological, inflammatory and PS changes in an *in vivo* model using injurious (V_T = 25mL/kg, no PEEP) ventilator strategies or conventional strategies (V_T = 9 mL/kg, PEEP = 5 cmH_2O) resembling clinical situations (10).

3. EXPERIMENTAL DESIGN

We established three experimental groups:

1) Control group: animals subjected to identical anesthetic and surgical procedures without being mechanical ventilated (n=15).

2) Low V_T ventilated group: V_T = 9 mL/kg, PEEP = 5 cm H_2O (n=24).

3) High V_T ventilated group: V_T = 25 mL/kg, zero PEEP (n=24).

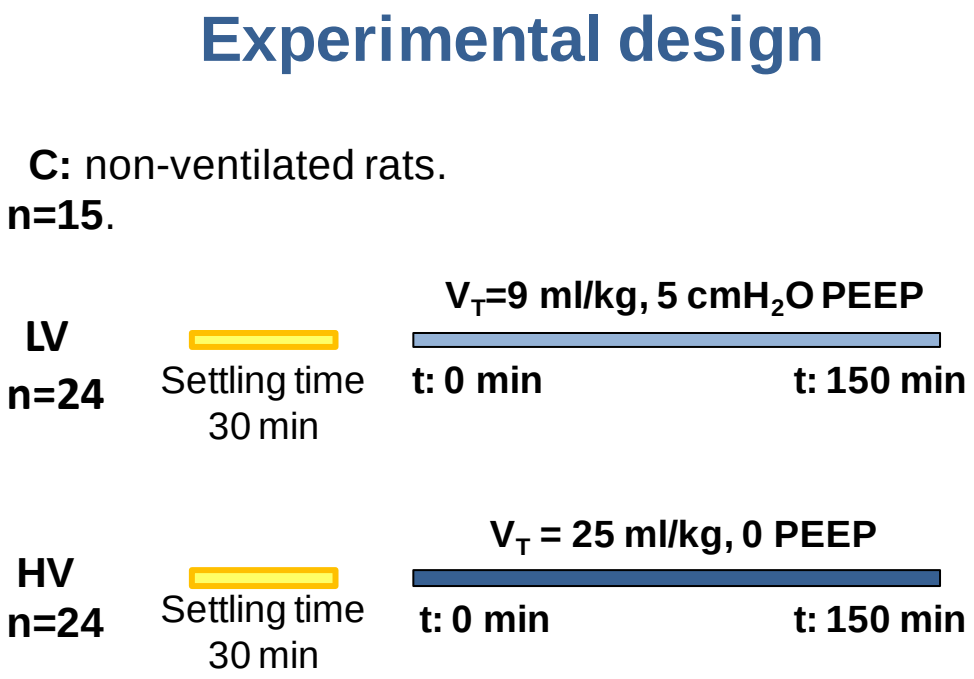

Figure 1: Experimental design. Representation of all groups established subdivided according to mechanical ventilation strategies.

In both MV groups, respiratory rate was 70 bpm, inspiratory time 0.3 seconds, expiratory time 0.56 seconds and FiO_2 0.35.

Animals were ventilated for an equilibration period of 30 min using the low V_T ventilation parameters. Then, they were assigned randomly to one of the groups. Dead-space ventilation was increased in animals ventilated with high V_T (by increasing the length of the ventilatory circuit) to attain comparable values of $PaCO_2$ during the ventilation period. The assigned V_T was administered starting at t=0 min up to 150 min.

At t=0 min and t=150 min, mean arterial pressure (MAP), peak airway pressure [P_{AW}], and dynamic respiratory system compliance [C_{RS}]) were registered. Blood samples were drawn at t=150 min to assess biochemical and gases analysis.

Animals were sacrificed by exsanguination after 150 min and subsequently we proceeded to sampling. We obtained lung tissue and bronchoalveolar lavage that it was separated from the alveolar fluid cells by centrifugation. The remaining bronchoalveolar lavage free of cells (BAL) was processed to obtain PS.

4. RESULTS

4.1. Physiology

Lung functionality was determined by hemodynamic and ventilatory measurements in both groups of study.

Ventilator parameters (P_{AW}, C_{RS}) and MAP were measured at the start and end of the ventilation period. As depicted in Table 1, rats ventilated with high V_T showed a significant increase in P_{AW} over time, as well as a significant decrease in C_{RS} and MAP.

Arterial blood gases, pH and lactate concentration were measured in blood at the end of MV. Rats exposed to high V_T MV presented systemic acidosis, hypoxemia and hyperlactatemia in contrast with rats ventilated with low V_T (Table 1). Specifically, PaO_2/FiO_2 ratio was below 300 mmHg in high-stretched rats (data not shown), criteria defined by the ARDSnet (2).

All these data suggest the existence of atelectasis in the animals ventilated with high V_T.

Table1: Changes in mechanical ventilatory parameters (P_{AW}, C_{RS}), mean arterial pressure (MAP), blood gases and lactate concentration in rats exposed to Low (V_T= 9 mL/kg) or High (V_T=25 mL/kg) mechanical ventilation strategies.

		Low V_T	High V_T
P_{AW} (cmH_2O)	t=0	17.36±0.38	28.86±0.72
	t=150	17.36±0.31	36.50±1.96 *
C_{RS} (mL/cmH_2O)	t=0	0.32±0.01	0.44±0.02
	t=150	0.32±0.01	0.34±0.03 *
MAP (mmHg)	t=0	114.16±4.23	115.59±4.49
	t=150	114.04±4.49	71.15±6.32 *
PaO_2 (mmHg)	t=150	146.75±3.37	88.00±12.32 #
$PaCO_2$ (mmHg)	t=150	30.35±1.17	39.13±1.14
pH	t=150	7.42±0.01	7.29±0.02 #
Lactate (mmol/L)	t=150	1.53±0.11	2.63±0.44 #

Definition of abbreviation: P_{AW}: peak airway pressure; C_{RS}: respiratory system compliance; MAP: mean arterial pressure; PaO_2: partial pressure of arterial oxygen; $PaCO_2$: partial pressure of arterial carbon dioxide.

P_{AW}, C_{RS} and MAP were measured at baseline (t=0) and after 150 minutes of mechanical ventilation. PaO_2, $PaCO_2$, pH and lactate concentration were measured at t=150 min. Data are mean ± S.E.M. * $p<0.05$, t=0 vs. t=150 min; #$p<0.05$ Low V_T vs. High V_T.

4.2. Alveolar injury

Several parameters were evaluated in order to characterize the injury induced by high V_T ventilation.

4.2.1. Cellular and histological analysis

Total cell counts in the alveolar fluid were significantly decreased in MV groups ($p<0.001$), having significant differences between them ($p<0.05$ HV vs. LV) as depicts Figure 2 (n=14 in all groups).

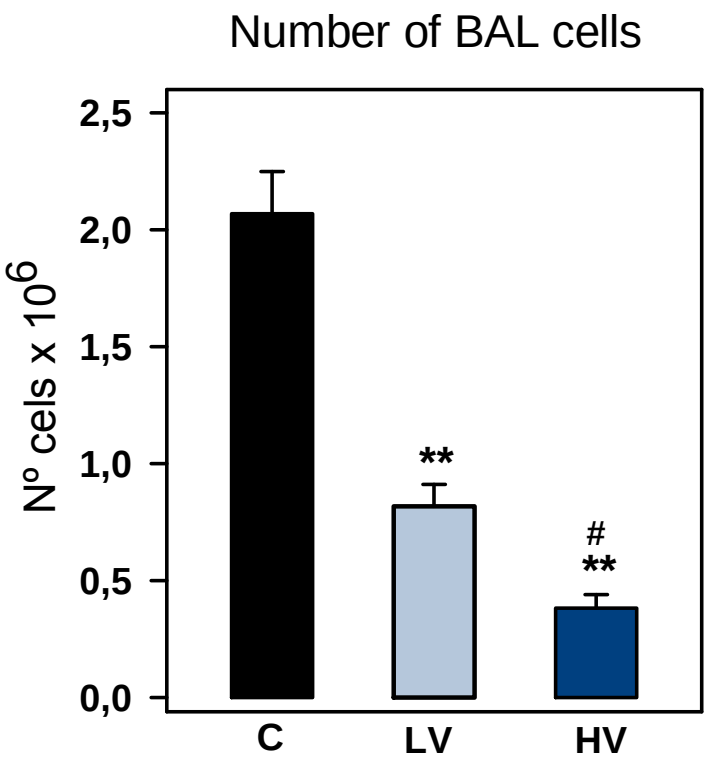

Figure 2: BAL cell counts in all experimental groups (all groups n=14).
The number of cells recovered in BAL was determined by cell viability with trypan blue dye exclusion. Data are mean ± S.E.M. ** $p< 0.001$ vs. C; # $p<0.05$ vs. LV.

As well, histopathological studies revealed alterations in the high-stretched animals. Figure 3 displays representative micrographs of n = 15 lungs examined in both MV groups. Left micrograph corresponds to LV rats, which had no evidence of morphological lung injury. In contrast, capillary congestion, alveolar type I cells necrosis, and hyaline membrane formation covering the denuded epithelial surface were presented in HV animals (Figure 3 [right]).

Lung tissue micrographs from MV groups

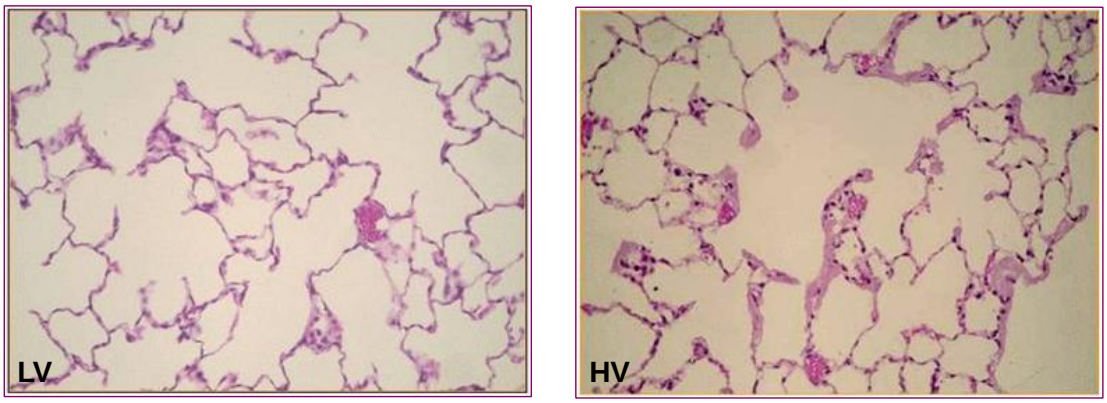

Figure 3: Histological micrographs of rats ventilated with Low or High tidal volumes during 150 min (all groups n=15).
Representative light micrographs obtained from isolated left lungs of LVgroup (left) and HV group (right) stained withhematoxylin-eosin.

4.2.2. Total protein and carbonylated proteins in BAL

Total amount of proteins in the alveolar fluid as well as their oxidized state were evaluated in BAL of n=8 and n=5 rats per group, respectively (Figure 4).

There was a significant increase in total protein presence in BAL in HV in contrast with all groups ($p<0.001$). This result reflects an increase of protein in BAL probably due to an increase of protein release in the alveolar space and alterations in the alveolar-capillary barrier allowing leakage of plasma proteins into the alveolar space.

As well, we observed in these rats an increase of carbonylated proteins in BAL of the rats injuriously MV in contrast with Control group ($p<0.01$).

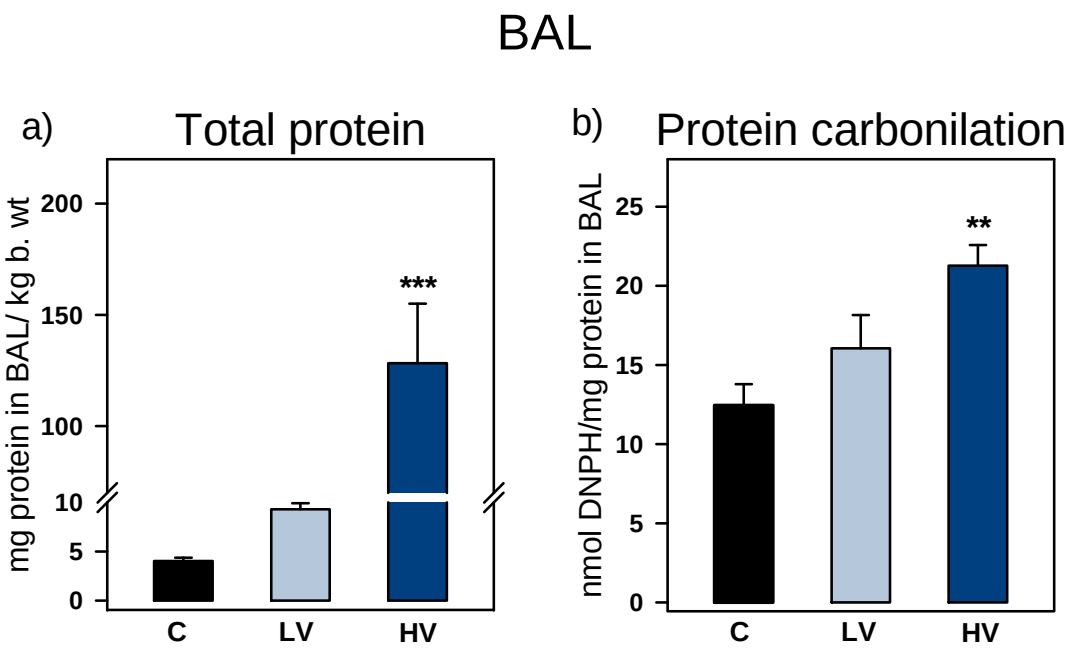

Figure 4: Total protein levels and its oxidized state in broncholalveolarlavage of Control and ventilated rats with Low/High tidal volumes during 150 min.
Total amount of proteins (a, n=8) and protein oxidation content (b, n=5) were assessed in BAL in all groups of study.
Data are mean ± S.E.M. **p< 0.01vs. Control and ***p< 0.001 vs. all groups.

4.2.3. Damage markers

We studied the presence of two damage markers in the alveolar space using n=5 animals per group: TNF-α and Acid Sphingomyelinase (ASMase) activity (Figure 5).

TNF-α is a pleiotropic cytokine with multiple functions in the inflammatory response(331). This cytokine increased significantly in BAL of HV group ($p<0.001$), while it was undetectable in plasma of both groups (Figure 5a).

On the other hand, ASMase catalyze the hydrolysis of sphingomyelin (SM) to ceramide and coline phosphate, being ASMase-derived ceramide a promoter of several pathways leading to ALI (332). We observed a significant increase of ASMase activity in BAL of MV groups, being significantly higher in HV group (Figure 5b). Interestingly, its levels in plasma did not vary between groups (data not shown).

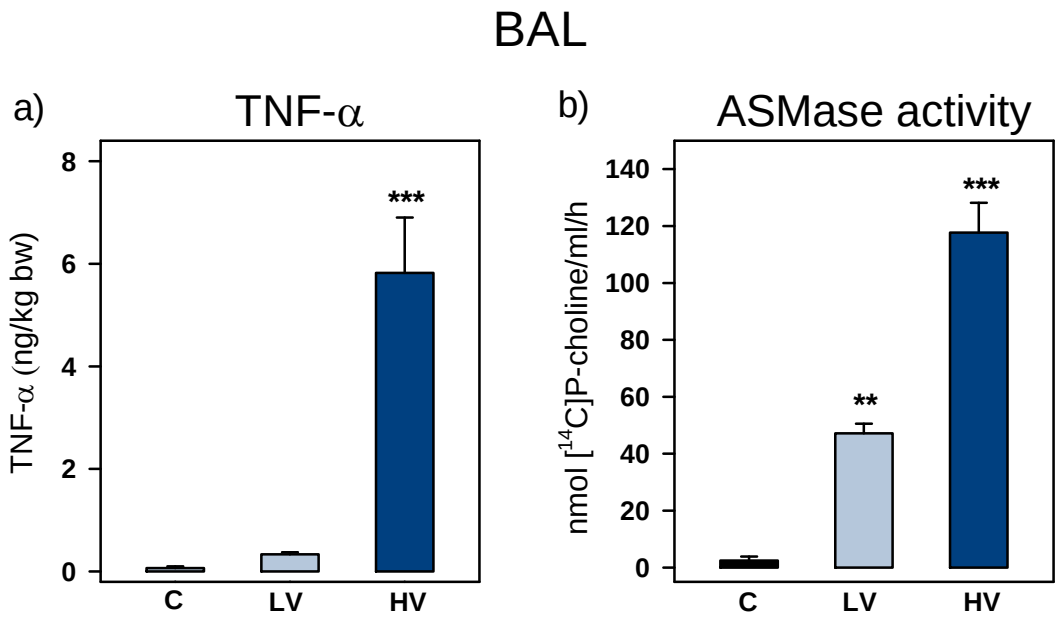

Figure 5: TNF-α and Acid Sphingomyelinase activity levelsin broncholalveolarlavage of control and ventilated rats with Low/High tidal volumes during 150 min.

a) TNF-αwas measured in BAL and plasma of all groups using a colorimetric rat ELISA kit (n=5 per group). There were significant differences between HV and all groups in BAL. Plasma levels were undetectable.

b) ASMase activity was measured in BAL and plasma of both ventilated groups performing an enzymatic assay (n=5 per group).There were significant differences between MV groups and Control group in BAL while there were no differences in plasma among groups (data not shown).

Data are mean ± S.E.M. ** p<0.01vs. Control and *** p< 0.001 vs. all groups.

4.3. Surfactant analysis

4.3.1. Composition analysis

PS is comprised of 90% lipids, predominantly phospholipids (PL), and 10% of proteins, mainly the PS-associated proteins: SP-A, SP-B, SP-C and SP-D. PS is secreted as its functional fraction (LA) by ATII to the alveolar space. In a normal lung, compression and expansion during respiration leads the conversion of LA to a non-functional fraction (SA), are either degraded or recycled by alveolar macrophages or ATII (314). Conversely, under pathological situations, there is an alteration of the conversion of LA to SA, being the increase of the SA/LA ratio a damage marker of VILI.

Therefore, we evaluate possible alterations in LA to SA conversion and their total PL amounts in n=11 rats per group (Figure 6). Moreover, we studied PS-associated protein levels in LA and its RNA expression in lung tissue of n=5 rats in all groups (Figures 7, 8 and 9).

The content of total PL in PS significantly increased in High V_T group ($p<0.001$). This increase was primary due to a significant increase of PL in SA fraction ($p<0.001$) while in LA did not differ among groups. Accordingly, SA/LA ratio was significantly altered in those rats exposed to high V_TMV ($p<0.001$). These data suggest that injurious MV increases PS secretion but also alters its metabolism.

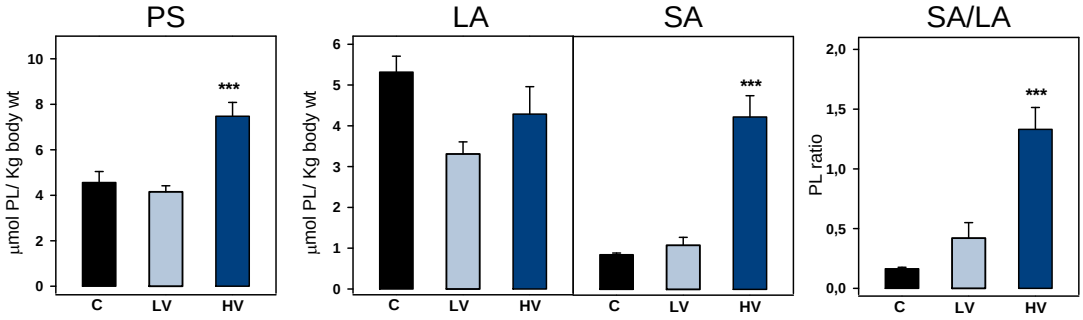

Figure 6: Total amount of phospholipids (PL) in pulmonary surfactant (PS) and PS fractions of rats ventilated with Low/High tidal volumes during 150 min.
Total PL content in PS and the active (LA) and inactive (SA) fractions of PS were measured in n=8 animals of both groups of study.As well, it was determined the ratio of PL content between SA and LA in both groups. We observed significant differences in HV group. Data represent mean ± S.E.M. ***p< 0.001 vs. all groups.

Figures 7, 8 and 9 represent RNA and protein levels of PS-associated proteins analyzed in n=5 animals of all groups of study.

Figure 7 represents SP-A data. Immunoblotting reveals a significant decrease of SP-A in HV groups in contrast with rest of groups ($p<0.01$). Additionally, we also detected a significant decrease of SP-A RNA levels in HV group vs. Control ($p<0.05$).

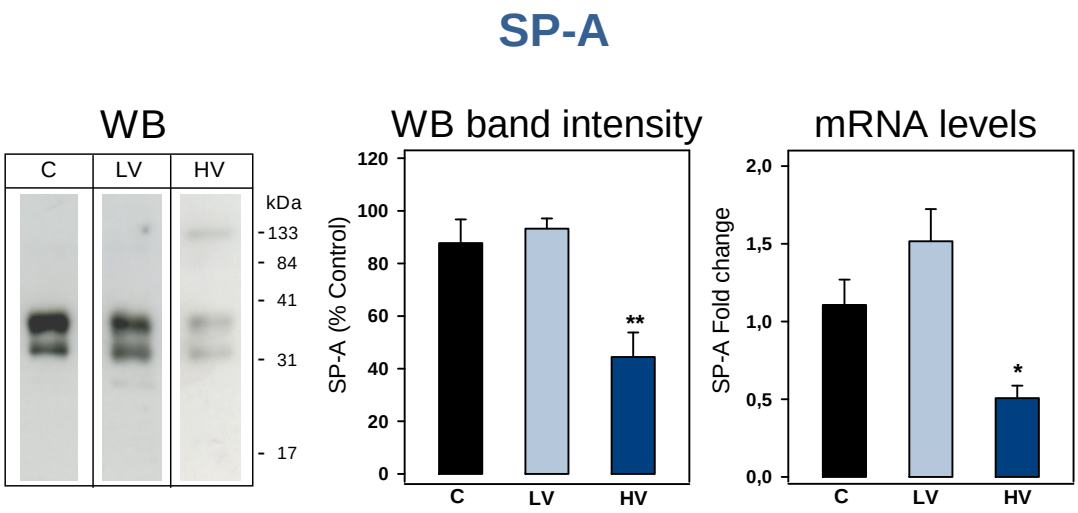

Figure 7: Presence of the collectin SP-A in large aggregates (left) and its RNA expression in lung tissue (right) of n=5 rats ventilated with Low/High tidal volumes during 150 min or non-ventilated (C).
Protein levels of SP-A were detected in LA by Western blot (WB) after 12% reducing SDS/PAGE loading 1 µg of total protein and quantified by densitometric evaluation.
RNA expression of SP-A in lung tissue was assessed using total RNA isolated from the lower lobe of the right lung. cDNA synthesis was performed using 1µg total RNA as input and it was amplified by RT-PCR using specific primers.
Data represent mean ± S.E.M. * $p<0.01$ vs. C and ** $p<0.01$ vs. all groups.

On the other hand, Figure 8 depicts SP-B results. Interestingly, we detected a significant decrease in HV group of both protein and RNA levels vs. Control whereas we observed and increasing trend of SP-B protein levels in LV group together with a significant increaseof its RNA levels in this group ($p<0.01$).

SP-C results showed in Figure 9, depicts a significant increase of protein levels in LV group in contrast with the significant decrease observed in HV group. As well, RT-PCR revealed a significant fold decrease of SP-C in HV group ($p<0.001$ vs. all groups).

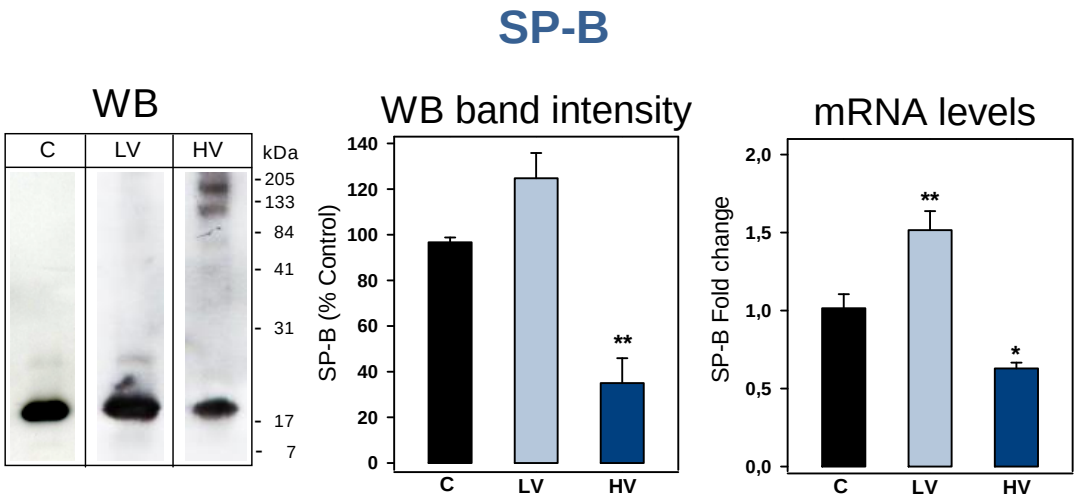

Figure 8: Presence of the hydrophobic peptide SP-B in large aggregates (LA) and their RNA expression in lung tissue of n=5 rats ventilated with Low/High tidal volumes during 150 min or non-ventilated (C).

Protein levels of SP-B were detected by WB after 12% SDS/PAGE under non-reducing conditions applying 5 nmol of total PL of LA (left) and quantified by densitometric evaluation (center). RNA expression of SP-B was assessed by RT-PCR using specific primers previous isolation of RNA from the lower lobe of the right lung. Results were analyzed using ΔΔCT method and expressed as normalized fold expression (right).

Data represent mean ± S.E.M. * p<0.05 vs. Control and ** p<0.01 vs. all groups.

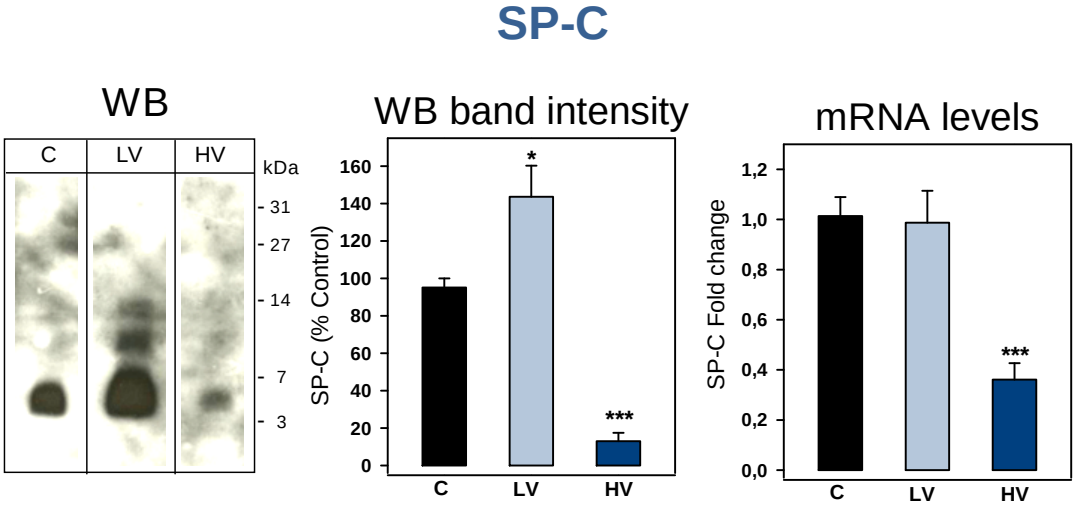

Figure 9: Presence of the hydrophobic peptide SP-C in large aggregates (LA) and their RNA expression in lung tissue of n=5 rats ventilated with Low/High tidal volumes during 150 min or non-ventilated (C).

Protein levels of SP-C were detected by WB after 18% SDS/PAGE under non-reducing conditions applying 3 nmol of total PL of LA (left) and quantified by densitometric evaluation (center).RNA expression of SP-C was detected using total RNA isolated from the lower lobe of the right lung. cDNA synthesis was performed using 1µg total RNA as input and it was amplified by RT-PCR using specific primers. Results were analyzed using ΔΔCT method and expressed as normalized fold expression (right).

Data represent mean ± S.E.M. * p<0.05 vs. Control and *** p<0.001 vs. all groups.

4.3.2. Pulmonary surfactant functionality

PS biophysical function was determined measuring the ability of LA to adsorb onto and spread at the air–water interface, by following the variation in surface pressure as a function of time (322).

Figure 10 depicts PS interfacial adsorption of all groups of study (n=5 per group). While Control and LV groups were near to the equilibrium pressure at 30 minutes, HV group pressure was significantly lower at the same time, suggesting functional impairment ($p<0.001$).

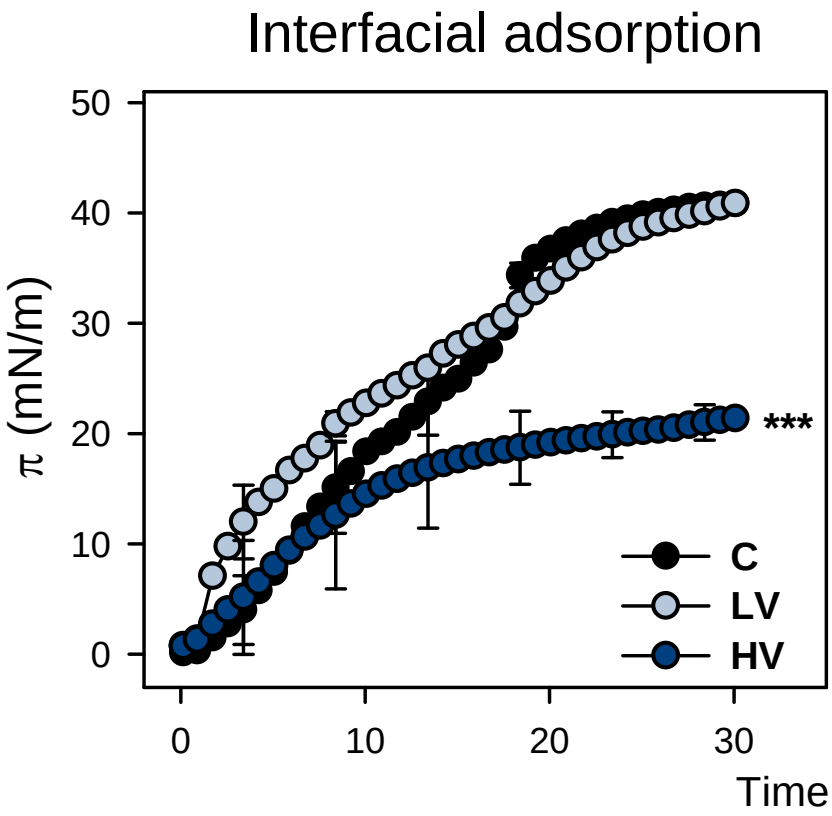

Figure 10: Pulmonary surfactant functionality of n=5 rats from all groups. Surfactant function was determined measuring its ability to adsorb onto and spread at an air-water interface. Surfactant interfacial adsorption in HV groups decreased significantly compared with rest of groups (*** $p< 0.001$). Data are mean ± S.E.M.

4.3.3. Presence of pulmonary surfactant inhibitors.

We studied several inhibitors of surfactant function previously described in other animal models and *in vitro* studies (6, 322, 333). For example, protein leakage into the alveolar space contributes to PS impairment due to the possible competition between LA and surface-active plasmatic proteins for reaching the air-liquid interface (6). According to this, we detected a significant contamination of proteins in the active fraction of PS in the HV group ($p<0.001$), depicted as protein to PL ratio in LA (Figure 11a, n=6 in both groups). Furthermore, we observed a significant increased in HV group of C-reactive protein (CRP) levels ($p<0.001$), determined in 4 rats per group as the percentage of CRP to PL in PS (Figure 11b). Previous studies in our laboratory determined that CRP is an acute-phase protein that inhibits PS functionality by binding to it when reaches the alveolar space (333). Therefore, this data indicates that CRP is implicated in PS impairment in this model.

On the other hand, it is widely accepted that mechanical stress stimulates reactive oxygen species (ROS) production (292) and some studies also demonstrated *in vitro* that PS oxidation is intimately related with PS impairment (334). Hence, we observed a significant increase of LA lipid peroxidation in HV group ($p<0.05$) as depicts Figure 11c (n=4 in both groups).

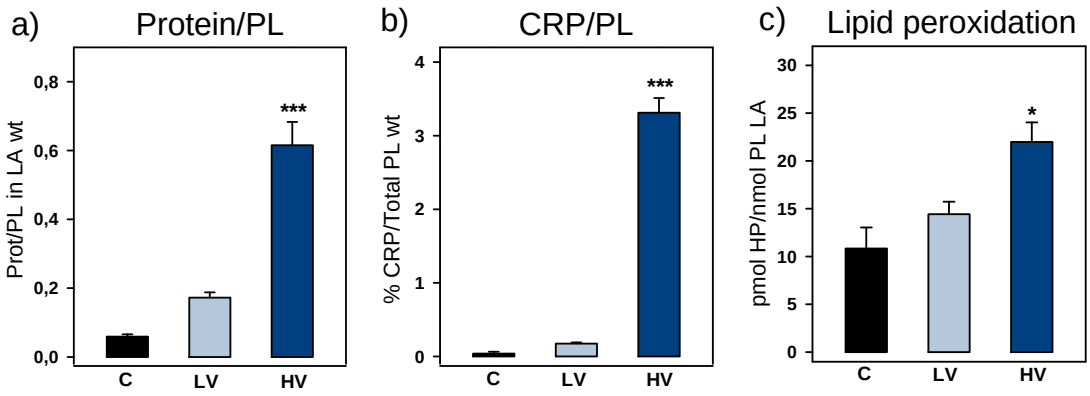

Figure 11: Presence of pulmonary surfactant inhibitors in all groups.
a) Total protein to PL ratio in LA was assessed in n=6 animals of all groups of study. This ratio significantly increased in HV group.
b) CRP was measured using a rat CRP ELISA kit. CRP to total PL in PS ratio significantly increased in HV group (n=4 per group).
c) Lipid hydroperoxides were quantified in lipid extracts of LA of n=4 samples by FOX method. Lipid hydroperoxides significantly increased in LA of HV group.
Data represent mean ± S.E.M. *$p<0.05$ vs. Control and ***$p<0.001$ vs. all groups.

5. DISCUSSION

The present study allows linking the alterations detected in the alveolar space due to VILI as well as highlights novel factors directly involved in PS alterations. This model depicts that injurious MV disturbs simultaneously three levels in the alveolar space: alveolar epithelium, alveolar fluid cells and PS.

Light micrographs from the injurious ventilated group showed alterations in the alveolar space concerning epithelial disturbances such as alveolar type I cells necrosis or thickening of the alveolar wall by hyaline membranes deposition. Also, we observed a decrease of alveolar fluid cells in this group. As hyaline membranes are composed by cellular debris and fibrin, our data suggest that the overinflation produced by high V_T and PEEP absence may induce alveolar cells necrosis comprising part of hyaline membranes. However, we also observed a significant decrease of alveolar fluid cells in LV group. As other groups have previously suggested that MV may induce alveolar cells adhesion to the epithelium (273, 309), we dare to speculate that MV may push alveolar cells to alveolar epithelium and depending on the overinflation produced,might lead to cell death. Therefore, it is reasonable to suggest that MV itself directly affects to alveolar cells by several mechanisms depending on the strategy applied.

Interestingly, tissue injury is usually linked with alterations in the alveolar capillary barrier (235). Accordingly, our data suggest similar alterations as we observed an increase of total protein in BAL. However, an increase of damage markers release in the alveolar space may contribute to this result.

In fact, we detected a significant increase of two damage markers in the alveolar space of HV group.

Sphingomyelinases are enzymes that catalyze the hydrolysis of sphingomyelin to ceramide and coline phosphate (335). Specifically, ASMase plays a key role in the SM/ceramide-signaling pathway, important for its implication in the pathogenesis of ALI (332). Several in vivo studies reported an increase of ASMase activity in lungs and serum (336, 337), and the lack of its presence showed an attenuation of inflammation (337) and edema (336) in ALI. Here we observed an increase of ASMase activity in BAL of MV groups, being its presence higher in high-ventilated animals. These data suggest that MV may induce the increment of ASMase activity in the alveolar space considering edema as a possible source in the case of HV group.

Additionally, we observed an increase of TNF-α exclusively in the alveolar compartment. Even though several models of VILI reported no changes in TNF-α levels in BAL (257, 294), many other VILI models including ours found an increment of this acute-phase cytokine in the alveolar space (250, 296).

However, an interesting role of this early acute inducible cytokine is its involvement in the production of reactive oxygen species (ROS) by various cell types (331, 338). It is known that patients with ARDS are subjected to an increase generation of ROS and reactive nitrogen species (RNS) produced by alveolar cells after proinflammatory stimulation, altering the endothelial barrier function and thus increasing its permeability (339, 340). Furthermore, stimulation of ROS production in response to elevated mechanical stretch has been mainly detected in endothelial cells, but also in epithelial cells, macrophages or fibroblasts, being widely accepted that they may contribute to the onset of VILI (290-292). However, sources and pathways leading to this production are still under discussion (290). Besides, we observed an increase in carbonyl proteins in BAL fluid together with lipid peroxidation increment in LA of high-stretched rats, suggesting that alveolar space is under oxidative stress.

It has been previously reported increments of carbonyl proteins in lung tissue (341) and malondialdehyde contents in the epithelial lining fluid (342) under MV as well as several studies confirm a relationship between PS biophysical activity impairment and its oxidation by different mechanisms (334). However, detection of LA peroxidation in a VILI *in vivo* model is a novelty and directly contributes to the PS impairment observed.

Conversely, we observed a significant increase of PS release in the alveolar space in those rats highly stretched. Interestingly, we only detected a significant increase of SA meanwhile LA remained stable, together with an increment of the SA/LA ratio. These findings are consistent with similar results previously obtained applying high V_T and no PEEP during 1h (294, 296, 297), being suggested that the increment of the SA/LA ratio due to the alteration of the LA to SA conversion is a damage marker in VILI (298). These data suggest that injurious MV induced PS release into the alveolar space but fresh PS may be rapidly altered by several damage markers in the alveolar space as depicts the increment of LA to SA conversion.

Together with LA peroxidation, we observed a significant increase of protein contamination in this fraction that may contribute to both functional impairment and alteration in LA to SA conversion. In fact, it is widely accepted that vascular leakage

of proteins into the alveolar space contributes to PS biophysical activity dysfunction (329). The increment of total protein to PL ratio in LA suggests a possible competition between LA and some surface-active plasmatic proteins such as albumin or fibrinogen, which has been shown to compete for reaching the air-liquid interface (6).

However, we studied CRP, an acute-phase protein that directly binds to PS inhibiting its biophysical function (322, 333). CRP is produced in humans and other animal species primarily by hepatocytes after inflammation or infection and secreted to the serum (343, 344). Besides, alveolar ATII and macrophages stimulated by pro-inflammatory mediators are also able to produce it (345-347). Previous studies in our laboratory detected elevated levels of CRP in BAL and plasma in patients with ischemia-reperfusion injury and studied the effect of CRP in PS functionality *in vivo* and *in vitro* (322, 333). In this study, we detected a significant increase of the percentage of CRP to total PL of PS ratio in injurious MV rats. Consequently, this study demonstrates for the first time the implication of CRP in the pathogenesis of VILI. In addition, previous studies in our group observed an increase in CRP associated with a decrease in SP-A under lung injury. This SP-A deficiency is critical because our laboratory demonstrated previously *in vitro* that SP-A binds to CRP, inhibiting its adverse effect (322, 333).

Accordingly, we observed a significant decrease of protein and RNA levels of SP-A in rats injuriously ventilated. The hydrophilic collectin SP-A is involved in several functions in the alveolar space such as lung defense or PS homeostasis. Specifically, SP-A contributes to LA maintenance, protects PS against inactivation by binding blockade and enhances PS adsorption (55). Hence, these data suggest that SP-A deficiency is also critical in VILI, as it cannot accomplish its protective and homeostatic role appropriately.

Moreover, we observed a decrement of protein and RNA levels of the hydrophobic peptides SP-B and SP-C, being both essential in PS adsorption and surface tension reduction (55). Interestingly, these protein decrease has been observed in several clinical studies of ARDS patients (5, 61, 348) as well as some VILI models revealed a decrease of SP-B and SP-C RNA levels (295) and SP-B protein levels (296).

However, it is the first time, as far as we know, that is detected a decrease of both, RNA and protein levels, of SP-A, SP-B and SP-C in VILI. Hence, these data

suggest that high-stretch MV altersPS-associated proteins production by ATII, being their lack a direct contributor of PS functionality impairment. A plausible explanation for the altered pattern of PS-associated proteins expression could be an increase of modulator factors in the alveolar space, such as proinflammatory mediators, leading to ATII alterations. For example, previous studies indicate a relation between increased TNF-α concentrations and a decreased of RNA levels of SP-B and SP-C (295). Nevertheless, degradation of these proteins in the alveolar space might be another contributor of their lack.

To summarize, injurious MV instigates the release of inflammatory factors by alveolar epithelial and fluid cells as well as promote protein contamination due to the alteration of the alveolar-capillary barrier. These features are involved in signaling pathways that exacerbate the existing damage, being an important target PS.

As a result, the presence of damage markers in the alveolar space directly affects PS functionality by oxidizing its functional fraction or due to protein binding that directly inhibits its function. As well, PS composition is altered, probably caused by ATII alterations, directly affecting its functionality due to decrease of PS-associated proteins. Moreover, ATII and alveolar cells alterations are involved in LA to SA conversion and reuptake. Consequently alteration of PS metabolism and functionality, in turn triggers an increase of alveolar infiltrations by altering the equilibrium pressures between the alveoli and the capillaries, generating a damaging feedback leading to atelectasis and impairment of gas exchange.

Therefore, this study allows interrelating many of the factors directly involved in acute lung injury that also contributes to pulmonary surfactant impairment.

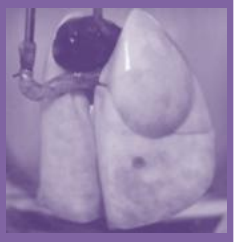

Chapter 2

Factors involved in the resistance to ventilator-induced lung injury

1. ABSTRACT

Ventilator-induced lung injury is a pulmonary damage caused by injurious mechanical ventilation that besides having a wide range of known alveolar alterations it also has a heterogeneous outcome.

The aim of the present study was to elucidate the possible different responses to the application of the same injurious high-stretch ventilation, trying to identify factors involved in the resistance to ventilator-induced lung injury.

Sprague-Dawley rats were randomly distributed in the following groups: Control (n=5), low-stretch ventilation (LV) (V_T = 9 ml/kg, PEEP = 5 cm H_2O) (n=5) or high-stretch ventilation (HV) (V_T = 25 ml/kg, PEEP = 0cm H_2O) (n=17). HV group was subdivided in two groups: 1) animals greatly susceptible to HV (sHV), showing a substantial PaO_2/FiO_2 reduction at 60 min of ventilation; and 2) animals resistant to HV (rHV), with insignificant changes inPaO_2/FiO_2 at 60 min. Lung tissue, plasma, bronchoalveolar fluid (BAL), BAL cells and lung surfactant were analyzed in all groups.

Injurious high-stretch ventilation induced a vulnerable and a resistant response. The vulnerable group was characterized by hyaline membranes formation, pronounced decrease of alveolar macrophages, intra-alveolar edema, inflammatory markers in BAL (TNF-α, MIP-2, MCP-1 and acid sphingomyelinase activity) and alterations in the composition and biophysical activity of lung surfactant, which contained significant levels of peroxides. In contrast, the resistant group was distinguished by an attenuate lung inflammatory response (characterized by IL-6 increase), high amounts of fully active surfactant, absence of edema and normal physiological parameters after 150 min of HV.

These findings suggest that an attenuate inflammatory response together with increased release of active surfactant into the alveolar space prevent edema and a worsened response to high-stretch ventilation.

2. INTRODUCTION

Acute lung injury (ALI) and its severe form, acute respiratory distress syndrome (ARDS), are the major acute respiratory failures with an elevated incidence in critical care units (175). However, the determination of their incidence has been complicated to assess due to their etiologic variability. These syndromes are closely related with insults that directly or indirectly affects to the lungs (e.g. pneumonia, sepsis, respectively.), contributing to their heterogeneity outcome (173). Furthermore, some studies suggest age and race as other factors involved in mortality risk (173, 175). Despite this, mortality rates have decreased significantly in the last decade (47, 173).

The main factor involved in this mortality reduction is the improvement of protective ventilation strategies, the only effective treatment to date (173). However, these studies also highlighted ventilator strategies that worsening the existing damage or even initiate it. Therefore, knowing the alterations attributable to mechanical ventilation (MV) has an essential clinical relevance that led to develop several clinical trials and establish numerous animal models to characterize it.

Clinical studies concluded that even applying the same stress to the lungs of different patients, forces that reach to their cells and the corresponding response are quite heterogeneous and variable (299), presuming that personalizing ventilator strategies according to the particular patient injury status will improve their outcome (349).

On the other hand, several experimental models have been performed in order to elucidate the main features attributable to MV. As a result, many groups studied inflammatory responses under different stretching stimuli (238, 293). Also some studies were aimed at discovering mechanisms leading to vascular permeability (236, 327, 336), detecting physiological variables alterations (328) or examining pulmonary surfactant alterations due to MV (294-298, 330). However, few studies addressed a global study in a single model *in vivo* (Chapter 1). Consequently, the experimental design variability and the variation of factors influencing this injury, lead to a wide range of biologic outcomes that limited a consensus on the importance of the factors determined and their link to systemic dysfunction (256, 350).

Nonetheless, some studies attribute these heterogeneity outcomes to different degrees of susceptibility to mechanical stress, arguing that a failure in the activation

of protective mechanisms or their inhibition may lead to a damaging imbalance (299, 351, 352).

On the basis of the above information, we formulate the following questions:

Experimental animals facing the same injurious mechanical stress may develop different responses according to their susceptibility?

If they do so, which are the main factors contributing to these different responses to damage? Some of these factors could be useful to develop therapeutic strategies?

To address these questions we established a model of injurious MV which was subdivided in two groups according to variations in mean arterial pressure (MAP) at 60 min. Subsequently, we investigate the possible different responses to injurious MV at different levels: physiological, histological, cellular, molecular and biochemical, focusing especially on pulmonary surfactant.

3. EXPERIMENTAL DESIGN

Male *Sprague-Dawley* rats were anesthetized and a surgical tracheotomy was performed to ventilate them. Subsequently, animals were randomly distributed in the following groups:

- Control group (C) (n=5): animals undergoing identical anesthetic and surgical procedures than the other groups but without applying MV.
- Low-stretch ventilation group (LV) (n=5): rats were ventilated applying this protective parameters: Tidal volume (V_T) = 9 ml/kg, positive end-expiratory pressure (PEEP) = 5 cmH_2O, during 150 min.

High-stretch ventilation group (HV) (n=17): animals were ventilated under damaging conditions: V_T = 25 ml/kg, PEEP = 0 cm H_2O, during 150 min.

In both ventilated groups, respiratory rate was 70 bpm, inspiratory time 0.35 sec., expiratory time 0.56 sec. and FiO_2 0.35. Animals were ventilated for an equilibration period of 30 min using the low V_T ventilation parameters. Then, the assigned V_T was administered starting at t=0 min up to 150 min.

Ventilatory and hemodynamic parameters of ventilated groups were registered and controlled during the ventilatory process. HV group was subdivided according to the variations in MAP at one hour:

- Animals resistant to HV (rHV) (n=6): animals with no changes in MAP at 60 min, sacrificed at 150 min.
- Animals susceptible to HV (sHV) (n=11): animals with a significant MAP reduction at 60 min and sacrificed at this point (MAP≤50 mmHg).

Hemodynamic and ventilatory parameters were registered at t=0 min, t=60 min and t=150 min. Blood samples were drawn before and after the ventilatory procedure for blood gases determination and its biochemical analysis.

At the end of the ventilatory period, the animals were sacrificed by exsanguination and subsequently we proceeded to obtain bronchoalveolar lavage free of cells (BAL), alveolar fluid cells and lung tissue.

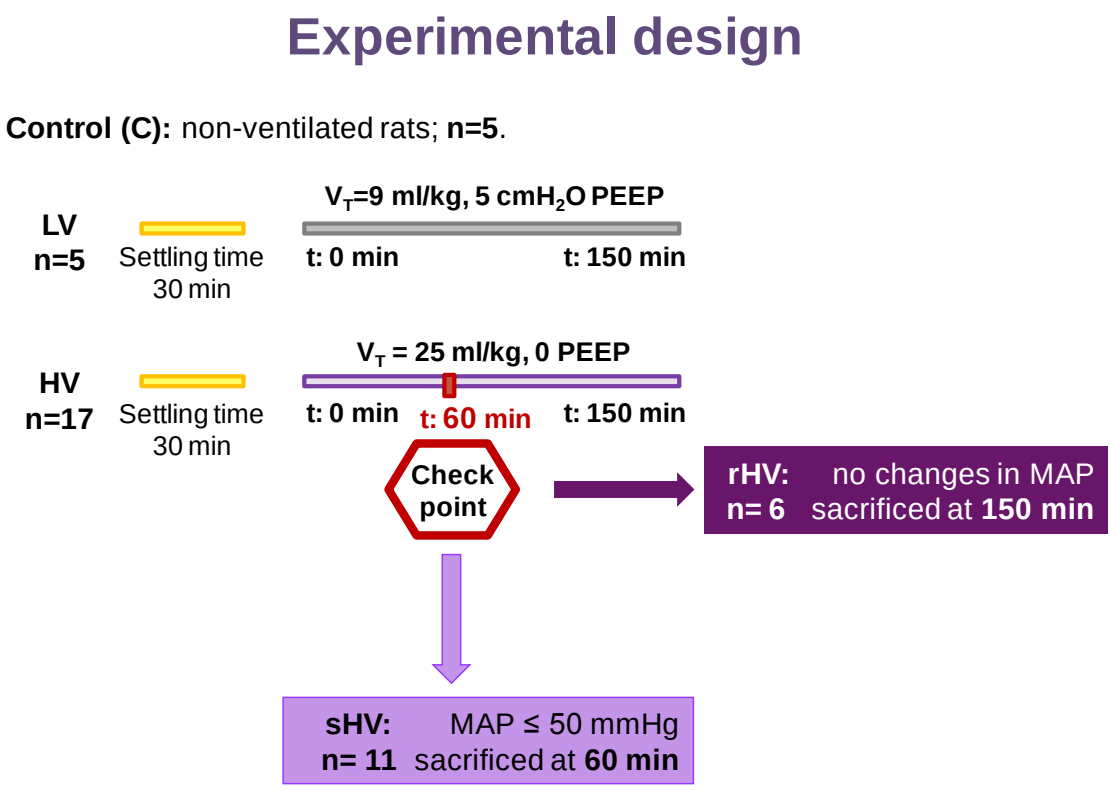

Figure 1: Experimental design. Representation of all groups established subdivided according to the mechanical ventilation strategies.

4. RESULTS

4.1. Physiology

We measured hemodinamic and ventilatory parameters in five rats per ventilated group. Peak inspiratory pressure (PIP) and mean arterial pressure (MAP) were analyzed at t=0 min, t=60 min and t=150 min of the ventilation period. As a result, significant changes in MAP resulted in the subdivision of HV group according to this criterion: MAP≤50 mmHg (Figure 2a). Interestingly, PIP already increased significantly at the beginning of HV in sHV group ($p<0.01$ vs. rHV) and kept growing during the following hour ($p<0.001$ vs. rHV), suggesting that PIP may be a good early damage marker in the prediction of VILI (Figure 3). We also detected a severe hypoxemia at the end of the ventilator period of sHV in contrast with rHV ($p<0.01$) as depicted PaO_2/FiO_2 ratio in Figure 2b.

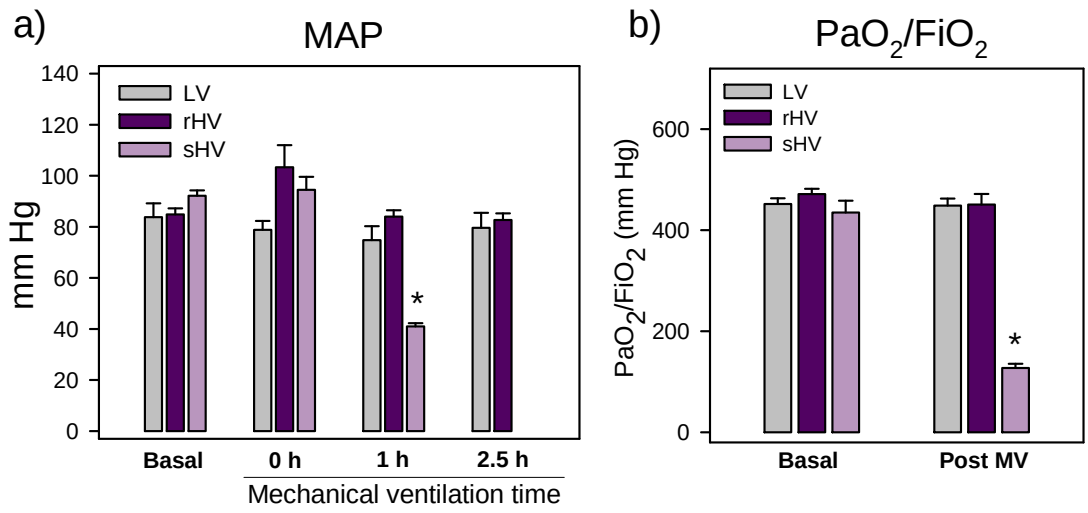

Figure 2: Changes during the mechanical ventilation (MV) period in hemodynamic variables in n=5 rats from ventilated groups with Low or High tidal volumes.

a) Mean arterial pressure (MAP) was measured at baseline, start and after 1 and 2.5 hours of MV. b) Arterial partial pressure of oxygen (PaO_2)-to-fractional inspired oxygen (FiO_2) ratio values were assessed before and after MV.

Data represent mean ± S.E.M of n=5 rats per group. *$p<0.001$ vs. rHV.

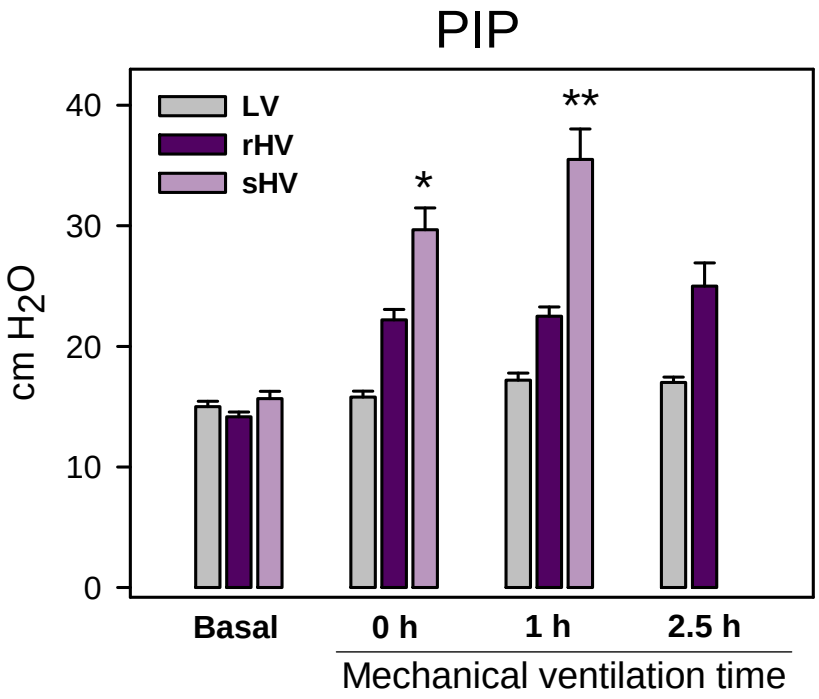

Figure 3: Changes during the mechanical ventilation (MV) period in peak inspiratory pressure (PIP) in n=5 rats from ventilated groups with Low or High tidal volumes.
PIP was measured at baseline, start and after 1 and 2.5 hours of MV. Data represent mean ± S.E.M of n=5 rats per group. *p<0.01 and **p<0.001 vs. rHV.

We also measured pH and lactate concentration in arterial blood at the end of MV. Rats from sHV group presented systemic acidosis and hyperlactatemia in contrast with both LV and rHV in the same time frame (Table 1). Furthermore, we determined the levels of glucose, creatinine, lactate aminotrasferase (LDH) and creatinine kinase (CK) enzymes in blood harvested at the end of MV. There was a significant increase of glucose and LDH in sHV group vs. LV and rHV groups. Also CK significantly increased vs. LV group (Table 1). Our data suggest an increase of anaerobic metabolism in sHV group.

Table 1: Changes in pH, blood enzymes and blood metabolites in rats subjected to Low (LV) or High mechanical ventilation strategies during 60 (sHV) or 150 min (rHV).

Parameter	LV	rHV	sHV
pH	7.27±0.01	7.28±0.02	7.18±0.02* ###
Lactate (mmol/L)	0.73±0.13	0.87±0.08	2.85±0.39*** ###
Glucose (mg/dL)	121.8±6.73	147.85±10.47	253.5±20.64*** ###
Creatinine (mg/dL)	0.76±0.08	0.57±0.04	0.75±0.06
LDH (IU/L)	366.4±101.8	502.83±61.64	876.83±119.38* #
CK (IU/L)	317.2±33.78	756.3±176.3	1423.67±386.72*

Definition of abbreviation: LDH: lactate aminotrasferase; CK: creatinine kinase.

All factors were measured at the end of the ventilator period. Data are mean ± S.E.M. *p<0.05, **p<0.01, ***p<0.001, vs. LV; #p<0.05, ##p<0.01, ###p<0.001, vs. rHV.

4.2. Alveolar injury

Changes in the alveolar space due to MV were characterized by the evaluation of histological score, alveolar fluid cells alterations and damage markers presence.

4.2.1. Alterations in the alveolar space

Histological score was evaluated in 5 animals per group and revealed alterations in high-stretched animals, being significant in sHV group ($p<0.05$) (Figure 4a). Interestingly, edema presence, represented as total amount of proteins in BAL determined in 5 animals per group, only appeared in sHV group ($p<0.001$) (Figure 4b).

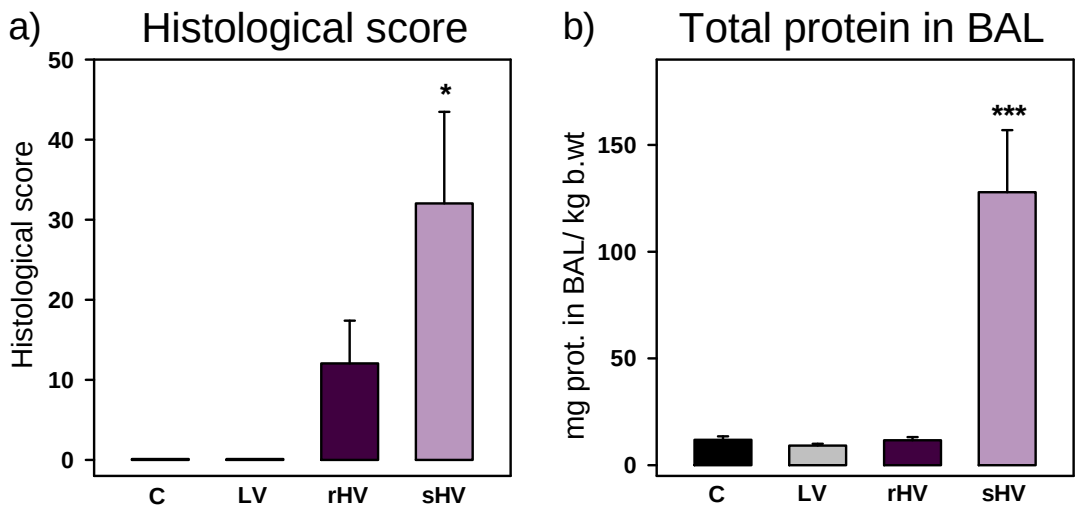

Figure 4: Alveolar injury in the different experimental groups.
Histological score was assessed by hematoxylin-eosin staining of the isolated and fixated left lungs of n=5 animals of all groups. Edema presence was measured as total protein content of bronchoalveolar fluid in n=5 animal per group.
Data represent mean ± S.E.M. *p<0.05, ***p<0.001 vs. Control.

4.2.2. Alveolar fluid cells

Total cell counts in BAL were assessed in five animals of all groups. Interestingly, alveolar cell counts decreased when MV was applied. In particular, cell counts significantly decreased in the rHV ($p<0.05$) and sHV ($p<0.001$) groups (Figure 5a, left panel). Also, macrophages proportion significantly decreased in rHV ($p<0.05$) and sHV ($p<0.001$) groups (Figure 4a, right panel). Hence, MV may change alveolar fluid cells profile as depict the representative flow cytometric side scatter (SSC, relative complexity)/forward scatter (FSC, relative size) dot plots from all experimental groups (Figure 5b).

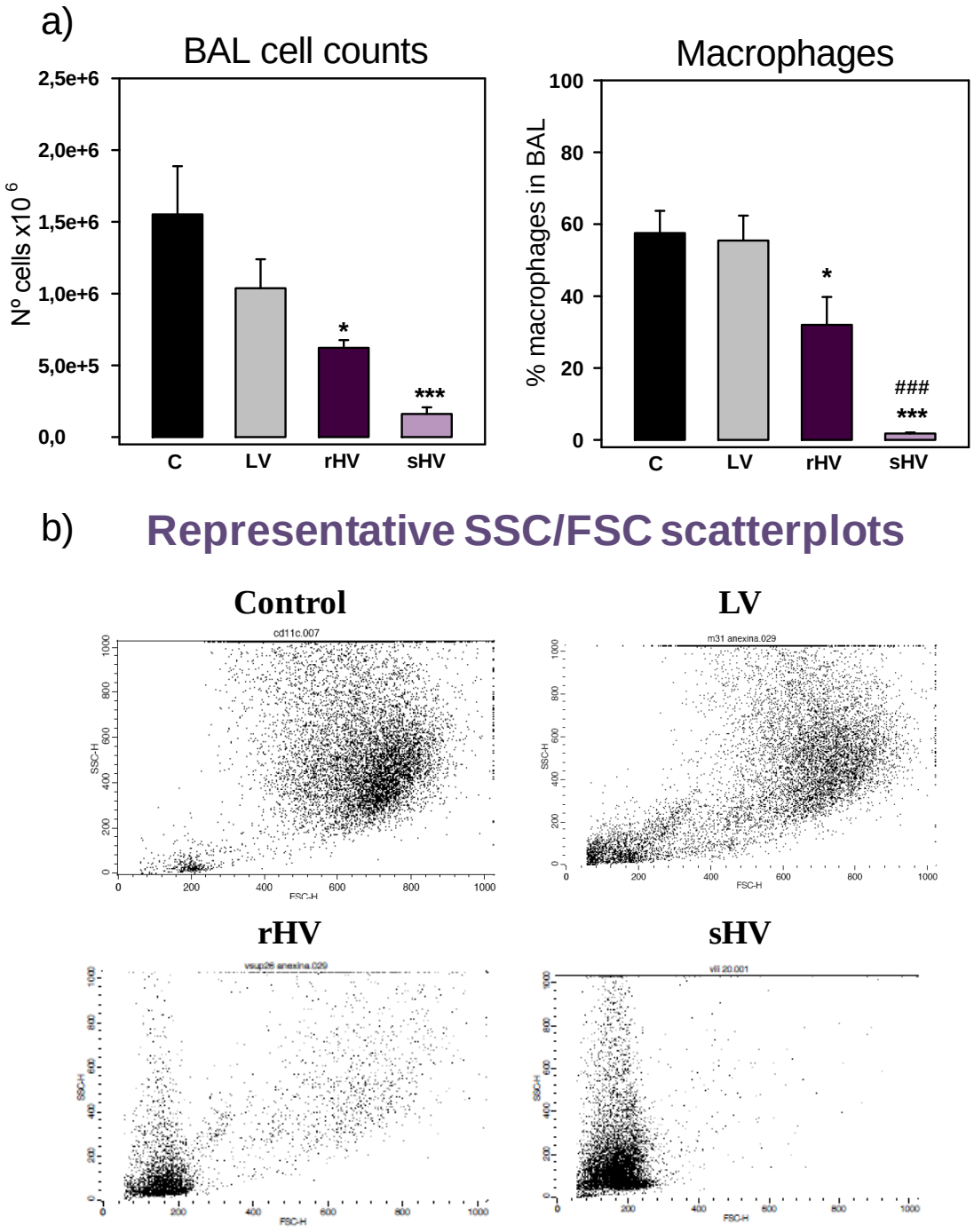

Figure 5: Alveolar cells profile in all experimental groups (n=5).

a) Left panel represent total cell counts recovered in BALdetermined by assessing cell viability with trypan blue dye exclusion. Right panel depicted the proportion of alveolar macrophages in BAL fluid determined by fluorescence flow cytometry using a specific monoclonal antibodies anti-CD11c for alveolar. n=5 animal per group were analyzed.

Data represent mean ± S.E.M. *$p<0.05$, ***$p<0.001$ vs. Control; $^{###}p<0.001$ vs. rHV.

b) Representative side scatter (SSC)/forward scatter (FSC) dot plots of the flow cytometric profile of total alveolar fluid cells from all groups of study.

.

4.2.3. Damage markers

The presence of cytokines (n=4) and chemokines (n=5) was determined in BAL (Figure 6a and 6b) and plasma (Table 2) as well as the presence of acid sphingomyelinase (ASMase) activity in these fluids (n=3) (Figure 6c and table 2).

IL-6 is a pleiotropic cytokine with multiple functions in the inflammatory response (353). This cytokine only increased significantly in rHV group ($p<0.05$) while its levels in plasma did not change among groups. Another pleiotropic cytokine involved in acute inflammatory responses, TNF-α (331), also increased its levels in the HV groups, being significant in sHV vs. Control ($p<0.001$), while it was undetectable in plasma of all groups of study.

We also studied the presence of chemokines MCP-1 and MIP-2. MCP-1 is a chemokine involved in proinflammatory responses, recruitment of monocytes and memory T cells as well as a contributor of macrophages activation (354, 355). Interestingly, MCP-1 significantly increased in BAL sHV ($p<0.001$ vs. Control and $p<0.05$ vs. rHV). On the other hand, MIP-2 is a well-known neutrophil chemoattractant involved in the elicitation of pulmonary neutrophilia (356), which was significantly increased in rHV ($p<0.05$) and sHV ($p<0.001$ vs. Control and $p<0.05$ vs. rHV) groups in BAL and also was significantly increased in plasma of sHV ($p<0.05$).

In order to assess the possible modulatory role of IL-6, we determined a ratio between each cytokine evaluated in BAL (TNF-α, MCP-1 and MIP-2) and IL-6. As a result, we observe in Table 2 a significant increase of these ratios in sHV group in contrast with control group values.

These data suggest that there are different inflammatory responses between HV groups being exacerbated in sHV group.

ASMase catalyze the hydrolysis of sphingomyelin (SM) to ceramide and coline phosphate, being ASMase-derived ceramide a promoter of several pathways leading to ALI (332). ASMase activity significantly increases in BAL of sHV group ($p<0.05$) compared with all groups whereas its levels in plasma did not vary among groups (Table 2).

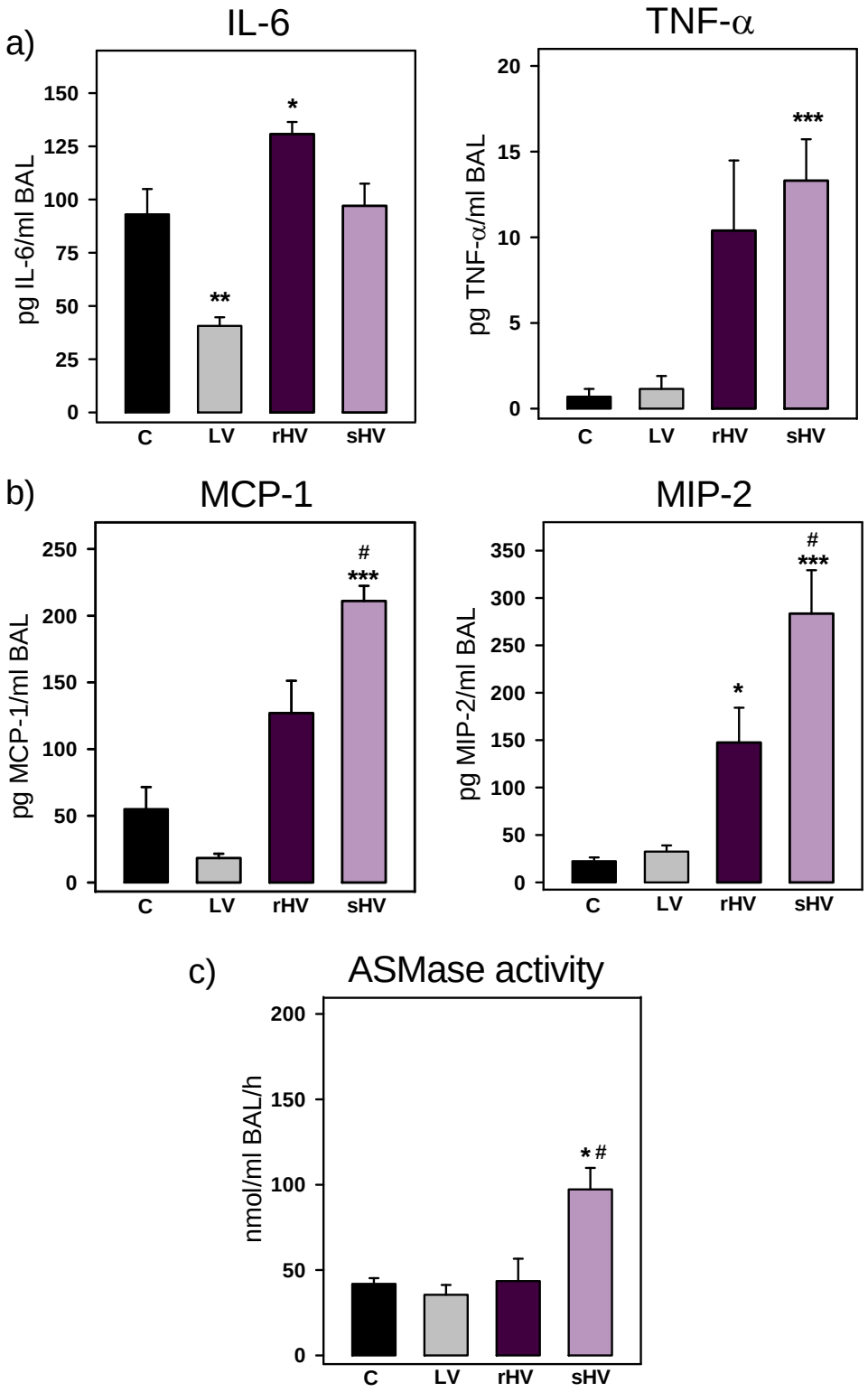

Figure 6: Damage markers detected in BAL of all groups.

a) Inflammatory cytokines IL-6 and TNF-αwere measured in BAL of n=4 rats per group by colorimetric rat ELISA kits. TNF-α levels increase in High V_T groups and significantly in sHV while IL-6 levels augment in High V_T groups and significantly in rHV.

b) Inflammatory chemokines MCP-1 and MIP-2 were both detected by ELISA kits in BAL on five rats per group. MCP-1 levels significantly increases in BAL of sHV group and MIP-2 significantly increases in both high-ventilated groups.

c) ASMase activity in BAL was measured by performing an enzymatic assay (n=3). ASMase activity values in BAL increase in sHV vs. all groups.

Data represent mean ± S.E.M. *p<0.05, **p<0.01, ***p<0.001 vs. Control; $^{\#}$p<0.05 vs. rHV.

Table 2: Relative content of cytokines referred to IL-6 levels in BAL and damage markers in plasma of Control (C) and rats subjected to Low (LV) or High mechanical ventilation strategies during 60 (sHV) or 150 min (rHV).

Groups	BAL			Plasma		
	TNF-α/IL-6	MIP-2/IL-6	MCP-1/IL-6	IL-6 (pg/ml)	MIP-2 (pg/ml)	ASMase activity (nmol/ml/h)
C	$7.1e^{-3}$±$4.9e^{-3}$	0.3±0.11	0.55±0.17	29.12±6	10.04±1.58	170.9±11.9
LV	0.03±0.017	0.8±0.2	0.49±0.1	40.5±2.3	8.1±2.1	178.3±13.5
rHV	0.066±0.03	1.1±0.3	0.95±0.15	42.3±1.5	13.65±1.82	161.7±15.3
sHV	0.16±0.04**	2.9±0.45***	2.25±0.35***	48.4±7.25	35.2±14.7*	152.6±15.3

Definition of abbreviation: TNF-α: Tumor necrosis factor alpha; IL-6: Interleukin 6; MIP-2: macrophage inflammatory protein 2; MCP-1: monocyte chemotactic protein 1; ASMase: Acid sphingomyelinase.
All factors were measured at the end of the ventilator period. Data are mean ± S.E.M.* $p<0.05$ and **$p<0.01$ vs. Control; *** $p<0.001$ vs. all groups.

4.3. Surfactant analysis

4.3.1. Pulmonary surfactant composition analysis

Pulmonary surfactant is a surface-active lipoprotein complex mainly composed by 90% lipids, most of them PL but also a small proportion of neutral lipids and cholesterol, and 10% of proteins being four the PS-associated proteins: SP-A, SP-B, SP-C and SP-D. PS is secreted by ATII as large aggregates (LA), which accomplish its main function. In a normal lung, compression and expansion during respiration leads the conversion of LA to a non-functional fraction, the small aggregates (SA), which are either degraded or recycled by alveolar macrophages or ATII (314). Conversely, under pathological situations, there is an alteration of the conversion of LA to SA, being the increase of the SA/LA ratio a damage marker of VILI.

Therefore, we evaluate possible alterations in total PL amounts in PS and its fractions (Figure 7). Also we assess PS-associated protein levels and its RNA expression in lung tissue (Figure 8).

The content of PL in PS is significantly increased in both high MV groups. However, rHV group had LA significantly increased compared with all groups ($p<0.001$) whereas sHV had significantly increased SA ($p<0.001$) as well as its SA/LA ratio ($p<0.001$) in contrast with all groups. Therefore, high MV may induce PS release into the alveolar space but in sHV is rapidly conversed to non-functional aggregates.

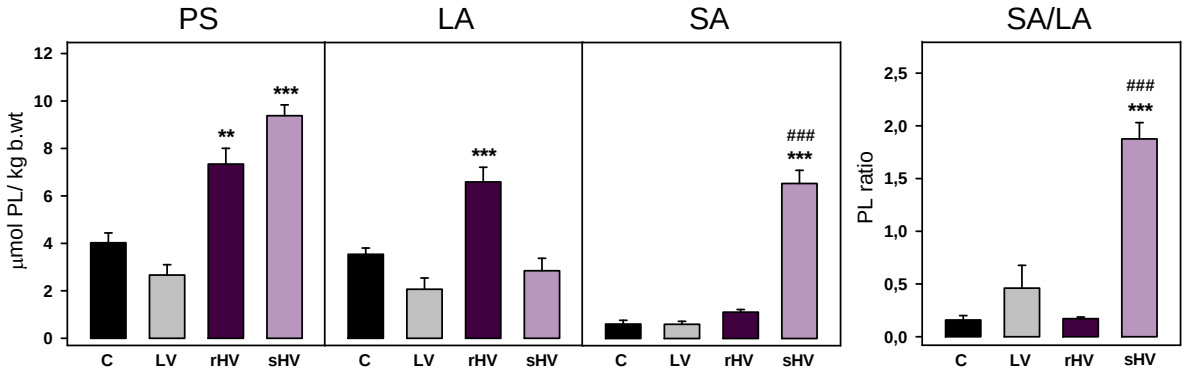

Figure 7: Total amount of phospholipids (PL) in pulmonary surfactant (PS)and its fractions of all experimental groups (n=5).
Total PL content in PS and its active (LA) and inactive (SA) fractions were measured in all groups of study. As well, it was determined the ratio of PL content between SA and LA. There was a significant increase of PS in high-stretched groups. Interestingly, there was a significant increase of the LA amounts in rHV whereas sHV had a significant increase in SA and SA/LA ratio.
Data represent mean ± S.E.M. ** $p<0.01$ and ***$p<0.001$ vs. Control; $^{###}p<0.001$ vs. rHV.

Figure 8 shows protein and RNA levels of the specific surfactant proteins SP-A, SP-B and SP-C of all MV groups.

Immunoblotting reveals a significant decrease of SP-A ($p<0.05$ vs. rHV) and SP-B ($p<0.001$ vs. rHV and $p<0.01$ vs. LV) levels in sHV group analyzing four animals per ventilator group. SP-C protein levels were analyzed in two animals per ventilator group. The results depicted significant decrease of SP-C levels in HV groups ($p<0.001$ vs. LV), obtaining significant differences between them ($p<0.05$).

As well, RNA levels were evaluated in four animals per HV group and two animals in LV group. As a result, we detected a significant fold decrease of the RNA levels of the three PS-associated proteins evaluated in both HV groups in contrast with LV.

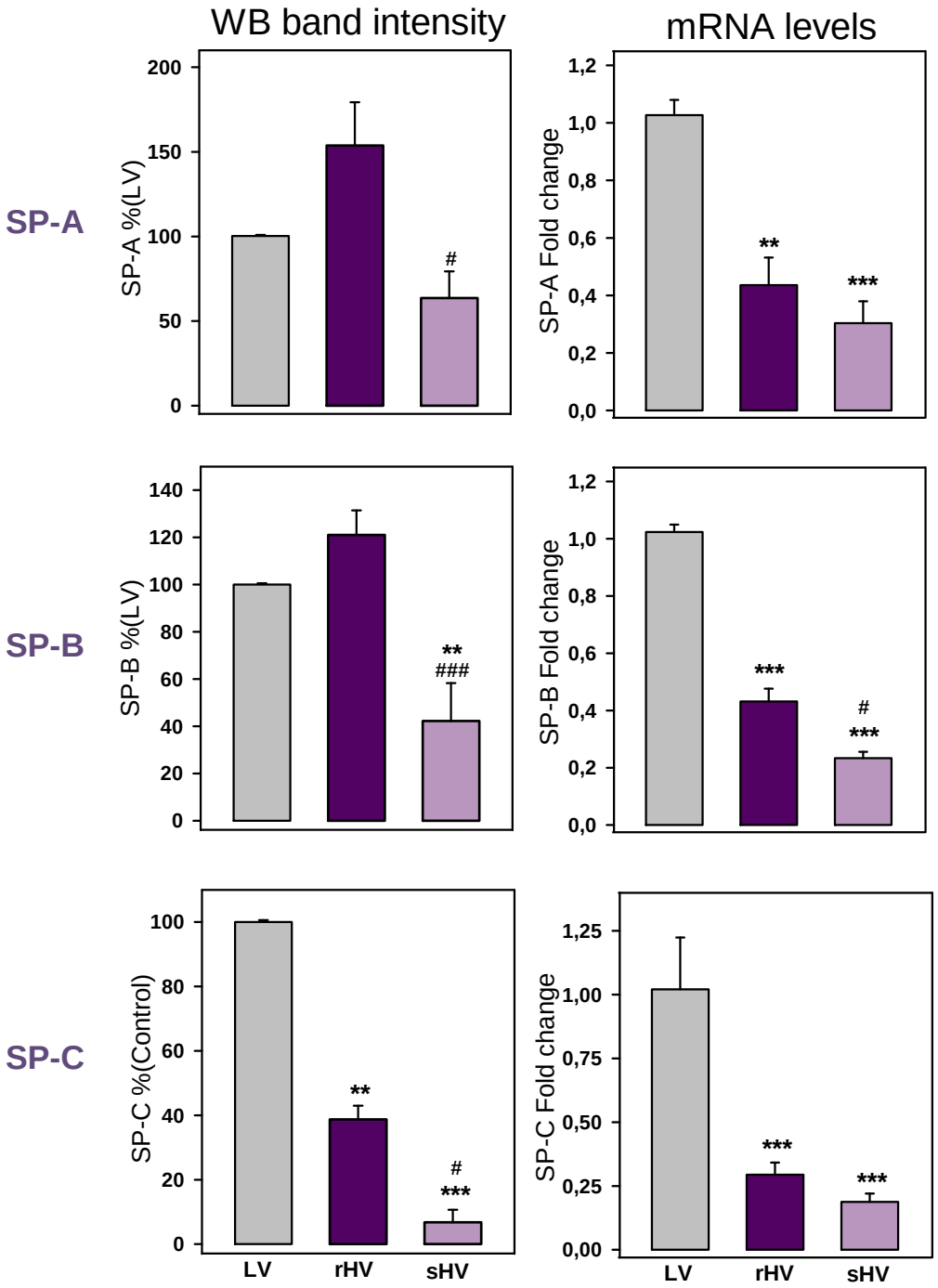

Figure 8: Presence of specific surfactant proteins SP-A, SP-B and SP-C in large aggregates (LA) and its RNA expression in lung tissue of all ventilated groups.

Protein levels were detected in LA samples by Western blot. Proteins quantification was achieved by densitometric evaluation (n=4 per group in SP-A and SP-B; n=2 per group in SPC).

RNA expression of SP-A, SP-B and SP-C was detected using total RNA isolated from the lower lobe of the right lung. cDNA synthesis was performed using 1µg total RNA as input and it was amplified by RT-PCR using specific primers. Results were analyzed using ΔΔCT method and expressed as normalized fold expression. (n=4 per HV group and n=2 in LV group).

Data represent mean ± S.E.M. **p<0.01 and***p<0.001 vs. LV; $^{\#}$p<0.05 and $^{\#\#\#}$p<0.001 vs.rHV.

4.3.2. Pulmonary surfactant functionality

Pulmonary surfactant biophysical function was determined using to techniques: Interfacial adsorption assay and Captive Bubble Surfactometry.

4.3.2.1. Interfacial adsorption

The ability of LA to adsorb onto and spread at the air–water interface was measuredin four rats per experimental group using a Wilhelmy-like high-sensitive surface microbalance, coupled to a teflon dish of very small size by following the variation in surface pressure as a function of time, as previously described (322). This ability has been significantly impaired in sHVgroup at 30 min in contrast with all groups ($p<0.001$), as shows Figure 9.

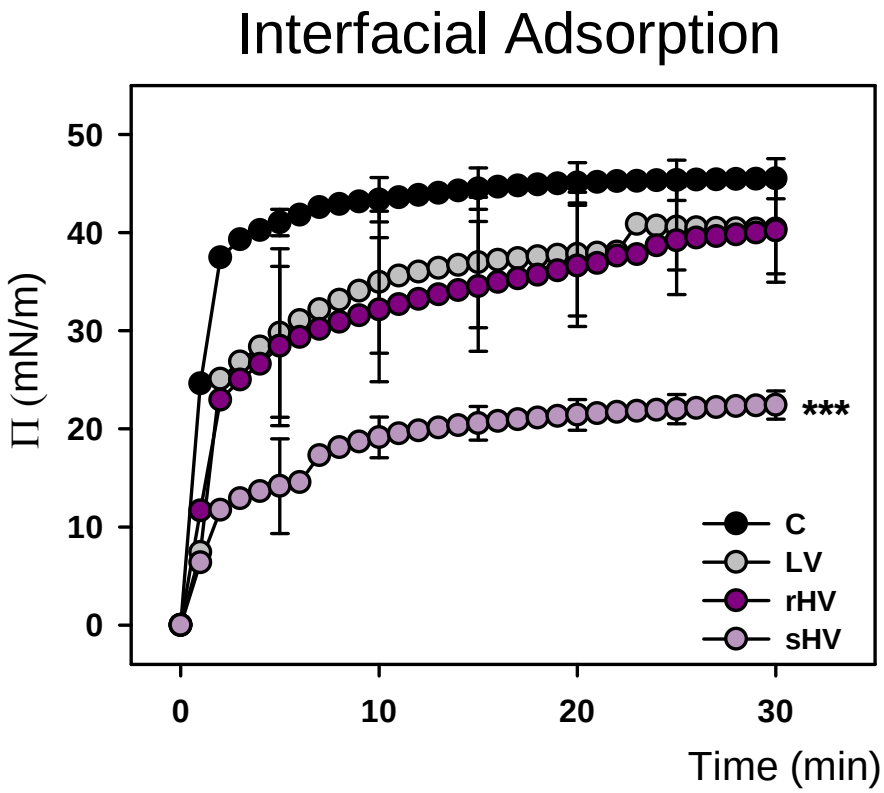

Figure 9: Interfacial adsorption of the active fraction of pulmonary surfactant of all experimental groups (n=4).
Surfactant interfacial adsorption was determined in a Wilhelmy-like high-sensitive surface microbalance. Surfactant interfacial adsorption of sHV is significantly altered.
Data represent mean ± S.E.M. ***$p<0.001$ vs. all groups, by one-way ANOVA using a Bonferroni pos hoc test when appropriate.

4.3.2.2. Captive Bubble Surfactometry

This is the best technique to simulate the compression-expansion cycling that happens at the breathing interface in order to evaluate the three main characteristic dynamic properties of PS: very rapid interfacial adsorption (~23 mN/m), low surface tension upon compression (less than 2mN/m) and efficient re-extension upon expansion (325, 357, 358). Figure 10 compares interfacial adsorption kinetics of 20 mg/ml of LA of three rats from HV groups and Control group assessed after deposition at the interface of the captive air bubble in the captive bubble surfactometer. Control group adsorbs to form a stable surface film with a minimum equilibrium surface tension of ~23 mN/m within the first seconds after deposition. rHV also reached this surface tension but it takes more time. However, sHV LA was far from reaching the equilibrium tension (41.6 ± 0.7 mN/m; $p<0.001$ vs. all groups) (Table 3). Also, re-adsorption of excess material upon expansion of the bubble (see the lower panel in figure 10) had the same pattern in all groups than in initial adsorption measurements, being significantly increased the equilibrium tension of sHV LA ($p<0.001$ vs. all groups) (Table 3).

Cycling isotherms acquired from LA of three rats from Control and rHV rats did not represent any compression/expansion hysteresis along dynamic cycles (Figure 11). Only the first dynamic cycle of rHV group exhibited hysteresis presence, which was lost in the subsequent cycles. All isotherms reached surface tensions ~4mN/m with <15% compression. In contrast, isotherms of sHV LA (n=3) depicted a marginal hysteresis as well as maximal and minimal surface tensions significantly higher than the other groups associated with ~30% compression (Figure 11 and Table 4).

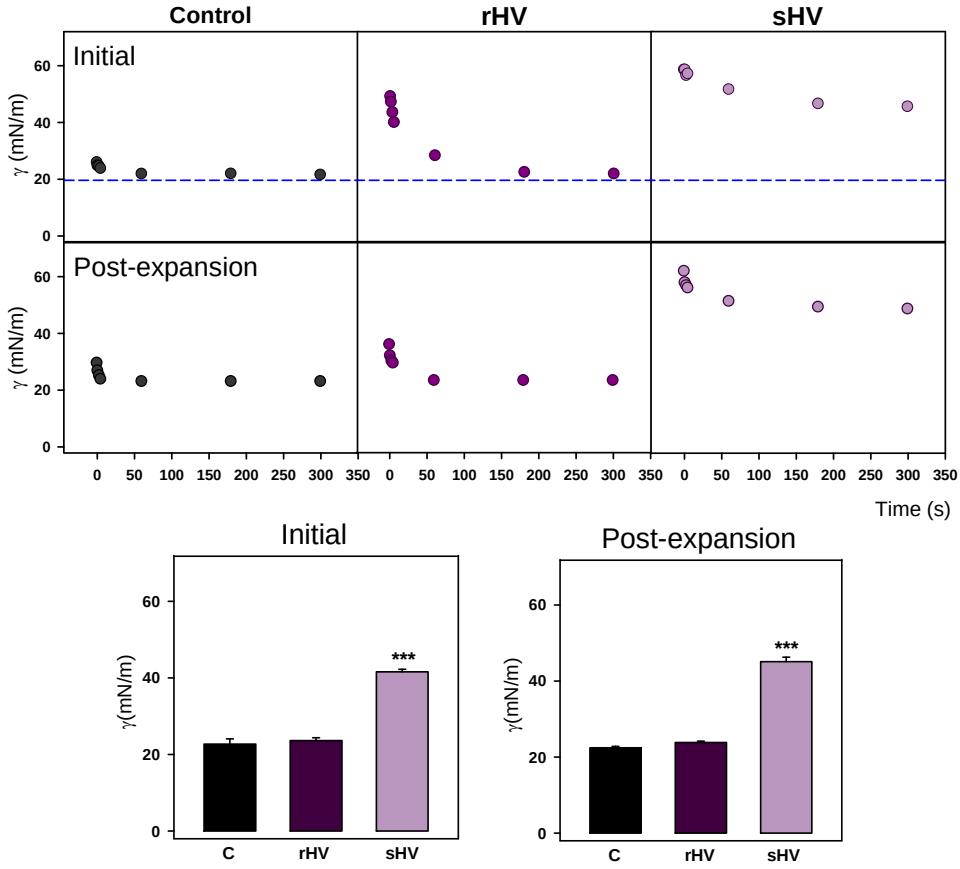

Figure 10: Initial and post-expansion adsorption of the active fraction (LA) of pulmonary surfactant from n=3 animals of Control and high-ventilated groups evaluated in captive bubble surfactometer.

Upper panels are representative samples of initial adsorption (top) immediately after the application of 20 mg/ml of LA into the bubble's air-liquid interface and post-expansion adsorption (below) of all samples. As well, media values of the minimum surface tension (γ_i) reached at 5 min after sample application and media values of the minimum surface tension (γ_{post}) reached at 5 min after interface expansion are represented (lower panels).

Data represent mean ± S.E.M. ***p<0.001 vs. all groups.

Table 3: Initial adsorption and post-expansion adsorption of pulmonary surfactant from control rats and rats injuriously ventilated during 60 (sHV) or 150 min (rHV) assessed in a captive bubble surfactometer.

Groups	Interfacial adsorption γ_{min} (mN/m) t=5 min	Post-expansion adsorption γ_{min} (mN/m) t=5 min
C	22.7±1.4	22.4±0.4
rHV	23.6±0.8	23.8±0.4
sHV	41.6±0.7***	45.1±1.2***

Definition of abbreviation: γ_{min}: minimum surface tension.

Data are mean ± S.E.M. ***p<0.001 vs. all groups.

Dynamic cycles

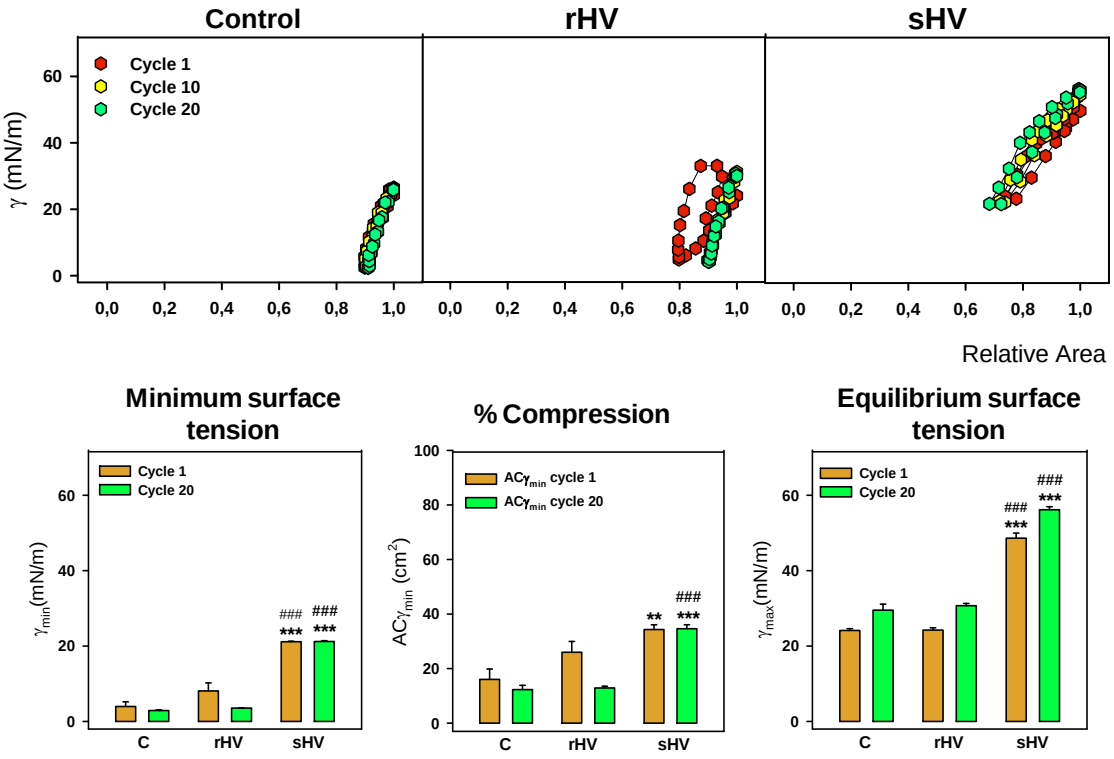

Figure 11: Dynamic compression-expansion isotherms of the active fraction (LA) of pulmonary surfactant fromn=3 animals of Control and high-stretched groups evaluated in captive bubble surfactometer.

Upper panels are representative surface tension/relative area isotherms obtained from 1º, 10º and 20º cycles during the dynamic cycling process of 20 cycles/min. Lower panels depict media values of minimum (γ_{min}) and maximum (γ_{max}) surface tensions as well as compressed area values at γ_{min} ($AC\gamma_{min}$) registered during the first and last cycle from dynamic processes. Data represent mean ± S.E.M. **p<0.01, ***p<0.001 vs. Control; $^{###}$p<0.001 vs. rHV.

Table 4: Effect of injurious mechanical ventilation during 60 (sHV) or 150 min (rHV) on the active fraction of pulmonary surfactant surface activity assessed in a captive bubble surfactometer under dynamic conditions.

Groups	Dynamic Cycles					
	Cycle 1			Cycle 20		
	γ_{min} (mN/m)	$AC\gamma_{min}$ (%)	γ_{max} (mN/m)	γ_{min} (mN/m)	$AC\gamma_{min}$ (%)	γ_{max} (mN/m)
C	4±1.2	16.1±3.8	24.1±0.5	2.9±0.2	12.3±1.6	29.5±1.6
rHV	8±2	26±4	24.3±0.6	3.5±0.1	13±0.6	30.7±0.6
sHV	21.2±0.2$^{***###}$	34.3±1.7**	48.6±1.4$^{***###}$	21.2±0.2$^{***###}$	34.6±1.5$^{***###}$	56.2±0.8$^{***###}$

Definition of abbreviation: γ_{min}: minimum surface tension; $AC\gamma_{min}$: relative area of compression at minimum surface tension; γ_{max}: maximum surface tension.

Data are mean ± S.E.M. **p<0.01 and ***p<0.001 vs. Control; $^{###}$p<0.001 vs. rHV.

4.3.3. Presence of pulmonary surfactant functionality inhibitors.

Previous studies in our laboratory demonstrate that C-Reactive Protein (CRP) and lipid peroxidation are main causes of surfactant impairment in VILI (Chapter 1).
CRP is an acute-phase protein that inhibits pulmonary surfactant by binding to it when reaches the alveolar space (333). As we can see in Figure 12b, CRP to PL ratio significantly increased in sHV group compared with Control ($p<0.01$) (n=3 per group).

On the other hand, is widely accepted that mechanical stress stimulates ROS production (292). As a result, this oxidative environment directly affects PS by lipid peroxidation of LA. We observed a significant increase of LA lipid peroxidation in sHV group in contrast with rHV ($p<0.05$) in Figure 12d (n=4 per group).

Finally, we also assessed total protein and Ch content in LA in five and four animal per group respectively, as they are considered potential inhibitors of PS functionality (296). Accordingly, we observed a significant increase of both, protein to PL ratio in LA ($p<0.001$ vs. all groups) and the molar percentage of Ch to PL ratio in LA of sHV group ($p<0.05$ vs. Control and rHV) (Figure 12a and 12c). These data suggest alterations in LA composition as well as plasma protein contamination, which may lead to surfactant biophysical activity impairment.

Therefore, the presence of all these factors contributes to PS functionality dysfunction.

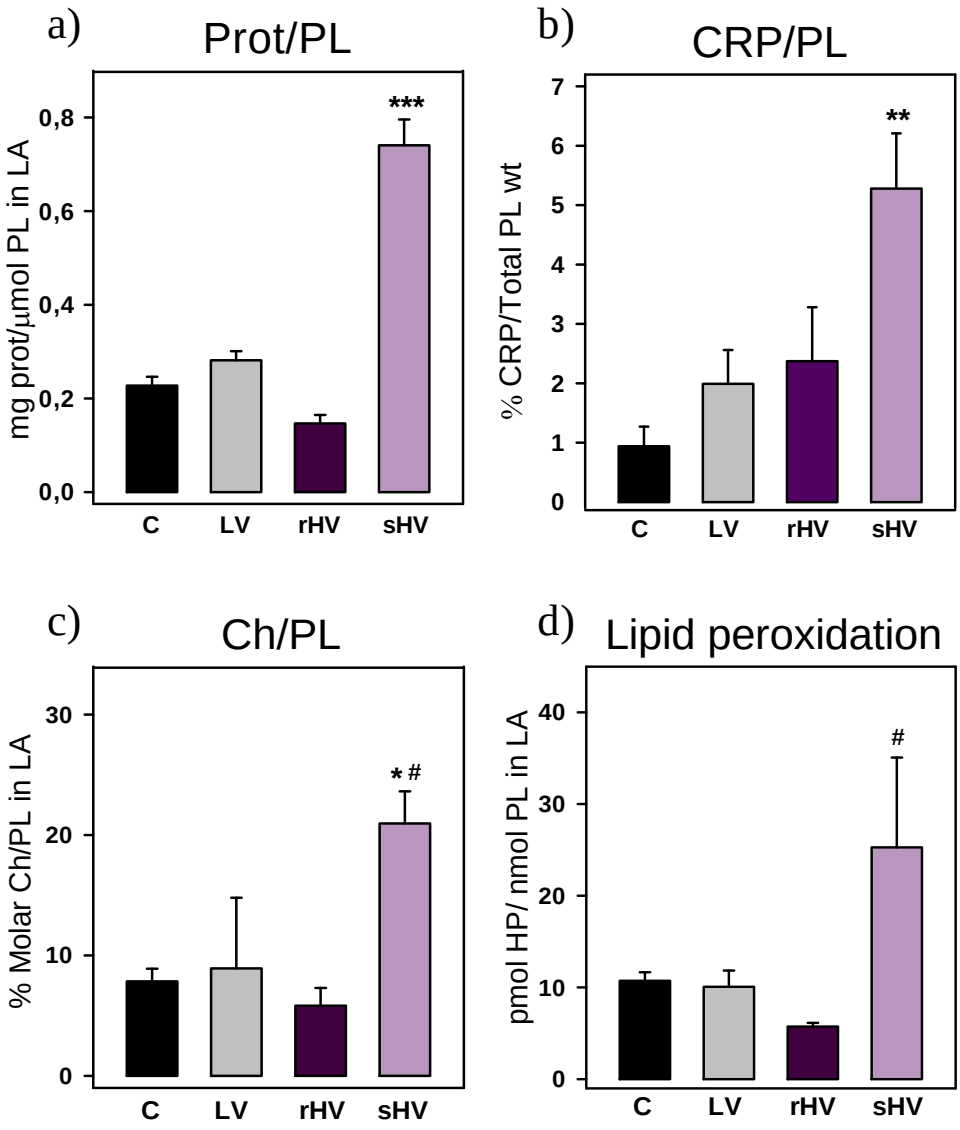

Figure 12: Presence of pulmonary surfactant inactivators in all groups of study.
a) Total protein to PL ratio in LA was assessed in five animals of all groups of study. This ratio significantly increases in sHV group as a result of plasma-derived proteins contamination.
b) CRP was measured using a rat CRP ELISA kit. CRP to PL in pulmonary surfactant ratio significantly increased in sHV (n=3 per group).
c) Analysis of Ch was performed using an enzymatic colorimetric kit (n=4 per group). Molar percentage of Ch to PL ratio in LA of sHV significantly increases vs. Control and rHV groups.
d) Lipid hydroperoxides were quantified in lipid extracts of LA from n=4 animals per group by FOX method. Lipid hydroperoxides significantly increase in LA of sHV group vs. rHV group.
Data represent mean ± S.E.M. *$p<0.05$ and **$p<0.01$ vs. Control; ***$p<0.001$ vs. all groups; $^{\#}p<0.05$ vs. rHV.

5. DISCUSSION

This study demonstrated that under the same injurious MV stress, experimental animals had two different outcomes: a susceptible response (sHV) or a resistant outcome to injurious MV (rHV). These two phenotypes almost differed in all levels studied involving several factors.

Previous studies in our laboratory observed a relationship between MV and a reduction of total number of fluid cells (Chapter 1), being remarkable under injurious MV. In this research we also observed this pattern together with a decrement of alveolar macrophages in HV groups, being stronger in sHV group. Furthermore, this decrease was accompanied by an injury score increase in HV groups, characterized by presence of capillary congestion, type I pneumocyte necrosis and hyaline membrane formation covering the denuded epithelial surface, being noteworthy in sHV. As hyaline membranes are composed by cellular debris and fibrin, our data suggest that alveolar macrophages from sHV group are more susceptible to overinflation produced by high V_T and PEEP absence and therefore to necrosis, comprising part of hyaline membranes. Conversely, alveolar macrophages from rHV group may be more resistant to overinflation as proof their higher rates. Therefore, it is reasonable to suggest that MV itself directly affects to alveolar cells by several mechanisms depending on their susceptibility. Interestingly, this susceptibility may also explain the different inflammatory responses observed in HV groups.

IL-6 is a typical early inducible cytokine synthesized by many cell types participating in initiation and regulation of inflammation (213, 359). Interestingly, while there is no doubt about the proinflammatory role of other early inducible cytokines such as TNF-α and MIP-2 after applying an insult to the lung, IL-6 seems to be more than a merely acute phase reaction-inducing cytokine (353), it should be defined as a resolution factor that balances pro- and anti-inflammatory outcomes to further the immunological response (213). In fact, some studies of acute inflammation demonstrated that the lack of IL-6 was related with higher levels of MIP-2 and TNF-α, which in high doses is considered a pathological inflammatory mediator causing cells activation and affecting permeability in combination with other cytokines (353, 359). Our results indicate a possible modulator role of proinflammatory cytokine sby IL-6 as we observed a contradictory pattern in HV groups: while in the alveolar fluid of rHVgroup IL-6 levels significantly increased, TNF-α, MCP-1 and MIP-2 levels

were slightly increased, whereas in BAL of sHV group TNF-α, MCP-1 and MIP-2 significantly increased while IL-6 remained at basal levels. Furthermore, TNF-α/IL-6 ratio, as well as MIP-2/IL-6 ratio and MCP-1/IL-6 ratio significantly increased in sHV group while remained similar in rest of groups. These data suggest a regulation role of IL-6 in rHV that is altered in sHV group leading to an exacerbated proinflammatory status. It is important to note that the only significant difference observe in plasma of ventilated groups was in sHV where MIP-2 levels significantly increased, suggesting a loss of compartmentalization.

All these data suggest that alveolar cells from HV groups had different responses to MV with high V_T and absence of PEEP, which may entail an attenuated or exacerbated inflammatory response in the alveolar space leading to different outcomes.

Also, as previously detected in our laboratory (Chapter 1), we observed an increase of ASMase activity in BAL of sHV group without changes in plasma levels among groups. Interestingly, ASMase activity-derived ceramide increase is involved in permeability alterations and promotes edema formation in models of ALI (336).

Here, we observed a significant increase of total protein in the alveolar space only in sHV group, suggesting edema presence probably due to alterations in the alveolar-capillary barrier while considering the increase of cytokines release as a contributor of this protein increment. Interestingly, an activated proinflammatory status in the alveolar space is considered a main contributor of alterations in alveolar-capillary barrier and tissue injury (173), which are usually linked (235), as we also detected in sHV group. Therefore, these data support the hypothesis that the same stress may induce different activation pathways that leads to an attenuated or exacerbated outcome depending on their susceptibility to injurious MV.

Indeed, we detected other factors that are known to be contributors of alveolar-capillary alterations in VILI. Many studies reported that ventilation with elevated PIP promotes edema (235) as well as few studies reported an increase of PIP values among time under injurious MVstrategies (296, 360). Here we observed a significant increase of PIP in sHV group in contrast with rHV group just at the beginning of high-stretch strategy setup that is aggravated at 1h of injurious MV. This result led us to speculate that PIP under V_T fixated strategies might be an early marker of MV susceptibility.

As well, another contributor to alter alveolar-capillary barrier leading to edema formation is PS impairment (298). An alteration in PS functionality by increasing surface tension at the air-liquid interface in the alveoli not only alters the gradient pressures across the barrier but also leads to decrease pulmonary compliance, atelectasis and hypoxemia associated with anaerobic metabolism (9, 298). Interestingly, we have detected these physiological alterations related with surfactant impairment and PIP increased values in sHV group while rHV had a proper functionality. We observed alterations in interfacial adsorption of sHV using two different techniques. As well, we further evaluated the other dynamic properties of PS detecting a surface tension decrease upon compression that did not reach appropriate values as well as an inefficient re-extension upon expansion of sHV group. Besides PS impairment in sHV, there was also a change in endogenous PS system and its composition.

Several studies reported the conversion of the active fraction of PS (LA) to the inactive fraction (SA) as a primary mechanism of PS impairment, being considered an increase in SA/LA ratio as a damage marker of VILI (298, 361). Here, we observed an alteration of SA/LA conversion in sHV together with a decrease in RNA levels and protein levels of PS-associated proteins, an increase of Ch values relative to PL amount in LA and presence of lipid peroxidation in LA. These findings are consistent with similar results previously obtained in our laboratory (Chapter 1) and other studies using *ex vivo* models (294, 297). However, PS from rHV group had an opposite outcome. We observed adequate biophysical dynamic properties and optimum levels of PS-associated proteins, Ch and absence of peroxidation in this group.

Interestingly, both injuriously MV groups had in common an increase of total PS release into the alveolar space. Previous studies, including ours, have demonstrated that high V_T ventilation increased PS secretion (Chapter 1) (296). However, while rHV group had significantly increased the LA pool without changes in SA, sHV group has the opposite pattern. Therefore injurious MV induced PS release into the alveolar space but depending on animal susceptibility may be rapidly altered probably due to the exacerbated inflammatory status in the alveolar space or may remain stable probably helping to ensure the attenuated response to injurious MV. As a result, a proper maintenance of PS against VILI may contribute to attenuate immune responses, as some studies reported immuno-modulator properties of PS PL (88, 148)

as well as maintain the alveolar barrier integrity.

In fact, it is worth highlighting that PS alterations contributing to edema presence provokes a vicious circle of surfactant inactivation as several plasma-derived proteins are able to even compete with PS for reaching the air-liquid interface (6) or directly binding to it. In this research we have detected protein contamination in LA in sHV group as well as a significant increase of CRP, an acute-phase protein that inhibits PS functionality by binding to it (Chapter 1) (333).

To summarize, we demonstrated that injurious MV could develop two different outcomes according to the animal susceptibility. The main factor that seems to contribute to protect the lung against injurious MV is an attenuated inflammatory response where IL-6 seems to play a key role. As a result, lack of edema, tissue injury or PS alterations are the main characteristic factors of this resistant outcome against VILI. Interestingly, our data indicated that VILI occurred only in animal models when surfactant is inactivated. Therefore, these results show that there is a direct link between pronounced proinflammatory response and surfactant inactivation. Consequently, we suggest that the best approach for early intervention, prior to exposition to mechanical ventilation, would be the administration of antiinflammatory agents. Given the beneficial effects of high surfactant secretion in survival animals exposed to high VT, surfactant-like nanoliposomes could be useful as carriers for delivering antiinflammatory agents to the alveolar spaces. Surfactant-like vesicles used as a vehicle could ensure drug contact with the alveolar spaces and could increase the potency of anti-inflammatory agents on alveolar epithelial cells and macrophages, facilitating their entrance into the cells. At the same time, exogenous surfactant administration could contribute to improve pulmonary function.

To conclude, these results depicts that an attenuated inflammatory response together with increasing endogenous, fully active, lung surfactant into the alveolar space prevents edema and a worsened outcome to high-stretch ventilation.

Chapter 3

Effect of prolonged low-stretch ventilation after injurious high-stretch ventilation in resistant rats

1. ABSTRACT

The aim of the present study was to elucidate the effect of prolonged conventional low-stretch ventilation, with or without previous exposition to injurious high-stretch ventilation.

Sprague-Dawley rats were randomly assigned to control conditions (no MV), low-stretch ventilation during 8.5 h (LV) [Tidal volume (V_T) = 9 ml/kg, positive-end expiratory pressure (PEEP) = 5 cm H_2O] or injurious ventilation [V_T = 25 ml/kg, PEEP = 0cm H_2O] during 2.5 h followed by 6 h of low stretch-ventilation (HV+LV). Subsequently, lung tissue, plasma, bronchoalveolar fluid (BAL), BAL cells, and isolated surfactant were analyzed.

Animals subjected to prolonged low-stretch MV after high-stretch ventilation had two different outcomes according to their susceptibility. Susceptible animals s(HV+LV) had a characteristic ventilator-induced lung injury (VILI) outcome distinguish by surfactant alterations, proinflammatory cytokines increase in BAL, edema and hypoxemia (PaO_2/FiO_2<200 mmHg). Resistant animals r(HV+LV) were characterized by alterations in the alveolar capillary-barrier, an increase of neutrophils in BAL, increased levels of MIP-2 and ASMase activity in plasma and slight alterations in gas exchange. Animals exclusively subjected to low-stretch ventilation strategies developed inflammatory changes without histological or physiological alterations.

To conclude conventional low-stretch ventilation length is directly related with the development of lung inflammation regardless of whether animals were or not previously exposed to high-stretch ventilation. In this context, lung surfactant alterations do not precede the onset of acute lung injury induced by prolonged low-stretch ventilation after high-stretch ventilation but its proper functioning is essential for survival.

2. INTRODUCTION

Numerous direct and indirect pulmonary clinical factors contribute to develop acute lung injury (ALI) hampering the assessment of its remarkable incidence (173). Despite of the etiological variability of this syndrome, its mortality rates has successfully decreased over the last two decades (173). The main factor contributing to this decrement is the improvement of mechanical ventilation strategies (MV). In fact, MV is an integral part of ALI therapy, but an inappropriate application can lead to side effects,

called ventilator-induced lung injury (VILI) (299). To date, limiting VILI through lower tidal volumes (V_T) is the only intervention demonstrated to reduce ALI mortality rates (362). However, some clinical trials have been developed to determine the possible effects of low V_T MV parameters (363).

Conversely, other clinical studies concluded that even applying the same MV stress to different patients, forces reaching to alveolar cells and their corresponding response are quite heterogeneous and variable (299), presuming that a personalization of the ventilator strategies according to the patient's condition will improve the outcome (349).

As clinical studies provide descriptive data about the onset and evolution of ALI leading to hypothesize about its mechanisms of injury, animal models yield straightforward methods to study in depth those assumptions.

The most frequent animal model of ALI is the application of MV (232) due to its clinical relevance (173).As a result, several harmful protocols characterized by the application of high V_T, high peak-pressures and/or the lack of positive end-expiratory pressure (PEEP) have been performed to characterized VILI (7). Generally, VILI models are no longer ventilated than 8 h depending on ventilatory settings and support (206), being usual to not exceed 4 h of high V_T or peak-pressures in rodents due to survival (206, 305, 364). These high-stretched models result in alveolar hemorrhage, hyaline membranes formation, neutrophilic infiltration, decreased compliance and gas-exchange abnormalities (232). Interestingly, a previous study in our laboratory described two different outcomes to the same injurious MV strategy, highlighting the existence of variability in stress susceptibility to MV in animal models (Chapter 2). Conversely, some experimental models recently studied the possible adverse effects of low V_T ventilation (286). Indeed, even there are many studies concerning the application of protective MV combined with other insults (365), little research has been performed related to the possible effects of protective MV after the induction of lung injury, specifically VILI (206).

Therefore, the aim of the present study was to characterize the effect of prolonged low V_T MV and specifically in animals resistant to previous application of injurious MV. To accomplish this objective, we established a rodent model of low or high V_T MV during 2.5 h followed by 6 more hours of low V_T MV to characterize the physiological, inflammatory and pulmonary surfactant changes in the lung.

3. EXPERIMENTAL PROTOCOL

Male *Sprague-Dawley* rats were randomly distributed in the following groups:

- *Control group (n=5):* animals undergoing identical anesthetic and surgical procedures than the other groups but without applying MV.
- *Low-stretched group during 8.5 h. (LV) (n=7):* animals subjected to protective MV parameters during 2.5 h followed by 6 more hours under this ventilation protocol until their sacrifice.
- *High-stretched group during 8.5 h. (HV+LV) (n=10):* animals subjected to injurious MV parameters during 2.5 h followed by 6 more hours applying protective MV until their sacrifice. Interestingly, some of the animals subjected to this MV protocol did not survive to the 6 h of protective MV. As a result, we obtained two groups: animals that finished the experimental protocol [r*(HV+LV), n=7]* and animals that did not reached the 8.5 h of MV *[s(HV+LV), n=3]*.

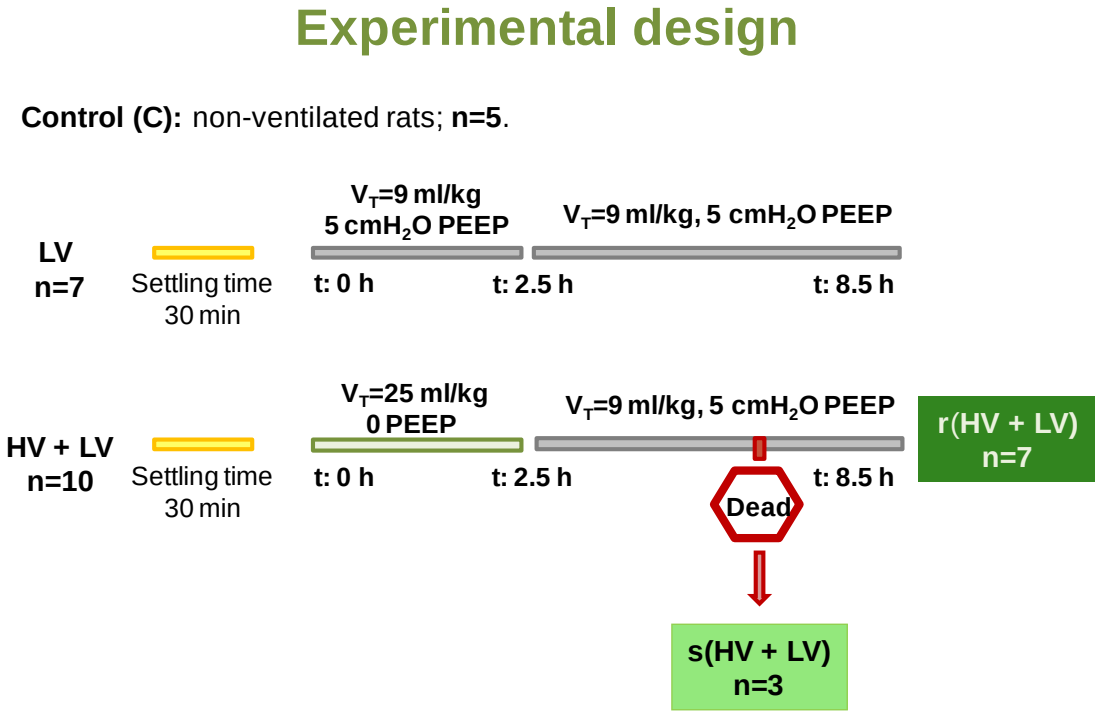

Figure 1: Experimental design. Representation of all groups established for the study subdivided according to the mechanical ventilation strategies.

In all ventilated groups, respiratory rate was 70 bpm, inspiratory time 0.35 sec., expiratory time 0.56 sec. and FiO_2 0.35. Animals were ventilated for an equilibration period of 30 min using the low V_T ventilation parameters. Then, the assigned V_T was administered starting at t=0 min.

Hemodynamic and ventilatory parameters were registered at t=0 min, t=2.5 h and t=8.5 h. Blood samples were collected at the beginning and end of the ventilatory procedure to gases analysis.

Animals were sacrificed by exsanguination after the established ventilatory period and subsequently we proceeded to sampling. We obtained lung tissue and bronchoalveola rlavage that it was separated from the alveolar fluid cells by centrifugation. The remaining bronchoalveolar lavage free of cells (BAL) was processed to obtain pulmonary surfactant (PS).

4. RESULTS

4.1. Alterations under long exposure to MV

4.1.1. Physiology

Lung function [peak inspiratory pressure (PIP) and respiratory system compliance (C_{RS})] were significantly altered in s(HV+LV) group in contrast with r(HV+LV) group just starting injurious MV as depicts Figure 2.

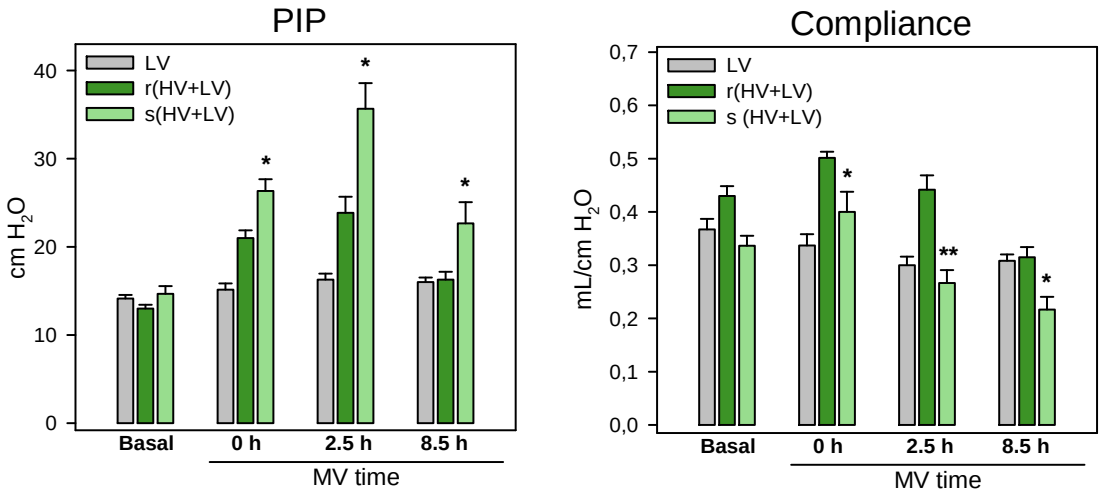

Figure 2: Changes during the ventilator period in peak inspiratory pressure (PIP) and respiratory system compliance (C_{RS}) in rats ventilated with Low or High tidal volumes.

PIP and C_{RS} were measured at baseline, start and after 2.5 and 8.5 hours of mechanical ventilation according to the experimental protocol requirements.

Data represent mean ± S.E.M. *p<0.05 and **p<0.01 vs. r(HV+LV) group.

As well, mean arterial pressure (MAP) and arterial partial pressure of oxygen (PaO_2)-to-fractional inspired oxygen (FiO_2) ratio were significantly decreased at 8.5 h in s(HV+LV) group together with a significant increased of arterial partial pressure of carbon dioxide ($PaCO_2$) in this group (Figure 3). Interestingly, PaO_2/FiO_2 ratio was also slightly decreased in r(HV+LV) group, without reaching the damaging values fixed by the ARDSnet (2).

These data suggest alterations in gas exchange and atelectasis in s(HV+LV).

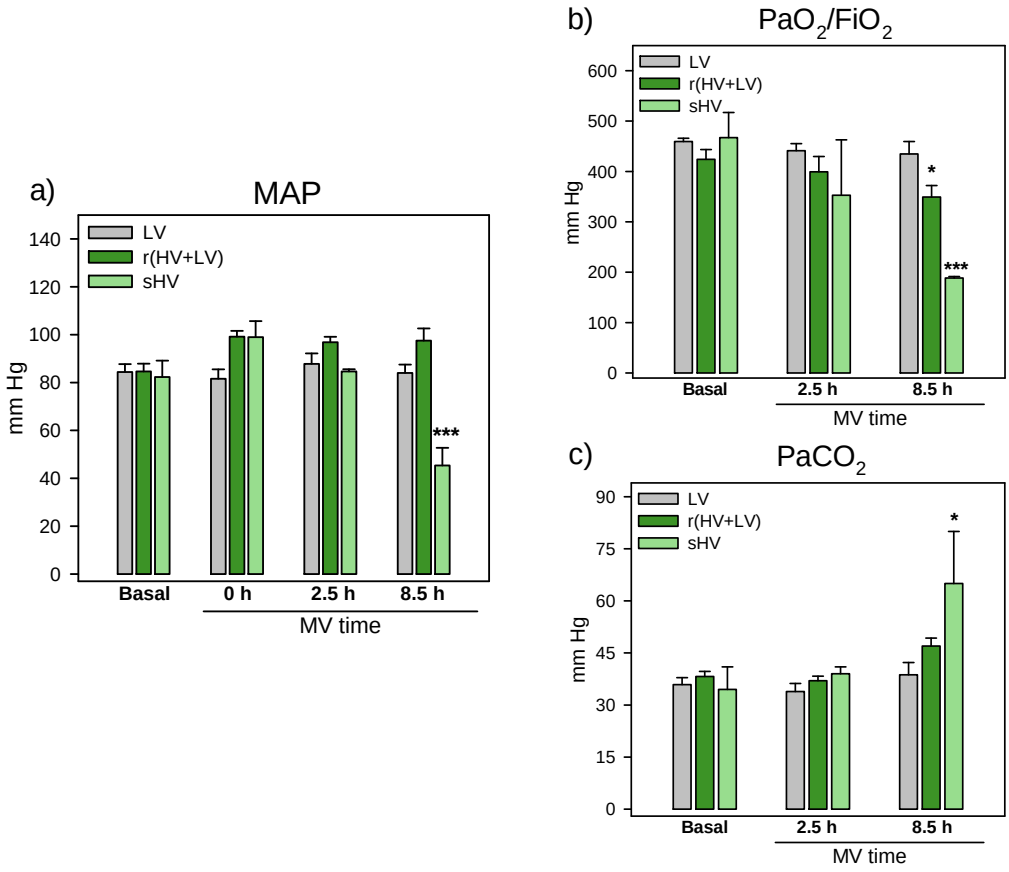

Figure 3: Changes during the mechanical ventilation (MV) period in hemodynamic variables in rats ventilated groups with Low or High tidal volumes.

a) Mean arterial pressure (MAP) was measured at baseline, start and after 2.5 and 8.5 hours of MV. b) Arterial partial pressure of oxygen (PaO_2)-to-fractional inspired oxygen (FiO_2) ratio values were assessed before and after 2.5 and 8.5 hours of MV. c) Arterial partial pressure of carbon dioxide ($PaCO_2$) was evaluated before and after 2.5 and 8.5 hours of MV.

Data represent mean ± S.E.M. *$p<0.05$ vs. Control and*** $p<0.001$ vs. all groups.

4.1.2. Alveolar injury

Changes in the alveolar space due to long exposure to MV were characterized evaluating presence of edema and alveolar fluid cells alterations as well as assessing the histological score and damage markers levels.

4.1.2.1. Intra-alveolar edema and histological injury score

Histological score revealed significant alterations in s(HV+LV) group whereas edema presence, represented as total amount of proteins in BAL, had an increasing trend in both HV groups, being significant in s(HV+LV) group (Figure 4).

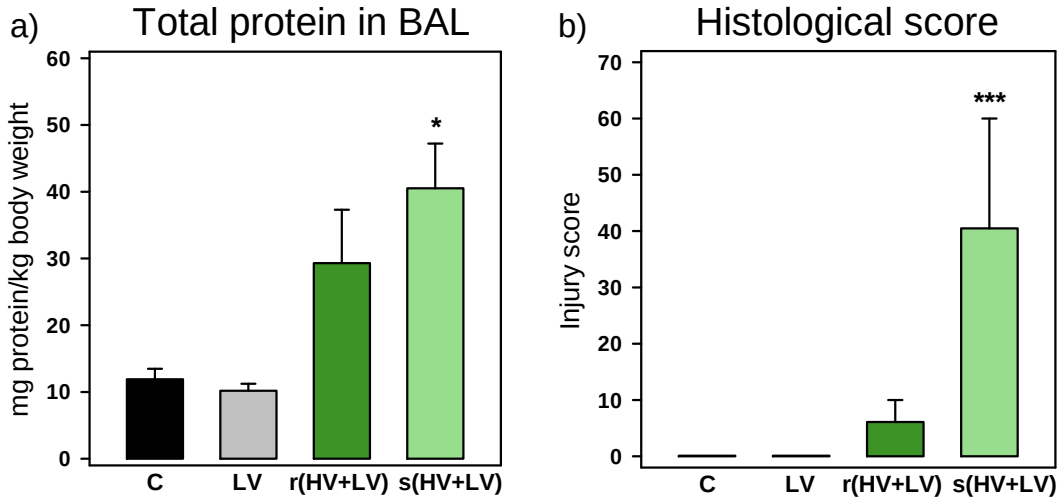

Figure 4: Alveolar injury in the different experimental groups.
a) Edema presence was measured as total protein content in bronchoalveolar fluid. b) Histological score was assessed by hematoxylin-eosin staining of isolated and fixated left lungs of all groups.
Data represent mean ± S.E.M. *p<0.05 vs. Control and ***p<0.001 vs. all groups.

4.1.2.2. Alveolar fluid cells

Total cell counts in BAL presented a decreasing trend when prolonged MV is applied. In particular, cell counts significantly decreased in s(HV+LV) group (Figure 5a, left panel). In addition, the proportion of alveolar macrophages significantly decreased in all HV groups. Interestingly, only neutrophils proportion was significantly raised in r(HV+LV) group though there was an increasing trend in all prolonged MV groups (Figure 5b, right panel), suggesting that prolonged protective MV may promote

neutrophils infiltration in the alveolar space together with alveolar macrophages decrement.

Hence, MV may change alveolar fluid cells profile as depict the representative flow cytometric side scatter (SSC, relative complexity)/forward scatter (FSC, relative size) dot plots from all experimental groups (Figure 5b).

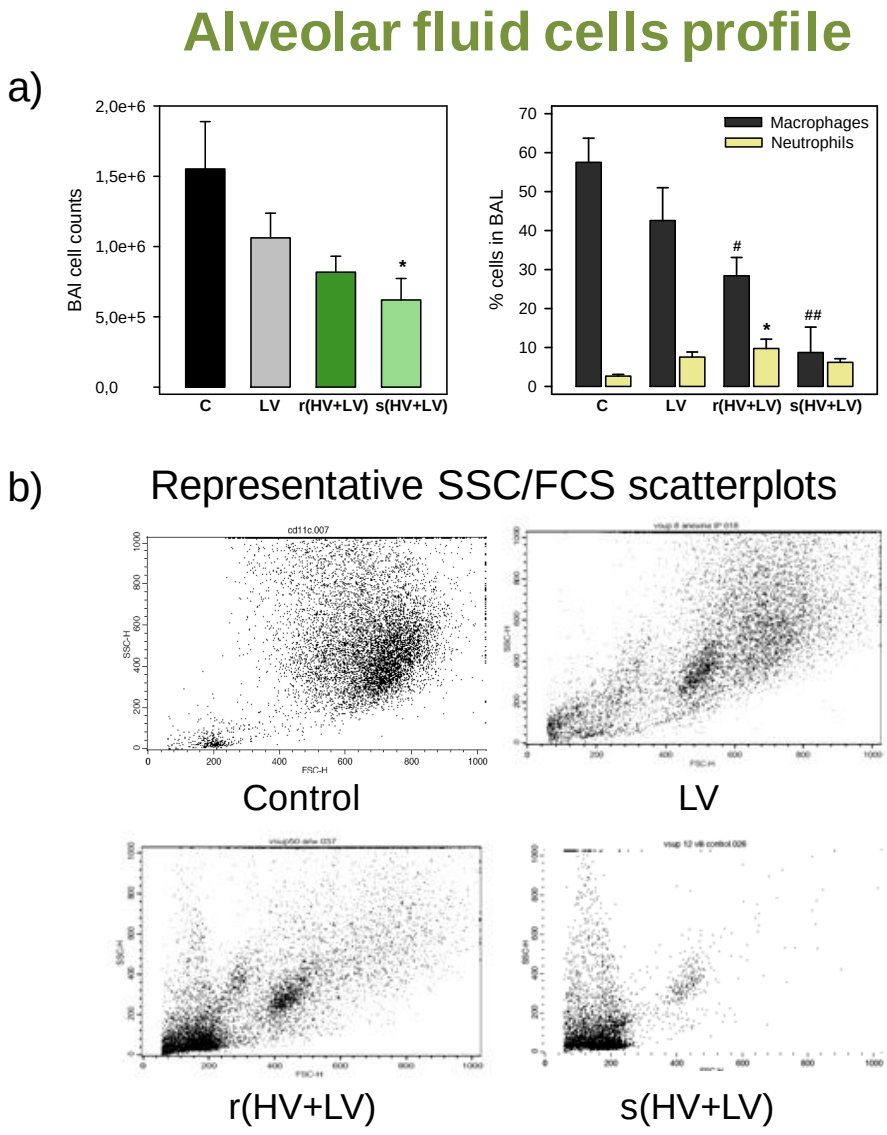

Figure 5: Alveolar fluid cells profile in all experimental groups.

a) Left panel represents total cell counts recovered in BALdetermined by assessing cell viability with trypan blue dye exclusion. Data represent mean ± S.E.M. *p<0.05 vs. Control. Right panel depicts the proportion of alveolar macrophages and neutrophils in BAL fluid determined by fluorescence flow cytometry assays using specific monoclonal antibodies (anti-CD11c for alveolar macrophages and anti-RP-1 for blood neutrophils). Data represent mean ± S.E.M. *p<0.05 vs. Control of neutrophils. $^{\#}$p<0.05 and $^{\#\#}$p<0.01 vs. Control of alveolar macrophages.

b) Representative side scatter (SSC)/forward scatter (FSC) dot plots of the flow cytometric profile of total alveolar fluid cells from all groups of study.

4.1.2.3. Damage markers

We determined the presence of the inflammatory cytokines TNF-α, IL-6, MIP-2 and MCP-1 in BAL (Figure 6a) and plasma (Figure 6b). In addition, we studied the acid sphingomyelinase (ASMase) activity in these fluids as well as its RNA levels in lung tissue (Figure 7).

Cytokines results indicated an exacerbated increase of all the cytokines studied in BAL in s(HV+LV) group. Furthermore, we observed a significant increase of IL-6 and MIP-2 levels in plasma in this group while TNF-α was undetectable in all groups and MCP-1 plasma levels did not change among groups (data not shown). It is worth noting that we observed a significant increase of MIP-2 levels in BAL and plasma of r(HV+LV) group, chemokine tightly related with neutrophils recruitment. Interestingly, we also observed changes in the low-stretched group. Specifically, we detected a significant increase of MIP-2 and IL-6 levels in BAL. Moreover, we observed an increase of IL-6 levels in plasma in LV group and also in r(HV+LV) group.

These data suggest an activation of inflammatory processes under prolonged MV even under protective strategies.

According to the results related to ASMase activity, we did not observe changes among groups in BAL, whose values were lower than those obtained in plasma. Conversely, we detected a significant increase of this enzymatic activity in plasma together with a significant increase of its RNA expression in lung tissue in r(HV+LV) group. These data let us to speculate that prolonged conventional MV after high-stretch MV up-regulates ASMase production and release to the bloodstream and therefore activating ASMase-derived ceramide pathway a promoter of several routes leading to ALI (332).

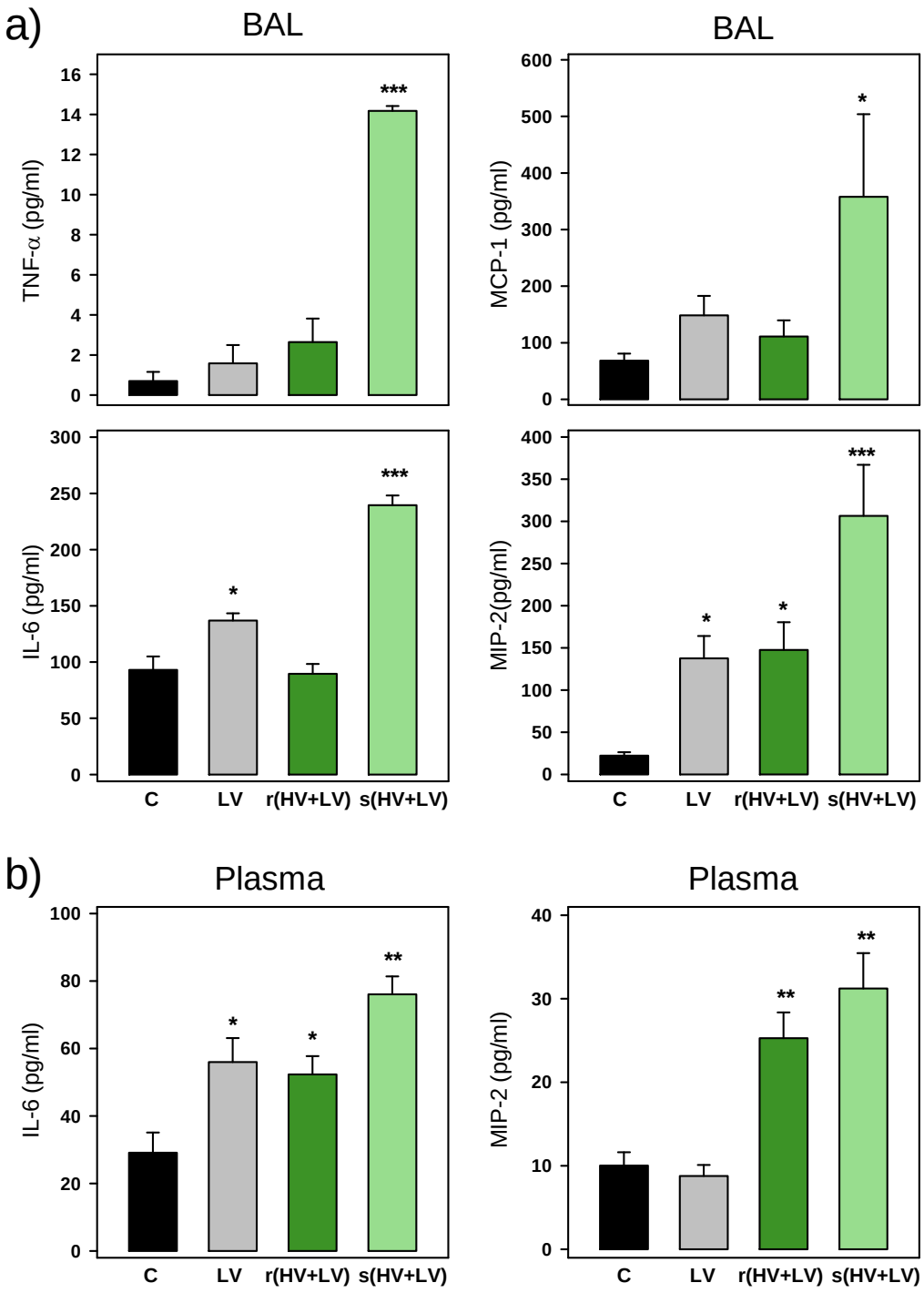

Figure 6: Inflammatory cytokines detected in all the experimental groups.
All cytokines were measured in BAL and plasma by colorimetric rat ELISA kits following the instructions provided by the supplier. TNF-α levels in plasma were undetectable and MCP-1 levels in plasma did not changed among groups (data not shown).
Data represent mean ± S.E.M. *p<0.05 and **p<0.01 vs. Control; ***p<0.001 vs. all groups.

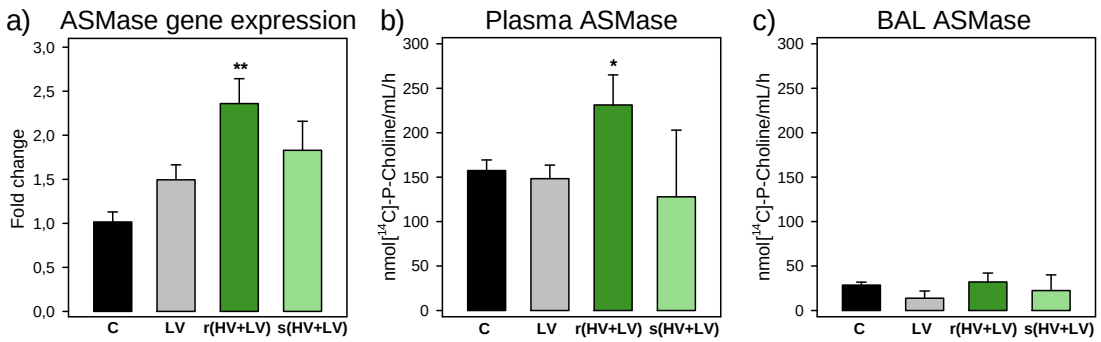

Figure 7: Acid sphingomyelinase activity in BAL and plasma and its RNA expression in lung tissue of all experimental groups.
a) RNA expression of ASMase was detected using total RNA isolated from the lower lobe of the right lung. cDNA synthesis was performed using 1µg total RNA as input and it was amplified by RT-PCR using specific primers. Results were analyzed using ΔΔCT method and expressed as normalized fold expression. b and c) ASMase activity in BAL and plasma measured performing an enzymatic assay. ASMase activity values in BAL were similar between groups and smaller than the values observed in plasma.
Data represent mean ± S.E.M.*p<0.05 and ** p<0.01 vs. Control.

4.1.3. Pulmonary surfactant analysis

Pulmonary surfactant (PS) is comprised of 90% lipids, predominantly phospholipids (PL), and 10% of proteins, mainly the PS-associated proteins: SP-A, SP-B, SP-C and SP-D. PS is secreted into the alveolar space by alveolar type II cells (ATII) as high-organized lipoprotein structures capable of establishing a surface film that stabilize the alveoli by the reduction of the surface tension at the air-liquid interface. This function is accomplished by PS large aggregates (LA), which may be transformed to a non-functional fraction, called small aggregates (SA), due to compression and expansion movements during respiration (314). Under pathological situations, LA to SA conversion is altered, being the SA/LA ratio increase a damage marker of VILI.

Therefore, we assessed PS biophysical function as well as presence of protein contamination in LA which is considered a potential inhibitor of PS functionality (296). Also, we evaluated possible alterations in LA to SA conversion and determined PS-associated protein levels in LA (Figure 8).

Pulmonary surfactant biophysical function was determined performing an interfacial adsorption assay. The ability of LA to adsorb onto and spread at the air–water interface was measured using a Wilhelmy-like high-sensitive surface microbalance, coupled to a teflon dish of very small size by following the variation in

surface pressure as a function of time, as previously described (322). This ability is significantly impaired in s(HV+LV) group at 30 min as represents figure 8a.

Accordingly, we observed a significant increase of SA/LA ratio in s(HV+LV) group, indicating alterations in PS conversion probably due to the alterations detected in the alveolar space (Figure 8b). Specifically, we observed protein contamination in the active fraction of s(HV+LV) group (Figure d) which may alter PS function. Also, the variation on PS-associated proteins levels might be considered as another marker of alveolar alterations due to injurious MV that directly affects PS (Chapter 1 and 2). As a result, we observed no difference among groups of SP-A protein levels in LA (data not shown). Conversely, we observed a significant decrease of SP-B and SP-C levels in s(HV+LV) group.

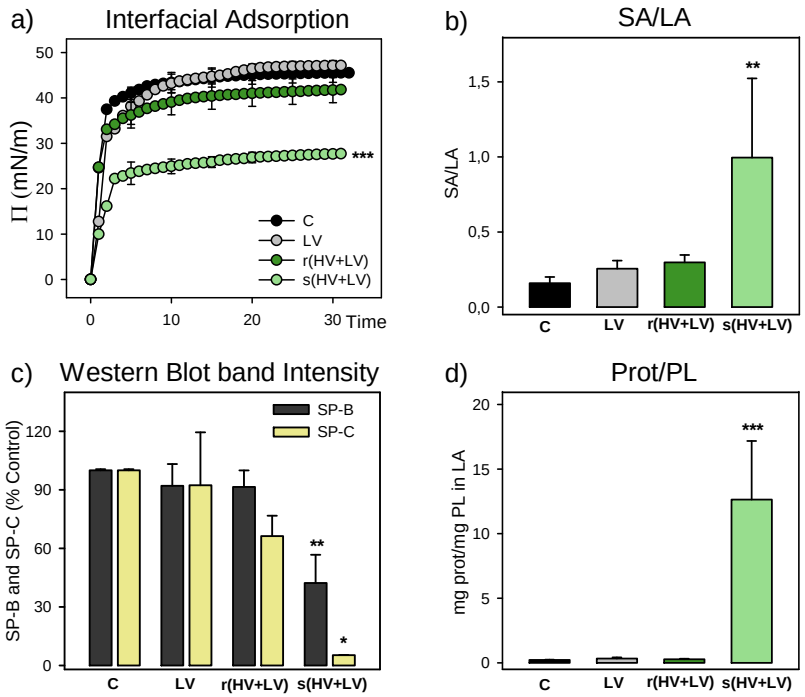

Figure 8: Pulmonary surfactant alterations due to prolonged mechanical ventilation.
a) Surfactant interfacial adsorption was determined in all groups of study in a Wilhelmy-like high-sensitive surface microbalance by following the variation in surface pressure as a function of time. Interfacial adsorption was impaired in s(HV+LV) group. b) LA to SA conversion as the ratio of PL content between SA and LA of all experimental groups. This ratio significantly increased in s(HV+LV) group. c) Pulmonary surfactant-associated proteinswere detected by Western blot analysis (WB) in LA samples. Proteins quantification was achieved by densitometric evaluation of the bands obtained in WB. SP-B and SP-C levels significantly decreased in s(HV+LV) group. d) Total protein to PL ratio in LA was assessed in all groups of study. This ratio significantly increased in s(HV+LV) group.
Data represent mean ± S.E.M. * $p<0.05$, ** $p<0.01$ and *** $p<0.001$ vs. Control.

4.2. Comparison between short and long exposure to MV under the same ventilation strategy.

In order to discern possible factors attributable to longer exposure to MV under conventional parameters we compared these data with the results obtained from the resistant groups to high-stretch MV studied in Chapter 2 (Table 1). As well, we assessed neutrophils proportion in BAL of n=5 rats per group under short strategies used in Chapter 2 to compare neutrophil infiltration values between short and long exposures to MV (Table 1). Furthermore, we also studied gene expression in lung tissue of factors usually observed in a later-stage of ALI such transforming growth beta (TGF-β) and matrix metalloproteinase-2 (MMP-2) in short and long-ventilated rats under both MV strategies (Figure 9).

Interestingly, in Table 1 we observed differences between HV groups but also among LV groups, suggesting that prolonged MV even under conventional strategies lead changes in the alveolar space. Specifically, we observed a significant increase of neutrophils percentage in the alveolar fluid along with a significant increase of chemokines (MCP-1 and MIP-2) and IL-6 in BAL in prolonged conventional mechanical ventilated animals in contrast with the short low-stretched group. Also we observed a significant increase of IL-6 in plasma in the prolonged low-stretched group. However, SP-A protein levels significantly decreased in the prolonged low-stretched group in contrast with the short LV group.

On the other hand, rHV and r(HV+LV) differed in almost all variables represented in Table 1. In particular, r(HV+LV) group was characterized by an increase of edema presence, neutrophils percentage and MIP-2 and IL-6 levels in plasma in contrast with rHV group. Conversely, the levels of the early inducible pleiotropic cytokines involved in acute inflammatory responses TNF-α and IL-6 (331, 353) were significantly decrease in BAL of r(HV+LV) group in contrast with rHV. However, MCP-1 and MIP-2 levels, chemokines involved in the attraction of leukocytes like monocytes, lymphocytes or neutrophils (355, 366, 367) were similar among rHV and r(HV+LV) groups and higher than in control group. Interestingly, rHV had a significant increase in PS secretion levels and SP-A protein levels.

Table 1: Differences between resistant animals subjected to short (2.5h) or long exposure (2.5h + 6h) to mechanical ventilation (MV) under conventional (Low tidal volume [V_T]) or injurious (High V_T) MV strategies.

Variables	Groups				
	Control	Low V_T MV		Resistant to High V_T MV	
		2.5h	2.5h + 6h	2.5h	2.5h + 6h (Low V_T)
Edema (BAL protein)	11.91±1.57	9.2±0.83	10.19±1.04	11.65±1.51	$36.6±9.8^{\#}$
% Neutrophils in BAL	2.65± 0.43	3.24±0.87	7.53±1.3*	3.65±0.73	$9.74±2.39^{\#}$
TNF-α (BAL)	0.7±0.46	1.15±0.75	1.58±0.92	$9.3±2.4^{\#}$	2.65±1.17
IL-6 (BAL)	93.1±11.88	40.64± 4.04	136.9±6.4***	$130.7±5.7^{\#\#}$	89.58±8.75
MIP-2 (BAL)	22.28±4.05	32.5±6.5	137.55±26.58**	147.55±36.69	147.55±32.82
MCP-1 (BAL)	68.38±12.49	18.35±3.24	148.37±34.39*	126.99±24.28	92.75±28.71
IL-6 (Plasma)	29.12±5.98	40.5±2.3	59.975±7.575*	43.73±0.48	$56.3±4.75^{\#}$
MIP-2 (Plasma)	10.04±1.58	8.1±2.1	8.78±1.33	13.66±1.82	$25.27±3.09^{\#}$
PS secretion	4.03±0.04	2.66±0.44	2.9±0.6	$7.34±0.66^{\#}$	4.58±0.73
SP-A (WB band intensity)	100%	174.07±9.83***	79.74±3.56	$185.73±26.95^{\#}$	86.58±9.01

Definition of abbreviation: BAL: bronchoalveolar lavage; TNF-α: Tumor necrosis factor alpha; IL-6: Interleukin 6; MIP-2: macrophage inflammatory protein 2; MCP-1: monocyte chemotactic protein 1. PS: pulmonary surfactant; SP-A: pulmonary surfactant-associated protein A; WB: western blot.

All factors were measured at the end of the ventilator period. Data are mean ± S.E.M; A two-tailed unpaired Student T-test was performed between groups of the same mechanical ventilation strategy. * $p<0.05$, ** $p<0.01$ and $p<0.001$ vs. LV; $^{\#}p<0.05$ and $^{\#\#}p<0.01$ vs. HV.

We also analyze TGF-β and MMP-2 gene expression in lung tissue from all the experimental groups of this Chapter and Chapter 2.

TGF-β1 RNA expression levels revealed a significant increase of its expression in r(HV+LV) group. On the other hand, Matrix metalloproteinase 2 (MMP-2) is a zinc-dependent endopeptidase that degrades several components of the extracellular matrix

(ECM), including type IV collagen and laminin (368). Our data indicated that MMP-2 RNA expression overcame a significant decrease in all HV groups and long-exposure animals to conventional MV.

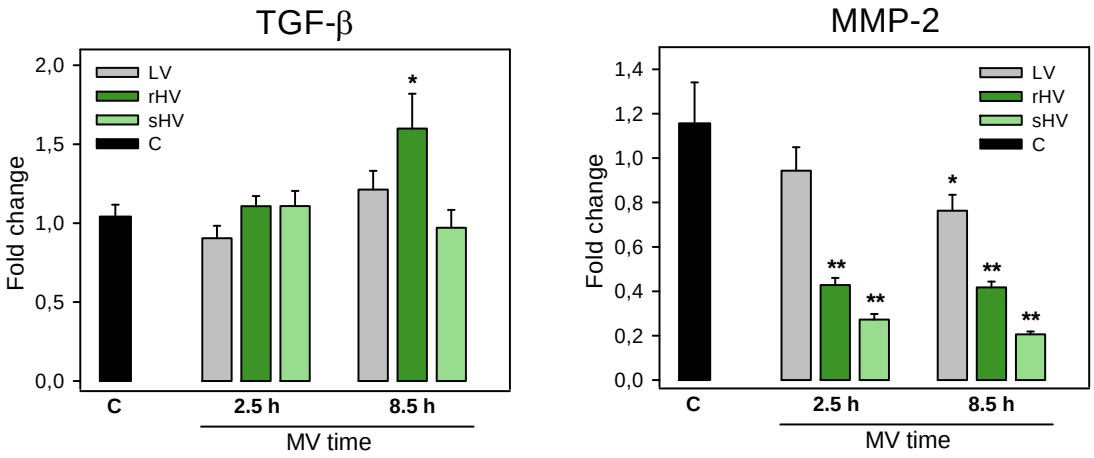

Figure 7: RNA expression of TGF-β and MMP-2 in lung tissue of animals exposed to short or long exposure to MV under conventional or injurious strategies.
RNA expression of TGF-β and MMP-2 was detected using total RNA isolated from the lower lobe of the right lung. cDNA synthesis was performed using 1µg total RNA as input and it was amplified by qPCR using specific primers. Results were analyzed using ΔΔCT method and expressed as normalized fold expression. Data represent mean ± S.E.M. * $p<0.05$ and ** $p<0.001$ vs. Control.

5. DISCUSSION

This study highlights that prolonged low-stretch MV usually applied in clinic, has effects not as harmless as could be expected. Thus, animals ventilated under the same low-stretch MV strategy during all the experimentdeveloped an inflammatory status in the alveolar space. However, animals subjected to previous high-stretch MV having a resistant outcome before prolonged low-stretch MV developed two different responses according to their resistance.

In line with the results previously obtained in our laboratory (Chapter 1 & 2), we observed that MV decreased total alveolar cells counts, being significantly decreased in s(HV+LV) group. Suitably, alveolar macrophages proportion had also a decreasing trend in all MV groups being significant in HV+LV groups. Interestingly, we also detected an increasing trend in neutrophils percentage in MV groups, being significant

in r(HV+LV) group. These data suggest that prolonged MV lead changes in the alveolar fluid cells profile, due to neutrophils infiltration and macrophages decrease, as depicts the side scatter/ forward scatter dot plot profile obtained by flow cytometry measurements of alveolar fluid cells from all experimental groups. It is noteworthy that the animals subjected to low or high MV strategies during 2.5 h had significantly lower levels of neutrophils than prolonged MV groups suggesting that prolonged MV may promote neutrophils infiltration in the alveolar space.

Furthermore, we studied the presence of MIP-2, also named CXCL-2, which is the most relevant chemokine for neutrophil recruitment into the lung of rodents (369) and its elevated expression exclusively in the alveolar compartment paralleled neutrophil sequestration in VILI (367). Accordingly, we observed a significant increase of MIP-2 levels in BAL of all prolonged MV groups. Interestingly, this MIP-2 levels were similar to those observed in the group resistant to 2.5 h of injurious MV studied in Chapter 2 [r(HV)]. Therefore, these data support the hypothesis that prolonged MV may induce neutrophil recruitment into the alveolar space, being an important factor the over-expression of MIP-2 in the alveolar compartment that may begin at early stages under injurious MV. In fact, some studies suggested that short ventilator strategies applied in small animals did not allow a massive recruitment (235). Nevertheless, our prolonged MV model permits to assess the evolution of neutrophils recruitment to the alveolar space.

Interestingly we also assessed a significant increase of MIP-2 levels in plasma only in HV+LV groups, suggesting that this rising values might be considered as possible damage biomarkers. Probably this increase might be related with the alveolar-capillary barrier alterations observed in these groups without rejecting the possibility of MIP-2 release by other cells susceptible to the mechanical stress generated by this MV strategy.

Alveolar-capillary barrier alterations were assessed measuring total protein content in BAL of all groups, detecting a significant increase in both HV+LV groups. Moreover, we observed presence of histological injury in both HV+LV groups being significant in s(HV+LV) group. Conversely, we did not find a trail of histological alterations or edema in LV group. Furthermore, the histological score values of r(HV+LV) were similar to the values obtained in rHV group but total protein levels differed due to a significant increase in r(HV+LV) group. Consequently, these data let

us to speculate that prolonged MV after high-stretch MV promotes alterations in the alveolar-capillary barrier.

As previous studies related neutrophils increment with hyaline membranes deposition (264), basement membrane destruction and increased permeability of the alveolar–capillary barrier (173, 206), we suspect that one of the main contributors to these alterations in our HV+LV groups is neutrophils infiltration, being the increased MIP-2 levels in plasma a good biomarker to realize it.

However, many other factors modulating inflammatory responses contribute to explain their different outcomes.

Specifically, we observed an exacerbated proinflammatory status in the alveolar space of s(HV+LV) group characterized by a significant increase of all cytokines measured in BAL. However, r(HV+LV) group had only increased MIP-2 as previously described. Furthermore, we observed that rHV had significantly increased TNF-α and IL-6 values in BAL in contrast with r(HV+LV) group explained by the fact that there are considered early inducible proinflammatory cytokines involved in acute inflammatory responses (331, 353). Conversely, we observed a significant increase of IL-6 in LV group together with a significant increase of this pleiotropic cytokine in plasma of all prolonged MV groups.

IL-6 is defined as a resolution factor that balances pro- and anti-inflammatory outcomes to further the immunological response (213), suggesting a complex role for IL-6 in lung injury (370). However, many studies reported a protective role of IL-6 by the attenuation of lung inflammation or pulmonary edema (353, 370). Specifically, IL-6 limits alveolar barrier disruption and therefore edema, by reducing neutrophil contact with the endothelium in VILI (370). These data support our findings, suggesting that an increase of IL-6 in BAL may protect the alveolar space against alterations in the alveolar-capillary barrier by limiting neutrophil contact with the endothelial cells in LV group. Conversely, the basal levels of IL-6 observed in BAL of r(HV+LV) group may not be enough to protect the alveolar-capillary barrier against neutrophils. Interestingly, we observed a significant increase of IL-6 levels in plasma of all prolonged MV groups. A wide range of cells besides cells from the alveolar compartment, including fibroblasts, vascular endothelial and smooth muscle cells (SMC) secretes IL-6 (371). Moreover, some studies suggest that alveolar SMC secreted IL-6 under certain proinflammatory stimuli (372) and others detected that vascular endothelial and SMC cells induced IL-6 expression under mechanical stress (373, 374). Therefore, we dare to

speculate that prolonged MV might promote IL-6 release to the bloodstream by cells closely related to the alveolar space suffering the mechanical stress.

Nevertheless, we have also reported other factors that may contribute to the alteration of the alveolar-capillary barrier in r(HV+LV) group. Specifically, we detected a significant increase of RNA expression of ASMase in lung tissue along with a significant increase of its activity in plasma of r(HV+LV) group. ASMase is mainly released by alveolar endothelial cells and has two subtypes, lysosomal and secretory ASMase both derived from the same gene (SMPD1) (332). As we observed that prolonged MV tend to stimulate ASMase RNA expression, only r(HV+LV) group had a significant detection of its action exclusively in plasma while there is an absence of ASMase activity increase either in BAL or plasma of the rest of groups. These results suggest a secretory ASMase translation in r(HV+LV) group to the bloodstream. Interestingly, secretory ASMase activity-derived ceramide is involved in alter vascular permeability and promote edema formation when this enzyme is increased in plasma in models of ALI (336). These data suggest that an increase of ASMase activity in plasma may contribute to alter the alveolar-capillary barrier in r(HV+LV) group and might be considered as possible damage biomarker of VILI.

On the other hand, it has been reported that an increase of TGF-ß1 gene expression levels contributes to develop alveolar flooding in a model of bleomycin-induced lung injury as well as is intimately related with an increase of ECM deposition in VILI (309, 375, 376). However, TGF-ß1 has a complex and critical role at late phases of ALI leading to antagonistic outcomes due to the activation of different effector pathways according to the presence of other stimuli in the alveolar space and the state of the target cells (377). Thus, some studies reported that TGF-ß1 has an important antiinflammatory and fibrotic effect inducing wound repair though other investigations concluded that TGF-ß1 has a proinflammatory effect, promoting fibrogenesis and consequently underlying the progression of tissue injury and fibrosis (376-378). Therefore, TGF-ß1 transcriptional responses seem to be involved in both inflammatory and proliferative phases of ALI (378). Interestingly, we observed a significant increase of TGF-ß1 RNA expression in lung tissue of r(HV+LV) group. This result suggests a possible implication of TGF-ß1 in alveolar-capillary barrier alterations as well as a possible role in the absence of hyaline membranes resolution, indicating a possible fibroproliferative stage at the proliferative phase. Thus, future studies with prolonged MV periods may elucidate this possibility.

Many studies related the increase of the active presence of MMP-2 with acute inflammation and fibrosis development in ALI and pulmonary fibrosis (379, 380). Conversely, others described that MMP-2 active presence is a key factor of injury repair and its inhibition seems to impair repair processes (206, 381). In this study we observed a strong decrease of MMP-2 RNA levels in lung tissue observed in HV groups. As some previous studies using models of mechanical stretch observed a significant increase of MMP-2 levels *in vitro* (382) and *in vivo* (308, 379), a recent two-hit model *in vivo*, detected a MMP-2 gene expression decrement after 8 h of MV (383). These data suggest that MMP-2 RNA strong inhibition due to high MV contributes to alterations in the alveolar space. However, though structural cells including fibroblasts, endothelial and alveolar epithelial cells mainly secrete MMP-2, we cannot reject the possibility of its release by leukocytes or even the release of other MMPs. Importantly, an *in vitro* study observed that MMP-2 up-regulation by TGF-ß1 resulted in injury repair (381). As we observed TGF-ß1 gene expression increment in r(HV+LV) group we could speculate about possible up-regulation of MMP-2 in later phases. Therefore, further investigation must be done in order to elucidate the pathway that leads to MMP-2 inhibition as well as its contribution over time.

Previous studies in our laboratory observed that HV induced a significant secretion of PS to the alveolar space (Chapters 1 and 2). Interestingly, rHV groups observed in Chapter 2 had increased the active fraction of PS together with a significant increase of SP-A protein levels in contrast with r(HV+LV) group which reached basal levels. SP-A prevents the inhibition of PS by binding proteins (384), is involved in control PS secretion and reuptake by alveolar cells and also contributes to maintain LA forms during surface-area cycling by stabilizing tubular myelin and multilamellar structures, avoiding LA to SA conversion (314, 385, 386). Therefore, SP-A may play a critical role in PS homeostasis in resistant HV groups at short times that it is loss during prolonged MV. Despite we did not found any trail of PS alterations in r(HV+LV) group, we reported that s(HV+LV) had impaired PS functionality together with alterations in LA to SA conversion (SA/LA ratio), total protein contamination in LA and significant decrease of the hydrophobic peptides SP-B and SP-C. As previous studies in our laboratory observed that animals susceptible to HV had associated PS alterations (Chapters 1 & 2), we hypothesize that PS alterations are closely linked with an exacerbated inflammatory status in the alveolar space of animals developing VILI. Therefore, these data suggest that PS impairment is a damage marker of VILI.

In fact, PS functional alteration by increasing surface tension at the air-liquid interface in the alveoli is associated with alterations in the gradient pressures across alveolar-capillary barrier, pulmonary compliance decrease, atelectasis and hypoxemia (9, 298), as we also observed in s(HV+LV) group.

Furthermore, previous studies in our laboratory observed a relation between PIP increment values and susceptibility to injurious MV, suggesting PIP as an early marker of VILI (Chapter 2). Our results are consistent with these previous observations as s(HV+LV) group significantly increased PIP values in contrast with r(HV+LV) group at the beginning and during the high-stretch strategy setup. Furthermore after the settlement of LV strategy, PIP values remained significantly higher in s(HV+LV) groups while r(HV+LV) PIP values reached LV group values. Accordingly to these results and taking into account that many studies reported that ventilation with elevated PIP promotes edema (235), we hypothesize that PIP values under high V_T strategies might be an early marker of susceptibility to develop VILI.

To summarize prolonged low-stretch MV led changes in the alveolar space that differed accordingly to the ventilation strategy applied. An exclusively prolonged low-stretch ventilation strategy develops inflammatory changes that do not impact on histological or physiological parameters. However, if prolonged low-stretch MV is applied after high-stretch ventilation, we observed two different outcomes according to their susceptibility. As a result, susceptible animals develop VILI characterized by PS alterations, inflammatory exacerbation, edema and hypoxemia. Conversely, resistant animals reveal alterations in the alveolar-capillary barrier together with neutrophils infiltration, increased levels of MIP-2 and ASMase activity in plasma and slight alterations in gas exchange.

Consequently, these data suggest that long exposure to low-stretch MV is directly related with the development of inflammatory responses in animals previously subjected to high-stretch mechanical ventilation or not. Furthermore, these results allow us to conclude that adequate pulmonary surfactant functioning is essential for survival of rats exposed to injurious and/or prolonged non-injurious mechanical ventilation and its impairment does not precede the onset of acute lung injury in this model.

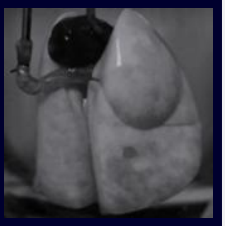

General Discussion

The main objective of this thesis was to address the impact of mechanical ventilation in the alveolar space and in particular the effects on the pulmonary surfactant system. The thesis employed a translational animal model that permits investigation of mechanical ventilation effects using different biochemical, biophysical, immunological, cellular, and physiological techniques. As a result, we obtained significant data that support the suggestion that proper functioning of pulmonary surfactant is essential for the survival of animals exposed to high-stretch ventilation.

As is currently known, the development of ALI is due to multiple closely linked factors, which hinders prognosis and diagnosis (173). This difficulty is transferred to animal models where the variety of damage-inducing factors combines with the assortment of animal and experimental designs to increase complexity (256, 350). Thus, in 2010 an ATS Official Committee established the main features that characterize ALI animal models (4). These features include histological evidence of tissue injury, alteration of the alveolar-capillary barrier, presence of inflammatory responses, and evidence of physiological dysfunction.

This thesis employed an animal model of VILI (10) due to its clinical relevance, as MV is currently the only effective treatment for ALI (173). Accordingly, a model of VILI using high tidal volumes (V_T=25 ml/kg) and absence of positive end-expiratory pressure application was established, as our aim was to provoke alveolar alterations. Moreover, we also used a ventilator strategy characterized by the application of moderated tidal volume and positive end-expiratory pressure (V_T=9 ml/kg, PEEP=5 cm H_2O) because this is a conventional strategy widely applied in critical care units.

The first chapter of this thesis reported that our VILI model fulfilled all the requirements established by the ATS Official Committee (4). In particular we observed a significant decrease of arterial oxygen tension/inspiratory oxygen fraction ratio (PaO_2/FiO_2< 300 mmHg), histological evidences of tissue injury, an increase of inflammatory markers such as TNF-α and acidic sphingomyelinase activity together with increased levels of protein carbonyls in BAL and leakage of plasma proteins into the alveoli. Besides, we also determined alterations in the composition and functionality of pulmonary surfactant. In particular, we observed a marked decrease in levels of surfactant apolipoproteins (SP-A, SP-B, and SP-C) and reduced expression of these proteins by lung tissue. Furthermore, we observed that even though high-stretch ventilation stimulated surfactant secretion by type II cells, surfactant was rapidly

inactivated. This inactivation can emerge due to presence of lipid peroxidation of surfactant membranes, low content of surfactant apolipoproteins, and increased levels of surfactant inhibitors such as C reactive protein (CRP) that insert into surfactant membranes and critically affect surfactant physical properties (1).

Consequently, these results showed that injurious high-stretch ventilation produces direct damage to the lung, promoting inflammation, oxidative stress, leakage of plasma proteins into the alveolar space, and release of factors that altogether contributes to inactivate lung surfactant.

However, during the previous study we realized that a small number of animals subjected to high-stretch ventilation did not show evidence of physiological lung dysfunction. Interestingly, prior to this study, Nin and co-workers also observed rats resistant to injurious high-stretch ventilation (305). In light of all this information we hypothesized that experimental animals facing the same stress may have heterogeneous outcomes, as clinical patients have been observed to have different responses to the same mechanical ventilation strategy (299, 349).

Hence, the aim of the next chapter was to identify factors involved in the resistance outcome to ventilator-induced lung injury. To this end, we designed an experimental model applying an endpoint criterion defined by the sacrifice of those animals with mean arterial pressure values below 50 mmHg at 60 min, as these values are incompatible with life in the short term. This criterion permitted us to establish two different groups differentiated not only by hemodynamic and ventilatory values but also by different alveolar alteration profiles.

As a result, in **the second chapter**, we observed that high-stretch ventilation induced a susceptible and a resistant response. The susceptible response corresponded to the damage profile observed in chapter 1. In particular, we observed that injurious high-stretch ventilation induced exacerbated inflammatory response together with alterations in the alveolar epithelial cells. On the other hand, even though the secretion of pulmonary surfactant increased by high-stretch ventilation, the exacerbated inflammatory response provokes surfactant inactivation, hindering the possibility of fresh-active pulmonary surfactant replacement in the air-liquid interface. Consequently, surface tension at the air-liquid interface increases, resulting in edema, hypoxemia, and death.

On the other hand, the animals resistant to injurious high-stretch ventilation increased the secretion of fresh pulmonary surfactant. However, pulmonary surfactant from these resistant rats had normal protein and lipid composition, absence of lipid peroxides and accomplished its biophysical, functions appropriately. As well, we observed an attenuated proinflammatory response, indicated by increased levels of IL-6 but reduced levels of TNF-α, MCP-1, and MIP-2 and absence of acidic sphingomyelinase activity in BAL. All together may contribute to the absence of edema or gas exchange alterations. Therefore, these data suggest that injurious MV could develop two different outcomes according to animal vulnerability. The key to their survival resides in their weakened inflammatory response and the good functioning of pulmonary surfactant, which seems to be a good damage maker as its impairment is intimately related to worse outcomes.

Thus, these results suggest that there is a direct link between pronounced proinflammatory response and surfactant inactivation in high-stretched rats. Also, they reinforced our statement that correct functioning of pulmonary surfactant is essential for survival in high-stretch ventilated rats.

This conclusion was further supported by the studies conducted in **the third chapter**. Given the demonstration of heterogeneous outcomes, we speculated on possible outcomes of the resistant group under low-stretch mechanical ventilation over time. This study would attempt to simulate clinical situations in which stable patients with pulmonary alterations would be subjected to conventional low-stretch mechanical ventilation.

Unexpectedly, we observed that the maintenance of conventional low-stretch mechanical ventilation worsened the animal's condition. In particular, we observed that the animals ventilated under conventional low-stretch ventilation during prolonged periods of time developed an inflammatory status characterized by neutrophils infiltration and an increase in the concentration of pr-inflammatory cytokines in BAL (IL-6 and MIP-2, but not TNF-α) and plasma (IL-6). However, the inflammatory status was not damaging enough to alter the epithelial cells and the pulmonary surfactant system.

In addition, we discovered that animals subjected to prolonged low-stretch ventilation after exposition to high-stretch ventilation showed edema together with neutrophils infiltration and slight alterations in gas exchange, whereas before the

application of prolonged low-stretch ventilation there was an attenuated inflammatory status and absence of edema. Moreover, few animals did not survive the whole ventilation process and were characterized by an exacerbated inflammatory response, edema, alterations in pulmonary surfactant system and hypoxemia. These results were consistent with the damage profile defined in the other chapters.

Therefore, the application of prolonged conventional low-stretch ventilation triggers mechanotransduction processes that activate different pathways according to the strategy applied and the vulnerability of the experimental animals to it. However, only the vulnerable animals had altered pulmonary surfactant system and its function. Consequently, these results suggested that the maintenance of conventional low-stretch ventilation promotes alterations in the alveolar space, corroborated the existence of different outcomes depending on vulnerability to mechanical ventilation, and strengthened the hypothesis that proper functioning of pulmonary surfactant is essential for survival in high-stretched rats. Furthermore, these results indicated that changes in surfactant composition and function do not precede the onset of acute lung injury induced by mechanical ventilation.

To conclude, the studies conducted in this thesis suggest that mechanical ventilation developed two different outcomes according to animal vulnerability. This vulnerability is mainly due to the outbreak of an exacerbated inflammatory response that may promote alterations in the alveolar-capillary barrier and pulmonary surfactant. Thus, we can conclude that impairment of pulmonary surfactant is an unequivocal VILI characteristic tightly linked with the exacerbation of the inflammatory response.

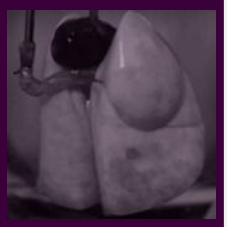

Conclusions

The research presented in this thesis highlights alterations in the lungs after exposition to mechanical ventilation. This research emphasizes the important role of pulmonary surfactant. The results obtained using a translational animal model of acute lung injury induced by mechanical ventilation allow us to conclude that:

- Injurious high-stretch ventilation produces direct damage to the lung, promoting pronounced inflammation, oxidative stress, leakage of plasma proteins into the alveolar space, and release of factors that together contribute to pulmonary surfactant impairment. Our results indicated that changes in lung surfactant composition and function do not precede the onset of acute lung injury induced by mechanical ventilation.

- Experimental animals treated with the same mechanical ventilation strategy have different outcomes according to their vulnerability to mechanical ventilation, which are mainly differentiated by their inflammatory response.

- VILI occurred in animal models only when surfactant was inactivated. There is a direct link between pronounced proinflammatory response and surfactant inactivation. In addition, we conclude that an attenuated inflammatory response together with increasing endogenous, fully active surfactant pools protect against the hypoxia and protein leakage that usually occur when ventilating animals with injurious high-stretch ventilation.

- With respect to the effect of non-injurious low-stretch ventilation, our results indicate that inflammation in the lung was directly related to the duration of conventional low-stretch ventilation and that proper functioning of pulmonary surfactant is essential for survival of rats exposed to injurious and/or prolonged non-injurious mechanical ventilation.

References

1. Casals C, Canadas O. Role of lipid ordered/disordered phase coexistence in pulmonary surfactant function. Biochim Biophys Acta. 2012;1818(11):2550-62. Epub 2012/06/05.
2. Bernard GR, Artigas A, Brigham KL, Carlet J, Falke K, Hudson L, et al. The American-European Consensus Conference on ARDS. Definitions, mechanisms, relevant outcomes, and clinical trial coordination. Am J Respir Crit Care Med. 1994;149(3 Pt 1):818-24. Epub 1994/03/01.
3. Ware LB, Matthay MA. The acute respiratory distress syndrome. N Engl J Med. 2000;342(18):1334-49. Epub 2000/05/04.
4. Matute-Bello G, Downey G, Moore BB, Groshong SD, Matthay MA, Slutsky AS, et al. An official American Thoracic Society workshop report: features and measurements of experimental acute lung injury in animals. Am J Respir Cell Mol Biol. 2011;44(5):725-38. Epub 2011/05/03.
5. Gunther A, Ruppert C, Schmidt R, Markart P, Grimminger F, Walmrath D, et al. Surfactant alteration and replacement in acute respiratory distress syndrome. Respiratory research. 2001;2(6):353-64. Epub 2001/12/12.
6. Zuo YY, Veldhuizen RA, Neumann AW, Petersen NO, Possmayer F. Current perspectives in pulmonary surfactant--inhibition, enhancement and evaluation. Biochim Biophys Acta. 2008;1778(10):1947-77. Epub 2008/04/25.
7. de Prost N, Ricard JD, Saumon G, Dreyfuss D. Ventilator-induced lung injury: historical perspectives and clinical implications. Ann Intensive Care. 2011;1(1):28. Epub 2011/09/13.
8. Esteban A, Anzueto A, Frutos F, Alia I, Brochard L, Stewart TE, et al. Characteristics and outcomes in adult patients receiving mechanical ventilation: a 28-day international study. JAMA. 2002;287(3):345-55. Epub 2002/01/16.
9. Albert RK. The role of ventilation-induced surfactant dysfunction and atelectasis in causing acute respiratory distress syndrome. Am J Respir Crit Care Med. 2012;185(7):702-8. Epub 2012/01/10.
10. Menendez C, Martinez-Caro L, Moreno L, Nin N, Moral-Sanz J, Morales D, et al. Pulmonary vascular dysfunction induced by high tidal volume mechanical ventilation*. Crit Care Med. 2013;41(8):e149-55. Epub 2013/03/22.
11. Criner GJ, Barnette RE., D'Alonzo GE. Critical Care Study Guide: Text and Review. Second Edition ed. New York: Springer Science + Business media; 2010.
12. Michael JA. Fundamentals of Medical Physiology. New York: Thieme Medical Publishers, Inc.; 2011.
13. Weibel ER. The Lung: Scietific Foundations. 2d ed ed. Philadelphia: Lippincot-Raven; 1977.
14. Fuhrman BP, Zimmerman, J. Pediatric Critical Care. 4d. ed ed. Philadelphia: Elsevier Sanders; 2011.
15. West JB. Respiratory and Physiology: the essentials. 6d ed. ed. Baltimore: Lippincott Williams & Wilkings; 2003.
16. Simionescu M. Lung endothelium: structure-function correlates. In: Crystal RG WJB, editor. The Lung: Scientific Foundations. 2d ed ed. Philadelphia: Lippincot-Raven; 1997. p. 615-28.

17. Gladwin MT. Role of the red blood cell in nitric oxide homeostasis and hypoxic vasodilation. Adv Exp Med Biol. 2006;588:189-205. Epub 2006/11/09.
18. Fishman AP. Endothelium: a distributed organ of diverse capabilities. Annals of the New York Academy of Sciences. 1982;401:1-8. Epub 1982/01/01.
19. Cines DB, Pollak ES, Buck CA, Loscalzo J, Zimmerman GA, McEver RP, et al. Endothelial cells in physiology and in the pathophysiology of vascular disorders. Blood. 1998;91(10):3527-61. Epub 1998/06/20.
20. Mitchell JA, Ali F, Bailey L, Moreno L, Harrington LS. Role of nitric oxide and prostacyclin as vasoactive hormones released by the endothelium. Experimental physiology. 2008;93(1):141-7. Epub 2007/10/30.
21. Rao RM, Yang L, Garcia-Cardena G, Luscinskas FW. Endothelial-dependent mechanisms of leukocyte recruitment to the vascular wall. Circulation research. 2007;101(3):234-47. Epub 2007/08/04.
22. Kumar V, Fausto, N., Abbas, A. Robbins and Contran Pathologic Basis of Disease. 7d ed, ed: Elsevier Saunders; 2004.
23. Gil J, Martinez-Hernandez A. The connective tissue of the rat lung: electron immunohistochemical studies. The journal of histochemistry and cytochemistry : official journal of the Histochemistry Society. 1984;32(2):230-8. Epub 1984/02/01.
24. Clark RA, Lanigan JM, DellaPelle P, Manseau E, Dvorak HF, Colvin RB. Fibronectin and fibrin provide a provisional matrix for epidermal cell migration during wound reepithelialization. The Journal of investigative dermatology. 1982;79(5):264-9. Epub 1982/11/01.
25. Torikata C, Villiger B, Kuhn C, 3rd, McDonald JA. Ultrastructural distribution of fibronectin in normal and fibrotic human lung. Laboratory investigation; a journal of technical methods and pathology. 1985;52(4):399-408. Epub 1985/04/01.
26. Lwebuga-Mukasa JS. Matrix-driven pneumocyte differentiation. Am Rev Respir Dis. 1991;144(2):452-7. Epub 1991/08/01.
27. Sannes PL. Differences in basement membrane-associated microdomains of type I and type II pneumocytes in the rat and rabbit lung. The journal of histochemistry and cytochemistry : official journal of the Histochemistry Society. 1984;32(8):827-33. Epub 1984/08/01.
28. Vaccaro CA, Brody JS. Structural features of alveolar wall basement membrane in the adult rat lung. The Journal of cell biology. 1981;91(2 Pt 1):427-37. Epub 1981/11/01.
29. Crowell RE, Heaphy E, Valdez YE, Mold C, Lehnert BE. Alveolar and interstitial macrophage populations in the murine lung. Experimental lung research. 1992;18(4):435-46. Epub 1992/07/01.
30. Laskin DL, Weinberger B, Laskin JD. Functional heterogeneity in liver and lung macrophages. Journal of leukocyte biology. 2001;70(2):163-70. Epub 2001/08/09.
31. Low FN. Electron microscopy of the rat lung. The Anatomical record. 1952;113(4):437-49. Epub 1952/08/01.

32. Johnson MD, Widdicombe JH, Allen L, Barbry P, Dobbs LG. Alveolar epithelial type I cells contain transport proteins and transport sodium, supporting an active role for type I cells in regulation of lung liquid homeostasis. Proc Natl Acad Sci U S A. 2002;99(4):1966-71. Epub 2002/02/14.
33. Taylor AE, Gaar KA, Jr. Estimation of equivalent pore radii of pulmonary capillary and alveolar membranes. The American journal of physiology. 1970;218(4):1133-40. Epub 1970/04/11.
34. Matthay MA, Folkesson HG, Clerici C. Lung epithelial fluid transport and the resolution of pulmonary edema. Physiological reviews. 2002;82(3):569-600. Epub 2002/06/28.
35. Crapo JD, Young SL, Fram EK, Pinkerton KE, Barry BE, Crapo RO. Morphometric characteristics of cells in the alveolar region of mammalian lungs. Am Rev Respir Dis. 1983;128(2 Pt 2):S42-6. Epub 1983/08/01.
36. Haies DM, Gil J, Weibel ER. Morphometric study of rat lung cells. I. Numerical and dimensional characteristics of parenchymal cell population. Am Rev Respir Dis. 1981;123(5):533-41. Epub 1981/05/01.
37. Schneeberger EE. Airway and alveolar epithelian cell junctions. In: Crystal RG WJB, editor. The Lung: Scientific Foundations: Lippincot-Raven; 1991. p. 205-14.
38. Johnson MD. Ion transport in alveolar type I cells. Molecular bioSystems. 2007;3(3):178-86. Epub 2007/02/20.
39. Mason RJ, Williams, M. C. Alveolar type II cells. In: Crystal RG WJB, editor. The Lung: Scientific Foundations: Lippincot-Raven; 1991. p. 235-46.
40. Fehrenbach H. Alveolar epithelial type II cell: defender of the alveolus revisited. Respiratory research. 2001;2(1):33-46. Epub 2001/11/01.
41. Davis IC, Matalon S. Epithelial sodium channels in the adult lung--important modulators of pulmonary health and disease. Adv Exp Med Biol. 2007;618:127-40. Epub 2008/02/14.
42. Mason RJ. Biology of alveolar type II cells. Respirology. 2006;11 Suppl:S12-5. Epub 2006/01/21.
43. Goerke J. Pulmonary surfactant: functions and molecular composition. Biochim Biophys Acta. 1998;1408(2-3):79-89. Epub 1998/11/14.
44. Avery ME, Mead J. Surface properties in relation to atelectasis and hyaline membrane disease. AMA journal of diseases of children. 1959;97(5, Part 1):517-23. Epub 1959/05/01.
45. Blanco O, Cruz A, Ospina OL, Lopez-Rodriguez E, Vazquez L, Perez-Gil J. Interfacial behavior and structural properties of a clinical lung surfactant from porcine source. Biochim Biophys Acta. 2012;1818(11):2756-66. Epub 2012/07/10.
46. Perez-Gil J, Weaver TE. Pulmonary surfactant pathophysiology: current models and open questions. Physiology (Bethesda). 2010;25(3):132-41. Epub 2010/06/17.
47. Zambon M, Vincent JL. Mortality rates for patients with acute lung injury/ARDS have decreased over time. Chest. 2008;133(5):1120-7. Epub 2008/02/12.

48. Daniels CB, Orgeig S. The comparative biology of pulmonary surfactant: past, present and future. Comparative biochemistry and physiology Part A, Molecular & integrative physiology. 2001;129(1):9-36. Epub 2001/05/23.
49. Postle AD, Heeley EL, Wilton DC. A comparison of the molecular species compositions of mammalian lung surfactant phospholipids. Comparative biochemistry and physiology Part A, Molecular & integrative physiology. 2001;129(1):65-73. Epub 2001/05/23.
50. Veldhuizen R, Nag K, Orgeig S, Possmayer F. The role of lipids in pulmonary surfactant. Biochim Biophys Acta. 1998;1408(2-3):90-108. Epub 1998/11/14.
51. Notter RH. Lung Surfactants: Basic Science and Clinical Applications. . New York: Marcel Dekker, Inc.; 2000.
52. Lang CJ, Postle AD, Orgeig S, Possmayer F, Bernhard W, Panda AK, et al. Dipalmitoylphosphatidylcholine is not the major surfactant phospholipid species in all mammals. American journal of physiology Regulatory, integrative and comparative physiology. 2005;289(5):R1426-39. Epub 2005/07/23.
53. Veldhuizen EJ, Haagsman HP. Role of pulmonary surfactant components in surface film formation and dynamics. Biochim Biophys Acta. 2000;1467(2):255-70. Epub 2000/10/13.
54. Possmayer F. A proposed nomenclature for pulmonary surfactant-associated proteins. Am Rev Respir Dis. 1988;138(4):990-8. Epub 1988/10/01.
55. Orgeig S, Hiemstra PS, Veldhuizen EJ, Casals C, Clark HW, Haczku A, et al. Recent advances in alveolar biology: evolution and function of alveolar proteins. Respiratory physiology & neurobiology. 2010;173 Suppl:S43-54. Epub 2010/05/04.
56. Perez-Gil J. Structure of pulmonary surfactant membranes and films: the role of proteins and lipid-protein interactions. Biochim Biophys Acta. 2008;1778(7-8):1676-95. Epub 2008/06/03.
57. Possmayer F, Nag K, Rodriguez K, Qanbar R, Schurch S. Surface activity in vitro: role of surfactant proteins. Comparative biochemistry and physiology Part A, Molecular & integrative physiology. 2001;129(1):209-20. Epub 2001/05/23.
58. Serrano AG, Perez-Gil J. Protein-lipid interactions and surface activity in the pulmonary surfactant system. Chemistry and physics of lipids. 2006;141(1-2):105-18. Epub 2006/04/08.
59. Casals C, Garcia-Verdugo, I. . Molecular and functional properties of surfactant protein A. In: Nag K, editor. Developments in Lung Surfactant Dysfunction in Lung Biology in Health and Disease. New York: Marcel Dekker Inc.; 2005. p. 55–84.
60. Voss T, Eistetter H, Schafer KP, Engel J. Macromolecular organization of natural and recombinant lung surfactant protein SP 28-36. Structural homology with the complement factor C1q. Journal of molecular biology. 1988;201(1):219-27. Epub 1988/05/05.
61. Wright JR. Immunoregulatory functions of surfactant proteins. Nature reviews Immunology. 2005;5(1):58-68. Epub 2005/01/05.

62. Casals C. Role of surfactant protein A (SP-A)/lipid interactions for SP-A functions in the lung. Pediatric pathology & molecular medicine. 2001;20(4):249-68. Epub 2001/08/07.
63. Hoover RR, Floros J. Organization of the human SP-A and SP-D loci at 10q22-q23. Physical and radiation hybrid mapping reveal gene order and orientation. Am J Respir Cell Mol Biol. 1998;18(3):353-62. Epub 1998/04/04.
64. Fisher JH, Emrie PA, Shannon J, Sano K, Hattler B, Mason RJ. Rat pulmonary surfactant protein A is expressed as two differently sized mRNA species which arise from differential polyadenylation of one transcript. Biochim Biophys Acta. 1988;950(3):338-45. Epub 1988/09/07.
65. Floros J, Kala P. Surfactant proteins: molecular genetics of neonatal pulmonary diseases. Annu Rev Physiol. 1998;60:365-84. Epub 1998/04/29.
66. Voss T, Melchers K, Scheirle G, Schafer KP. Structural comparison of recombinant pulmonary surfactant protein SP-A derived from two human coding sequences: implications for the chain composition of natural human SP-A. Am J Respir Cell Mol Biol. 1991;4(1):88-94. Epub 1991/01/01.
67. Kuroki Y, Takahashi M, Nishitani C. Pulmonary collectins in innate immunity of the lung. Cellular microbiology. 2007;9(8):1871-9. Epub 2007/05/11.
68. Benne CA, Benaissa-Trouw B, van Strijp JA, Kraaijeveld CA, van Iwaarden JF. Surfactant protein A, but not surfactant protein D, is an opsonin for influenza A virus phagocytosis by rat alveolar macrophages. European journal of immunology. 1997;27(4):886-90. Epub 1997/04/01.
69. Griese M. Respiratory syncytial virus and pulmonary surfactant. Viral immunology. 2002;15(2):357-63. Epub 2002/06/26.
70. Van Iwaarden JF, Pikaar JC, Storm J, Brouwer E, Verhoef J, Oosting RS, et al. Binding of surfactant protein A to the lipid A moiety of bacterial lipopolysaccharides. The Biochemical journal. 1994;303 (Pt 2):407-11. Epub 1994/10/15.
71. Yamada C, Sano H, Shimizu T, Mitsuzawa H, Nishitani C, Himi T, et al. Surfactant protein A directly interacts with TLR4 and MD-2 and regulates inflammatory cellular response. Importance of supratrimeric oligomerization. J Biol Chem. 2006;281(31):21771-80. Epub 2006/06/07.
72. Janssen WJ, McPhillips KA, Dickinson MG, Linderman DJ, Morimoto K, Xiao YQ, et al. Surfactant proteins A and D suppress alveolar macrophage phagocytosis via interaction with SIRP alpha. Am J Respir Crit Care Med. 2008;178(2):158-67. Epub 2008/04/19.
73. Henning LN, Azad AK, Parsa KV, Crowther JE, Tridandapani S, Schlesinger LS. Pulmonary surfactant protein A regulates TLR expression and activity in human macrophages. J Immunol. 2008;180(12):7847-58. Epub 2008/06/05.
74. Kazi AS, Tao JQ, Feinstein SI, Zhang L, Fisher AB, Bates SR. Role of the PI3-kinase signaling pathway in trafficking of the surfactant protein A receptor P63 (CKAP4) on type II pneumocytes. Am J Physiol Lung Cell Mol Physiol. 2010;299(6):L794-807. Epub 2010/09/28.

75. White MK, Strayer DS. Survival signaling in type II pneumocytes activated by surfactant protein-A. Experimental cell research. 2002;280(2):270-9. Epub 2002/11/05.
76. Crouch EC. Collectins and pulmonary host defense. Am J Respir Cell Mol Biol. 1998;19(2):177-201. Epub 1998/08/12.
77. Crouch EC. Structure, biologic properties, and expression of surfactant protein D (SP-D). Biochim Biophys Acta. 1998;1408(2-3):278-89. Epub 1998/11/14.
78. Nayak A, Dodagatta-Marri E, Tsolaki AG, Kishore U. An Insight into the Diverse Roles of Surfactant Proteins, SP-A and SP-D in Innate and Adaptive Immunity. Frontiers in immunology. 2012;3:131. Epub 2012/06/16.
79. Kuan SF, Rust K, Crouch E. Interactions of surfactant protein D with bacterial lipopolysaccharides. Surfactant protein D is an Escherichia coli-binding protein in bronchoalveolar lavage. J Clin Invest. 1992;90(1):97-106. Epub 1992/07/01.
80. Chroneos ZC, Sever-Chroneos Z, Shepherd VL. Pulmonary surfactant: an immunological perspective. Cell Physiol Biochem. 2010;25(1):13-26. Epub 2010/01/08.
81. Pilot-Matias TJ, Kister SE, Fox JL, Kropp K, Glasser SW, Whitsett JA. Structure and organization of the gene encoding human pulmonary surfactant proteolipid SP-B. DNA. 1989;8(2):75-86. Epub 1989/03/01.
82. Moore KJ, D'Amore-Bruno MA, Korfhagen TR, Glasser SW, Whitsett JA, Jenkins NA, et al. Chromosomal localization of three pulmonary surfactant protein genes in the mouse. Genomics. 1992;12(2):388-93. Epub 1992/02/01.
83. Hawgood S, Derrick M, Poulain F. Structure and properties of surfactant protein B. Biochim Biophys Acta. 1998;1408(2-3):150-60. Epub 1998/11/14.
84. Hawgood S, Benson BJ, Schilling J, Damm D, Clements JA, White RT. Nucleotide and amino acid sequences of pulmonary surfactant protein SP 18 and evidence for cooperation between SP 18 and SP 28-36 in surfactant lipid adsorption. Proc Natl Acad Sci U S A. 1987;84(1):66-70. Epub 1987/01/01.
85. Patthy L. Homology of the precursor of pulmonary surfactant-associated protein SP-B with prosaposin and sulfated glycoprotein 1. J Biol Chem. 1991;266(10):6035-7. Epub 1991/04/05.
86. Johansson J, Curstedt T, Jornvall H. Surfactant protein B: disulfide bridges, structural properties, and kringle similarities. Biochemistry. 1991;30(28):6917-21. Epub 1991/07/16.
87. Andersson M, Curstedt T, Jornvall H, Johansson J. An amphipathic helical motif common to tumourolytic polypeptide NK-lysin and pulmonary surfactant polypeptide SP-B. FEBS letters. 1995;362(3):328-32. Epub 1995/04/10.
88. Blanco O, Perez-Gil J. Biochemical and pharmacological differences between preparations of exogenous natural surfactant used to treat Respiratory Distress Syndrome: role of the different components in an efficient pulmonary surfactant. European journal of pharmacology. 2007;568(1-3):1-15. Epub 2007/06/05.
89. Perez-Gil J, Casals C, Marsh D. Interactions of hydrophobic lung surfactant proteins SP-B and SP-C with dipalmitoylphosphatidylcholine and

dipalmitoylphosphatidylglycerol bilayers studied by electron spin resonance spectroscopy. Biochemistry. 1995;34(12):3964-71. Epub 1995/03/28.
90. Breitenstein D, Batenburg JJ, Hagenhoff B, Galla HJ. Lipid specificity of surfactant protein B studied by time-of-flight secondary ion mass spectrometry. Biophysical journal. 2006;91(4):1347-56. Epub 2006/04/25.
91. Nogee LM, Garnier G, Dietz HC, Singer L, Murphy AM, deMello DE, et al. A mutation in the surfactant protein B gene responsible for fatal neonatal respiratory disease in multiple kindreds. J Clin Invest. 1994;93(4):1860-3. Epub 1994/04/01.
92. Glasser SW, Burhans MS, Korfhagen TR, Na CL, Sly PD, Ross GF, et al. Altered stability of pulmonary surfactant in SP-C-deficient mice. Proc Natl Acad Sci U S A. 2001;98(11):6366-71. Epub 2001/05/10.
93. Glasser SW, Korfhagen TR, Perme CM, Pilot-Matias TJ, Kister SE, Whitsett JA. Two SP-C genes encoding human pulmonary surfactant proteolipid. J Biol Chem. 1988;263(21):10326-31. Epub 1988/07/25.
94. Weaver TE, Whitsett JA. Function and regulation of expression of pulmonary surfactant-associated proteins. The Biochemical journal. 1991;273(Pt 2):249-64. Epub 1991/01/15.
95. Fisher JH, Shannon JM, Hofmann T, Mason RJ. Nucleotide and deduced amino acid sequence of the hydrophobic surfactant protein SP-C from rat: expression in alveolar type II cells and homology with SP-C from other species. Biochim Biophys Acta. 1989;995(3):225-30. Epub 1989/05/01.
96. Johnson AL, Braidotti P, Pietra GG, Russo SJ, Kabore A, Wang WJ, et al. Post-translational processing of surfactant protein-C proprotein: targeting motifs in the NH(2)-terminal flanking domain are cleaved in late compartments. Am J Respir Cell Mol Biol. 2001;24(3):253-63. Epub 2001/03/14.
97. Johansson J. Structure and properties of surfactant protein C. Biochim Biophys Acta. 1998;1408(2-3):161-72. Epub 1998/11/14.
98. Beers MF, Mulugeta S. Surfactant protein C biosynthesis and its emerging role in conformational lung disease. Annu Rev Physiol. 2005;67:663-96. Epub 2005/02/16.
99. Oosterlaken-Dijksterhuis MA, Haagsman HP, van Golde LM, Demel RA. Interaction of lipid vesicles with monomolecular layers containing lung surfactant proteins SP-B or SP-C. Biochemistry. 1991;30(33):8276-81. Epub 1991/08/20.
100. Plasencia I, Rivas L, Keough KM, Marsh D, Perez-Gil J. The N-terminal segment of pulmonary surfactant lipopeptide SP-C has intrinsic propensity to interact with and perturb phospholipid bilayers. The Biochemical journal. 2004;377(Pt 1):183-93. Epub 2003/09/30.
101. Plasencia I, Keough KM, Perez-Gil J. Interaction of the N-terminal segment of pulmonary surfactant protein SP-C with interfacial phospholipid films. Biochim Biophys Acta. 2005;1713(2):118-28. Epub 2005/07/09.
102. Perez-Gil J, Keough KM. Interfacial properties of surfactant proteins. Biochim Biophys Acta. 1998;1408(2-3):203-17. Epub 1998/11/14.
103. Kramer A, Wintergalen A, Sieber M, Galla HJ, Amrein M, Guckenberger R. Distribution of the surfactant-associated protein C within a lung surfactant model film

investigated by near-field optical microscopy. Biophysical journal. 2000;78(1):458-65. Epub 2000/01/05.

104. Gustafsson M, Palmblad M, Curstedt T, Johansson J, Schurch S. Palmitoylation of a pulmonary surfactant protein C analogue affects the surface associated lipid reservoir and film stability. Biochim Biophys Acta. 2000;1466(1-2):169-78. Epub 2000/05/29.

105. Glasser SW, Witt TL, Senft AP, Baatz JE, Folger D, Maxfield MD, et al. Surfactant protein C-deficient mice are susceptible to respiratory syncytial virus infection. Am J Physiol Lung Cell Mol Physiol. 2009;297(1):L64-72. Epub 2009/03/24.

106. Glasser SW, Senft AP, Whitsett JA, Maxfield MD, Ross GF, Richardson TR, et al. Macrophage dysfunction and susceptibility to pulmonary Pseudomonas aeruginosa infection in surfactant protein C-deficient mice. J Immunol. 2008;181(1):621-8. Epub 2008/06/21.

107. Madala SK, Maxfield MD, Davidson CR, Schmidt SM, Garry D, Ikegami M, et al. Rapamycin Regulates Bleomycin-Induced Lung Damage in SP-C-Deficient Mice. Pulmonary medicine. 2011;2011:653524. Epub 2011/06/11.

108. Augusto LA, Li J, Synguelakis M, Johansson J, Chaby R. Structural basis for interactions between lung surfactant protein C and bacterial lipopolysaccharide. J Biol Chem. 2002;277(26):23484-92. Epub 2002/05/01.

109. Augusto L, Le Blay K, Auger G, Blanot D, Chaby R. Interaction of bacterial lipopolysaccharide with mouse surfactant protein C inserted into lipid vesicles. Am J Physiol Lung Cell Mol Physiol. 2001;281(4):L776-85. Epub 2001/09/15.

110. Garcia-Verdugo I, Garcia de Paco E, Espinassous Q, Gonzalez-Horta A, Synguelakis M, Kanellopoulos J, et al. Synthetic peptides representing the N-terminal segment of surfactant protein C modulate LPS-stimulated TNF-alpha production by macrophages. Innate immunity. 2009;15(1):53-62. Epub 2009/02/10.

111. Patterson CE, Rhoades RA. Substrate utilization in the perinatal lung. The American journal of physiology. 1989;257(6 Pt 1):L318-30. Epub 1989/12/01.

112. Batenburg JJ. Surfactant phospholipids: synthesis and storage. The American journal of physiology. 1992;262(4 Pt 1):L367-85. Epub 1992/04/01.

113. Ikegami M, Le Cras TD, Hardie WD, Stahlman MT, Whitsett JA, Korfhagen TR. TGF-alpha perturbs surfactant homeostasis in vivo. Am J Physiol Lung Cell Mol Physiol. 2005;289(1):L34-43. Epub 2005/03/15.

114. Nichols KV, Floros J, Dynia DW, Veletza SV, Wilson CM, Gross I. Regulation of surfactant protein A mRNA by hormones and butyrate in cultured fetal rat lung. The American journal of physiology. 1990;259(6 Pt 1):L488-95. Epub 1990/12/01.

115. Scavo LM, Ertsey R, Gao BQ. Human surfactant proteins A1 and A2 are differentially regulated during development and by soluble factors. The American journal of physiology. 1998;275(4 Pt 1):L653-69. Epub 1998/10/01.

116. Hallman M, Miyai K, Wagner RM. Isolated lamellar bodies from rat lung: correlated ultrastructural and biochemical studies. Laboratory investigation; a journal of technical methods and pathology. 1976;35(1):79-86. Epub 1976/07/01.

117. Stratton CJ. The high resolution ultrastructure of the periodicity and architecture of lipid-retained and extracted lung multilamellar body laminations. Tissue & cell. 1976;8(4):713-28. Epub 1976/01/01.
118. Stratton CJ. The three-dimensional aspect of mammalian lung multilamellar bodies. Tissue & cell. 1976;8(4):693-712. Epub 1976/01/01.
119. Weaver TE, Na CL, Stahlman M. Biogenesis of lamellar bodies, lysosome-related organelles involved in storage and secretion of pulmonary surfactant. Seminars in cell & developmental biology. 2002;13(4):263-70. Epub 2002/09/24.
120. Weaver TE. Synthesis, processing and secretion of surfactant proteins B and C. Biochim Biophys Acta. 1998;1408(2-3):173-9. Epub 1998/11/14.
121. Wissel H, Lehfeldt A, Klein P, Muller T, Stevens PA. Endocytosed SP-A and surfactant lipids are sorted to different organelles in rat type II pneumocytes. Am J Physiol Lung Cell Mol Physiol. 2001;281(2):L345-60. Epub 2001/07/04.
122. van Meer G, Voelker DR, Feigenson GW. Membrane lipids: where they are and how they behave. Nature reviews Molecular cell biology. 2008;9(2):112-24. Epub 2008/01/25.
123. Chevalier G, Collet AJ. In vivo incorporation of choline- 3 H, leucine- 3 H and galactose- 3 H in alveolar type II pneumocytes in relation to surfactant synthesis. A quantitative radoautographic study in mouse by electron microscopy. The Anatomical record. 1972;174(3):289-310. Epub 1972/11/01.
124. Osanai K, Mason RJ, Voelker DR. Pulmonary surfactant phosphatidylcholine transport bypasses the brefeldin A sensitive compartment of alveolar type II cells. Biochim Biophys Acta. 2001;1531(3):222-9. Epub 2001/04/28.
125. Yamano G, Funahashi H, Kawanami O, Zhao LX, Ban N, Uchida Y, et al. ABCA3 is a lamellar body membrane protein in human lung alveolar type II cells. FEBS letters. 2001;508(2):221-5. Epub 2001/11/24.
126. Mulugeta S, Gray JM, Notarfrancesco KL, Gonzales LW, Koval M, Feinstein SI, et al. Identification of LBM180, a lamellar body limiting membrane protein of alveolar type II cells, as the ABC transporter protein ABCA3. J Biol Chem. 2002;277(25):22147-55. Epub 2002/04/10.
127. Cheong N, Zhang H, Madesh M, Zhao M, Yu K, Dodia C, et al. ABCA3 is critical for lamellar body biogenesis in vivo. J Biol Chem. 2007;282(33):23811-7. Epub 2007/06/02.
128. Hammel M, Michel G, Hoefer C, Klaften M, Muller-Hocker J, de Angelis MH, et al. Targeted inactivation of the murine Abca3 gene leads to respiratory failure in newborns with defective lamellar bodies. Biochemical and biophysical research communications. 2007;359(4):947-51. Epub 2007/06/20.
129. Rooney SA. Regulation of surfactant secretion. Comparative biochemistry and physiology Part A, Molecular & integrative physiology. 2001;129(1):233-43. Epub 2001/05/23.
130. Frick M, Bertocchi C, Jennings P, Haller T, Mair N, Singer W, et al. Ca2+ entry is essential for cell strain-induced lamellar body fusion in isolated rat type II pneumocytes. Am J Physiol Lung Cell Mol Physiol. 2004;286(1):L210-20. Epub 2003/09/25.

131. Pattle RE. Surface Lining of Lung Alveoli. Physiological reviews. 1965;45:48-79. Epub 1965/01/01.
132. Clements JA, Brown ES, Johnson RP. Pulmonary surface tension and the mucus lining of the lungs: some theoretical considerations. J Appl Physiol. 1958;12(2):262-8. Epub 1958/03/01.
133. Bachofen H, Gerber U, Gehr P, Amrein M, Schurch S. Structures of pulmonary surfactant films adsorbed to an air-liquid interface in vitro. Biochim Biophys Acta. 2005;1720(1-2):59-72. Epub 2006/01/13.
134. Yu SH, Possmayer F. Lipid compositional analysis of pulmonary surfactant monolayers and monolayer-associated reservoirs. Journal of lipid research. 2003;44(3):621-9. Epub 2003/02/04.
135. Amrein M, von Nahmen A, Sieber M. A scanning force- and fluorescence light microscopy study of the structure and function of a model pulmonary surfactant. European biophysics journal : EBJ. 1997;26(5):349-57. Epub 1997/01/01.
136. Follows D, Tiberg F, Thomas RK, Larsson M. Multilayers at the surface of solutions of exogenous lung surfactant: direct observation by neutron reflection. Biochim Biophys Acta. 2007;1768(2):228-35. Epub 2006/12/13.
137. Rodriguez-Capote K, Manzanares D, Haines T, Possmayer F. Reactive oxygen species inactivation of surfactant involves structural and functional alterations to surfactant proteins SP-B and SP-C. Biophysical journal. 2006;90(8):2808-21. Epub 2006/01/31.
138. Putman E, Creuwels LA, van Golde LM, Haagsman HP. Surface properties, morphology and protein composition of pulmonary surfactant subtypes. The Biochemical journal. 1996;320 (Pt 2):599-605. Epub 1996/12/01.
139. Veldhuizen RA, Ito Y, Marcou J, Yao LJ, McCaig L, Lewis JF. Effects of lung injury on pulmonary surfactant aggregate conversion in vivo and in vitro. The American journal of physiology. 1997;272(5 Pt 1):L872-8. Epub 1997/05/01.
140. Ito Y, Veldhuizen RA, Yao LJ, McCaig LA, Bartlett AJ, Lewis JF. Ventilation strategies affect surfactant aggregate conversion in acute lung injury. Am J Respir Crit Care Med. 1997;155(2):493-9. Epub 1997/02/01.
141. Wright JR, Dobbs LG. Regulation of pulmonary surfactant secretion and clearance. Annu Rev Physiol. 1991;53:395-414. Epub 1991/01/01.
142. Forbes A, Pickell M, Foroughian M, Yao LJ, Lewis J, Veldhuizen R. Alveolar macrophage depletion is associated with increased surfactant pool sizes in adult rats. J Appl Physiol. 2007;103(2):637-45. Epub 2007/04/21.
143. Baritussio AG, Magoon MW, Goerke J, Clements JA. Precursor-product relationship between rabbit type II cell lamellar bodies and alveolar surface-active material. Surfactant turnover time. Biochim Biophys Acta. 1981;666(3):382-93. Epub 1981/12/23.
144. Willson DF, Chess, P. R., Wang, Z., Notter, R. H. Pulmonary Surfactant: Biology an therapy. In: Wheeler D. S. STP, Wong H.R., editor. The respiratory tract in pediatric critical illness and injury. London: Springer-Verlag; 2009.
145. Ganter CC, Jakob SM, Takala J. Pulmonary capillary pressure. A review. Minerva anestesiologica. 2006;72(1-2):21-36. Epub 2006/01/13.

146. Chase MA, Wheeler, D. S. Disorders of the pediatric chest. In: Wheeler D. S. STP, Wong H.R., editor. Pediatric critical care medicine: basic science and clinal evidence. London: Springer-Verlag; 2007.
147. Topulos GP, Brown RE, Butler JP. Increased surface tension decreases pulmonary capillary volume and compliance. J Appl Physiol. 2002;93(3):1023-9. Epub 2002/08/17.
148. Glasser JR, Mallampalli RK. Surfactant and its role in the pathobiology of pulmonary infection. Microbes and infection / Institut Pasteur. 2012;14(1):17-25. Epub 2011/09/29.
149. Wu H, Kuzmenko A, Wan S, Schaffer L, Weiss A, Fisher JH, et al. Surfactant proteins A and D inhibit the growth of Gram-negative bacteria by increasing membrane permeability. J Clin Invest. 2003;111(10):1589-602. Epub 2003/05/17.
150. Kuronuma K, Mitsuzawa H, Takeda K, Nishitani C, Chan ED, Kuroki Y, et al. Anionic pulmonary surfactant phospholipids inhibit inflammatory responses from alveolar macrophages and U937 cells by binding the lipopolysaccharide-interacting proteins CD14 and MD-2. J Biol Chem. 2009;284(38):25488-500. Epub 2009/07/09.
151. Numata M, Kandasamy P, Voelker DR. Anionic pulmonary surfactant lipid regulation of innate immunity. Expert review of respiratory medicine. 2012;6(3):243-6. Epub 2012/07/14.
152. Perino J, Crouzier D, Spehner D, Debouzy JC, Garin D, Crance JM, et al. Lung surfactant DPPG phospholipid inhibits vaccinia virus infection. Antiviral research. 2011;89(1):89-97. Epub 2010/11/26.
153. Abate W, Alghaithy AA, Parton J, Jones KP, Jackson SK. Surfactant lipids regulate LPS-induced interleukin-8 production in A549 lung epithelial cells by inhibiting translocation of TLR4 into lipid raft domains. Journal of lipid research. 2010;51(2):334-44. Epub 2009/08/04.
154. Gille C, Spring B, Bernhard W, Gebhard C, Basile D, Lauber K, et al. Differential effect of surfactant and its saturated phosphatidylcholines on human blood macrophages. Journal of lipid research. 2007;48(2):307-17. Epub 2006/11/14.
155. Ikegami M, Whitsett JA, Martis PC, Weaver TE. Reversibility of lung inflammation caused by SP-B deficiency. Am J Physiol Lung Cell Mol Physiol. 2005;289(6):L962-70. Epub 2005/07/19.
156. Epaud R, Ikegami M, Whitsett JA, Jobe AH, Weaver TE, Akinbi HT. Surfactant protein B inhibits endotoxin-induced lung inflammation. Am J Respir Cell Mol Biol. 2003;28(3):373-8. Epub 2003/02/21.
157. Mulugeta S, Beers MF. Surfactant protein C: its unique properties and emerging immunomodulatory role in the lung. Microbes and infection / Institut Pasteur. 2006;8(8):2317-23. Epub 2006/06/20.
158. Green GM, Jakab GJ, Low RB, Davis GS. Defense mechanisms of the respiratory membrane. Am Rev Respir Dis. 1977;115(3):479-514. Epub 1977/03/01.
159. Beutler B. Innate immunity: an overview. Molecular immunology. 2004;40(12):845-59. Epub 2003/12/31.
160. Martin TR, Frevert CW. Innate immunity in the lungs. Proceedings of the American Thoracic Society. 2005;2(5):403-11. Epub 2005/12/03.

161. Lehrer RI. Primate defensins. Nature reviews Microbiology. 2004;2(9):727-38. Epub 2004/09/17.
162. Martin TR, Rubenfeld GD, Ruzinski JT, Goodman RB, Steinberg KP, Leturcq DJ, et al. Relationship between soluble CD14, lipopolysaccharide binding protein, and the alveolar inflammatory response in patients with acute respiratory distress syndrome. Am J Respir Crit Care Med. 1997;155(3):937-44. Epub 1997/03/01.
163. Martin TR, Mathison JC, Tobias PS, Leturcq DJ, Moriarty AM, Maunder RJ, et al. Lipopolysaccharide binding protein enhances the responsiveness of alveolar macrophages to bacterial lipopolysaccharide. Implications for cytokine production in normal and injured lungs. J Clin Invest. 1992;90(6):2209-19. Epub 1992/12/01.
164. Mizgerd JP. Acute lower respiratory tract infection. N Engl J Med. 2008;358(7):716-27. Epub 2008/02/15.
165. Byers DE, Holtzman MJ. Alternatively activated macrophages and airway disease. Chest. 2011;140(3):768-74. Epub 2011/09/08.
166. Mosser DM, Edwards JP. Exploring the full spectrum of macrophage activation. Nature reviews Immunology. 2008;8(12):958-69. Epub 2008/11/26.
167. Burns AR, Smith CW, Walker DC. Unique structural features that influence neutrophil emigration into the lung. Physiological reviews. 2003;83(2):309-36. Epub 2003/03/29.
168. Ashbaugh DG, Bigelow DB, Petty TL, Levine BE. Acute respiratory distress in adults. Lancet. 1967;2(7511):319-23. Epub 1967/08/12.
169. Murray JF, Matthay MA, Luce JM, Flick MR. An expanded definition of the adult respiratory distress syndrome. Am Rev Respir Dis. 1988;138(3):720-3. Epub 1988/09/01.
170. Fowler AA, Hamman RF, Good JT, Benson KN, Baird M, Eberle DJ, et al. Adult respiratory distress syndrome: risk with common predispositions. Ann Intern Med. 1983;98(5 Pt 1):593-7. Epub 1983/05/01.
171. Milberg JA, Davis DR, Steinberg KP, Hudson LD. Improved survival of patients with acute respiratory distress syndrome (ARDS): 1983-1993. JAMA. 1995;273(4):306-9. Epub 1995/01/25.
172. Villar J, Slutsky AS. The incidence of the adult respiratory distress syndrome. Am Rev Respir Dis. 1989;140(3):814-6. Epub 1989/09/01.
173. Johnson ER, Matthay MA. Acute lung injury: epidemiology, pathogenesis, and treatment. J Aerosol Med Pulm Drug Deliv. 2010;23(4):243-52. Epub 2010/01/16.
174. Goss CH, Brower RG, Hudson LD, Rubenfeld GD. Incidence of acute lung injury in the United States. Crit Care Med. 2003;31(6):1607-11. Epub 2003/06/10.
175. Rubenfeld GD, Caldwell E, Peabody E, Weaver J, Martin DP, Neff M, et al. Incidence and outcomes of acute lung injury. N Engl J Med. 2005;353(16):1685-93. Epub 2005/10/21.
176. Eisner MD, Thompson T, Hudson LD, Luce JM, Hayden D, Schoenfeld D, et al. Efficacy of low tidal volume ventilation in patients with different clinical risk factors for acute lung injury and the acute respiratory distress syndrome. Am J Respir Crit Care Med. 2001;164(2):231-6. Epub 2001/07/21.

177. Erickson SE, Shlipak MG, Martin GS, Wheeler AP, Ancukiewicz M, Matthay MA, et al. Racial and ethnic disparities in mortality from acute lung injury. Crit Care Med. 2009;37(1):1-6. Epub 2008/12/04.
178. Weinert CR, Gross CR, Kangas JR, Bury CL, Marinelli WA. Health-related quality of life after acute lung injury. Am J Respir Crit Care Med. 1997;156(4 Pt 1):1120-8. Epub 1997/11/14.
179. Herridge MS, Cheung AM, Tansey CM, Matte-Martyn A, Diaz-Granados N, Al-Saidi F, et al. One-year outcomes in survivors of the acute respiratory distress syndrome. N Engl J Med. 2003;348(8):683-93. Epub 2003/02/21.
180. McHugh LG, Milberg JA, Whitcomb ME, Schoene RB, Maunder RJ, Hudson LD. Recovery of function in survivors of the acute respiratory distress syndrome. Am J Respir Crit Care Med. 1994;150(1):90-4. Epub 1994/07/01.
181. Goodman RB, Strieter RM, Martin DP, Steinberg KP, Milberg JA, Maunder RJ, et al. Inflammatory cytokines in patients with persistence of the acute respiratory distress syndrome. Am J Respir Crit Care Med. 1996;154(3 Pt 1):602-11. Epub 1996/09/01.
182. Park WY, Goodman RB, Steinberg KP, Ruzinski JT, Radella F, 2nd, Park DR, et al. Cytokine balance in the lungs of patients with acute respiratory distress syndrome. Am J Respir Crit Care Med. 2001;164(10 Pt 1):1896-903. Epub 2001/12/06.
183. Pugin J, Verghese G, Widmer MC, Matthay MA. The alveolar space is the site of intense inflammatory and profibrotic reactions in the early phase of acute respiratory distress syndrome. Crit Care Med. 1999;27(2):304-12. Epub 1999/03/13.
184. Tomashefski J. Pulmonary Pathology of the Acute Respiratory Distress Syndrome- Diffuse Alveolar Damage. In: Matthay M, editor. Acute Respiratory Distress Syndrome. New York: Marcel Dekker; 2003.
185. Bigatello LM, Zapol WM. New approaches to acute lung injury. British journal of anaesthesia. 1996;77(1):99-109. Epub 1996/07/01.
186. Ware LB, Conner ER, Matthay MA. von Willebrand factor antigen is an independent marker of poor outcome in patients with early acute lung injury. Crit Care Med. 2001;29(12):2325-31. Epub 2002/01/22.
187. Ware LB, Eisner MD, Thompson BT, Parsons PE, Matthay MA. Significance of von Willebrand factor in septic and nonseptic patients with acute lung injury. Am J Respir Crit Care Med. 2004;170(7):766-72. Epub 2004/06/18.
188. Flori HR, Ware LB, Milet M, Matthay MA. Early elevation of plasma von Willebrand factor antigen in pediatric acute lung injury is associated with an increased risk of death and prolonged mechanical ventilation. Pediatric critical care medicine : a journal of the Society of Critical Care Medicine and the World Federation of Pediatric Intensive and Critical Care Societies. 2007;8(2):96-101. Epub 2007/02/03.
189. Flori HR, Ware LB, Glidden D, Matthay MA. Early elevation of plasma soluble intercellular adhesion molecule-1 in pediatric acute lung injury identifies patients at increased risk of death and prolonged mechanical ventilation. Pediatric critical care medicine : a journal of the Society of Critical Care Medicine and the

World Federation of Pediatric Intensive and Critical Care Societies. 2003;4(3):315-21. Epub 2003/07/02.

190. Calfee CS, Eisner MD, Parsons PE, Thompson BT, Conner ER, Jr., Matthay MA, et al. Soluble intercellular adhesion molecule-1 and clinical outcomes in patients with acute lung injury. Intensive Care Med. 2009;35(2):248-57. Epub 2008/08/02.

191. Greene KE, Wright JR, Steinberg KP, Ruzinski JT, Caldwell E, Wong WB, et al. Serial changes in surfactant-associated proteins in lung and serum before and after onset of ARDS. Am J Respir Crit Care Med. 1999;160(6):1843-50. Epub 1999/12/10.

192. Bitterman PB. Pathogenesis of fibrosis in acute lung injury. The American journal of medicine. 1992;92(6A):39S-43S. Epub 1992/06/22.

193. Kurahashi K, Kajikawa O, Sawa T, Ohara M, Gropper MA, Frank DW, et al. Pathogenesis of septic shock in Pseudomonas aeruginosa pneumonia. J Clin Invest. 1999;104(6):743-50. Epub 1999/09/24.

194. Pittet JF, Mackersie RC, Martin TR, Matthay MA. Biological markers of acute lung injury: prognostic and pathogenetic significance. Am J Respir Crit Care Med. 1997;155(4):1187-205. Epub 1997/04/01.

195. Canonico AE, Brigham, K. L. Biology of Acute Injury. In: Crystal RG WJB, Barnes PJ, Weibel ER., editor. The Lung: Scientific Foundations. Philadelphia: Lippincot-Raven; 1997.

196. Libby P, Ordovas JM, Auger KR, Robbins AH, Birinyi LK, Dinarello CA. Endotoxin and tumor necrosis factor induce interleukin-1 gene expression in adult human vascular endothelial cells. The American journal of pathology. 1986;124(2):179-85. Epub 1986/08/01.

197. Podor TJ, Jirik FR, Loskutoff DJ, Carson DA, Lotz M. Human endothelial cells produce IL-6. Lack of responses to exogenous IL-6. Annals of the New York Academy of Sciences. 1989;557:374-85; discussion 86-7. Epub 1989/01/01.

198. Sica A, Matsushima K, Van Damme J, Wang JM, Polentarutti N, Dejana E, et al. IL-1 transcriptionally activates the neutrophil chemotactic factor/IL-8 gene in endothelial cells. Immunology. 1990;69(4):548-53. Epub 1990/04/01.

199. Kwon OJ, Au BT, Collins PD, Adcock IM, Mak JC, Robbins RR, et al. Tumor necrosis factor-induced interleukin-8 expression in cultured human airway epithelial cells. The American journal of physiology. 1994;267(4 Pt 1):L398-405. Epub 1994/10/01.

200. Tosi MF, Stark JM, Smith CW, Hamedani A, Gruenert DC, Infeld MD. Induction of ICAM-1 expression on human airway epithelial cells by inflammatory cytokines: effects on neutrophil-epithelial cell adhesion. Am J Respir Cell Mol Biol. 1992;7(2):214-21. Epub 1992/08/01.

201. Springer TA. Adhesion receptors of the immune system. Nature. 1990;346(6283):425-34. Epub 1990/08/02.

202. Orfanos SE, Mavrommati I, Korovesi I, Roussos C. Pulmonary endothelium in acute lung injury: from basic science to the critically ill. Intensive Care Med. 2004;30(9):1702-14. Epub 2004/07/20.

203. Bachofen M, Weibel ER. Structural alterations of lung parenchyma in the adult respiratory distress syndrome. Clinics in chest medicine. 1982;3(1):35-56. Epub 1982/01/01.
204. Abraham E, Carmody A, Shenkar R, Arcaroli J. Neutrophils as early immunologic effectors in hemorrhage- or endotoxemia-induced acute lung injury. Am J Physiol Lung Cell Mol Physiol. 2000;279(6):L1137-45. Epub 2000/11/15.
205. Lee WL, Downey GP. Neutrophil activation and acute lung injury. Current opinion in critical care. 2001;7(1):1-7. Epub 2001/05/25.
206. Zemans RL, Colgan SP, Downey GP. Transepithelial migration of neutrophils: mechanisms and implications for acute lung injury. Am J Respir Cell Mol Biol. 2009;40(5):519-35. Epub 2008/11/04.
207. Ginzberg HH, Shannon PT, Suzuki T, Hong O, Vachon E, Moraes T, et al. Leukocyte elastase induces epithelial apoptosis: role of mitochondial permeability changes and Akt. American journal of physiology Gastrointestinal and liver physiology. 2004;287(1):G286-98. Epub 2004/06/15.
208. Ginzberg HH, Cherapanov V, Dong Q, Cantin A, McCulloch CA, Shannon PT, et al. Neutrophil-mediated epithelial injury during transmigration: role of elastase. American journal of physiology Gastrointestinal and liver physiology. 2001;281(3):G705-17. Epub 2001/08/24.
209. Wiedermann FJ, Mayr AJ, Kaneider NC, Fuchs D, Mutz NJ, Schobersberger W. Alveolar granulocyte colony-stimulating factor and alpha-chemokines in relation to serum levels, pulmonary neutrophilia, and severity of lung injury in ARDS. Chest. 2004;125(1):212-9. Epub 2004/01/14.
210. Strieter RM, Belperio JA, Keane MP. Cytokines in innate host defense in the lung. J Clin Invest. 2002;109(6):699-705. Epub 2002/03/20.
211. Cross LJ, Matthay MA. Biomarkers in acute lung injury: insights into the pathogenesis of acute lung injury. Critical care clinics. 2011;27(2):355-77. Epub 2011/03/29.
212. Strieter RM, Kunkel SL. Acute lung injury: the role of cytokines in the elicitation of neutrophils. Journal of investigative medicine : the official publication of the American Federation for Clinical Research. 1994;42(4):640-51. Epub 1994/12/01.
213. Jones SA. Directing transition from innate to acquired immunity: defining a role for IL-6. J Immunol. 2005;175(6):3463-8. Epub 2005/09/09.
214. Strieter RM, Koch AE, Antony VB, Fick RB, Jr., Standiford TJ, Kunkel SL. The immunopathology of chemotactic cytokines: the role of interleukin-8 and monocyte chemoattractant protein-1. The Journal of laboratory and clinical medicine. 1994;123(2):183-97. Epub 1994/02/01.
215. Pugin J, Ricou B, Steinberg KP, Suter PM, Martin TR. Proinflammatory activity in bronchoalveolar lavage fluids from patients with ARDS, a prominent role for interleukin-1. Am J Respir Crit Care Med. 1996;153(6 Pt 1):1850-6. Epub 1996/06/01.
216. Meduri GU, Headley S, Kohler G, Stentz F, Tolley E, Umberger R, et al. Persistent elevation of inflammatory cytokines predicts a poor outcome in ARDS.

Plasma IL-1 beta and IL-6 levels are consistent and efficient predictors of outcome over time. Chest. 1995;107(4):1062-73. Epub 1995/04/01.
217. Stapleton RD, Dixon AE, Parsons PE, Ware LB, Suratt BT. The association between BMI and plasma cytokine levels in patients with acute lung injury. Chest. 2010;138(3):568-77. Epub 2010/05/04.
218. Meduri GU, Kohler G, Headley S, Tolley E, Stentz F, Postlethwaite A. Inflammatory cytokines in the BAL of patients with ARDS. Persistent elevation over time predicts poor outcome. Chest. 1995;108(5):1303-14. Epub 1995/11/01.
219. Slutsky AS, Ranieri VM. Mechanical ventilation: lessons from the ARDSNet trial. Respiratory research. 2000;1(2):73-7. Epub 2001/10/23.
220. Adhikari N, Burns KE, Meade MO. Pharmacologic treatments for acute respiratory distress syndrome and acute lung injury: systematic review and meta-analysis. Treatments in respiratory medicine. 2004;3(5):307-28. Epub 2004/12/21.
221. Berthiaume Y, Broaddus VC, Gropper MA, Tanita T, Matthay MA. Alveolar liquid and protein clearance from normal dog lungs. J Appl Physiol. 1988;65(2):585-93. Epub 1988/08/01.
222. Sakuma T, Folkesson HG, Suzuki S, Okaniwa G, Fujimura S, Matthay MA. Beta-adrenergic agonist stimulated alveolar fluid clearance in ex vivo human and rat lungs. Am J Respir Crit Care Med. 1997;155(2):506-12. Epub 1997/02/01.
223. Manocha S, Gordon AC, Salehifar E, Groshaus H, Walley KR, Russell JA. Inhaled beta-2 agonist salbutamol and acute lung injury: an association with improvement in acute lung injury. Crit Care. 2006;10(1):R12. Epub 2006/01/20.
224. Perkins GD, McAuley DF, Thickett DR, Gao F. The beta-agonist lung injury trial (BALTI): a randomized placebo-controlled clinical trial. Am J Respir Crit Care Med. 2006;173(3):281-7. Epub 2005/10/29.
225. Artinian V, Krayem H, DiGiovine B. Effects of early enteral feeding on the outcome of critically ill mechanically ventilated medical patients. Chest. 2006;129(4):960-7. Epub 2006/04/13.
226. Almog Y, Shefer A, Novack V, Maimon N, Barski L, Eizinger M, et al. Prior statin therapy is associated with a decreased rate of severe sepsis. Circulation. 2004;110(7):880-5. Epub 2004/08/04.
227. Kruger P, Fitzsimmons K, Cook D, Jones M, Nimmo G. Statin therapy is associated with fewer deaths in patients with bacteraemia. Intensive Care Med. 2006;32(1):75-9. Epub 2005/11/12.
228. Thomsen RW, Riis A, Kornum JB, Christensen S, Johnsen SP, Sorensen HT. Preadmission use of statins and outcomes after hospitalization with pneumonia: population-based cohort study of 29,900 patients. Archives of internal medicine. 2008;168(19):2081-7. Epub 2008/10/29.
229. Rojas M, Xu J, Woods CR, Mora AL, Spears W, Roman J, et al. Bone marrow-derived mesenchymal stem cells in repair of the injured lung. Am J Respir Cell Mol Biol. 2005;33(2):145-52. Epub 2005/05/14.
230. Gupta N, Su X, Popov B, Lee JW, Serikov V, Matthay MA. Intrapulmonary delivery of bone marrow-derived mesenchymal stem cells improves survival and

attenuates endotoxin-induced acute lung injury in mice. J Immunol. 2007;179(3):1855-63. Epub 2007/07/21.
231. Ware LB. Modeling human lung disease in animals. Am J Physiol Lung Cell Mol Physiol. 2008;294(2):L149-50. Epub 2007/11/21.
232. Matute-Bello G, Frevert CW, Martin TR. Animal models of acute lung injury. Am J Physiol Lung Cell Mol Physiol. 2008;295(3):L379-99. Epub 2008/07/16.
233. Irvin CG, Bates JH. Measuring the lung function in the mouse: the challenge of size. Respiratory research. 2003;4:4. Epub 2003/06/05.
234. Mestas J, Hughes CC. Of mice and not men: differences between mouse and human immunology. J Immunol. 2004;172(5):2731-8. Epub 2004/02/24.
235. Dreyfuss D, Saumon G. Ventilator-induced lung injury: lessons from experimental studies. Am J Respir Crit Care Med. 1998;157(1):294-323. Epub 1998/01/28.
236. Webb HH, Tierney DF. Experimental pulmonary edema due to intermittent positive pressure ventilation with high inflation pressures. Protection by positive end-expiratory pressure. Am Rev Respir Dis. 1974;110(5):556-65. Epub 1974/11/01.
237. Lang JD, Hickman-Davis JM. One-hit, two-hit . . . is there really any benefit? Clinical and experimental immunology. 2005;141(2):211-4. Epub 2005/07/06.
238. Frank JA, Parsons PE, Matthay MA. Pathogenetic significance of biological markers of ventilator-associated lung injury in experimental and clinical studies. Chest. 2006;130(6):1906-14. Epub 2006/12/15.
239. dos Santos CC, Slutsky AS. The contribution of biophysical lung injury to the development of biotrauma. Annu Rev Physiol. 2006;68:585-618. Epub 2006/02/08.
240. Dreyfuss D, Soler P, Basset G, Saumon G. High inflation pressure pulmonary edema. Respective effects of high airway pressure, high tidal volume, and positive end-expiratory pressure. Am Rev Respir Dis. 1988;137(5):1159-64. Epub 1988/05/01.
241. Hernandez LA, Peevy KJ, Moise AA, Parker JC. Chest wall restriction limits high airway pressure-induced lung injury in young rabbits. J Appl Physiol. 1989;66(5):2364-8. Epub 1989/05/01.
242. Carlton DP, Cummings JJ, Scheerer RG, Poulain FR, Bland RD. Lung overexpansion increases pulmonary microvascular protein permeability in young lambs. J Appl Physiol. 1990;69(2):577-83. Epub 1990/08/01.
243. Whitehead T, Slutsky AS. The pulmonary physician in critical care * 7: ventilator induced lung injury. Thorax. 2002;57(7):635-42. Epub 2002/07/04.
244. Schiller HJ, McCann UG, 2nd, Carney DE, Gatto LA, Steinberg JM, Nieman GF. Altered alveolar mechanics in the acutely injured lung. Crit Care Med. 2001;29(5):1049-55. Epub 2001/06/01.
245. Frank JA, Gutierrez JA, Jones KD, Allen L, Dobbs L, Matthay MA. Low tidal volume reduces epithelial and endothelial injury in acid-injured rat lungs. Am J Respir Crit Care Med. 2002;165(2):242-9. Epub 2002/01/16.
246. Ranieri VM, Suter PM, Tortorella C, De Tullio R, Dayer JM, Brienza A, et al. Effect of mechanical ventilation on inflammatory mediators in patients with acute respiratory distress syndrome: a randomized controlled trial. JAMA. 1999;282(1):54-61. Epub 1999/07/15.

247. Amato MB, Barbas CS, Medeiros DM, Magaldi RB, Schettino GP, Lorenzi-Filho G, et al. Effect of a protective-ventilation strategy on mortality in the acute respiratory distress syndrome. N Engl J Med. 1998;338(6):347-54. Epub 1998/02/05.
248. Uhlig S. Ventilation-induced lung injury and mechanotransduction: stretching it too far? Am J Physiol Lung Cell Mol Physiol. 2002;282(5):L892-6. Epub 2002/04/12.
249. Chiumello D, Pristine G, Slutsky AS. Mechanical ventilation affects local and systemic cytokines in an animal model of acute respiratory distress syndrome. Am J Respir Crit Care Med. 1999;160(1):109-16. Epub 1999/07/03.
250. Tremblay L, Valenza F, Ribeiro SP, Li J, Slutsky AS. Injurious ventilatory strategies increase cytokines and c-fos m-RNA expression in an isolated rat lung model. J Clin Invest. 1997;99(5):944-52. Epub 1997/03/01.
251. Montgomery AB, Stager MA, Carrico CJ, Hudson LD. Causes of mortality in patients with the adult respiratory distress syndrome. Am Rev Respir Dis. 1985;132(3):485-9. Epub 1985/09/01.
252. Parsons PE, Eisner MD, Thompson BT, Matthay MA, Ancukiewicz M, Bernard GR, et al. Lower tidal volume ventilation and plasma cytokine markers of inflammation in patients with acute lung injury. Crit Care Med. 2005;33(1):1-6; discussion 230-2. Epub 2005/01/13.
253. Ranieri VM, Giunta F, Suter PM, Slutsky AS. Mechanical ventilation as a mediator of multisystem organ failure in acute respiratory distress syndrome. JAMA. 2000;284(1):43-4. Epub 2000/06/29.
254. Stuber F, Wrigge H, Schroeder S, Wetegrove S, Zinserling J, Hoeft A, et al. Kinetic and reversibility of mechanical ventilation-associated pulmonary and systemic inflammatory response in patients with acute lung injury. Intensive Care Med. 2002;28(7):834-41. Epub 2002/07/18.
255. Pugin J. Is the ventilator responsible for lung and systemic inflammation? Intensive Care Med. 2002;28(7):817-9. Epub 2002/09/28.
256. Dreyfuss D, Ricard JD, Saumon G. On the physiologic and clinical relevance of lung-borne cytokines during ventilator-induced lung injury. Am J Respir Crit Care Med. 2003;167(11):1467-71. Epub 2003/05/29.
257. Ricard JD, Dreyfuss D, Saumon G. Production of inflammatory cytokines in ventilator-induced lung injury: a reappraisal. Am J Respir Crit Care Med. 2001;163(5):1176-80. Epub 2001/04/24.
258. Shikata Y, Rios A, Kawkitinarong K, DePaola N, Garcia JG, Birukov KG. Differential effects of shear stress and cyclic stretch on focal adhesion remodeling, site-specific FAK phosphorylation, and small GTPases in human lung endothelial cells. Experimental cell research. 2005;304(1):40-9. Epub 2005/02/15.
259. Nonas SA, Moreno-Vinasco L, Ma SF, Jacobson JR, Desai AA, Dudek SM, et al. Use of consomic rats for genomic insights into ventilator-associated lung injury. Am J Physiol Lung Cell Mol Physiol. 2007;293(2):L292-302. Epub 2007/05/01.
260. Dreyfuss D, Soler P, Saumon G. Spontaneous resolution of pulmonary edema caused by short periods of cyclic overinflation. J Appl Physiol. 1992;72(6):2081-9. Epub 1992/06/01.

261. Dreyfuss D, Basset G, Soler P, Saumon G. Intermittent positive-pressure hyperventilation with high inflation pressures produces pulmonary microvascular injury in rats. Am Rev Respir Dis. 1985;132(4):880-4. Epub 1985/10/01.
262. Tsuno K, Miura K, Takeya M, Kolobow T, Morioka T. Histopathologic pulmonary changes from mechanical ventilation at high peak airway pressures. Am Rev Respir Dis. 1991;143(5 Pt 1):1115-20. Epub 1991/05/01.
263. John E, McDevitt M, Wilborn W, Cassady G. Ultrastructure of the lung after ventilation. British journal of experimental pathology. 1982;63(4):401-7. Epub 1982/08/01.
264. Kawano T, Mori S, Cybulsky M, Burger R, Ballin A, Cutz E, et al. Effect of granulocyte depletion in a ventilated surfactant-depleted lung. J Appl Physiol. 1987;62(1):27-33. Epub 1987/01/01.
265. Cooper JA, van der Zee H, Line BR, Malik AB. Relationship of end-expiratory pressure, lung volume, and 99mTc-DTPA clearance. J Appl Physiol. 1987;63(4):1586-90. Epub 1987/10/01.
266. O'Brodovich H, Coates G, Marrin M. Effect of inspiratory resistance and PEEP on 99mTc-DTPA clearance. J Appl Physiol. 1986;60(5):1461-5. Epub 1986/05/01.
267. Marks JD, Luce JM, Lazar NM, Wu JN, Lipavsky A, Murray JF. Effect of increases in lung volume on clearance of aerosolized solute from human lungs. J Appl Physiol. 1985;59(4):1242-8. Epub 1985/10/01.
268. Nolop KB, Maxwell DL, Royston D, Hughes JM. Effect of raised thoracic pressure and volume on 99mTc-DTPA clearance in humans. J Appl Physiol. 1986;60(5):1493-7. Epub 1986/05/01.
269. Egan EA. Lung inflation, lung solute permeability, and alveolar edema. J Appl Physiol. 1982;53(1):121-5. Epub 1982/07/01.
270. Kim KJ, Crandall ED. Effects of lung inflation on alveolar epithelial solute and water transport properties. J Appl Physiol. 1982;52(6):1498-505. Epub 1982/06/01.
271. Parker JC, Townsley MI, Rippe B, Taylor AE, Thigpen J. Increased microvascular permeability in dog lungs due to high peak airway pressures. J Appl Physiol. 1984;57(6):1809-16. Epub 1984/12/01.
272. Rippe B, Townsley M, Thigpen J, Parker JC, Korthuis RJ, Taylor AE. Effects of vascular pressure on the pulmonary microvasculature in isolated dog lungs. J Appl Physiol. 1984;57(1):233-9. Epub 1984/07/01.
273. Frank JA, Wray CM, McAuley DF, Schwendener R, Matthay MA. Alveolar macrophages contribute to alveolar barrier dysfunction in ventilator-induced lung injury. Am J Physiol Lung Cell Mol Physiol. 2006;291(6):L1191-8. Epub 2006/08/01.
274. Pugin J, Dunn I, Jolliet P, Tassaux D, Magnenat JL, Nicod LP, et al. Activation of human macrophages by mechanical ventilation in vitro. The American journal of physiology. 1998;275(6 Pt 1):L1040-50. Epub 1998/12/09.
275. Eyal FG, Hamm CR, Parker JC. Reduction in alveolar macrophages attenuates acute ventilator induced lung injury in rats. Intensive Care Med. 2007;33(7):1212-8. Epub 2007/05/01.

276. Downey GP, Dong Q, Kruger J, Dedhar S, Cherapanov V. Regulation of neutrophil activation in acute lung injury. Chest. 1999;116(1 Suppl):46S-54S. Epub 1999/07/29.
277. Tremblay LN, Slutsky AS. Ventilator-induced injury: from barotrauma to biotrauma. Proc Assoc Am Physicians. 1998;110(6):482-8. Epub 1998/11/21.
278. Zhang H, Downey GP, Suter PM, Slutsky AS, Ranieri VM. Conventional mechanical ventilation is associated with bronchoalveolar lavage-induced activation of polymorphonuclear leukocytes: a possible mechanism to explain the systemic consequences of ventilator-induced lung injury in patients with ARDS. Anesthesiology. 2002;97(6):1426-33. Epub 2002/12/03.
279. Martin TR, Pistorese BP, Chi EY, Goodman RB, Matthay MA. Effects of leukotriene B4 in the human lung. Recruitment of neutrophils into the alveolar spaces without a change in protein permeability. J Clin Invest. 1989;84(5):1609-19. Epub 1989/11/01.
280. Vlahakis NE, Schroeder MA, Limper AH, Hubmayr RD. Stretch induces cytokine release by alveolar epithelial cells in vitro. The American journal of physiology. 1999;277(1 Pt 1):L167-73. Epub 1999/07/17.
281. Wilson MR, Choudhury S, Goddard ME, O'Dea KP, Nicholson AG, Takata M. High tidal volume upregulates intrapulmonary cytokines in an in vivo mouse model of ventilator-induced lung injury. J Appl Physiol. 2003;95(4):1385-93. Epub 2003/06/17.
282. Hoegl S, Boost KA, Flondor M, Scheiermann P, Muhl H, Pfeilschifter J, et al. Short-term exposure to high-pressure ventilation leads to pulmonary biotrauma and systemic inflammation in the rat. International journal of molecular medicine. 2008;21(4):513-9. Epub 2008/03/25.
283. Haitsma JJ, Uhlig S, Goggel R, Verbrugge SJ, Lachmann U, Lachmann B. Ventilator-induced lung injury leads to loss of alveolar and systemic compartmentalization of tumor necrosis factor-alpha. Intensive Care Med. 2000;26(10):1515-22. Epub 2000/12/29.
284. Naik AS, Kallapur SG, Bachurski CJ, Jobe AH, Michna J, Kramer BW, et al. Effects of ventilation with different positive end-expiratory pressures on cytokine expression in the preterm lamb lung. Am J Respir Crit Care Med. 2001;164(3):494-8. Epub 2001/08/14.
285. Veldhuizen RA, Slutsky AS, Joseph M, McCaig L. Effects of mechanical ventilation of isolated mouse lungs on surfactant and inflammatory cytokines. The European respiratory journal : official journal of the European Society for Clinical Respiratory Physiology. 2001;17(3):488-94. Epub 2001/06/19.
286. Wolthuis EK, Vlaar AP, Choi G, Roelofs JJ, Juffermans NP, Schultz MJ. Mechanical ventilation using non-injurious ventilation settings causes lung injury in the absence of pre-existing lung injury in healthy mice. Crit Care. 2009;13(1):R1. Epub 2009/01/21.
287. Determann RM, Royakkers A, Wolthuis EK, Vlaar AP, Choi G, Paulus F, et al. Ventilation with lower tidal volumes as compared with conventional tidal volumes

for patients without acute lung injury: a preventive randomized controlled trial. Crit Care. 2010;14(1):R1. Epub 2010/01/09.
288. Jaecklin T, Otulakowski G, Kavanagh BP. Do soluble mediators cause ventilator-induced lung injury and multi-organ failure? Intensive Care Med. 2010;36(5):750-7. Epub 2010/03/17.
289. Albaiceta GM, Gutierrez-Fernandez A, Garcia-Prieto E, Puente XS, Parra D, Astudillo A, et al. Absence or inhibition of matrix metalloproteinase-8 decreases ventilator-induced lung injury. Am J Respir Cell Mol Biol. 2010;43(5):555-63. Epub 2009/12/10.
290. Waters CM. Reactive oxygen species in mechanotransduction. Am J Physiol Lung Cell Mol Physiol. 2004;287(3):L484-5. Epub 2004/08/17.
291. Chabot F, Mitchell JA, Gutteridge JM, Evans TW. Reactive oxygen species in acute lung injury. The European respiratory journal : official journal of the European Society for Clinical Respiratory Physiology. 1998;11(3):745-57. Epub 1998/05/22.
292. Birukov KG. Cyclic stretch, reactive oxygen species, and vascular remodeling. Antioxidants & redox signaling. 2009;11(7):1651-67. Epub 2009/02/04.
293. Edwards YS. Stretch stimulation: its effects on alveolar type II cell function in the lung. Comparative biochemistry and physiology Part A, Molecular & integrative physiology. 2001;129(1):245-60. Epub 2001/05/23.
294. Nakamura T, Malloy J, McCaig L, Yao LJ, Joseph M, Lewis J, et al. Mechanical ventilation of isolated septic rat lungs: effects on surfactant and inflammatory cytokines. J Appl Physiol. 2001;91(2):811-20. Epub 2001/07/18.
295. Veldhuizen RA, Tremblay LN, Govindarajan A, van Rozendaal BA, Haagsman HP, Slutsky AS. Pulmonary surfactant is altered during mechanical ventilation of isolated rat lung. Crit Care Med. 2000;28(7):2545-51. Epub 2000/08/02.
296. Maruscak AA, Vockeroth DW, Girardi B, Sheikh T, Possmayer F, Lewis JF, et al. Alterations to surfactant precede physiological deterioration during high tidal volume ventilation. Am J Physiol Lung Cell Mol Physiol. 2008;294(5):L974-83. Epub 2008/03/18.
297. Veldhuizen RA, Welk B, Harbottle R, Hearn S, Nag K, Petersen N, et al. Mechanical ventilation of isolated rat lungs changes the structure and biophysical properties of surfactant. J Appl Physiol. 2002;92(3):1169-75. Epub 2002/02/14.
298. Verbrugge SJ, Bohm SH, Gommers D, Zimmerman LJ, Lachmann B. Surfactant impairment after mechanical ventilation with large alveolar surface area changes and effects of positive end-expiratory pressure. British journal of anaesthesia. 1998;80(3):360-4. Epub 1998/06/12.
299. Plataki M, Hubmayr RD. The physical basis of ventilator-induced lung injury. Expert review of respiratory medicine. 2010;4(3):373-85. Epub 2010/06/09.
300. Jobe AH. Pulmonary surfactant therapy. N Engl J Med. 1993;328(12):861-8. Epub 1993/03/25.
301. Chesnutt AN, Matthay MA, Tibayan FA, Clark JG. Early detection of type III procollagen peptide in acute lung injury. Pathogenetic and prognostic significance. Am J Respir Crit Care Med. 1997;156(3 Pt 1):840-5. Epub 1997/10/06.

302. Wesselkamper SC, Case LM, Henning LN, Borchers MT, Tichelaar JW, Mason JM, et al. Gene expression changes during the development of acute lung injury: role of transforming growth factor beta. Am J Respir Crit Care Med. 2005;172(11):1399-411. Epub 2005/08/16.
303. Crystal RG, Fulmer JD, Baum BJ, Bernardo J, Bradley KH, Bruel SD, et al. Cells, collagen and idiopathic pulmonary fibrosis. Lung. 1978;155(3):199-224. Epub 1978/01/01.
304. Keogh BA, Crystal RG. Alveolitis: the key to the interstitial lung disorders. Thorax. 1982;37(1):1-10. Epub 1982/01/01.
305. Nin N, Lorente JA, de Paula M, El Assar M, Vallejo S, Penuelas O, et al. Rats surviving injurious mechanical ventilation show reversible pulmonary, vascular and inflammatory changes. Intensive Care Med. 2008;34(5):948-56. Epub 2008/01/09.
306. Curley GF, Contreras M, Higgins B, O'Kane C, McAuley DF, O'Toole D, et al. Evolution of the inflammatory and fibroproliferative responses during resolution and repair after ventilator-induced lung injury in the rat. Anesthesiology. 2011;115(5):1022-32. Epub 2011/09/29.
307. Brew N, Hooper SB, Allison BJ, Wallace MJ, Harding R. Injury and repair in the very immature lung following brief mechanical ventilation. Am J Physiol Lung Cell Mol Physiol. 2011;301(6):L917-26. Epub 2011/09/06.
308. Gonzalez-Lopez A, Astudillo A, Garcia-Prieto E, Fernandez-Garcia MS, Lopez-Vazquez A, Batalla-Solis E, et al. Inflammation and matrix remodeling during repair of ventilator-induced lung injury. Am J Physiol Lung Cell Mol Physiol. 2011;301(4):L500-9. Epub 2011/07/12.
309. Imanaka H, Shimaoka M, Matsuura N, Nishimura M, Ohta N, Kiyono H. Ventilator-induced lung injury is associated with neutrophil infiltration, macrophage activation, and TGF-beta 1 mRNA upregulation in rat lungs. Anesthesia and analgesia. 2001;92(2):428-36. Epub 2001/02/13.
310. van Rijt LS, Kuipers H, Vos N, Hijdra D, Hoogsteden HC, Lambrecht BN. A rapid flow cytometric method for determining the cellular composition of bronchoalveolar lavage fluid cells in mouse models of asthma. Journal of immunological methods. 2004;288(1-2):111-21. Epub 2004/06/09.
311. Muscedere JG, Mullen JB, Gan K, Slutsky AS. Tidal ventilation at low airway pressures can augment lung injury. Am J Respir Crit Care Med. 1994;149(5):1327-34. Epub 1994/05/01.
312. Copland IB, Kavanagh BP, Engelberts D, McKerlie C, Belik J, Post M. Early changes in lung gene expression due to high tidal volume. Am J Respir Crit Care Med. 2003;168(9):1051-9. Epub 2003/06/21.
313. Yamada T, Ikegami M, Jobe AH. Effects of surfactant subfractions on preterm rabbit lung function. Pediatr Res. 1990;27(6):592-8. Epub 1990/06/01.
314. Wright JR, Clements JA. Metabolism and turnover of lung surfactant. Am Rev Respir Dis. 1987;136(2):426-44. Epub 1987/08/01.
315. Bligh EG, Dyer WJ. A rapid method of total lipid extraction and purification. Can J Biochem Physiol. 1959;37(8):911-7. Epub 1959/08/01.

316. Rouser G, Siakotos AN, Fleischer S. Quantitative analysis of phospholipids by thin-layer chromatography and phosphorus analysis of spots. Lipids. 1966;1(1):85-6. Epub 1966/01/01.
317. Gay C, Collins J, Gebicki JM. Hydroperoxide assay with the ferric-xylenol orange complex. Anal Biochem. 1999;273(2):149-55. Epub 1999/09/02.
318. Lowry OH, Rosebrough NJ, Farr AL, Randall RJ. Protein measurement with the Folin phenol reagent. J Biol Chem. 1951;193(1):265-75. Epub 1951/11/01.
319. Levine RL, Williams JA, Stadtman ER, Shacter E. Carbonyl assays for determination of oxidatively modified proteins. Methods Enzymol. 1994;233:346-57. Epub 1994/01/01.
320. Casals C, Herrera L, Miguel E, Garcia-Barreno P, Municio AM. Comparison between intra- and extracellular surfactant in respiratory distress induced by oleic acid. Biochim Biophys Acta. 1989;1003(2):201-3. Epub 1989/06/08.
321. Livak KJ, Schmittgen TD. Analysis of relative gene expression data using real-time quantitative PCR and the 2(-Delta Delta C(T)) Method. Methods. 2001;25(4):402-8. Epub 2002/02/16.
322. Casals C, Varela A, Ruano ML, Valino F, Perez-Gil J, Torre N, et al. Increase of C-reactive protein and decrease of surfactant protein A in surfactant after lung transplantation. Am J Respir Crit Care Med. 1998;157(1):43-9. Epub 1998/01/28.
323. Valino F, Casals C, Guerrero R, Alvarez L, Santos M, Saenz A, et al. Inhaled nitric oxide affects endogenous surfactant in experimental lung transplantation. Transplantation. 2004;77(6):812-8. Epub 2004/04/13.
324. Schurch S, Bachofen H, Goerke J, Possmayer F. A captive bubble method reproduces the in situ behavior of lung surfactant monolayers. J Appl Physiol. 1989;67(6):2389-96. Epub 1989/12/01.
325. Schoel WM, Schurch S, Goerke J. The captive bubble method for the evaluation of pulmonary surfactant: surface tension, area, and volume calculations. Biochim Biophys Acta. 1994;1200(3):281-90. Epub 1994/08/18.
326. Vockeroth D, Gunasekara L, Amrein M, Possmayer F, Lewis JF, Veldhuizen RA. Role of cholesterol in the biophysical dysfunction of surfactant in ventilator-induced lung injury. Am J Physiol Lung Cell Mol Physiol. 2010;298(1):L117-25. Epub 2009/11/10.
327. Marini JJ, Hotchkiss JR, Broccard AF. Bench-to-bedside review: microvascular and airspace linkage in ventilator-induced lung injury. Crit Care. 2003;7(6):435-44. Epub 2003/11/20.
328. Dries DJ, Adams AB, Marini JJ. Time course of physiologic variables in response to ventilator-induced lung injury. Respiratory care. 2007;52(1):31-7. Epub 2006/12/30.
329. Da Silva K, McCaig LA, Veldhuizen RA, Possmayer F. Protein inhibition of surfactant during mechanical ventilation of isolated rat lungs. Experimental lung research. 2005;31(7):745-58. Epub 2005/10/06.
330. Panda AK, Nag K, Harbottle RR, Rodriguez-Capote K, Veldhuizen RA, Petersen NO, et al. Effect of acute lung injury on structure and function of pulmonary surfactant films. Am J Respir Cell Mol Biol. 2004;30(5):641-50. Epub 2003/11/25.

331. Beutler BA. The role of tumor necrosis factor in health and disease. The Journal of rheumatology Supplement. 1999;57:16-21. Epub 1999/05/18.
332. Uhlig S, Gulbins E. Sphingolipids in the lungs. Am J Respir Crit Care Med. 2008;178(11):1100-14. Epub 2008/08/30.
333. Saenz A, Lopez-Sanchez A, Mojica-Lazaro J, Martinez-Caro L, Nin N, Bagatolli LA, et al. Fluidizing effects of C-reactive protein on lung surfactant membranes: protective role of surfactant protein A. FASEB J. 2010;24(10):3662-73. Epub 2010/05/21.
334. Bailey TC, Maruscak AA, Petersen A, White S, Lewis JF, Veldhuizen RA. Physiological effects of oxidized exogenous surfactant in vivo: effects of high tidal volume and surfactant protein A. Am J Physiol Lung Cell Mol Physiol. 2006;291(4):L703-9. Epub 2006/04/25.
335. Spence MW. Sphingomyelinases. Adv Lipid Res. 1993;26:3-23. Epub 1993/01/01.
336. Goggel R, Winoto-Morbach S, Vielhaber G, Imai Y, Lindner K, Brade L, et al. PAF-mediated pulmonary edema: a new role for acid sphingomyelinase and ceramide. Nat Med. 2004;10(2):155-60. Epub 2004/01/06.
337. von Bismarck P, Wistadt CF, Klemm K, Winoto-Morbach S, Uhlig U, Schutze S, et al. Improved pulmonary function by acid sphingomyelinase inhibition in a newborn piglet lavage model. Am J Respir Crit Care Med. 2008;177(11):1233-41. Epub 2008/03/04.
338. Chandel NS, Schumacker PT, Arch RH. Reactive oxygen species are downstream products of TRAF-mediated signal transduction. J Biol Chem. 2001;276(46):42728-36. Epub 2001/09/18.
339. Lang JD, McArdle PJ, O'Reilly PJ, Matalon S. Oxidant-antioxidant balance in acute lung injury. Chest. 2002;122(6 Suppl):314S-20S. Epub 2002/12/12.
340. Bhatia M, Moochhala S. Role of inflammatory mediators in the pathophysiology of acute respiratory distress syndrome. The Journal of pathology. 2004;202(2):145-56. Epub 2004/01/27.
341. Marin-Corral J, Martinez-Caro L, Lorente JA, de Paula M, Pijuan L, Nin N, et al. Redox balance and cellular inflammation in the diaphragm, limb muscles, and lungs of mechanically ventilated rats. Anesthesiology.112(2):384-94. Epub 2010/01/14.
342. Collard KJ, Godeck S, Holley JE, Quinn MW. Pulmonary antioxidant concentrations and oxidative damage in ventilated premature babies. Archives of disease in childhood Fetal and neonatal edition. 2004;89(5):F412-6. Epub 2004/08/24.
343. Marnell L, Mold C, Du Clos TW. C-reactive protein: ligands, receptors and role in inflammation. Clin Immunol. 2005;117(2):104-11. Epub 2005/10/11.
344. Black S, Kushner I, Samols D. C-reactive Protein. J Biol Chem. 2004;279(47):48487-90. Epub 2004/09/01.
345. Dong Q, Wright JR. Expression of C-reactive protein by alveolar macrophages. J Immunol. 1996;156(12):4815-20. Epub 1996/06/15.
346. Gould JM, Weiser JN. Expression of C-reactive protein in the human respiratory tract. Infection and immunity. 2001;69(3):1747-54. Epub 2001/02/17.

347. Ramage L, Proudfoot L, Guy K. Expression of C-reactive protein in human lung epithelial cells and upregulation by cytokines and carbon particles. Inhalation toxicology. 2004;16(9):607-13. Epub 2005/07/23.
348. Schmidt R, Markart P, Ruppert C, Wygrecka M, Kuchenbuch T, Walmrath D, et al. Time-dependent changes in pulmonary surfactant function and composition in acute respiratory distress syndrome due to pneumonia or aspiration. Respiratory research. 2007;8:55. Epub 2007/07/31.
349. Smith BJ, Grant KA, Bates JH. Linking the Development of Ventilator-Induced Injury to Mechanical Function in the Lung. Annals of biomedical engineering. 2012. Epub 2012/11/20.
350. Henzler D, Hochhausen N, Chankalal R, Xu Z, Whynot SC, Slutsky AS, et al. Physiologic and biologic characteristics of three experimental models of acute lung injury in rats. Anesthesia and analgesia. 2011;112(5):1139-46. Epub 2011/04/09.
351. Vlahakis NE, Schroeder MA, Pagano RE, Hubmayr RD. Deformation-induced lipid trafficking in alveolar epithelial cells. Am J Physiol Lung Cell Mol Physiol. 2001;280(5):L938-46. Epub 2001/04/06.
352. Gajic O, Lee J, Doerr CH, Berrios JC, Myers JL, Hubmayr RD. Ventilator-induced cell wounding and repair in the intact lung. Am J Respir Crit Care Med. 2003;167(8):1057-63. Epub 2002/12/14.
353. Xing Z, Gauldie J, Cox G, Baumann H, Jordana M, Lei XF, et al. IL-6 is an antiinflammatory cytokine required for controlling local or systemic acute inflammatory responses. J Clin Invest. 1998;101(2):311-20. Epub 1998/02/07.
354. Roca H, Varsos ZS, Sud S, Craig MJ, Ying C, Pienta KJ. CCL2 and interleukin-6 promote survival of human CD11b+ peripheral blood mononuclear cells and induce M2-type macrophage polarization. J Biol Chem. 2009;284(49):34342-54. Epub 2009/10/17.
355. van Zoelen MA, Verstege MI, Draing C, de Beer R, van't Veer C, Florquin S, et al. Endogenous MCP-1 promotes lung inflammation induced by LPS and LTA. Molecular immunology. 2011;48(12-13):1468-76. Epub 2011/05/03.
356. Schmal H, Shanley TP, Jones ML, Friedl HP, Ward PA. Role for macrophage inflammatory protein-2 in lipopolysaccharide-induced lung injury in rats. J Immunol. 1996;156(5):1963-72. Epub 1996/03/01.
357. Schurch S, Green FH, Bachofen H. Formation and structure of surface films: captive bubble surfactometry. Biochim Biophys Acta. 1998;1408(2-3):180-202. Epub 1998/11/14.
358. Lopez-Rodriguez E, Echaide M, Cruz A, Taeusch HW, Perez-Gil J. Meconium impairs pulmonary surfactant by a combined action of cholesterol and bile acids. Biophysical journal. 2011;100(3):646-55. Epub 2011/02/02.
359. Kamkin AG, Kiseleva I. Mechanical stretch and cytokines. Dordrecht ; New York: Springer; 2012. xv, 236 p. p.
360. Sandhar BK, Niblett DJ, Argiras EP, Dunnill MS, Sykes MK. Effects of positive end-expiratory pressure on hyaline membrane formation in a rabbit model of the neonatal respiratory distress syndrome. Intensive Care Med. 1988;14(5):538-46. Epub 1988/01/01.

361. Lewis JF, Veldhuizen R. The role of exogenous surfactant in the treatment of acute lung injury. Annu Rev Physiol. 2003;65:613-42. Epub 2003/01/09.
362. Ventilation with lower tidal volumes as compared with traditional tidal volumes for acute lung injury and the acute respiratory distress syndrome. The Acute Respiratory Distress Syndrome Network. N Engl J Med. 2000;342(18):1301-8. Epub 2000/05/04.
363. Determann RM, Achouiti AA, El Solh AA, Bresser P, Vijfhuizen J, Spronk PE, et al. Infectious pleural effusions can be identified by sTREM-1 levels. Respiratory medicine. 2010;104(2):310-5. Epub 2009/10/17.
364. Schulz O, Pennington DJ, Hodivala-Dilke K, Febbraio M, Reis e Sousa C. CD36 or alphavbeta3 and alphavbeta5 integrins are not essential for MHC class I cross-presentation of cell-associated antigen by CD8 alpha+ murine dendritic cells. J Immunol. 2002;168(12):6057-65. Epub 2002/06/11.
365. Altemeier WA, Matute-Bello G, Gharib SA, Glenny RW, Martin TR, Liles WC. Modulation of lipopolysaccharide-induced gene transcription and promotion of lung injury by mechanical ventilation. J Immunol. 2005;175(5):3369-76. Epub 2005/08/24.
366. Guo RF, Ward PA. Mediators and regulation of neutrophil accumulation in inflammatory responses in lung: insights from the IgG immune complex model. Free radical biology & medicine. 2002;33(3):303-10. Epub 2002/07/20.
367. Belperio JA, Keane MP, Burdick MD, Londhe V, Xue YY, Li K, et al. Critical role for CXCR2 and CXCR2 ligands during the pathogenesis of ventilator-induced lung injury. J Clin Invest. 2002;110(11):1703-16. Epub 2002/12/05.
368. Woessner JF, Jr. Matrix metalloproteinases and their inhibitors in connective tissue remodeling. FASEB J. 1991;5(8):2145-54. Epub 1991/05/11.
369. Zucker S, Hymowitz M, Rollo EE, Mann R, Conner CE, Cao J, et al. Tumorigenic potential of extracellular matrix metalloproteinase inducer. The American journal of pathology. 2001;158(6):1921-8. Epub 2001/06/08.
370. Wolters PJ, Wray C, Sutherland RE, Kim SS, Koff J, Mao Y, et al. Neutrophil-derived IL-6 limits alveolar barrier disruption in experimental ventilator-induced lung injury. J Immunol. 2009;182(12):8056-62. Epub 2009/06/06.
371. Febbraio MA, Pedersen BK. Muscle-derived interleukin-6: mechanisms for activation and possible biological roles. FASEB J. 2002;16(11):1335-47. Epub 2002/09/03.
372. Howarth PH, Knox AJ, Amrani Y, Tliba O, Panettieri RA, Jr., Johnson M. Synthetic responses in airway smooth muscle. The Journal of allergy and clinical immunology. 2004;114(2 Suppl):S32-50. Epub 2004/08/17.
373. Zampetaki A, Zhang Z, Hu Y, Xu Q. Biomechanical stress induces IL-6 expression in smooth muscle cells via Ras/Rac1-p38 MAPK-NF-kappaB signaling pathways. American journal of physiology Heart and circulatory physiology. 2005;288(6):H2946-54. Epub 2005/02/01.
374. Kobayashi S, Nagino M, Komatsu S, Naruse K, Nimura Y, Nakanishi M, et al. Stretch-induced IL-6 secretion from endothelial cells requires NF-kappaB activation.

Biochemical and biophysical research communications. 2003;308(2):306-12. Epub 2003/08/07.
375. Kaminski N, Allard JD, Pittet JF, Zuo F, Griffiths MJ, Morris D, et al. Global analysis of gene expression in pulmonary fibrosis reveals distinct programs regulating lung inflammation and fibrosis. Proc Natl Acad Sci U S A. 2000;97(4):1778-83. Epub 2000/03/04.
376. Pittet JF, Griffiths MJ, Geiser T, Kaminski N, Dalton SL, Huang X, et al. TGF-beta is a critical mediator of acute lung injury. J Clin Invest. 2001;107(12):1537-44. Epub 2001/06/20.
377. Lee CG, Kang HR, Homer RJ, Chupp G, Elias JA. Transgenic modeling of transforming growth factor-beta(1): role of apoptosis in fibrosis and alveolar remodeling. Proceedings of the American Thoracic Society. 2006;3(5):418-23. Epub 2006/06/27.
378. Dos Santos CC. Advances in mechanisms of repair and remodelling in acute lung injury. Intensive Care Med. 2008;34(4):619-30. Epub 2008/02/12.
379. Foda HD, Rollo EE, Drews M, Conner C, Appelt K, Shalinsky DR, et al. Ventilator-induced lung injury upregulates and activates gelatinases and EMMPRIN: attenuation by the synthetic matrix metalloproteinase inhibitor, Prinomastat (AG3340). Am J Respir Cell Mol Biol. 2001;25(6):717-24. Epub 2001/12/01.
380. Corbel M, Belleguic C, Boichot E, Lagente V. Involvement of gelatinases (MMP-2 and MMP-9) in the development of airway inflammation and pulmonary fibrosis. Cell biology and toxicology. 2002;18(1):51-61. Epub 2002/05/07.
381. Lechapt-Zalcman E, Pruliere-Escabasse V, Advenier D, Galiacy S, Charriere-Bertrand C, Coste A, et al. Transforming growth factor-beta1 increases airway wound repair via MMP-2 upregulation: a new pathway for epithelial wound repair? Am J Physiol Lung Cell Mol Physiol. 2006;290(6):L1277-82. Epub 2006/01/18.
382. Haseneen NA, Vaday GG, Zucker S, Foda HD. Mechanical stretch induces MMP-2 release and activation in lung endothelium: role of EMMPRIN. Am J Physiol Lung Cell Mol Physiol. 2003;284(3):L541-7. Epub 2002/11/29.
383. Trummer-Menzi E, Gremlich S, Schittny JC, Denervaud V, Stampanoni M, Post M, et al. Evolution of gene expression changes in newborn rats after mechanical ventilation with reversible intubation. Pediatric pulmonology. 2012;47(12):1204-14. Epub 2012/07/12.
384. Rodriguez Capote K, McCormack FX, Possmayer F. Pulmonary surfactant protein-A (SP-A) restores the surface properties of surfactant after oxidation by a mechanism that requires the Cys6 interchain disulfide bond and the phospholipid binding domain. J Biol Chem. 2003;278(23):20461-74. Epub 2003/02/26.
385. Veldhuizen RA, Yao LJ, Hearn SA, Possmayer F, Lewis JF. Surfactant-associated protein A is important for maintaining surfactant large-aggregate forms during surface-area cycling. The Biochemical journal. 1996;313 (Pt 3):835-40. Epub 1996/02/01.
386. Quintero OA, Wright JR. Clearance of surfactant lipids by neutrophils and macrophages isolated from the acutely inflamed lung. Am J Physiol Lung Cell Mol Physiol. 2002;282(2):L330-9. Epub 2002/01/17.